

**DOCTORAL THESIS**

# Performance of Timber Structures Protected by Traditional Plaster Systems in Fire

Johanna Liblik

TALLINN UNIVERSITY OF TECHNOLOGY  
DOCTORAL THESIS  
23/2023

# **Performance of Timber Structures Protected by Traditional Plaster Systems in Fire**

JOHANNA LIBLIK



TALLINN UNIVERSITY OF TECHNOLOGY

School of Engineering

Department of Civil Engineering and Architecture

This dissertation was accepted for the defence of the degree 22/05/2023

**Supervisor:** Prof. Alar Just  
School of Engineering  
Department of Engineering and Architecture  
Tallinn University of Technology  
Tallinn, Estonia

**Opponents:** Prof. Andrea Frangi  
Department of Civil, Environmental and Geomatic Engineering  
Institute of Structural Engineering  
Eidgenössische Technische Hochschule Zürich  
Zürich, Switzerland

Assoc Prof. John Gales  
Department of Civil Engineering  
York University  
Toronto, Canada

**Reviewer:** Dr Michael Rauch  
Munich, Germany

**Defence of the thesis:** 04/07/2023, Tallinn

**Declaration:**

Hereby I declare that this doctoral thesis, my original investigation and achievement, submitted for the doctoral degree at Tallinn University of Technology has not been submitted for doctoral or equivalent academic degree.

Johanna Liblik

-----  
signature



European Union  
European Regional  
Development Fund



Investing  
in your future

Copyright: Johanna Liblik, 2023

ISSN 2585-6898 (publication)

ISBN 978-9949-83-991-9 (publication)

ISSN 2585-6901 (PDF)

ISBN 978-9949-83-992-6 (PDF)

Printed by Koopia Niini & Rauam

TALLINNA TEHNIKAÜLIKOOL  
DOKTORITÖÖ  
23/2023

# Traditsioonilise krohvisüsteemiga kaetud puitkonstruktsioonide tulepüsivus

JOHANNA LIBLIK





# Contents

Contents.....	5
List of publications .....	7
Author’s contribution to the publications .....	8
Preface .....	9
Abbreviations .....	10
Terms .....	11
Symbols .....	12
Greek letters .....	13
1 Introduction .....	14
1.1 Context .....	14
1.2 Problem statement .....	16
1.3 Aims and objectives .....	18
1.4 Methodology .....	19
1.5 Limitations .....	20
1.6 Thesis outline .....	21
2 Fire resistance of timber structures .....	22
2.1 Requirements and assessment .....	22
2.2 Design standard EN 1995-1-2.....	22
2.2.1 The European Charring Model .....	23
2.2.2 The Separating Function Method .....	27
2.2.3 Advanced design methods .....	29
2.3 Fire testing .....	29
3 Timber structures with plaster systems .....	31
3.1 Building structures .....	31
3.2 Traditional plaster systems .....	33
3.2.1 Clay plaster.....	33
3.2.2 Lime plaster.....	35
3.2.3 Plaster carriers and substrates.....	37
3.2.4 Plaster application.....	38
4 Literature review of plasters in fire.....	39
5 Experimental work .....	45
5.1 Test materials .....	45
5.2 Material tests .....	49
5.2.1 Thermogravimetric analysis .....	49
5.2.2 Transient plane heat source method .....	51
5.3 Cone heater tests .....	54
5.3.1 Test materials and programmes .....	54
5.3.2 Test set-up and procedure .....	56
5.4 Furnace tests .....	58
5.4.1 Test materials and programs .....	58
5.4.2 Test preparation and procedure .....	62

6 Results and analysis .....	67
6.1 Material tests and data for simulations .....	67
6.2 Cone heater tests .....	71
6.3 Furnace tests .....	79
6.3.1 Test results .....	79
6.3.2 Analysis of the charring performance of timber .....	90
6.4 Comparison of test results between cone and furnace tests .....	104
6.4.1 Clay plaster systems .....	104
6.4.2 Lime plaster systems .....	108
6.4.3 Discussion.....	109
6.5 Discussion on experimental work .....	111
7 Thermal simulations.....	117
7.1 Aim .....	117
7.2 Simulation program and model .....	117
7.3 Heat transfer simulations.....	120
7.4 Determination of effective thermal properties .....	128
8 Determination of the design equations .....	139
8.1 Basic protection time .....	139
8.2 Basic insulation time .....	141
8.3 Position coefficients .....	142
8.4 Protection factor .....	143
8.5 Failure time .....	144
8.6 Validation by full-scale tests .....	145
9 Small scale method for estimation of fire protection effect.....	152
10 Design principles and parameters.....	153
10.1 Limits of applicability .....	153
10.2 Design equations for plaster systems .....	154
11 Conclusions and outlook.....	158
11.1 Conclusions .....	158
11.2 Outlook.....	161
List of figures.....	163
List of tables .....	168
References .....	170
Acknowledgements.....	180
Abstract.....	181
Lühikokkuvõte.....	183
Appendix 1 .....	185
Appendix 2 .....	186
Curriculum vitae.....	188
Elulookirjeldus.....	189

## List of publications

The list of author's publications in peer-reviewed journals, on the basis of which the thesis has mainly been prepared:

- I Liblik, J., Nurk, M., Just, A. 2022. Charring performance of timber structures protected by traditional lime-based plasters. *Construction and Building Materials*, 347. DOI: 10.1016/j.conbuildmat.2022.128572.
- II Liblik, J. & Just, A. 2022. Small-scale assessment method for the fire resistance of historic plaster system and timber structures. *Fire and Materials*, <https://doi.org/10.1002/fam.3069>.
- III Liblik, J., Küppers, J., Just, A., Maaten, B., Pajusaar, S. 2021. Material properties of clay and lime plaster for structural fire design. *Fire and Materials*, 45 (3), 355–365. DOI: 10.1002/fam.2798.
- IV Liblik, J., Küppers, J., Maaten, B., Just, A. 2020. Fire protection provided by clay and lime plasters. *Wood Material Science & Engineering*, 16:5, 290–298, DOI: 10.1080/17480272.2020.1714726

### Other published works:

- V Liblik, J., Just, A., Küppers, J. 2020. Properties of clay plaster for the fire design of timber structures. LEHM2020 8th International Conference on Building with Earth, Weimar, Germany, Dachverband Lehm e.V.
- VI Liblik, J., Küppers, J., Just, A., Zehfuß, J., Ziegert, C. 2018. Fire safety of historic timber buildings with traditional plasters in Europe. *Proceedings of World Conference on Timber Engineering: World Conference on Timber Engineering*, Seoul, South Korea.
- VII Liblik, J., Järnefelt, K., Just, A., Möller, H., Lynch, P., Salminen, M. 2018. Renovation of a Wooden Building in a Historic Village – a Case Study from Finland. *Proceedings of World Conference on Timber Engineering: World Conference on Timber Engineering*, Seoul, South Korea.
- VIII Küppers, J., Gößwein, L., Liblik, J., Mäger, K. N. 2018. Numerical investigations on heat transfer through claddings of bio-based building materials. *Proceedings of 5th Symposium Structural Fire Engineering: 5th Symposium Structural Fire Engineering*, Braunschweig, Germany.
- IX Liblik, J. & Just, A. 2017. Design parameters for timber members protected by clay plaster at elevated temperatures. *Proceedings of the International Network on Timber Engineering Research (INTER), Meeting 50*, Kyoto, Japan. Ed. Görlacher, R. Karlsruhe: Forschungszentrum Karlsruhe, 375–389.
- X Liblik, J., Just, A. 2016. Performance of Constructions with Timber and Clay at Elevated Temperatures. *Energy Procedia, 96: Sustainable Built Environment Tallinn and Helsinki Conference SBE16 – Build Green and Renovate Deep*. Ed. J. Kurnitski. Elsevier, 717–728. DOI: 10.1016/j.egypro.2016.09.133.
- XI Liblik, J. & Just, A. 2015. Fire technical properties of clay plaster for the fire design of timber structures. *REHAB 2015. Book of proceedings: 2nd International Conference on Preservation, Maintenance and Rehabilitation of Historical Buildings and Structures*, Porto, Portugal, Green Lines Institute for Sustainable Development, 745–754.

## Author's contribution to the publications

Contribution to the peer-reviewed papers in this thesis are:

<b>I</b>	<b>Johanna Liblik</b>	concept of the study, experiments in furnace, preparation of test specimens, data curation and analysis, writing of the paper
	Meeri Nurk	cone heater experiments, preparation of test specimens, data curation, first analysis
	Alar Just	concept of the study, supervision, reviewing and editing
<b>II</b>	<b>Johanna Liblik</b>	concept of the study, cone heater experiments and furnace tests, preparation of test specimens, data collection and test analysis, writing of the paper
	Alar Just	concept of the study, supervision, reviewing and editing
<b>III</b>	<b>Johanna Liblik</b>	concept of the study, experimental work, preparation of test specimens, data collection and test analysis, numerical modelling, writing of the paper
	Judith Küppers	reviewing and editing
	Alar Just	concept of the study, supervision, reviewing and editing
	Birgit Maaten	experimental work of TGA, test analysis, writing of test procedure and results
	Siim Pajusaar	experimental work of XRD, test analysis, writing of test procedure and results
<b>IV</b>	<b>Johanna Liblik</b>	concept of the study, experimental work, preparation of test specimens, data collection and test analysis, writing of the paper
	Birgit Maaten	experimental work of TGA and test analysis, writing of test procedure and results
	Alar Just	concept of the study, supervision, reviewing and editing

## **Preface**

This work is the result of my PhD studies in the Department of Civil Engineering and Architecture at Tallinn University of Technology. The PhD programme was supported by the European Regional Development Fund and the Estonian Research Council grant TAR 16012 – ‘Zero energy and resource efficient smart buildings and districts’.

I met Prof. Alar Just during my master's studies at Tallinn University of Technology, who motivated me to become engaged in fire testing and research. Given my interest in historical buildings and natural building materials, the topic of the fire performance of timber structures and traditional plasters inspired me to continue researching these material combinations in my PhD studies.

This thesis provides an overview of the significance of the research topic as well as experimental and numerical investigations undertaken over the years to enhance our understanding of the fire protection provided by traditional types of plaster systems to timber structures.

## Abbreviations

CEN	European committee for standardisation
DIN	Deutsches Institut für Normung (German standardisation institute)
E	Integrity criterion
ECSM	Effective cross-section method
EMC	Equilibrium moisture content
EN	European norm
ETICS	External Thermal Insulation Composite System
FE	Finite elements
FSITB	European guideline <i>Fire Safety in Timber Buildings</i>
GtA	Gypsum plasterboard type A
GtF	Gypsum plasterboard type F
I	Insulation criterion
iBMB	Institut für Baustoffe, Massivbau und Brandschutz
ISO	International organisation for standardisation
MC	Moisture content
N/A	Not applicable
OSB	Oriented strand board
R	Load-bearing capacity criterion
RB	Reed board
RH	Relative humidity
RM	Reed mat
RISE	RISE Research Institutes of Sweden
SD	Standard deviation
SFM	Separating Function Method
TC	Thermocouples
TGA	Thermogravimetric analysis
TPS	Transient Plane Source (hot disc) method
TU	Technische Universität
WM	Wire mesh
XRD	X Ray Diffraction Analysis

## Terms

<b>plaster</b>	mixture of different materials (binders, additives, admixtures, water, aggregates) to obtain a surface finish which is applied internally to walls and ceilings [EN 13914-2:2016].
<b>plaster coat</b>	obtained by application of one or more layers with one or more mixes of the same product [EN 13914-2:2016].
<b>plaster system</b>	plaster coat or sequence of plaster coats to be applied to a substrate, including the possible use of a carrier and/or reinforcement [EN 13914-2:2016].
<b>reinforcement</b>	material incorporated within a plaster coat to improve resistance to cracking (e.g., glass fibre mesh, jute fabric).
<b>plaster carrier</b>	product attached to the substrate to which a plaster is applied so that the plaster system is largely independent of the substrate (e.g., reed mat, wire mesh).
<b>reed mat</b>	a plaster carrier that is a thin plaster base mat that is made of parallel natural reed stems (~70 stems per linear metre) held together by zinc-plated iron wires.
<b>steel wire mesh</b>	a plaster carrier that is a woven or resistance welded grid consisting of a series of parallel longitudinal wires with accurate spacing welded to cross wires at the required spacing.
<b>substrate</b>	material or product on which plaster is applied to (e.g., reed board, timber member).
<b>reed board</b>	a rigid building board made from natural reed, laid parallel and tightly bound using thin gauge galvanised wire.
<b>fire protection material</b>	material applied for the purpose of increasing fire resistance [prEN 1995-1-2:2022].
<b>protection time</b>	the time to reach the charring of entire thickness or temperature rise of 250 K behind the considered material or product [prEN 1995-1-2:2022].
<b>start time of charring</b>	time at the beginning of the fire exposure for initially unprotected sides of timber members, or time when the surface temperature for initially protected sides of timber members reaches 300°C [prEN 1995-1-2:2022].
<b>failure time of fire protection system</b>	time at which the fall-off of the fire protection system occurs.
<b>char-line</b>	the borderline between char layer and the residual cross-section, assumed to be equal with the position of the 300°C isotherm [prEN 1995-1-2:2022].
<b>charring depth</b>	distance from the original surface of the timber member to the char-line [prEN 1995-1-2:2022].
<b>residual cross-section</b>	cross-section of the original timber member reduced by the charring depth at heated sides of the timber member [prEN 1995-1-2:2022].
<b>effective cross-section</b>	cross-section of the original timber member reduced by the charring depth and the zero-strength layer at heated sides of the timber member.

## Symbols

$d_{char,n}$	notional charring depth within one charring phase, mm
$d_{char}$	charring depth measured in a test, mm
$h_i$	thickness of the considered layer, mm
$h_n$	thickness of the last layer $n$ , mm
$h_p$	material thickness, mm
$k_2$	protection factor
$k_3$	post-protection factor
$k_{pos,exp}$	position coefficient that takes into account the influence of layers preceding the layer considered
$k_{pos,unexp}$	position coefficient that takes into account the influence of layers backing the layer considered
$l_{a,min}$	minimum anchorage length of the fastener into the uncharred timber member, mm
$l_x$	penetration length of the fastener, mm
$l_{x,min}$	minimum penetration length of the fastener, mm
$t$	time, min
$t_0$	time until a constant charring rate is assumed, min
$t_a$	consolidation time, min
$t_{ch}$	start time of charring on the fire exposed side, min
$t_f$	failure time of panels (plaster systems) initially exposed to fire, min
$t_{f,pr}$	failure time of the fire protection system, min
$t_{ins}$	insulation time of the assembly, min
$t_{ins,0,n}$	basic insulation time of the last layer $n$ , min
$t_{ins,n}$	insulation time of the last layer $n$ of the assembly on the unexposed side, min
$t_{prot,0,i}$	basic protection time of the considered layer $i$ , min
$t_{prot,i}$	protection time of each layer $i$ , min
$v_{rec}$	recession speed, mm/min
$\Sigma t_{prot}$	sum of protection times, min
$\Sigma t_{prot}$	sum of protection times of the layers $i$ , min
$\Sigma t_{prot,i-1}$	sum of the protection times of the layers preceding the layer $i$ , min

## Greek letters

$\beta_0$	basic design charring rate, mm/min
$\beta_n$	notional design charring rate within one charring phase, mm/min
$\beta_{n,Phase2}$	notional design charring rate during the protected charring phase (Phase 2), mm/min
$\beta_{n,Phase3}$	notional design charring rate during the post-protected charring phase (Phase 3), mm/min
$\beta_2$	charring rate measured in a test, mm/min
$\lambda$	thermal conductivity, W/(m·K)
$\rho$	density, kg/m <sup>3</sup>
$C_v$	volumetric heat capacity, MJ/(m <sup>3</sup> K)
$c_p$	specific heat, J/(kg·K)

# 1 Introduction

## 1.1 Context

Continuing efforts toward sustainable construction have generated a growing demand for innovative design and the use of low-carbon building materials and technology (Pacheco-Torgal, 2014; Umar et al., 2012; Melià et al., 2014). The present situation has prompted a rediscovery of the advantages of natural (bio-based) building materials such as wood, clay (earth), straw, hemp, and materials derived from reeds (Golden, 2012; Klinge et al., 2016; Pacheco-Torgal et al., 2012; Asdrubali et al., 2016). Timber structures have seen a resurgence in recent decades as a result of their environmental credentials and societal goals for sustainable development with decreased energy consumption and less pollution (Tian et al., 2022).

Despite advances in the use of timber and other bio-based materials in the construction industry, there are still challenges to their wider adoption (COST Action FP1404, 2014). The combustibility of wood has traditionally been one of the key constraints to its widespread usage as a primary load-bearing structural element in buildings (Östman, 2022). However, throughout history, wood has been an important structural and construction material for most societies.

Historically, the use of timber and plaster in the construction of buildings has been widespread across the world (Hasemi et al., 2002; Röhlen et al., 2011; Historic England, 2016). In the past, the primary passive fire safety method for wooden structures has been the use of some protection material against direct fire exposure (Gales, 2013; Chorlton et al., 2020). Clay and lime are one of the oldest binders in plasters that were extensively used in European countries up until the end of 19th century when lime was largely superseded by cement (Ranesi et al., 2021). To this day, densely packed wooden towns and neighbourhoods may still be found in many regions of Europe, notably in Baltic and Scandinavian countries as well as in Germany (Graham, 2004). Nowadays, these buildings hold an important part of crafts in cultural heritage representing old building techniques, craftsmanship and local material use (Larsen et al., 2000). The significance and need to preserve the still existing old wooden structures and buildings is gaining attention in various parts of the world where issues related to the fire resistance performance of traditional building materials and structures are being addressed (Hasemi et al., 2002; Garcia-Castillo et al., 2021). Since these structures were constructed before contemporary fire regulations were developed, sufficient information about how they would behave in a fire is lacking.

In the last decades, the main concentration of interest of designers and academia with respect to fire safety design of timber structures has been in modern and high-rise buildings. Consequently, the research on fire resistance of timber structures and their combination with other traditional building materials (mainly found in historic buildings such as clay or lime plaster) has largely been neglected. As from the beginning of the Industrial Revolution, new materials have been constantly developed and the type of surface finish materials used in timber buildings have significantly been changed due to the shift from traditional to modern building construction. Today, building codes and standards of the fire safety design of wood buildings consist of a limited number of materials and present mainly design values for gypsum plasterboards to guarantee a required level of fire protection (e.g., EN 1995-1-2, 2004). There hardly exist any design equations or guidelines to determine the fire protection effect provided by plasters.

Today, on the other hand, an increasing awareness of the need for appropriate materials for the preservation and retrofitting building structures has led in the revival of traditional building materials, technologies, and applications in the case of historical or heritage buildings (Barbero-Barrera et al., 2014; Ranesi et al., 2021). Partly it has been related to the improper use of modern materials in old buildings that has frequently contributed to accelerating the degradation process of the built heritage, poor indoor climate and loss of authenticity and crafts. International organisations such as ICOMOS argue that any intervention in historic structure should, to the greatest extent feasible, respect the concept, techniques, and historical value of the original or earlier states of the structure (ICOMOS, 2017). For repairs and restorations, it is highly suggested to utilize materials with comparable composition and qualities to the originals. This approach permits the conservation and proper maintenance of buildings (Barbero-barrera et al., 2014).

Ongoing research and the knowledge about the performance and benefits of natural (traditional) materials such as plasters have resulted in their acceptance and their use seems to become once again much practiced in restoration works (Snow & Torney, 2014). An increased interest to find alternative surface finish materials such as plasters may also be encountered in contemporary buildings (e.g., straw bale buildings (Wachtling et al., 2013)). In the last decades, plasters have demonstrated list of benefits. Number of studies have suggested that clay plaster might be an effective passive removal material for ozone (Darling et al., 2012; Darling et al., 2016) and acts as an active agent to regulate indoor climate, while prospectively reducing the presence of indoor pollutants (Richter et al., 2021). It has been pointed out that traditional type of plasters have certain qualities that make them well suited for use on historically constructed timber buildings: i) high vapour permeability that prevents timber from deteriorating; ii) elasticity to absorb minor structural movement; iii) non-toxic and aesthetically pleasing (Snow & Torney, 2014). In moderately cold climates, individuals spend a significant amount of time inside, making air quality and a healthy atmosphere vital to their health. Consequently, materials used in buildings are regarded as essential components for attaining contemporary living standards.

Whilst the benefits of plasters are being rediscovered, up until today their fire-related performance has not been widely studied. Only limited number of research papers or technical sheets are available dealing with the fire protection assessment of plasters as protection material for timber structures (Chorlton et al., 2020; Jackman, 2009; BRE, 1988). Particularly rare are studies when plasters are exposed to standard fire exposure conditions (according to EN 1363-1) (Dalmais et al., 2019). However, amongst various requirements set for building constructions and materials, fire safety is one the most relevant criteria that needs to be guaranteed (European Commission, 2011). It is stated that constructions must be designed and built such that in the case of fire: i) load-bearing capacity can be assumed for a specific time; ii) generation and spread of fire and smoke is limited; iii) spread of fire to neighbouring constructions is limited. EN 13501-2 specifies the procedure for classification of construction products and building elements using data from fire resistance and smoke leakage tests. To comply with fire safety requirements, the performance of structures need to be guaranteed by calculation methods given in design standards (e.g., EN 1995-1-2) or if no design values exist, by conducting a full-scale fire test (e.g., EN 13381-7:2019).

The subject of this thesis is directly influenced by the heritage of the 19th and early 20th century architecture in Estonia, where old wooden buildings still dominate the

cityscapes. Previously, (Arumägi, 2015) has investigated the energy retrofit measures for these type of buildings (Arumägi et al., 2014). Yet, one of the challenges these buildings still face is adapting to a required fire resistance when plaster is to be used as a fire protection material (i.e., clay or lime-based plaster systems applied directly on wooden structures). There are currently no flexible design guidelines for the use of plaster systems as fire protection materials for timber structures. In this regard, the present thesis will have an important impact on the existing knowledge gap.

## 1.2 Problem statement

To verify the fire resistance of any building structure, full-scale testing or calculation using appropriate design models can be performed. The latter needs input values, which describe the material's contribution to the construction's overall fire resistance. In Europe, the design standard of structural fire design of timber structures (EN 1995-1-2:2004) gives principles and application rules for specified requirements with respect to the loadbearing capacity and separating function. This standard lists some materials (e.g., gypsum plasterboards) that could be used as a fire protection material. Design values are given to calculate the charring of timber when initially protected (i.e., the start time of charring, protection factor considering the reduced charring rate of timber while protected, fall-off times). Applying protection materials such as gypsum plasterboards is one of the simplest and proven ways to initially protect timber structures from direct fire exposure. However, today, no design values (with respect to the design principles of EN 1995-1-2:2004) for plaster systems are available.

At this moment, this standard is under revision and will be significantly improved (prEN 1995-1-2:2022). In practice, the calculation-based verification methods for the load-bearing capacity of timber elements are widely used, however the calculation models for the separating function are not well-known. During the last decades, design methods have been improved and new developments have been presented, e.g., the European technical guideline for timber buildings (Östman et al., 2010). In prEN 1995-1-2:2022, a separating function method (SFM) is proposed as a future design method to evaluate timber structures under standard fire exposure. This calculation method is based on work by (Schleifer, 2009) with the improvements by (Mäger et al., 2018), wherein the fire resistance of structures is calculated as a sum of the protection times of the individual layer of an assembly (explained in Chapter 2.2.2). The SFM supports the design freedom and flexible use of various materials and their combinations in respective structures, whereas the design flexibility can be seen particularly relevant and needed in the retrofitting of existing (historic) buildings and in modern buildings when new materials are used.

With the absence of design equations in building codes and lack of fire-related performance data on plaster systems, the designers as well as implementers, refrain from using traditional surface finish materials, e.g., clay and lime-based plasters. Thus, the problem related to the use of such plasters today is complicated. As a result, to use traditional materials (such as plasters) as fire protection, either a full-scale fire test is required or in practice, the existing material/construction in question is removed and replaced. Both alternatives are not favourable, as the full-scale testing has number of drawbacks (e.g., high costs, large equipment requirement and environmental impact) and is not preferable when various material combinations are in interest. It has been stressed that if the design data of the current materials in historical buildings is known, then needless renovations to show the fire safety of materials and structures may be

avoided (Jackman, 2009). The need of fire-related data on historical (traditional type) of plasters has previously been pointed out in other studies (Pachta et al., 2018) as well as the need to establishing technical documentation to enhance design standards has been emphasized (Barbero-Barrera et al., 2014). Furthermore, the absence of fire design guidelines places producers of such materials at a significant competitive disadvantage. Recently, the lack and need of fire design data on clay-based materials has been pointed out in the context of sustainable building designs (Baumberger et al., 2022).

In some countries, e.g., Germany, a design standard DIN 4102-4: 2016 presents fire resistance classes for some specific existing timber-frame walls with infill material ('Fachwerk'), protected by plaster (a minimum thickness is usually given to fulfil the criterion). In UK, a technical guideline by BRE has been published describing the possibilities to upgrade existing floor structures covered with lath and plaster (BRE, 1988). Yet, these documents reveal somewhat different opinions and regulations on the acceptable levels of fire resistance and means to achieve them. Additionally, the technical guidelines provide upgrading solutions for existing structures by incorporating mainly gypsum plasterboards; however, this approach is not favourable in historic buildings. Furthermore, these documents are limited to specific building structures and present limited design options, i.e., no flexible design calculations could be made.

In the last decades, plasters have mainly been tested in straw bale structures as a finishing layer (Wall et al., 2012; Wachtling et al., 2013). Performed tests demonstrate that plaster can stay intact to its underlying structure for a considerable time. Yet, often the test reports lack specific fire test data (e.g., temperature measurements behind the plaster) and observations such as the cracking or fall-off times of plaster are poor or not made at all. However, these factors are highly relevant when trying to understand the fire protection ability of plasters. Up until today, there are hardly any data available about the fire tests of plaster systems directly applied on timber structures under standard fire exposure conditions. In addition, the results obtained from straw bale testing are not directly applicable to the plaster system applied on solid timber elements due to different application techniques (e.g., use of plaster carriers) and substrates.

To develop an understanding of the behaviour of a building material subjected to fire and to define its fire protection ability, its temperature-dependent material properties must be known. To define the relevant material properties and design values (in view of EN 1995-1-2), various test methods have been used in the fire research community (Adl-Zarrabi et al., 2006; Sjöström et al., 2012; Tiso, 2018). In view of the implementation of new materials to the SFM, (Mäger et al., 2017) have proposed a procedure to determine the relevant design parameters by recommending specific material testing (e.g., TPS method) and furnace tests (EN 1363-1). The developed material specific thermal properties enable to carry out numerical investigations, while minimising the need for extensive physical testing. Today, there is limited data available on these properties (thermal conductivity, specific heat, and density) for traditional clay and lime-based plasters.

For investigating the fire resistance of new materials, small-scale testing methods can be very useful. Intermediate size furnace tests and other small-scale testing equipment have demonstrated means for assessing materials in roughly comparable fire exposure conditions (with certain limitations) as in full-scale. The potential and shortcomings of testing in different scales has been discussed by (Babrauskas, 2004). Today, a bench-scale testing device, cone calorimeter, has become a well-established tool for the determination of combustible characteristics of materials in accordance with ISO 5660-1. Owing to its

continuous widespread use around the world due to its simplicity and cost-efficiency, other potential uses of this device have been recognised, e.g., the assessment of the charring performance of timber (Mikkola, 1991; Xu et al., 2015). Testing in small-scale, while obtaining reliable test results comparable to the ones received in furnace may serve as an effective prediction and planning tool for full-scale testing. Small specimen size can be especially beneficial for the assessment of various (historic) plaster systems that may require fire resistance rating. Today, existing studies with the cone heater are rarely comparable due to different test set-ups and fire exposure conditions. No small-scale test method has been proposed.

This thesis is aimed at addressing the knowledge and research gaps described above, in view of the design principles given in EN 1995-1-2. This allows the results and perspective of this study to be compared and implemented in the current framework of fire design of timber structures.

### **1.3 Aims and objectives**

This thesis investigates the performance of traditional clay and lime-based plasters as fire protection systems for timber structures under fire-related conditions at various scales.

The aim of this thesis is to improve the fire design models for timber structures with clay and lime-based plaster systems by proposing relevant design parameters in compliance with Eurocode 5 Part 1-2.

Through the experimental programme in this research, this thesis also aims to propose a small-scale test method as an estimation tool for predicting the fire design parameters for plasters.

The primary objectives of this thesis are as follows:

- to determine the fire protection ability of various types of clay and lime-based plasters for timber using the cone heater of a cone calorimeter at high heat flux levels;
- to investigate the charring performance of timber structures protected by selected plaster systems in furnace under standard fire exposure conditions;
- to develop design parameters for traditional plaster systems for the simplified design models for the revision of Eurocode 5 Part 1-2;
- to determine the effective temperature-dependent material properties for traditional plaster systems for advanced fire design models presented in Eurocode 5 Part 1-2;
- to propose a small-scale test method for estimating the fire design parameters of plaster systems for timber structures in relation to furnace tests.

The fire resistance performance of selected plaster systems and timber structures is assessed by means of experimental studies and numerical heat transfer analysis.

### **Novelty and practical application**

The proposed design parameters enable the design and assessment of the fire resistance of timber structures protected by traditional clay and lime-based plaster systems. The performed study serves as a basis and facilitates the integration of traditional plaster systems to be incorporated in design guidelines and standards in the future (e.g., EN 1995-1-2). The proposed effective thermal properties for plaster systems could be used in advanced design methods and serve as a first input data for performance-based design as these data are scarce to date.

This work consists of fire investigations with traditional plaster systems that have seldom been assessed using contemporary fire testing equipment. Testing at different scales and under different fire exposure conditions allowed for a better understanding of the various test results that could be obtained. Test results outline the critical factors influencing the fire performance of plasters accompanied by future work.

The performed study attempts to reduce the need for extensive furnace tests by demonstrating a small-scale testing method as an estimation tool. To date, there is no established small-scale approach for assessing the fire protection effect of plasters in relation the furnace test results for determination of design values in view of EN 1995-1-2. The cone heater testing can be utilized for existing and future research of material's fire performance (incl. material development), providing a method to compare plasters in view of their fire protection ability.

The proposed design parameters can be used as a guidance to assess similar type of existing plaster systems in situ that require fire ratings, e.g., in renovation projects. This research contributes to the use of traditional building materials and techniques, thus the preservation of cultural built heritage.

## **1.4 Methodology**

The methodology of this thesis follows the objectives and is based on commonly used research methods for the assessment of fire resistance of building structures. The charring performance of timber is taken as the primary criteria for assessing the fire protection provided by plaster systems. The following provides the principal basis for the development of the fire design model and parameters for the selected plaster systems.

Firstly, a review on the various plaster systems and timber structures was carried out, to form a sufficient knowledge of selected plasters and their application. Subsequently, a state-of-the-art overview of previously performed fire-related studies was conducted to provide a frame of reference for the experimental and numerical studies.

The experimental work formed the principal part of this research to meet the aim of the thesis. The fire resistance of selected structures was assessed by small and intermediate-scale testing commonly used in this research field. The cone heater of a cone calorimeter (ISO 5660-1) was used to estimate and compare the fire protection ability of various plaster systems in a feasible way. The test set-up, procedure and obtained test results were later analysed to propose the use of cone heater testing as an estimation method for predicting the fire protection effect of plasters.

The intermediate-scale furnace tests enabled to subject the test specimens to the standard fire exposure conditions in accordance with EN 1363-1. The furnace tests were carried out in various scales that enabled to compare the test results obtained from different sizes of test specimens. Main design values of the start time of charring and charring rate behind the plaster systems were determined. Observations were made

about the fall-off times of plaster systems that also served as an estimation of their performance in full-scale tests according to EN 13381-7:2019.

For the simplified design method and advanced design methods described in EN 1995-1-2, numerical heat transfer analysis was carried out with the SAFIR software program. The input data for temperature-dependent thermal properties of plasters were defined by thermogravimetric analysis (TGA), the transient plane heat source method (TPS) and literature. The listed test methods are widely used to determine these material properties (Mäger et al., 2017). In view of prEN 1995-1-2:2022, the effective thermal properties of plasters were developed based on the obtained furnace test results. It was found that the data from the furnace experiments were sufficient for the separating function method (SFM) defined in prEN 1995-1-2:2022 to determine design parameters.

## 1.5 Limitations

This thesis was limited to the investigations of fire resistance performance of solid timber structures with plaster systems exposed to high heat flux levels and standard fire exposure conditions. Meaning, the materials were subjected to the fully developed fire phase, thus the development of material changes during the early stage of fire phase was not explicitly examined. Accordingly, material tests at elevated temperatures were only performed to support the analysis of furnace test results and to provide input data for the thermal simulations. No in-depth examination of temperature-dependent physico-mechanical properties of plasters was conducted.

This research was defined by the scope of the fire part of Eurocode 5. The development of design equations for the European Charring Model and the SFM were determined based on the performed fire tests, using a solid timber element (or insulation board) as the backing material for plaster systems. For the SFM, the set-up of a test specimen slightly differs from the requirement given in Annex G of prEN 1995-1-2:2022 (e.g., timber element was used instead of a wooden particleboard as a backing layer).

The temperature-dependent material properties (i.e., thermal conductivity, specific heat, and density) were mainly determined in accordance with the design principles presented in prEN 1995-1-2:2022. These properties were developed as effective values rather than physically measured real values taking into account effects (e.g., cracking of plaster) in a fire test, which were not explicitly considered in the thermal analysis.

The numerical investigations were performed with certain simplifications regarding the SAFIR software used for heat transfer analysis. The influence of moisture content and migration of the moisture within the materials were considered indirectly by the effective properties. In addition, the plaster carriers (i.e., the reed mat or metal wire mesh) were not regarded as independent materials in the simulations, thus they were taken into account indirectly. The objective of the thermal simulations was the thermal response of the whole plaster system (including the plaster carrier) as a fire protection system and the development of the respective effective material properties.

The performed furnace tests were limited to intermediate scale, using different sizes of furnaces up to 1.5 m<sup>3</sup>. All tests were conducted as non-loadbearing wall and ceiling elements. The validation was done by available full-scale test results.

The small-scale (cone heater) test method proposal was realized by comparing the test results obtained from tests carried out in small and intermediate scale. No explicit investigations were undertaken in terms of thermal boundary conditions, heat loss phenomena and heat transfer coefficients apparent in the cone heater testing.

The test materials and their application techniques were chosen on the basis of their traditional composition, recommended use in old buildings, and applicability to present-day practise. The selection of test materials was strongly influenced by their use in historic wooden buildings in Estonia. Primarily, plasters that fulfilled the requirements of the product standards were selected.

## **1.6 Thesis outline**

This thesis consists of 11 chapters. In the current chapter, the background and problem definition of this thesis are discussed. The aims and objectives of the thesis are presented, along with the research methodology and limitations that apply.

Chapter 2 discusses the framework of the fire safety concept of timber structures and its fire resistance assessment methods for particularly this research. The structural fire design of initially protected timber structures is explained in view of EN 1995-1-2:2022, along with the design parameters that are in the centre focus of this thesis.

Chapter 3 provides a review on timber constructions and plaster systems used in existing and new buildings. This forms a solid background for the experimental studies. The chapter concludes with an elaboration on the selection of plaster systems predominantly investigated in this thesis.

Chapter 4 discusses the literature overview of previously performed fire-related studies on plaster materials, plaster systems and timber structures. Main results and observations are reported for the frame of reference of the experimental studies carried out in the current thesis.

Chapter 5 describes the experimental program, which includes small- and medium-scale fire resistance tests and material-specific experiments. Tests are described in terms of their preparation, test setup, and the test methods used.

Chapter 6 presents test results obtained from the experimental work. Analysis and discussion of test results and observations are presented.

Chapter 7 presents and discusses the numerical investigations. SAFIR software is used for heat transfer analysis based on material properties derived from the experimental program and literature. The furnace test results are used to calibrate and determine the effective thermal properties for plaster systems.

Chapter 8 complements the previous chapter by presenting the determination of the design equations of plaster systems with respect to prEN 1995-1-2:2022.

Chapter 9 proposes the small-scale test method using the cone heater for estimating the design values of plaster systems as protection materials for wooden structures, which are usually determined in furnace.

Chapter 10 presents the design model and parameters for traditional plaster systems to be used in accordance with design standard EN 1995-1-2, alongside with limitations and design principles for plaster systems.

Chapter 11 provides conclusions and an outlook for future research.

## **2 Fire resistance of timber structures**

### **2.1 Requirements and assessment**

Structural fire safety measures are part of the requirements of the fire safety regulations set for buildings. Its main objective is to guarantee the load-bearing capacity (R criterion) of a structure and restrict the spread of fire to the room of origin for a required time (the integrity (E) and insulation (I) criteria). The fire resistance performance is applicable for structural and compartment separating building elements, whereas the building structures are subjected to a fully developed fire phase.

The verification of the requirements can be achieved by means of fire tests or calculations (if available) or both. The criterion of fire resistance is usually addressed with the duration of time or time of fire resistance for which the member fulfils certain requirements whilst exposed to a certain fire exposure condition. To compare products with each other, a standardised method of EN 13501-2 defines classification for resistance to fire of construction products and building elements, wherein main fire characteristics (R, E and I criteria) and fire resistance tests are described.

The considered fire load to determine the fire resistance of building structures is usually based on the standard temperature-time curve described in ISO 834. It is a simplified description of a fire exposure that indicates the temperature dependency over time. This nominal fire exposure is also adopted by the European standard on fire resistance tests EN 1363-1, which describes the general requirements and means of controlling the temperature-time curve by using the installed plate thermometers in the furnace.

In Europe, the fire part of Eurocode 5 (EN 1995-1-2) gives principles and application rules for the design of timber structures for specified requirements in respect of the abovementioned functions on R, E and I criteria. The calculation methods given in EN 1995-1-2 mainly apply to structures exposed to standard fire exposure conditions (EN 1363-1). Regarding the new generation of EN 1995-1-2 that is currently under revision, prEN 1995-1-2:2022, simplified design models are introduced for calculations in future: 'Effective Cross-Section Method' and 'Separating Function Method'. The design principles are explained in detail below (Section 2.2.1 and 2.2.2).

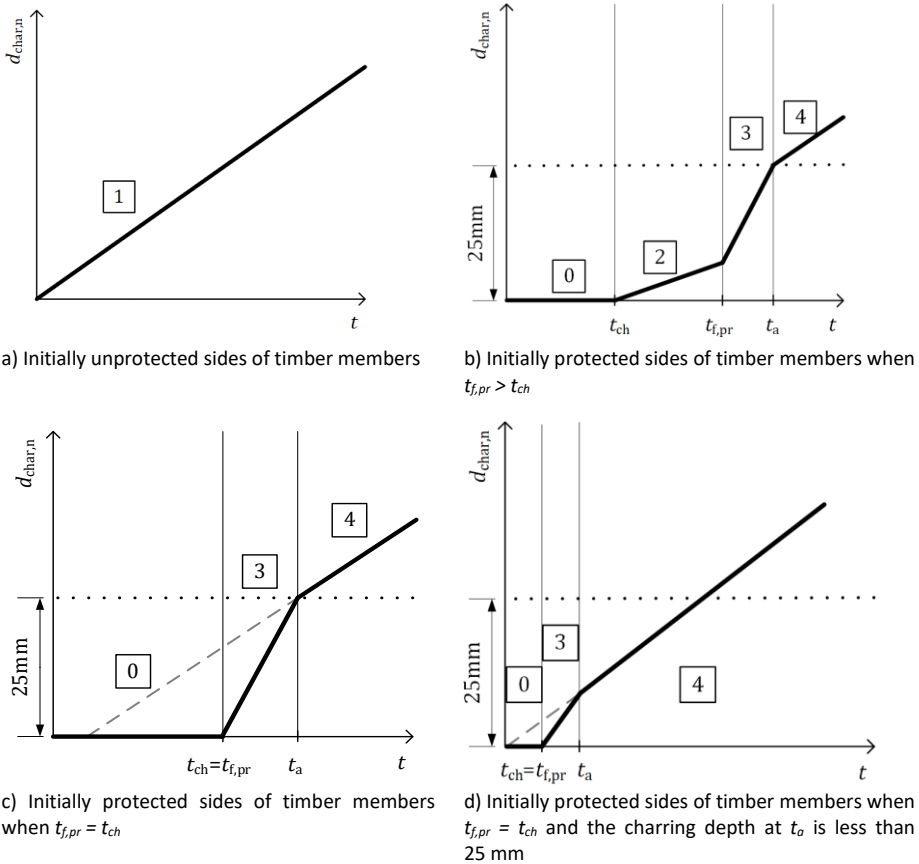
As the design standards have certain limitations, experimental full-scale fire testing is still widely practiced in the majority of jurisdictions. However, testing in full-scale has several drawbacks such as high cost, time requirements, limited use of test results etc. Therefore, calculation methods have become favourable to predict the fire resistance of structures as they present a cost-efficient and more flexible ways for design purposes.

### **2.2 Design standard EN 1995-1-2**

The EN 1995-1-2 is currently under revision. Improved calculation methods have recently been included to a final draft version (prEN 1995-1-2:2022). Following are the relevant design principles in accordance with prEN 1995-1-2:2022, which forms the basis for the development of design parameters for selected plaster systems in this thesis.

## 2.2.1 The European Charring Model

Design standard prEN 1995-1-2:2022 introduces the European charring model, which is a simplified model for the calculation of the residual cross-section of a timber member assuming linear charring rates during different charring phases. The model should be applied to standard fire exposure. The position of the char-line in timber members is assumed as the position of the 300°C isotherm. The different charring phases are presented in Figure 2-1.



Key:

1	Normal charring phase (Phase 1)
0	Encapsulated phase (Phase 0)
2	Protected charring phase (Phase 2)
3	Post-protected charring phase (Phase 3)
4	Consolidated charring phase (Phase 4)
$d_{char,n}$	Notional charring depth;
$t$	Time;
$t_a$	Consolidation time;
$t_{ch}$	Start time of charring;
$t_{f,pr}$	Failure time of the fire protection system.

Figure 2-1. The European charring model according to prEN 1995-1-2:2022.

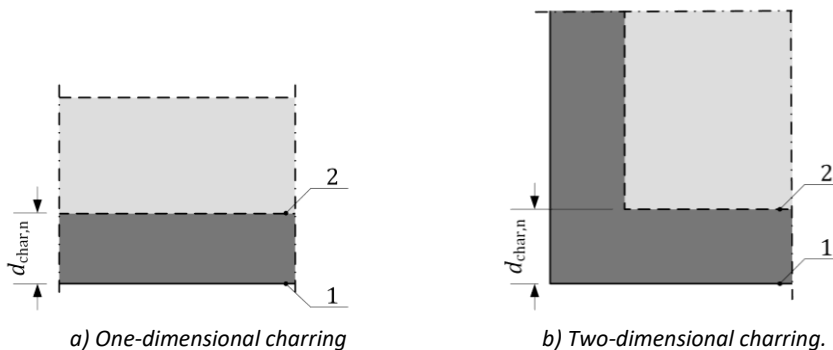
For initially unprotected sides of timber members a normal charring phase (Phase 1) applies, see Figure 2-1a. For initially protected sides of timber members different charring phases apply (Figure 2-1b, Figure 2-1c, Figure 2-1d): an encapsulation phase (Phase 0) when no charring occurs behind the fire protection system; protected charring phase (Phase 2) is the phase when charring occurs behind the fire protection system while the protection system is still in place; post-protected charring phase (Phase 3) is the phase after the failure of the fire protection system before a fully developed char layer (25 mm) has been formed; consolidated charring phase (Phase 4) is the phase with fully developed char layer.

If the timber member undergoes charring in different charring phases the European charring model shall be individually applied for each charring phase. The relevant charring rate is calculated considering various factors influencing its performance (see prEN1995-1-2:2022). In Figure 2-2, the notional charring depth  $d_{char,n}$  is the distance between the outer surface of the original timber member and the position of the char-line. It is calculated using the time of fire exposure  $t$  and the relevant notional charring rate  $\beta_n$ . The  $\beta_n$  should be calculated using the applicable modification factors for charring  $k_i$  given in prEN1995-1-2:2022. The notional charring depth  $d_{char,n}$  should be calculated as follows:

$$d_{char,n} = \sum_{Phases} (\beta_n \cdot t) \quad (1)$$

where:

- $d_{char,n}$  is the notional charring depth in mm;
- $\beta_n$  is the notional design charring rate within one charring phase in mm/min;
- $t$  is the time for the charring phase considered in min.



- Key:
- 1 Fire exposed side
  - 2 Border-line of the residual cross-section

Figure 2-2. Notional charring depth  $d_{char,n}$  (prEN 1995-1-2:2022)

According to the standard, charring shall be taken into account for all sides of timber members directly exposed to fire, and, where relevant, for initially protected sides, where charring occurs during the relevant time of fire exposure. The charring depth should be calculated using appropriate charring rates. The charring rates are normally different for initially unprotected sides of timber members, initially protected sides of timber members prior to failure of the protection and sides of timber members directly exposed to fire after failure of the protection.

In case of one-dimensional charring and considering no other influential factors, the charring rate of initially protected timber is influenced by two different protection phases. The one-dimensional charring of protected timber is considered as the protected charring phase (Phase 2) and should be calculated as follows:

$$\beta_{n,Phase2} = k_2\beta_0 \quad (2)$$

where:

- $k_2$  is the protection factor for Phase 2;
- $\beta_0$  is the basic design charring rate of timber, the design charring rates ( $\beta_0$ ) are given in EN 1995-1-2. For coniferous species  $\beta_0 = 0,65$  mm/min.

The post-protection phase is considered when the failure of the protection system has occurred. The charring in post-protection phase until the consolidation phase is calculated as follows:

$$\beta_{n,Phase3} = k_3\beta_0 \quad (3)$$

where:

- $k_3$  is the protection factor for Phase 3;
- $\beta_0$  is the basic design charring rate of timber, the design charring rates ( $\beta_0$ ) are given in EN 1995-1-2. For coniferous species  $\beta_0 = 0,65$  mm/min.

Unless rules are given in EN 1995-1-2, the post-protection factor  $k_3$  for Phase 3 should be assumed equal to 2.

### Start time of charring

According to prEN 1995-1-2:2022, the start time of charring  $t_{ch}$  behind the fire protection system should be calculated as follows:

$$t_{ch} = \min \left\{ \sum t_{prot}, t_{f,pr} \right\} \quad (4)$$

where:

- $t_{ch}$  is the start time of charring behind the fire protection system, in min;
- $t_{f,pr}$  is the failure time of the fire protection system, in min;
- $\sum t_{prot}$  is the sum of protection times of the fire protection system.

### The failure time of the fire protection system

The failure of fire protection systems mainly occurs due to the mechanical degradation of the protection material or insufficient fixation into uncharred timber. The latter may be caused by insufficient penetration depth, type of the fasteners or large distances between fasteners. For a fire protection system, the fastener should be chosen with respect to the applied fire protection system and to avoid failure of the fixation for a required time. The minimum penetration length of the fastener should be calculated as by design equation (7), see Figure 2-3. The minimum anchorage length into the uncharred part of the timber member should be taken as 10 mm. The anchorage failure of the fasteners could be avoided by respecting the given detailing rules.

The failure time of fire protection systems should be assessed on the basis of tests according to EN 13381-7:2019. For gypsum plasterboards, the generic values for  $t_{f,pr}$  are

given in prEN 1995-1-2:2022, along with the detailing and specifics regarding the boards and fasteners.

According to prEN 1995-1-2:2022, the failure time  $t_{f,pr}$  of the fire protection system should be calculated as follows:

$$t_{f,pr} = t_f \quad \text{for the fire protection system consisting only of panels} \quad (5)$$

$$t_{f,pr} = \max \left\{ \sum t_{prot} \right. \quad \text{for all other applications consisting of combinations of panels with other panels.} \quad (6)$$

where:

$t_f$  is the failure time of panels initially exposed to fire, in min;

$\sum t_{prot}$  is the sum of protection times of the fire protection system.

The minimum penetration length  $l_{x,min}$  of the fastener should be calculated as follows, see Figure 2-3:

$$l_{x,min} = (t_{f,pr} - t_{ch}) \cdot \beta_{n,Phase2} + l_{a,min} \quad (7)$$

where:

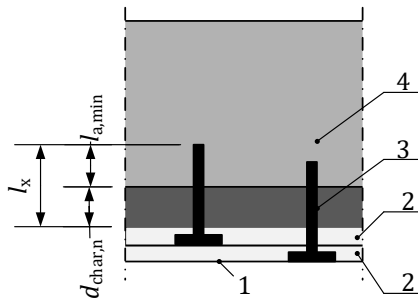
$t_{f,pr}$  is the failure time of fire protection system, in min;

$t_{ch}$  is the start time of charring, in min;

$l_{x,min}$  is the penetration length of the fastener, in mm;

$l_{a,min}$  is the minimum anchorage length of the fastener into the uncharred timber member, in mm;

$\beta_{n,Phase2}$  is the notional design charring rate during Phase 2, in mm/min.



Key:

1 Fire exposed side

2 Fire protection system

3 Fastener

4 Timber member

$d_{char,n}$  Notional charring depth in mm;

$l_{a,min}$  Minimum anchorage length of the fastener into the uncharred part of the timber member, in mm;

$l_x$  Penetration length of the fastener, in mm.

Figure 2-3. Minimum penetration length of the fastener and minimum anchorage length into the uncharred part of the timber member (prEN 1995-1-2:2022).

### 2.2.2 The Separating Function Method

The separating function method (SFM) defined in prEN 1995-1-2:2022 is an improved calculation model based on work by (Schleifer, 2009) and its improvements by (Mäger et al., 2018). The SFM should be applied for the verification of the separating function (integrity and/or insulation), for the calculation of the start time of charring of initially protected timber members.

The fire resistance according to SFM is determined by accounting the contribution of single layers in the entire layered assembly. Each layer is defined by a protection time ( $t_{prot,i}$ ) which is the time until its fire protective function is assumed to be lost. This is the time when temperature rises by 250 K on average or 270 K at any point on the unexposed side of the considered layer. This value is also considered as the start time of charring ( $t_{ch}$ ) in prEN 1995-1-2:2022. The protection time can be increased by the value  $\Delta t$  if layers on the exposed side remain on the construction, despite the temperature criterion of 270°C is reached on the unexposed side of this layer (e.g., gypsum plasterboard type F). The influence of adjacent layers is considered by using the position coefficients ( $k_{pos,exp,i}$ ,  $k_{pos,unexp,i}$ ). The influence of joints is considered by the joint coefficient ( $k_j$ ) that respectively reduces the protection or insulation time of a layer at a certain extent. The last layer (fire-unexposed side of an assembly) serves the insulating function (crucial failure criteria) that is prescribed by the insulation time ( $t_{ins,n}$ ) when the temperature rise on the unexposed side is 140 K on average or 180 K at any point. The insulation time of the entire timber assembly can be calculated from the sum of the protection times and the insulation time of the last layer. These temperature criteria are consistent with the insulation criterion requirements set in EN 13501-2. Using this calculation method, the integrity (E) criterion should be assumed as satisfied where insulation (I) is satisfied according to the general principles of SFM, if detailing is carried out accordingly and last layers on the unexposed side remain fixed to the unburnt part of the assembly. The insulation time  $t_{ins}$  of the assembly should be calculated as the sum of contributions of the individual layers used in the assembly as follows:

$$t_{ins} = \sum_{i=1}^{i=n-1} t_{prot,i} + t_{ins,n} \quad (8)$$

where:

- $t_{ins}$  is the insulation time of the assembly, in min;
- $t_{prot,i}$  is the protection time of each layer  $i$  in the direction of the heat flux, in min;
- $t_{ins,n}$  is the insulation time of the last layer  $n$  of the assembly on the unexposed side, in min.

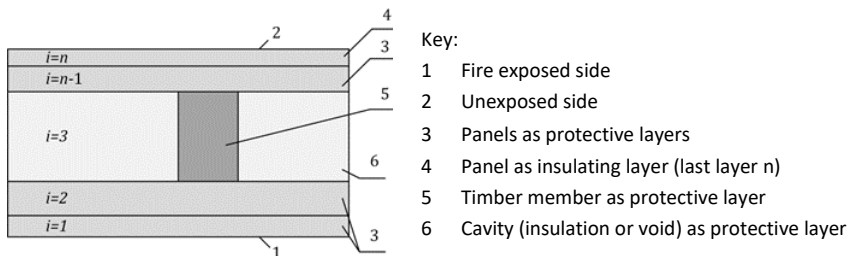


Figure 2-4. Numbering and function of the layers in the assembly (prEN 1995-1-2:2022).

According to prEN 1995-1-2:2022, the protection time  $t_{prot,i}$  for panels and insulation products should be calculated as follows:

$$t_{prot,i} = (t_{prot,0,i} \cdot k_{pos,exp,i} \cdot k_{pos,unexp,i} + \Delta t_i) \cdot k_{j,i} \quad (9)$$

where:

- $t_{prot,i}$  is the protection time of the considered layer  $i$ , in min;
- $t_{prot,0,i}$  is the basic protection time of the considered layer  $i$  in min;
- $k_{pos,exp,i}$  is the position coefficient that takes into account the influence of layers preceding the layer;
- $k_{pos,unexp,i}$  is the position coefficient that takes into account the influence of layers backing the layer;
- $k_{j,i}$  is the joint coefficient for layer  $i$  where relevant;
- $\Delta t_i$  is the correction time for considered layer  $i$  where relevant, in min.

The insulation time  $t_{ins,n}$  for timber members as last layer  $n$  should be calculated as follows:

$$t_{ins,n} = (t_{prot,n} - 10) \cdot k_{j,n} \quad (10)$$

where:

- $t_{ins,n}$  is the insulation time of the last layer  $n$ , in min;
- $t_{prot,n}$  is the protection time of the last layer  $n$ , in min;
- $k_{j,n}$  is the joint coefficient for the last layer  $n$ .

The insulation time  $t_{ins,n}$  for panels as last layer  $n$  should be calculated as follows:

$$t_{ins,n} = (t_{ins,0,n} \cdot k_{pos,exp,n} + \Delta t_n) \cdot k_{j,n} \quad (11)$$

where:

- $t_{ins,n}$  is the insulation time of the last layer  $n$ , in min;
- $t_{ins,0,n}$  is the basic insulation time of the last layer  $n$ , in min;
- $k_{pos,exp,n}$  is the position coefficient that takes into account the influence of layers preceding the last layer  $n$ ;
- $\Delta t_n$  is the correction time for the last layer  $n$  protected by fire protection system where relevant, in min;
- $k_{j,n}$  is the joint coefficient for the last layer  $n$  where relevant.

The SFM only applies to timber members exposed to standard fire exposure conditions. When design values for certain materials are unavailable, Annex G of prEN 1995-1-2:2022 provides guidelines for determining the design equations for new materials. This procedure of implementation of new materials into the SFM is based on the work of (Mäger et al., 2017). The development of design equations is based on numerical investigations and furnace testing. The procedure is specified in the respective paper and in the following subchapter explaining the development and use of effective thermal properties of fire protection materials.

### 2.2.3 Advanced design methods

The use of advanced calculation methods provides extensive means for the evaluation of thermal and structural performance of timber assemblies in fire. The calculations are undertaken using numerical models commonly based on finite element analyses. These methods are most likely to be employed in the case of complex structures with performance-based design, but they may also be particularly useful for evaluating the performance of new materials or those that cannot be tested. Advanced design methods may include separate calculation models for the determination of i) the development and distribution of the temperature within structural members; ii) the mechanical behaviour of the structure.

Advanced calculation models account for the fundamentals of heat transfer to predict the transient temperature distributions in building components, while implicitly accounting for the complex phenomena that materials undergo. Thus, a simple conductive heat transfer analysis may be conducted on solid anisotropic materials by using the 'effective' material properties (Buchanan & Östman, 2022). The thermal material properties specified in the Eurocodes have been calibrated using furnace test results. Thus, the given thermal properties are dependent on the whole global model of furnace testing and its possible errors (Zehfuß et al., 2020). These proposed values incorporate all forms of heat transfer occurring in a bulk solid. However, heat transfer in a solid is normally dominated by conduction. Thus, the effective properties are not physically measured values but rather characteristic values as they take into account the effects during fire exposure, which are not explicitly considered in the thermal analysis, e.g., increased heat transfer due to shrinkage cracks or degradation of materials. For example, in case of timber, the effective values consider the influence of char cracking.

Thermal simulations require a set of temperature-dependent material properties (thermal conductivity, specific heat, and density) that describe each material layer of a structure as input. If no input data exists, the first input may be obtained from material testing methods (e.g., TGA, TPS, and DSC). However, these methods are limited in their heating regime (not capable to follow ISO 834 curve), size of test samples etc. Therefore, the effective material properties as a function of temperature should be determined by calibration and validated on the basis of fire tests (prEN 1995-1-2:2022; Mäger et al., 2017). Today, for common materials such as gypsum plasterboards, the validated material properties for standard fire exposure conditions are provided (Schleifer, 2009; Östman et al., 2010; prEN 1995-1-2:2022).

## 2.3 Fire testing

When no design values exist, a full-scale fire test is required to verify the fire resistance of building structures. In most countries, the fire resistance of elements and assemblies is required to be evaluated in accordance with the standard temperature-time curve, as defined in ISO 834 and EN 1363-1. General requirements for fire resistance tests are given in EN 1363-1.

A fire resistance test represents a ventilation controlled, fully developed, post-flashover fire where the compartment shows a very limited oxygen concentration. Fire tests can be loaded or unloaded. Unloaded tests, EN 1364-1 for walls and EN 1364-2 for ceilings, are suitable to verify charring scenarios or separating function of the wall or floor assembly. Load-bearing capacity can then be calculated based on the remaining cross-section of the member and conservative design methods. Loaded full-scale fire tests can be used for verification of load-bearing capacity directly (e.g., EN 1365-1).

Full-scale fire testing is usually performed in a furnace with minimum dimensions 3 m x 3 m for walls and 3 m x 4 m for floors, depending on the applicable standard. In view of the initially protected timber structures, EN 13381-7:2019 specifies test methods for determining the contribution of fire protection systems to the fire resistance of structural timber members. The fire test methodology makes provision for the collection and presentation of data that can be used as direct input to the calculation of fire resistance of timber members in accordance with the procedures given in EN 1995-1-2.

For the purposes of research and product development, fire tests are also conducted in smaller-than-full-scale furnaces (Buchanan et al., 2022), such as medium scale fire test (also known as a model scale test) furnaces, which also follow the standard fire exposure conditions. The scale of a fire-exposed area of at least 1 m x 1 m allows assessment of the start time of charring according to EN 13381-7:2019 and charring rates according to EN 1995-1-2. Extensive research using a model scale furnace has been carried out by several authors to determine the fire protection and charring performance of timber under standard fire exposure conditions, e.g., work by (Tiso, 2018). Yet, this medium scale testing cannot generally be used to assess fall-off times of fire protection materials nor to determine the fire resistance of structural members (Buchanan & Östman, 2022). This is mainly due to the limitations of the size of test specimens, because solely the full-scale testing allows a proper assessment of materials' performance such as the thermal expansion, shrinkage, local damage, and deformation under load. Additionally, the severity of fire may be different in small and full-scale furnaces due to the variations in the heat transfer coefficients from the walls and hot gases of the furnace to the test specimens (Buchanan & Abu, 2017). Yet, it is noted that useful information could be obtained regarding thermal transmission. The effect on the different sizes of furnaces has been studied by (Sultan et al., 2003). It was demonstrated and explained that testing an assembly in an intermediate-scale furnace will provide a conservative performance compared to a full-scale furnace. As the furnace size increases, the convective heat to the specimen decreases and this may explain why the heat exposure in an intermediate-scale furnace is higher than in a full-scale furnace (Sultan et al., 2003).

In addition, worldwide, testing in small-scale to predict charring performance of timber by using the cone calorimeter device (ISO 5660-1) has become widely practiced. Owing to its ease of use and cost-effectiveness, additional applications of this device have been examined (Babrauskas, 2004). The difference of fire exposure conditions and heat transfer modes in the cone calorimeter and furnace have been investigated by (Ingason et al., 2007). An overview of previous research using the cone heater of a cone calorimeter (ISO 5660-1) to assess the charring of timber specimens is given in Chapter 4.

## 3 Timber structures with plaster systems

### 3.1 Building structures

The available forest resources and climatic conditions have resulted in a geographical distribution of various building techniques and materials used in buildings. In Northern and Central Europe, there is a long tradition of building with timber in combination with other readily available materials found in the region, e.g., earth, stones, wetland plants.

For centuries, in Scandinavia, UK and in Central Europe, one of the widespread building types was a timber-frame construction, where the frame cavities are filled with a walling material such as wattle and daub or earth brick masonry (Figure 3-1, left) (Graham, 2004). For wind proofing and thermal insulation, the external and internal walls or solely the frame panels were covered with plaster coats. These half-timbered constructions remained predominant for almost all kinds of buildings until the 19<sup>th</sup> century. In Estonia, for centuries, the buildings were mainly erected as a horizontal-log construction. The external walls are typically 120–160 mm thick without additional insulation. From the 20<sup>th</sup> century vertical double-plank walls as a novel framework was introduced that increased the mass construction of these houses in city landscapes (Eensalu et al., 2014). The walls of wooden planks are arranged in two rows with an overlap in order to improve airtightness. The exterior walls regardless of the wall structure are mainly clad with a wooden boarding (Figure 3-1, right) or plaster. Additionally, reed boards have been used in the past to increase the thermal insulation of the walls (Miljan et al., 2013). The inner walls were mainly finished with locally available surface finish materials such as clay and lime-based plasters that were sometimes painted or covered with wallpapers.



*Figure 3-1. Different type of timber constructions in Europe: Left – half-timbered buildings in Germany; Right – Wooden apartment buildings in Estonia.*

The typical floor construction consists of wooden joists filled with a combination of sand, clay, and natural fibres (that provided the sound insulation and fire safety during that time of building construction). The joists are covered with a boarding on top and they are left half or fully visible from below. However, most commonly the ceilings are covered with a lath and plasterwork (Tooming, National Heritage Board of Estonia; Fromme et al., 2021). In Germany, other techniques have been used where different type

of filling of panels between timber floor joists with light earth have been used such as earth reel floors or compacted earth floors (Claytec, 2017). The earth reel floors (floor system where the stakes made of unleft wood are wrapped with straw-clay and inserted between the floor joists) enabled to finish the ceilings directly with plaster (Volhard, 2016).

Plasters have been regarded a practical design solution throughout history since they not only improve the appearance of buildings, but also protect and maintain the building structures. Due to the low equilibrium moisture content by weight and capillary nature of earthen materials, the combination of wood and earth materials is effective; wood members in contact with earth are conserved by remaining dry, preventing insect and fungal growth (Volhard, 2016).

Historically, plasters were applied in thicker coats, and they required an underlying mechanical support to be firmly attached to timber surfaces. The historic plaster systems contained laths (thin strips of timber) that are nailed to log walls or timber joists/posts; then covered with plaster layers, Figure 3-2, left. The laths were spaced apart so that the plaster could fill the gaps between them. In the coastal regions, reed-based plaster carriers (Figure 3-2b, right) have been widely used (Alev, 2017; Graham, 2004; Köbbing et al., 2013; Ikonen et al., 2007). In Germany, the timber posts and beams of timber-framed buildings have been covered by plaster using the reed mat (Fromme et al., 2021; Claytec e.K.). Reed as a construction material has been widely used in Estonia to insulate the buildings (Kask, 2013).



*Figure 3-2. Examples of plaster support fixed on horizontal-log construction for the mechanical fixation of plaster: Left – Plaster applied on wooden lath and sticks. Right – Reed mat fixed to a log wall by using staples.*

In case of traditional (aerial) lime-based plasters, the application and hardening process is time-consuming as well as it may take years or decades for the plaster to gain its mechanical strength. Thus, as time progressed, gypsum or cement was added to minimise the setting time between layers, but plastering was a skilled craft and a time-consuming activity and so it was largely replaced using pre-manufactured plasterboard towards the middle of the 20th century.

Today, a revival of these traditional building materials such as timber and clay are acknowledged for achieving increased sustainability in buildings. Plasters are combined with other materials, such as clay-based boards or wooden fiberboards. Various wood frame assemblies using bio-based insulating materials and plaster-coated boards are used in practice, e.g., straw bale buildings. Owing to its weather resistance performance, lime-based plasters are extensively used in façade systems, e.g., ETICS (Küppers, 2020).

## 3.2 Traditional plaster systems

Plaster, along with its numerous composition and application variants, is one of humanity's oldest and most continuously used building materials. In simple terms, plaster may be described as a mixture of fine aggregates (sands), binder and water. Throughout history, clay and lime have been used as the main binders in plaster, depending on their regional availability (Minke, 2006; Barbero-Barrera et al., 2014).

Plasters are thin layers of mortar that are used to protect and decorate the walls and ceilings. In contrast to contemporary technology, which allows for the application of new (modern) plaster in a single layer, traditional plasters are usually applied in a layered system of two or more layers. The layered structure is probably the most prominent characteristic of traditional plasters. Its main underlying concept is to apply multiple coats of differentiated mortars with decreasing thickness towards the exterior. This old technology was deeply influenced by the characteristics of the binder (e.g., lime, which has low mechanical resistance, high porosity, and shrinkage (Nogueira et al., 2018).

Types of plaster can be distinguished according to their binder, function, and granularity. Each plaster coat has unique properties and functions in the whole plaster system. The first layer is made of a coarse mortar (i.e., undercoat plaster) with grain size of 0–4 mm. It has the mechanical resistance to adhere to the substrate, fill in any imperfections at the same time and provides a stable base for subsequent layers. For a smooth surface, the final coat is usually made with a fine mortar (grain size of 0–2 mm or 0–1 mm), applied in a thin layer (about 2–5 mm thick). Sometimes an intermediate coat is built between the first and finishing coats. Adhesion between the plaster coats is increased by giving the underlying coat a rough finish.

### 3.2.1 Clay plaster

Terms such as earth, clay, loam, and mud are often used while describing this respective plaster in literature or technical documents. In this thesis, the term clay is used as it refers to the binder in plaster.

Clay plasters are manufactured from clay, mineral additives, and fibre reinforcement, if necessary. Thus, a common clay plaster consists of clay, sand, and silt and (organic) fibres. Clay acts as a binding agent developing the adhesive and binding forces. Water activates the binding forces of clay. In contrast to other binding agents where hardening is a product of chemical curing, the cohesive effect of clay minerals derives primary from the physical attraction of the particles while the excess water added during the application process is lost (Röhlen et al., 2011). Aggregates such as sand and silt are relevant components for modifying the mechanical and physical properties of clay plaster. The performance of clay plasters with different clay/sand ratios has been assessed by (Emiroğlu et al., 2015).

Plant fibres are added to strengthen the inner cohesion of the mixture and to reduce the effect of drying shrinkage; various fibres are used in clay plaster: straw, cattail, flax, hemp, wood aggregates, etc (Laborel-Préneron 2016; Georgiev et al., 2013), see Figure 3-3. The fibre materials are described in (COST Action FP1303, 2017). The addition of fibres in plaster improves the workability and pliability of plaster. Fibres act as a reinforcement and help to resist stresses in the plaster caused by the movement in the substrate or tensile forces originating from thermal expansion or contraction (Röhlen et al., 2011). Studies by (Ashour et al., 2010) revealed that the thermal conductivity of the plaster material decreases with increasing fibre content and decreasing sand content.

Clay plaster can benefit from additional stabilisation ensured by a reinforcement fixed across the entire surface of the plaster such as a jute fabric (aka hessian mesh) or a flax mesh (Figure 3-4). Jute is a natural fibre obtained from the stems of the jute plant being one of the most common vegetable fibre materials. The description of jute fabric and performance in plaster has been studied by (Alcaraz et al., 2019). The reinforcement is embedded in the upper third of the entire plaster coat (Röhlen et al., 2011), whilst it is still wet and worked into the plaster, thereafter topcoat plaster is added after previous one is firm.

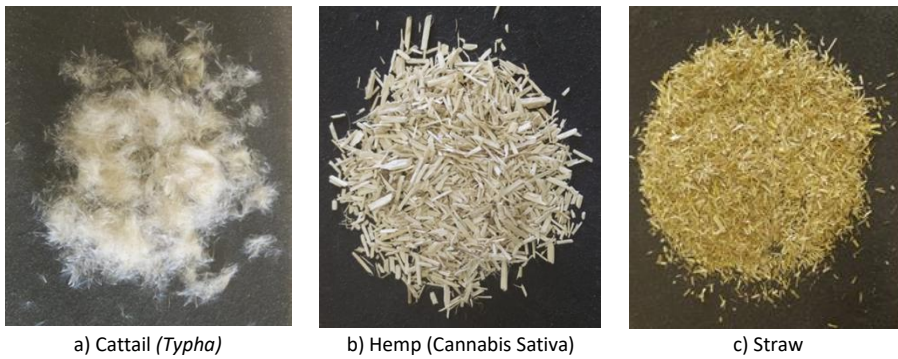


Figure 3-3. Different plant fibres used in clay plasters.



Figure 3-4. Application of reinforcement mesh into the clay plaster system: Left – Jute mesh; Right – Flax mesh embedded in the plaster.

Although there is currently no product standard for clay plaster at the European level, there has been significant work accomplished in Germany in developing product standards for clay-based products (Schroeder, 2018). In 2013, the first product standard DIN 18947 for clay plaster was published. It is mostly based on the standards of conventional plasters and is used for plastering walls and ceilings in interior and weatherproof external applications. From 2016, clay plaster is incorporated into the superior standards of application of (DIN 18550-2:2018), where it is implemented alongside other conventional plasters. Further, clay plaster is also described in the European design and application standard of interior plastering (EN 13914-2:2016).

DIN 18947 determines the terms, requirements, and test methods for clay plaster. According to this standard, clay plasters are divided with respect to their bulk density (e.g., plasters in a density range of 1610–1800 kg/m<sup>3</sup> are categorised in a density class 1.8). The manufacturers need to classify the strength class (SI and SII) of the plaster (minimum values are given for tensile, compressive, and adhesive strength; Chart 2 in

DIN 18947). The linear shrinkage of drying should be no more than 2%, for fibre reinforced plaster 3%. Shrinkage cracks occur due to the evaporation of the water used to prepare the mixture. If water evaporates, the interlamellar distance is reduced, since the lamellas arrange themselves in a parallel pattern due to the forces of electrical attraction (Minke, 2006). The colour of clay is not an indication of its properties (Röhlen et al., 2011).

Several studies have been carried out to determine the moisture content (MC) of clay plasters, addressing their different types and amounts of fibres in the plaster mix. Research by (Ashour et al., 2010) revealed that the moisture content increases with the wheat straw content in the plaster; average MC values were 2.78%, 1.3%, and 0.61% for fibres 75%, 50%, and 25%, respectively (plaster densities about 1120, 1420 and 1700 kg/m<sup>3</sup>, respectively). The average MC of plaster without fibre (density of 1804 kg/m<sup>3</sup>) was about 1.11%. The dry density decreases with increasing fibre content. A further study by (Ashour et al., 2011) concluded that the relative humidity (RH) has greater effect on the change of moisture content in plaster than temperature. Test results show that the equilibrium moisture content (EMC) of plasters increases with increasing relative humidity and decreases with rising temperature; the EMC of plaster without any fibres was determined in the range of 0.6–1.7% (1.7% refers to RH 90%). At around room temperature and RH 50%, the EMC was roughly 1%. Another research by (Navarro et al., 2015) determined the EMC at different RH levels for clay plasters incorporating a single fibre size, for all plasters the EMC was not higher than 1.8% at RH 80%, whereas at around RH 50%, the EMC was approximately 1%. A study from Estonia (Ruus, 2020) has also determined the moisture content of two clay plasters (densities ~1750 kg/m<sup>3</sup>). The EMC was determined less than 1% in case of both plasters in case of RH 40% and RH 60%.

### 3.2.2 Lime plaster

Lime as a building material has been used in construction from ancient times. Until the early 19th century, the main binder in mortars was lime. In the course of time as scientific knowledge and manufacturing processes improved, traditional limes began to be replaced by higher performance artificial hydraulic limes, and in 20<sup>th</sup> century the Portland cement (Nogueira et al., 2018). The advancements along with new additives enabled significantly faster setting times and improved the mechanical and insulation performance of plasters (Gulbe et al., 2017; Barbero-Barrera et al., 2014).

In the past, the lime mortar comprised a mixture of fine aggregates (sands), binder and water, and for rendering purposes vegetable fibers or animal hair was added. In modern times, additives such as glass fibers are used to improve the tensile strength of the paste, which increases the cohesion among mortars' components and reduces the shrinkage during setting (Nogueira et al., 2018). A review of strengths and weaknesses of traditional lime-based plasters has been presented by (Nogueira et al., 2018).

Lime refers to a product derived from limestone (calcium carbonate) by an industrial process known as calcination. Limestone is a naturally occurring sedimentary rock, which main constituent is calcite, CaCO<sub>3</sub> but it can also contain dolomite, MgCa(CO<sub>3</sub>)<sub>2</sub> and varying amounts of other mineral and impurities. During the calcination process (at around 800–900°C), calcium oxide (quicklime) and carbon dioxide are produced, which is ground to powder. When adding water, it becomes calcium hydroxide (hydrated lime). (Despotou et al., 2014) has presented a literature study about different types of lime plasters from the past. Generally, lime produced from limestone with less than 5% of magnesium carbonate is classified as high-calcium lime (HL), while limestone with a magnesium carbonate content above 20% produces dolomitic lime (DL). These differences

in aerial limes are made in the standard of building lime EN 459-1. The differences between the building limes and their performance as mortar has been carried out by (Garijo et al., 2020). This current thesis focuses on aerial lime mortars as the primary type of lime plaster due to their traditional use in Estonia and elsewhere until today.

Unlike gypsum plaster, which goes through a chemical reaction to harden, aerial lime plaster, largely composed by CaO, goes through a carbonisation process in the presence of air, which results in the plaster absorbing carbon dioxide (Lawrence, 2006). As a result, it takes a long time for the plaster to harden completely. The carbonation reaction in mortars is a rather complicated process. It involves CO<sub>2</sub> diffusing through the pores and dissolving in the capillary pore water, where it reacts with calcium hydroxide to form calcium carbonate crystals (CaCO<sub>3</sub>). This is called the hardening mechanism. The carbonation is the fundamental process for the hardening of lime-based plasters that is deeply studied by (Balén, 2005). Various factors have a direct impact on the carbonation rate; in the recent decades, the research focus is on the carbonation speed which impacts the strength development and the factors that influence this rate. There are several factors such as are the mixture composition, moisture content and permeability of the mortar as well as surrounding environment (temperature, relative humidity, CO<sub>2</sub> concentration) (Oliveira et al., 2017). (Elert et al., 2002) has shown that the carbonation reaction proceeds from the outside inward; thus, the thickness of the mortar and its permeability significantly influence the rate of carbonation. It was cited that the diffusion of carbon dioxide to the reaction site will be a limiting factor and carbonation time will become impracticably long if this distance is more than 25mm for porous mortars and more than 5mm for dense, impermeable mortars.

Various researchers found that the carbonation process may continue for many years. Rapid drying, on the other hand, retarded the process and can result in poor ultimate strength. It is recommended to protect the finished work by encouraging good air circulation (Elert et al., 2002). Furthermore, it may take weeks to pass for the first plaster layer to take up enough before the second layer could be applied. This is the case for each layer that is applied to construct the whole plaster system. Plasters whose thickness is limited to few centimetres can be considered as having reached their final carbonation levels, i.e., 80% to 92% within 1 to 2 years (Despotou et al., 2014). A study by (Garijo et al., 2020) assessed the evaluation of the carbonization depth in natural hydraulic and aerial lime mortars and observed that the carbonation process only begins once excess pore blocking water is evaporated, thus little carbonation can occur within the first weeks. It was concluded that even small variations in the binder type, the dosage, the water content, or the curing conditions can affect the porosity of the material and therefore, the CO<sub>2</sub> access and carbonation process (Garijo et al., 2020). An experimental study on aerial lime mortars by (Oliveira et al., 2017) concluded that both drying, and carbonation processes seem to have influence on the development of compressive strength; highlighting that the drying process is probably responsible for a significant part of the initial gain of strength.

(Nogueira et al., 2018) presents a review of the main aspects that govern the design and behavior of traditional lime-based plasters and renders. It also provides a critical appraisal of the strengths and weaknesses shown by the traditional lime-based mortars technology. In the paper, (Nogueira et al., 2018) have compiled a list of published research work on different historic lime-based plasters. In the case of lime plaster, the best reported behavior of the multilayer system is primarily due to shrinkage, which induces lower tensile stress because the coats are thinner; carbonation is faster for thinner coats;

and cracking is limited to the thickness of each coat and does not cross the entire plaster (Nogueira et al., 2018). The application of the first plaster coat is shown in Figure 3-5a.

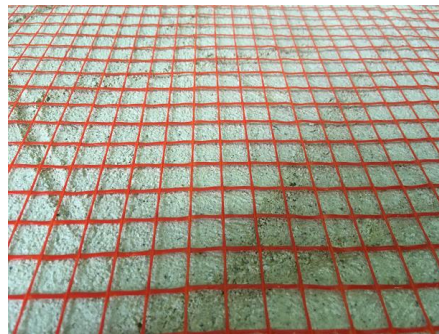
Nowadays, cement is frequently used in lime-based plasters to enhance their mechanical properties. Lime-cement plasters are resistant to moisture and therefore also suitable in damp and wet rooms. They are preferable as they are stronger than pure lime plasters and develop their strength properties in a controlled manner. The addition of reinforcement meshes also increase the tensile strength of the plaster, Figure 3-5b.

The moisture properties of (lime) mortar have been discussed in a document by (Straube, 2000). The sorption isotherm, which is unique to each material, describes the relationship between the relative humidity and moisture content; for mortar at RH 60%, the moisture content is shown to be not higher than 2%. In terms of vapour permeability, the mixtures of pure cement and sand are relatively resistant, but the mixtures of pure lime and sand were the most permeable. Studies have shown that clay plasters are generally more permeable than lime plasters (Minke, 2006).

The performance of lime-based plasters is specified in design standard EN 998-1 that is applicable to factory made rendering/plastering mortar based on inorganic binders for external (rendering) and internal (plastering) use on walls, ceilings, columns, and partitions. Requirement categories for the compressive strength (CS I, CS II, CS III, CS IV), the capillary water absorption and the thermal conductivity are given to be determined for lime plasters. The CS I refer to the lowest strength of plaster which is in range of 0.4–2.5 N/mm<sup>2</sup> measured after 28 days. In the standard it is noted that the plastering mortars do not attain their final characteristics until properly hardened after application. The functions performed by the plaster depend on the properties of the type of materials used, on the thickness of the coats and the type of application.



a) Application of the first layer of lime plaster using a trowel.



b) Glass fibre mesh on a lime plaster layer before the subsequent layer is added.

*Figure 3-5. Application of lime plaster system.*

### **3.2.3 Plaster carriers and substrates**

In practice, the mechanical resistance of the plasters and their compatibility with the substrate is important to ensure their performance. Consequently, plaster usually requires a mechanical support when applied directly to wooden surfaces (i.e., plaster carrier that provides a mechanical fastening system for plaster to timber). Various kinds of plaster carriers have been used throughout history, and some of them are still in use today (e.g., in renovations) because they fit well with the material characteristics of traditional type of plasters.

In the twentieth century, wooden laths were extensively used in historic timber structures, until metal and gypsum laths gained popularity in the 1940s. The wooden lath is constructed from spaced-apart, thin, narrow strips of wood. When wet plaster is applied, it pushes through the gaps and develops a key with the substrate and the laths, holding it in place. Wooden lath was nailed directly to the structural members. Later, metal wire meshes were commonly used as plaster carriers. The metal lath included more gaps than wood lath and increased the number of keys, thus providing more effective bond to hold the plaster compared to the wooden lath. Their significant benefits over sawn wood lath include incombustibility, ease of application, stability, unit uniformity, availability.

The reed-based materials are another extensively used material that works well for plaster substrates (Wegerer, 2011; Asdrubali et al., 2016; Richter et al., 2021). The Common Reed (*Phragmites australis*) is one of the most widely found plant species occurring in European land-water ecotones (Ikonen et al., 2007). From the prehistoric times, it has been used widely as a roofing and insulating material in the Baltic Sea area. Reed has long been used in Estonia for thatching and insulation purposes, and this tradition has survived to this day, foremost in old buildings (Kask, 2013). Also, in Germany, various reed products are manufactured for buildings and used in restoration projects (e.g., HISS REET GmbH, Claytec e. K.).

For plastering, there are primarily two kinds of reed-based materials: a reed mat and a reed board. A reed mat is a thin mat (< 10 mm in thickness) applied directly on a wooden surface. The distances of reed stems in a reed mat suit well for the coarse grain of plaster to achieve a good mechanical bond. Reed boards, on the other hand, comprise reed stems that are squeezed against each other and fixed together with a wire to form thick lightweight construction panels. The board thickness usually varies from 25 mm to 50 mm. Plaster is applied directly on the boards, being squeezed onto the panel that ensures its mechanical key.

Nowadays, in contemporary buildings, plasters are used as a finishing layer on various construction boards, such as wooden fiberboards or clay boards (Küppers, 2020). In the case of boards, no plaster carrier is used, but a reinforcement mesh is often applied to the joints and gaps of the boards before plastering. Plaster is applied directly on the boards with a total thickness ranging normally between 3–10 mm, as compared to the plaster thicknesses in range of 15–40 mm found in old buildings.

#### **3.2.4 Plaster application**

The design considerations and essential principles for internal plastering systems and application of plastering systems is given in (EN 13914-2, 2016). This standard also refers to the relevance of the instructions recommended by the product manufacturers which must be followed with care. For the application of plaster to any substrate, water is added to the dry mix of plaster to activate its binding strength and to achieve workability. The amount of water is usually specified by the producer, where the water content is restricted to fall between the liquid and the plastic limits of the binder. There are different types of water in plaster such as free water, chemically bound water, absorbed and capillary water. Except the structural water that is released between 400–900°C, other types of water are released by 105°C. The period during which wet plaster reaches its equilibrium moisture content is called the 'drying period'. Product specific guidance on the preparation and design applications of plaster systems with their use of various types of plaster carriers are given in respective standards and should be carefully followed to guarantee the quality of the plasterwork.

## 4 Literature review of plasters in fire

The materials and testing methods relevant to this thesis were the focus of a literature review. Previous studies on the material properties of plasters at elevated temperatures, cone heater tests, and fire resistance studies conducted at different scales with plaster and timber structures is presented.

Fire affects materials in a variety of ways, altering their physical, mechanical, and chemical properties. As wood is a porous material, heat transfer occurs via conduction, convection, and radiation. When exposed to high heat fluxes, wood undergoes pyrolysis, a process in which its components decompose to volatiles, tar, and carbonaceous char. Gas-phase oxidation of volatiles and tar creates flame combustion, while solid-phase oxidation of char produces glowing or smouldering combustion (Buchanan & Östman, 2022). The thermal composition of timber as a function of temperature is explained by (Bartlett et al., 2019). Overall, there is strong agreement that temperatures around 300°C represent the onset of rapid pyrolysis and char formation, which is also considered as the start time of charring in EN 1995-1-2:2004 and in furnace tests (EN 13381-7:2019).

Charring is a highly important factor for determining the fire resistance of structural timber elements exposed to fire, since it influences the load-bearing capacity. The chemical and physical complexity of wood influences its behaviour at high temperatures, including material properties such as density, moisture content, chemical composition, grain orientation, permeability, scale effect, char contraction, and char oxidation. Additionally, environmental elements like oxygen content, thermal exposure, and opening factor have an impact on the charring of wood. Today, the charring of wood and its performance under a wide range of experimental conditions has been assessed and a good agreement is found in the fire science community (Bartlett et al., 2019).

According to the current design standard EN 1995-1-2, a basic charring rate value of 0.65 mm/min is commonly used for solid timber elements made of softwood. A review of studies by (Babrauskas, 2004) concludes that a charring rate of 0.5–0.8 mm/min has typically been found for solid timber structures in fire resistance furnaces. This variance is attributed to random variations (Babrauskas, 2004); in addition, a time-period effect has been reported, which links longer fire exposures to slower charring rates. (Friquin, 2010) assessed the charring rates of heavy timber structures for fire safety design. A review of factors affecting the burning behaviour of wood has been investigated by (Bartlett et al., 2019). A recent work by (Fahrni et al., 2021) evaluated the relationship between the charring rate of solid timber panels and fire duration (30 minutes up to 120 minutes) in a model scale furnace; the mean charring rates were obtained in the range of 0.67–0.60 mm/min.

Testing in small-scale using the cone heater of a cone calorimeter (ISO 5660-1), has been widely practiced in the research community. Several studies have been performed to determine the charring rate of various wood products as well as to estimate the charring rate usually obtained from the furnace tests (White, 1971; Mikkola, 1991; Tsantaridis et al., 1998; Crewe et al., 2010). Previous studies have proposed various expressions for the charring rate that represent correlations between the charring rate and the exposed heat flux, charring time, and density of wood (Babrauskas, 2004). A study by (Tsantaridis et al., 1998) concluded that the charring depths obtained in cone calorimeter tests at constant heat flux level of 50 kW/m<sup>2</sup> were similar to those obtained in furnace tests during 30–40 minutes. In addition, a relationship between the char depths at a particular time was provided for the cone and furnace tests. Based on the

test data presented in this paper (Tsantaridis et al., 1998; Silcock et al., 2001) introduced a concept of local fire intensity to link large scale and small-scale test environments in terms of the estimation and prediction of char formation. It was demonstrated that the char depth profiles resulting from the exposure of wood in a furnace can be equated to the exposure of similar wood specimens set at a constant heat flux level of 50 kW/m<sup>2</sup>. A recent study by (Xu et al., 2015) used three different heat flux levels of 25, 50 and 75 kW/m<sup>2</sup> to investigate the charring of timber specimens. It was found that the charring rate increased with heat flux and decreased with fire exposure time. When the fire exposure time exceeded 30 minutes, the rate of charring tended to remain almost constant. An average charring rate of 0.8 mm/min was obtained for Scots pine (430 kg/m<sup>3</sup>, at MC 12%), while exposed to constant heat flux of 50 kW/m<sup>2</sup> for 30–60 minutes.

Despite the studies with timber specimens using the cone calorimeter device, limited research has been done on the fire protection materials for timber. Studies by (Tsantaridis et al., 1999, 1998) tested gypsum plasterboards of type A and F applied on a timber stud (45 mm x 100 mm) with different depths of 50 mm (maximum depth according to ISO 5660-1) and 145 mm (to simulate the size in furnace tests). For the two wood stud depths, all temperature curves for unprotected and protected wood studs had almost identical shapes. The time it took to reach 300°C behind gypsum plasterboards was almost the same for both depths of wood studs. It was concluded that the best prediction of start time of charring is obtained by using the board thickness as the prediction parameter. The charring rate of wood protected by gypsum plasterboard was said to be best predicted using the area weight of the boards, however for gypsum plasterboards commonly used as wall and ceiling linings, the prediction is reasonably accurate using board thickness only. The chosen heat flux of 50 kW/m<sup>2</sup> in relation to the heat flux level occurring in furnace is explained in the paper (Tsantaridis et al., 1998). The study showed that the charring depths clearly demonstrated the relationship between fire exposure and time. Without boards, the charring depth exhibits a sharper slope with exposure time to the furnace than the cone calorimeter, with identical depths at around 32 minutes. The charring depths of type A boards were equal until the boards fail in the furnace tests after approximately 25 minutes. In case of type F boards, the charring depths significantly decreased after around 27 minutes and onwards. This is directly related to the continued increase in heat flux with time in furnace, reaching as high as 125 kW/m<sup>2</sup> after around 45–60 minutes. Another study with gypsum plasterboards type F tested on CLT elements (5 layers, 45 mm x 95 mm, depth of 95 mm) and massive timber (45 mm x 100 mm, depth of 135 mm) has been carried out by (Tiso et al., 2015). The sides of the timber elements were protected by insulation, similar set-up as used in (Tsantaridis et al., 1998). In this work, the heat flux level was adjusted to achieve a better fit with the heat flux levels measured in furnace (Tsantaridis & Östman, 1998). Thus, in-between 20–30 minutes, the heat flux level was raised gradually in three steps from 50–75 kW/m<sup>2</sup>. The test results demonstrated good repeatability and the start time of charring determined around 28 min agreed well with the design value given in EN 1995-1-2:2004 for 15 mm thick gypsum plasterboard. The charring depths obtained from the model-scale furnace tests agreed well with EN 1995-1-2:2004 for an infinitely wide element. The cone test results on the charring obtained a better agreement with the infinitely wide element than with the non-infinitely wide element, especially at around 60 minutes of testing. The results indicated that the increase in the heat flux level was justified, as it has been highlighted that the heat flux levels in cone testing are not

capable of producing fire exposure levels in furnace for prolonged test durations (COST Action FP1303, 2017). The thermal exposure and measured heat flux in relation with time has been investigated by (Tsantaridis et al., 1998; Babrauskas, 2004) and (Sultan et al., 2003).

Whilst the performance of plasterboards is widely investigated, limited studies with plaster exist using modern fire testing methods. One of the few studies has been carried out within a research project about the fire protection in straw bale buildings at TU Braunschweig by (Wachtling et al., 2013). This study tested various types of clay plasters under cone heater exposed to heat flux of 40 kW/m<sup>2</sup> until the temperature criterion of 270°C was reached on timber. An estimation based on cone tests was made that a rather thick clay plaster (> 60mm) is needed if the K<sub>2</sub>60 criteria is to be achieved in furnace tests. However, it was recognised that the use of a specific additive in plaster increases its protection ability. Intermediate scale furnace tests (DIN 4102-8) were performed. A test in floor position with a 10 mm clay plaster (without fibres) and a 45 mm clay board applied on a chipboard was successful to demonstrate that the temperature rise behind plaster did not reach the limit temperature of 270°C on the chipboard in 60 minutes. Another test with a 60 mm lightweight plaster applied on a straw panel was also carried out that succeeded to demonstrate lower temperature rise than 200°C on straw in 60 minutes. An earlier study by (Niemann, 2010) examined different types of clay and lime plasters on straw panels using the cone heater and a small-scale furnace under standard fire, which resulted in a conclusion that a relatively thick plaster coat (55 mm) is required to receive higher fire resistance ratings, e.g., K<sub>2</sub>60.

Another recent research work has been conducted by (Chorlton et al., 2020) using the cone calorimeter to evaluate the fire protection provided by historic encapsulation materials such as lime-based plasters and steel-plates. The materials were attached to plywood and subjected to 50 kW/m<sup>2</sup>. The test period was limited to 5 minutes, which was deemed sufficient to detect no burning but some smoke. After testing, the plaster was easily removed from the plywood. It was concluded that plaster might theoretically increase the fire resistance of timber buildings but is not reliable in the event of a fire due to their limited ability to stay attached to the underlying structure. Another study by (Dalmais et al., 2019) has been carried out within a European research project ISOBIO that aimed to develop a multi-layered wall solution made of bio-based materials. In one of the furnace tests, clay plaster was also tested, and it was concluded that the fire resistance of wall assemblies appears to be directly related to the integrity of the exposed layer (plaster) and the thermo-mechanical stability of all the constitutive layers. It was shown that the plaster has a significant impact in fire behaviour of the wall assembly.

The relevance of the condition and key of the plaster on its substrate has been highlighted in a fire technical guideline of upgrading existing timber floors by (BRE, 1988). Additionally, it indicates that greater plaster thickness may not provide enhanced fire protection as the added weight may fail earlier than thinner plaster. The attachment of the plaster to the structures has also been noted as an important factor by (Ryan, 1962). This specific research examined the effects of mix, aggregate, and conditioning of gypsum plaster on the fire resistance, in terms of limiting temperature rise behind the plaster. Test results showed that in case of different mix ratio of gypsum to aggregate has little, if any, influence on the temperature rise of 250°C. Additional tests with perlite and vermiculite aggregate plasters exhibited significantly longer temperature-rise times than did the sanded gypsum plasters mainly due to the lower thermal conductivity values. In view of historic building structures, an article by (Jackman, 2009), who was a

lead author of the British standard for fire tests on building materials and a major contributor to the EN and ISO equivalent standards, refers to limited published data on the fire resistance of existing lath and lime plaster ceilings. However, it was recognised that the post-war building studies have revealed wide variations in performance of such constructions when tested under the standard furnace conditions. Factors such as the aging of lime plaster has a major influence on its fire resistance performance as the maximum strength is achieved when fully carbonated that may take months or even years (Jackman, 2009). It has been noted that the evolution of the mechanical properties of lime mortars is linked with depth of carbonation (Garijo et al., 2020).

The material-specific performance of lime plasters has been studied by (Pachta et al., 2018) that additionally cite other research indicating that compressive strength seems to be one of the most significant representative values for the behaviour of mortars (plasters) at elevated temperatures. (Pachta et al., 2018) conducted experiments to study the physico-mechanical performance of lime-based plasters before and after being subjected to temperatures of up to 1000°C. The results showed that the selected mortars maintained their structure, physical and mechanical properties up to 800°C, while at 1000°C their volume and mass was still preserved but exhibiting reduced strength; above 400°C they started to gradually lose their elasticity and should be envisaged. This research used a specific heating program and relatively small test specimens in size; thus, no direct parallel could be drawn to their real performance in case of standard fire exposure conditions. The study highlighted that the investigation of materials' performance should be carried out in relation to their mineralogical alterations that take place at different temperatures. A further study (Pachta et al., 2021) examined the lime-cement plaster and a comparison was made in view of the physico-mechanical performance: lime-based mortars had low initial strength (1–4 MPa), yet they performed more steadily and efficiently at higher temperatures, making them more resistant in the early stages of fire. At 800–1000°C, cement-based mortars performed better. It was concluded that the binding system influences the performance of mortars at high temperatures. Adding lime to traditional or contemporary mortar systems seems to improve their performance at high temperatures. Another study on the strength of sand cement plaster has determined that the aggregate grain size distribution in the plaster affects the flexural strength, yet the degree of influence from the temperature was found to be the same over 450°C (Ünal et al., 2017). It was observed that the strength of the plaster fell in large quantities as the temperatures increased. The colour of the plaster samples varied depending on the degree of temperature exposure.

Plasters are heterogeneous materials, thus the effects of high temperatures on their paste and aggregates depend on their constituents and thermal stresses (e.g., expansion of aggregates, shrinkage deformations of the paste). Temperature-dependent expansion coefficients of minerals are well-documented. At 570°C, for instance, quartz undergoes a polymorphic transition; at 800°C, limestone and dolomite transform into CaO and MgO, respectively. Therefore, plasters (e.g., sand cement plasters) are damaged by these transformations (Ünal et al., 2017). Thermal expansion coefficients of plaster made from heavy loam (clay) are in the range of 0.0043–0.0052 mm/mK, for a sandy mud mortar has a value of 0.005 mm/mK, and strong cement mortar 0.01 mm/mK, the same as a concrete (Minke, 2006).

Numerous studies have been conducted on concrete and cement-based plasters, wherein the temperature-dependent changes occurring in a material are presented. (Pachta et al., 2018) describes that around 100–200°C the free moisture of the materials

evaporates, while above 250°C the dehydration or loss of the bonded water begins. Above 300°C the silicate hydrates of the cement paste decompose and above 500°C portlandite, influencing the stability of the matrix. In the case of cement-based mortars, the residual strength is maintained for temperatures up to 300°C, while between 300°C and 500°C it is decreased around 15–40%. In the case of lime-based mortars, compressive strength is significantly increased up to 600°C; it is reduced at 800°C and minimized at 1000°C.

The effect of elevated temperatures upon the properties of clay plaster has hardly been examined. Numerous studies exist on clay, sand, and soil (Han et al., 2017; Alrtimi et al., 2016) that provide rather specific material data, but not their performance in a standard fire test. During the heating process, there is a series of changes in particle size distribution, mass loss, mineralogy, and permeability (Zihms et al., 2013). Research about clay at elevated temperatures by (Han et al., 2017) indicate that when temperature reaches more than 100°C, free and absorbed water dissipates and pores are filled with air. The porosity increases while the temperature continues to rise to 400°C. In the temperature range of 400–600°C, the original minerals of clay transform, and the chemically bound water is lost. Above 400°C, the properties of clay are close to rock. The inner structure recombines due to the dehydration of kaolinite in clay and phase transformation of quartz. Changes in kaolinite are considered the primary cause of the variation of physical and mechanical properties of clay under elevated temperatures (Sun, Zhang, & Qian, 2016; Sun, Zhang, Zhang, et al., 2016). The dehydration of kaolinite improves the bond between particles. Around 900°C the clay particles start to fuse and form ceramic structures. The size, shape and orientation of pores influence the properties of thermal conductivity of earthen plasters. A study by (Randazzo et al., 2016) investigated the thermal conductivity of clay plasters, indicating that pores act as heat barriers thus affecting thermal conductivity. Therefore, the thermal conductivity of dry rock-based minerals is a function of mineralogical composition (i.e., thermal conductivities of the individual components, and several textural features such as the degree of cementation, porosity, grain shape and size). Another work indicated that the differences in mineralogy, sand, silt, and clay fractions could be primary reasons that govern the specific heat (Abu-Hamdeh, 2014). These aspects have also been highlighted in concrete studies at elevated temperatures, e.g., the specific heat property is sensitive to various physical and chemical transformations that take place in concrete (Fletcher et al., 2007).

The materials' mineralogical alterations are directly linked to its thermal properties at high temperatures. For accurate predictions of temperature profiles in structures, it is necessary to understand how the thermal properties of materials change with temperature. Today, the required temperature-dependent properties (thermal conductivity, specific heat, and density) for some materials like wood and gypsum plasterboards are given in the FSITB and prEN 1995-1-2:2022. One of the only studies known to the author carried out by (Küppers, 2020) has determined these properties for a specific light-weight lime plaster, mineral clay plaster and clay boards. However, the fire tests under standard fire exposure conditions were conducted only with thick plaster coats (50–60 mm), applied on straw bale panels.

In order to determine these material properties, several test methods are available and proposed to be used (Mäger et al., 2017). TGA is frequently used for the compositional analysis of materials, since it measures the weight loss resulting from the thermal decomposition (Despotou et al., 2014). Temperature-dependent mass loss may be evaluated using TGA (Mäger et al., 2017; Küppers, 2020). A TPS method is used to

determine thermal diffusivity and thermal conductivity (also, indirectly specific heat (Jansson, 2004, (Sjöström et al., 2012; Berge et al., 2013; Küppers et al., 2018). Previous research using TPS test method has proven to show an encouraging compliance with the temperature measurements obtained from fire tests (Adl-Zarrabi et al., 2004) it was concluded that the measured effect of temperature on the thermal properties on wood were approximately the same as shown in literature. A further study by (Adl-Zarrabi et al., 2006) used the TPS method to determine the thermal properties for concrete, which has proven to show an encouraging compliance with the values found in literature and the temperature measurements obtained from fire tests. However, it has also been argued that large-scale fire testing does not give insight in the processes of moisture and vapour movement that can have a large influence on the materials' properties (van der Heijden et al., 2011). Thus, in case of real physical properties are in interest, more specific testing methods should be used.

As today there is limited data on temperature-dependent thermal properties available on the plasters, remarkable number of research on concrete has been carried out demonstrating a wide variation of materials' thermal properties, which depend on the recipe and type of constituents in concrete as well as its quality, age, moisture content, etc (Jansson, 2013). Traditional type of heavy weight plaster has somewhat similarities to concrete as they are composite materials consisting of various aggregates, additives, and binder, that when mixed with water, undergo a hardening process after its application. Most recently, a paper by (Zehfuß et al., 2020) discusses the impact of thermal material properties of concrete on the heat transfer, highlighting that the most influential property impacting the temperature distribution in concrete structural elements is thermal conductivity. Furthermore, it comments the simplification of material properties given in EN1992-1-2, including the assumption made that the thermal properties are independent of the type of aggregates.

In addition to material testing, numerous lime-based plasters have been evaluated as a finishing material for straw bale structures in furnaces of varying sizes during the last decades (Džidić, 2017). A study by (Wall et al., 2012) examined the fire resistance of a prefabricated straw bale panel in a full-scale furnace under standard fire exposure conditions; the panel was sprayed with three coats of formulated lime render. The lime render (thickness of 30–35 mm) stayed in place for approximately 90 minutes before it fell off and exposed straw directly to fire. Furnace tests by (Wachtling et al., 2013) did not show any fall-off of plaster. As reported, plaster systems may stay intact for long time if properly applied and attached on a suitable substrate. Based on the full-scale test results of the straw bale structures; the plasters seem to have a great potential to contribute as a protection material. However, the plaster systems could exhibit cracking or other types of failure modes associated with their mechanical fastening and the type of substrate its applied to, that are not well understood. In case of concrete structures, the spalling behaviour has been identified as a complex phenomenon, wherein the scale effect of a test specimen and different boundary conditions in case of fire has still not yet been quantified but are found highly relevant to understand the influence of different boundary conditions and scaling effects to the spalling behaviour (Jansson, 2013). Similar aspects of material performance (e.g., cracking or layer detachment) and specimen size could also have an influence on the behaviour of plasters in fire due to the moisture/vapour movement and built-up of thermal stresses in the composite material.

## 5 Experimental work

The experimental study was carried out in three parts:

- i) Material tests (TGA, TPS);
- ii) Cone heater tests at high heat flux levels;
- iii) Furnace tests under standard fire exposure conditions.

This research work and main results have been published in the peer-review journal papers (Liblik et al., 2019, 2020, 2022, 2023). An overview of the experimental study is presented below.

### 5.1 Test materials

The materials and their set-up as test specimens were selected and prepared according to their application in historic timber buildings, e.g., plaster system applied directly on solid wall and floor structures. The plasters were not obtained from a historic building structure *in situ*, but they were chosen in terms of their traditional composition, their recommended use in old buildings (declared by professionals) and their applicability in today's practice, i.e., approved by building authorities. This was considered as a justification for the selection and source of materials, as the test results would have a high practical value in building projects.

The selection of plasters was mainly based on their availability and use at the Estonian market. In the case of clay plaster, one of the German producers was also selected since their plasters have been tested in compliance with DIN 19847. In this research, only traditional type of plasters was of interest as they represent authentic/similar plaster compositions in existing buildings, i.e., plasters are produced and deemed suitable for use in historic structures; they are composed of only natural materials and applied in layers to build up thicker plaster systems, like in the past. These types of plasters are also favoured in renovation and conservation projects.

The selected types of plasters and their physical properties declared by manufacturers are presented for clay and lime-based plasters in Table 5-1 and Table 5-2, respectively. Each type of plaster is characterized by their producer (which refers to the two-letter combination in the plasters' reference) and their grain size distribution (which refers to the number combination in the plasters' reference). The number combination of 04 denotes an undercoat (basecoat) plaster, as the 02 and 01 refer to the topcoat plasters. Abbreviation NF refers to no fibres in the plaster mix, i.e., purely mineral plaster.

Material physical properties are declared by the manufacturers in accordance with a relevant product standard: DIN 19847 is used for clay plaster and EN 998-1 applies for lime-based plasters. For some plasters, not all material properties have been declared, therefore they are marked as not available (n/a). Product standard DIN 19847 does not apply to plasters with a thickness of less than 3 mm (i.e., the topcoat plasters). In case of clay plasters, the declared physical properties of tensile and compressive strength refer to material class SII according to DIN 19847. The composition of the dry-mix plasters was determined by XRD analysis (Appendix 1).

The range of density and thickness of plaster systems were mainly selected by their use in old buildings. Density of clay plasters was mainly declared in a gross density class 1.8 (DIN 19847) that corresponds to a density range of 1610–1800 kg/m<sup>3</sup>. The range of thicknesses was prepared from 10 mm up to 44 mm (as often encountered in buildings), measured from the substrate. The selected clay plasters consist of three main components:

clay (5–8% of total dry plaster volume), sand and organic fibres such as barley straw, hemp, and cattail.

Table 5-1. Type of clay plasters selected for this research.

Plaster reference	Type of fibre in plaster	Grain size	Dry bulk density	Tensile strength	Compressive strength	Thermal conductivity	Country of origin
			[kg/m <sup>3</sup> ]	[N/mm]		[W/mK]	
ClaySU04	hemp	0-4	1610-1800	0.7	2.0	0.91	Estonia
ClayCT04	straw*	0-4	1610-1800	0.7	1.5	0.91	Germany
ClaySF04	cattail	0-4	~1700	n/a	n/a	n/a	Estonia
ClaySU02	cattail	0-2	1610-1800	n/a	n/a	n/a	Estonia
ClayCT02	straw**	0-2	1610-1800	0.7	2.0	0.91	Germany
ClaySU01	cattail	0-1	~1700	-	-	-	Estonia
ClayCT01	flax	0-1	~1700	-	-	-	Germany
ClaySU04NF	-	0-1	~1700	-	-	-	Estonia
ClayCT04NF	-	0-1	~1700	-	-	-	Germany
ClaySU01NF	-	0-1	~1700	-	-	-	Estonia
ClayCT01NF	-	0-1	~1700	-	-	-	Germany

\*Barley straw < 30 mm

\*\*Barley straw 10 mm

Regarding lime-based plasters, five different plaster mixes were tested (Table 5-2). Plasters LimeSF04, LimeSU04, LimeSAK and LimeUNI are industrially produced ready-made dry-mixes available at the Estonian market. Plaster LimeSUC04 was the only lab-made plaster mix in this test program. According to the product manufacturers, the composition of plaster mixes LimeSF04 and LimeSU04 follow the traditional recipe of historic lime plasters (to ensure their compatibility with the ones already seen in old buildings). For plaster LimeSU04, a material test report was available, and its specific composition was known: 10% high-grade hydrated lime CL90, 40% crushed limestone sand and 50% selected sand using a special grading curve (Test Report 16027, 2016). As this data was available, Plaster LimeSUC04 was additionally prepared (lab-made) analogue to plaster LimeSU04, except the addition of 4% of cement in the total dry volume of the plaster mix. The objective was to evaluate the cement component's direct effect on the fire protection performance. Plaster LimeSAK and LimeUNI are widely used commercial ready-made dry-mixes, however limited material properties were known. According to the product declaration, plaster LimeSAK contains up to 4% of cement in the volume of the dry mix. In Table 5-2, the material strength class CS I indicates that the compressive strength after 28 days of drying is 0.4 up to 2.5 N/mm<sup>2</sup>. All lime-based plasters are classified in a reaction to fire class A1 as they are purely mineral.

Table 5-2. Type of lime-based plasters selected for this research.

Plaster reference	Type of lime	Lime in dry mix	Cement in dry mix	Grain size	Compressive strength class	Dry bulk density	Thermal conductivity	Capillary Water absorption
		[%]	[%]	[mm]		[kg/m <sup>3</sup> ]	P=50 [W/mK]	
LimeSF04	DL 80	n/a	0	0 - 4	n/a	~1700	n/a	n/a
LimeSU04	CL 90	10	0	0 - 4	C I	1840	0.82	W0
LimeSAK	n.a.	n/a	≤ 4	0 - 1	CS I	~1400	≤ 0.47	W0
LimeCSU04	CL 90	10	4	0 - 4	n/a	~1800	n/a	n/a
LimeUNI	n.a.	n/a	0	0 - 1.5	n/a	~1400	0.27	W2

In order to increase tensile strength and minimize the likelihood of plaster cracking during the hardening process (and over the plaster’s full-service life in practice), reinforcement meshes were included into the plaster systems of select test specimens. Three different types were used in this study, see Figure 5-1. Jute fabric and flax mesh were used for clay plasters (Figure 3-4). The mesh sizes for the jute and flax mesh were about 4.5 x 4.5 mm and 5 x 5 mm, respectively, and the width of both meshes was 100 cm. In case of lime plaster system tested in furnace (in TP4), a fiberglass mesh was used that has a high tear and tensile strength. Fiberglass mesh of 11 mm x 11 mm (width of 100 cm) was used with a density of 105 g/m<sup>2</sup>.

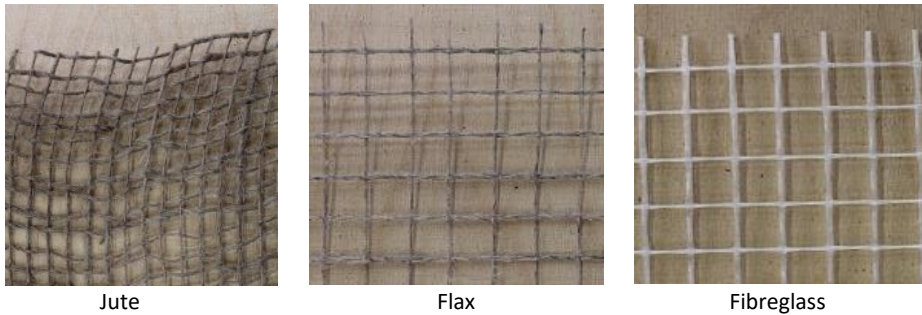
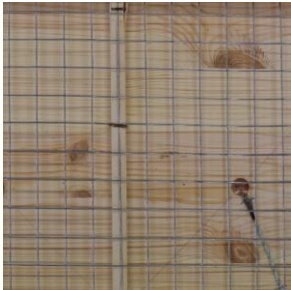


Figure 5-1. Types of reinforcement meshes used in plaster systems.

Table 5-3 presents the plaster carriers (reed mat and wire mesh) used in this research. Reed-based materials were given the most attention because they represent historic plaster support systems used in old buildings up to the present day. Because of its excellent workability and compatibility with traditional type of plasters, reed mat is the preferred material by professionals for plastering wooden surfaces.

Table 5-3. Plaster carriers used in this research.

Description	Reed mat	Wire mesh
Photo		
Thickness	≤ 10 mm	~ 1 mm
Density	190 kg/m <sup>3</sup>	-
Fixation	Staples (Length – 25 mm; distance ~10 cm)	Staples (Length – 25 mm; distance ~10 mm)

A reed mat (as a plaster carrier) consists of ca. 6–10 mm thick reed stems with approximate 70 stems per linear metre. A galvanized carrier wire and a thinner binding wire are used to bind the reed stems together. The wires are fixed in ~10 cm apart perpendicular to the reed stems along the mat. The carrier wire is fixed with staples to

timber, hence presses the reed stems firmly against the wooden surface. The distance between staples (width of 10 mm, length of 25 mm) was set to ~10–15 cm.

In addition, a galvanized wire mesh was used as a plaster carrier that is considered as a modern design solution and is occasionally favored because to its simplicity of application. It is fixed on timber with staples using thin wooden strips that provides a distance (< 10 mm) from the wooden surface for plaster to adhere mechanically around the mesh. The selected mesh size was 19 mm x 19 mm and a wire diameter ~1 mm.

In practice, a reed board is used as a plaster substrate and was selected for testing. It is a rigid building board made from natural reeds that are laid in parallel and braided with gauge-galvanised wire to ensure the strength (compactness) of the board (Figure 5-2, Figure 5-18c). The board density is 225 kg/m<sup>3</sup> and thermal conductivity of 0.056 W/mK. Reed board is fixed with screws using fastening clips on the wires (Figure 5-2a). The distance between screws on the wire support is about 15–20 cm. In this study, a 50 mm thick reed board was used. The plaster system applied on board is shown in Figure 5-2b.



a) Fastening of reed board to timber



b) Plaster system on reed board

Figure 5-2. Reed board as a plaster substrate on timber structures.

The application process of plaster layers using a plaster carrier on timber is presented in Figure 5-3. The same application method applies to reed board, except for the use of a plaster carrier. The preparation of the plaster was conducted in line with the producers' stated technical and practical use. The procedure for preparing the plaster was intended to replicate the actual building conditions as closely as possible. Plasterer-judged volumes of water (20–25 wt.%) were added gradually to dry ready-mix powder in accordance with the manufacturer's specifications to create a homogeneous slurry. The protection system for timber elements was applied such that charring would occur perpendicular to the grain. Test specimens were prepared and set-up with respect to the test method and scale (see Chapter 5.2, 5.3 and 5.4).

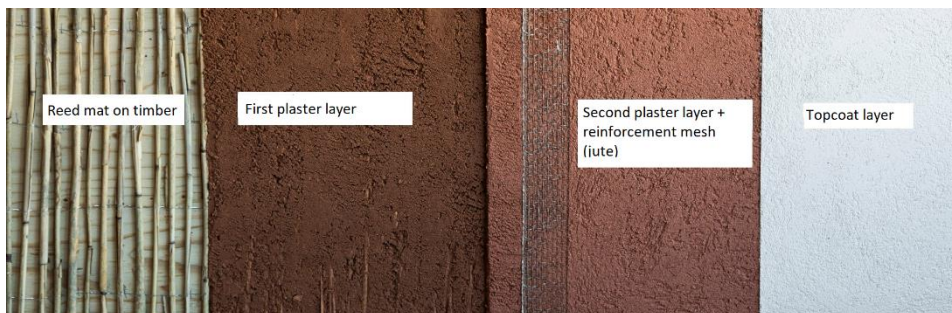


Figure 5-3. An example of a plaster system on timber element.

## 5.2 Material tests

Plaster is a relatively complex mix of components that comprise different minerals, organic matter as well as air and water that is locked between and in the pores. Thus, the material behaviour at high temperatures is influenced by various parameters such as type of aggregates, density, water content, volumetric proportion of components, type of binder and sand, mineralogy, particle size, air voids etc.

In this research, the determination of material thermal properties was limited to the materials and test methods used and present no explicit assessment on the thermo-physical changes in plaster. The aim of material tests was to determine and provide input data for heat transfer simulations to calculate their correspondence to the temperature measurements obtained from furnace tests. This aided the development of design parameters for selected plaster systems in view of the design concept given in Eurocode 5 Part 1-2. The material tests have been discussed in papers (Liblik et al. 2019, 2020).

### 5.2.1 Thermogravimetric analysis

TGA enables to investigate the thermal stability of a material. The device continuously weighs a sample as it is heated to temperatures of higher than 1000°C. By monitoring the weight of a sample while heating at a constant rate, it measures mass changes as a function of temperature that is associated with decomposition, oxidation and other physical or chemical changes. The chemical and physical thermal reaction types and their appearance on thermo-analytical curves is given in Table 10 in a handbook by (Földvári, 2011).

In this work, TG analysis was conducted on a NETZSCH STA 449 F3 Jupiter® TG-DSC analyser coupled with a NETZSCH QMS Aëolos® mass spectrometer. The samples were heated under a mixture of 80% nitrogen and 20% oxygen. Prior to each test, the TGA system was flushed with the same mixture to ensure a correct atmosphere. To follow a similar increase of temperature in time as in fire tests (ISO 834-1), the sample was first heated to 770°C with a heating rate of 40°C/min and then to 970°C with a heating rate of 4°C/min. To eliminate any buoyancy effects (apparent mass gain), correction runs with empty crucibles were run and the afforded data was subtracted from the measured data. The samples were analysed in Al<sub>2</sub>O<sub>3</sub> crucibles with pierced lids. Temperature calibration was performed using In, Sn, Zn, Al and Au standards.

Description of selected test samples and obtained test results are presented in Table 5-4. Samples of crushed dry-mix plasters were selected appropriate for the test method. Solely the undercoat dry-mix plasters were tested as they build up the main volume of the plaster system used in practise. As a reference, a sample of gypsum plasterboard (denoted as Gypsum PB in Table 5-4) was also tested with an aim to position the results for plasters in a broader context. The results from TGA may slightly fluctuate as the test sample consistency may vary at some extent; selective double testing confirmed similar test results with small differences. This was also confirmed by additional tests wherein a constant heating rate of 10 K/min or 20 K/min was used (Liblik & Maaten, 2019).

Figure 5-4 presents the test results. No mass change occurred until 100°C since solely dry crushed particles were tested. Test samples of clay plaster mixes retained a rough steady mass until 400–500°C, some decrease in their mass was detectable that can be explained by the start of transformation of the original minerals of clay (temperature range of 400–600°C) resulting in the loss of chemically bound water. At around 700–850°C, a significant mass loss took place for all clay plasters, apart from other two

clay plasters with a total mass loss around 4–7%; ClaySF04 presented the greatest total mass loss of 11%. The difference may be attributed to the different type or volume of compounds in the plaster mix (e.g., calcite and dolomite) that decompose at temperatures above 600°C (Lawrence, 2006).

Table 5-4. Test materials and results of TG analysis.

Plaster reference	Weight of test sample	First mass loss change (before 500°C)	Total mass loss change (after 900°C)
	[mg]	[%]	[%]
ClaySU04	8.970	0.42	6.43
ClaySF04	9.677	0.59	11.18
ClayCT04	5.345	1.37	4.81
LimeSU04	6.397	3.53	25.81
LimeSAK	7.038	1.46	9.62
LimeUNI	6.315	3.03	12.12
Gypsum PB	3.623	18.41	20.69

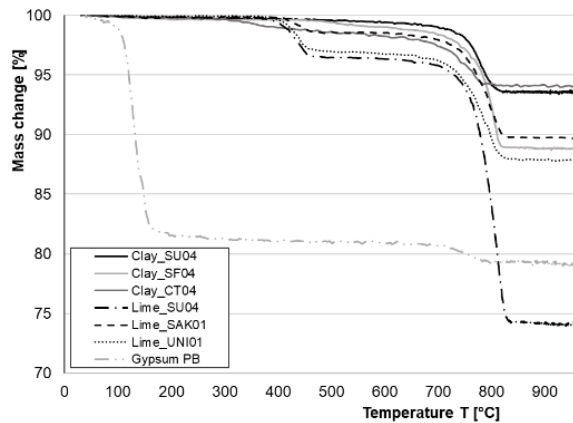


Figure 5-4. TGA test results of the relationship between mass loss and temperature.

Lime plasters presented greater total mass loss compared to clay plasters. LimeSU04 demonstrated two distinct mass loss stages that correspond to the dehydroxylation and decarboxylation processes. The mass loss around 400°C is due the decomposition of calcium hydroxide  $\text{Ca}(\text{OH})_2$ , the higher temperature range around 700°C to 850°C corresponds to the thermal decomposition of calcium carbonate (i.e. evaporation of  $\text{CO}_2$ ) (Lawrence, 2006). The second weight drop occurred at a similar temperature range as for clay plaster mixes, thus the total mass loss of 26% for LimeSU04 is more than a double value compared to clay plasters. In contrast, the other two types of commercial lime-based plaster mixes performed distinctly different (smaller total mass loss) compared to the plaster LimeSU04 that most probably refers to the fewer components (mainly calcium carbonate) that decompose at this temperature range (Appendix 1).

In case of the test sample of gypsum plasterboard, a large amount of crystallized water around 100°C is lost that consequently demonstrates its well-known performance as an effective fire protection material delaying the heat transfer to an underlying structure. At around 700–800°C a significantly smaller mass loss was observed, after 900°C a total mass of 20.7% was determined (Table 5-4).

### 5.2.2 Transient plane heat source method

The TPS method is used to determine the temperature-dependent thermal properties of materials from room temperature up until 700°C. (Log et al., 1995) have described the principles of using this methodology. This method uses a sensor which functions as a heat source and resistance thermometer. A constant power is supplied to the sensor and the temperature in the sensor is continuously measured. The thermal properties of the sample can be calculated by using the temperature development in the sensor. In this research, this method was used in accordance with ISO 22007-2 to determine the thermal conductivity and thermal diffusivity, hence the specific heat capacity per unit volume.

Test specimens of three different types of plasters were prepared and tested, see Table 5-5. The clay plasters were prepared with the same amount of water (150 ml of water was added to a 0.5 kg dry mix, following the manufacturer's instructions, that refer for 5.5 litres of water per 25 kg to prepare the plaster mix for application). The amount of water in lime plaster was 130 ml per 0.5 kg dry mix, according to the instruction by producer. Each test specimen comprised two sample halves, both prepared in a cylinder shape with a diameter of 68 mm and depth of 25 mm. Deviation in measurements was  $\pm 2$  mm. Figure 5-5 illustrates the preparation of test samples. A hot disc probe (a Mica sensor 4922, sensor radius of 14.6 mm) which serves as both a heater and a temperature detector was embedded in-between the two specimen halves. The specimens were left for curing for five weeks at ambient room conditions. Before testing, the specimens were conditioned at  $23 \pm 2^\circ\text{C}$  and  $50 \pm 5\%$  RH in a climate chamber for three days.

Table 5-5. Description of test samples in TPS tests.

Plaster reference	Density of specimen before test	Weight of specimen before test	Weight of specimen after test (~500°C)	Total mass loss after test (~500°C)
	[kg/m <sup>3</sup> ]	[g]	[g]	[%]
ClaySU04	1814.8	146.4	144.8	1.08
ClaySF04	1855.7	159.3	157.3	1.25
LimeSU04	1893.6	162.9	160.5	1.48

Tests were carried out in an electrical furnace. An average of five reliable measurement values per temperature step were obtained. Measuring problems were encountered at higher temperatures at around 400–500°C that resulted in less measurement points. The evaporation of chemically bound water and material changes resulted in the cracking of test specimens, which hindered the determination of measurements and restricted to continue testing at higher temperatures (number of reliable measurements only two or three). Figure 5-6 presents a documentation of test specimens after testing. Sample LimeSU04 cracked around 450–500°C, while the ClaySU04 and ClaySF04 cracked at around 500°C. This indicates that measurements in this temperature range may not be correct if the samples cracked during the time of measurement. In general, the variation of measurements could have some influence from the quality of the bond contact between the test samples and the sensor as some air pockets could add some uncertainty to the test results. However, all samples were prepared alike and with proper care to minimize these types of factors.

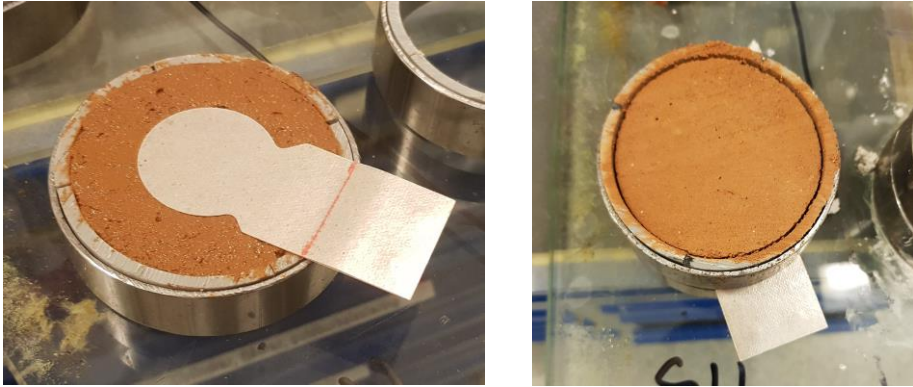


Figure 5-5. Preparation of test samples for TPS method: Left – MICA sensor fixed on one of the sample halves; Right – Test specimen after hardening and before the removal of the metal cylinder.



Figure 5-6. Documentation of test specimens after TPS tests: Left – Close-up of ClaySU04 after testing; Right – Cracking of LimeSU04 when tested in the electric furnace.

Test results of thermal conductivity are presented in Figure 5-7 and Figure 5-8. There is a significant difference in the obtained values of thermal conductivity for ClaySU04 and ClaySF04, despite their similar densities, see Table 5-5. Foremost, this variation may be attributed to a difference in the initial moisture content and type of fibre, which may have an impact. ClaySU04 has hemp fibres while the ClaySF04 incorporates cattail fibres. It could be argued that the hemp fibres absorb more water into the plaster mix compared to cattail (due to its physical characteristics, see Figure 3-3). The difference in clay minerals may also have some influence; however, the clay component in the total plaster mixture is about 6–8%, thus it is unlikely to have a such a significant impact on the measured thermal conductivities. The thermal conductivity of ClaySU04 was determined 1.6 W/mK at room temperature, which is significantly higher compared to the one declared by the manufacturer for the same plaster (0.91 W/mK, see Table 5-1). The higher thermal conductivity is attributable to a greater initial moisture content, as shown by the measurements at 21°C and 89°C, when the thermal conductivity decreases by almost 0.3 W/mK (see Table 5-5, left).

In contrast, ClaySF04 exhibited readings similar to those reported by the manufacturer at room temperature (thermal conductivity of 0.93 W/mK). However, it showed only a slight reduction in thermal conductivity of ~0.05 W/mK at 90°C. This relates to a much

lower initial free water content in ClaySF04 compared to ClaySU04, since the thermal conductivity is directly related to the evaporation of free water around 100°C, i.e., the water pores are filled with air. ClaySF04 demonstrates roughly constant values until 400°C, whilst there is a clear trend of decrease in the thermal conductivity for ClaySU04. It is notable that the measurements for both clay plasters around 400°C show relatively good agreement (difference in average is only 0.078 W/mK) compared to the significant difference in measurements at lower temperatures. Measurements at 494°C were also achieved for ClaySF04, wherein a significant drop of thermal conductivity was determined that could be explained by the evaporation of crystallised water of clay minerals but can additionally be related to some other components starting to undergo transformation around 400°C.

Figure 5-8 shows the test results for LimeSU04, in which a distinct reduction in thermal conductivity with increasing temperature is seen. At temperatures higher than 250°C, there is a greater deviation of measurements at certain temperatures, which is likely due to the onset of chemical reactions in the plaster mixture. The thermal diffusivity of plasters was also simultaneously determined, the results are presented in Table 6-1, Table 6-2, Table 6-3.

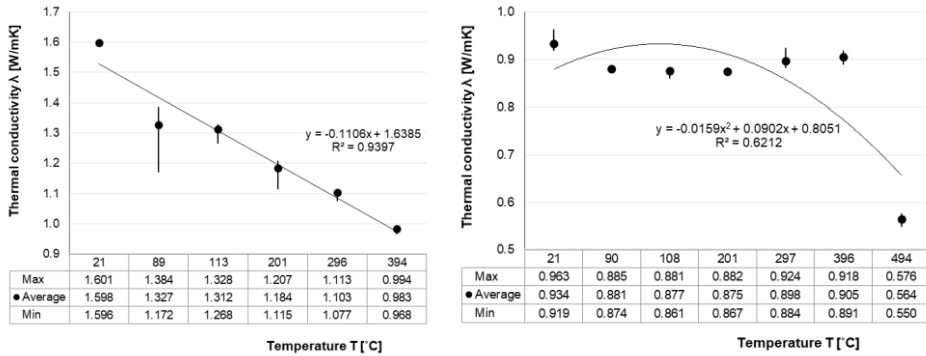


Figure 5-7. Thermal conductivity of clay plasters as determined by TPS tests: Left – ClaySU04; Right – ClaySF04.

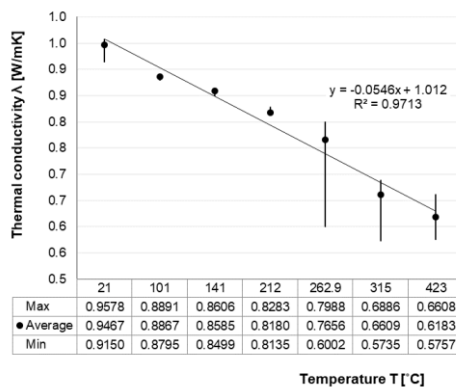


Figure 5-8. Thermal conductivity of lime plaster (LimeSU04) as determined by TPS tests.

## 5.3 Cone heater tests

### 5.3.1 Test materials and programs

Cone heater tests were performed in four test programs (TP), see Table 5-6. TP1 was regarded as a preliminary study (the bulk of tests were conducted as part of the author’s master’s thesis) to explore the feasibility of the cone heater testing method and the repeatability of test results. The first study (TP1, (Liblik, 2015)) was followed by further cone testing (TP2, (Liblik, 2016; Liblik, 2017)). These test data are compared to and subjected to additional analysis in this current thesis. TP2 comprised two ready-made clay plaster dry-mixes available at the Estonian and German market. These tests were conducted to compliment the furnace tests (Chapter 5.4) in order to compare the test results obtained from different test methods. TP3 was carried out to test mainly the lime-based plasters, the preliminary work was conducted by (Nurk, 2021). For an extended analysis of the charring rate of timber and determination of  $k_2$  using the cone heater, additional tests were carried out solely with timber specimens in TP4.

Different heat flux scenarios were used (Figure 5-9). The duration of cone tests varied between 40–60 minutes. The test equipment of cone calorimeter (ISO 5660-1) determined the size of test specimens; however, some modifications were made for this study (described in Chapter 5.3.2). In TP1, TP2 and TP3, the test specimens composed of a plaster system and a solid timber element. The dimensions of timber elements were selected 100 mm x 100 mm x 100 mm and 50 mm x 100 mm x 100 mm ( $\pm 1$  mm tolerance).

Table 5-6. Overview of test programs of cone heater tests.

Test program	No of Tests	Size of the timber specimen [mm x mm x mm]	Plaster reference	Type of plaster carrier	Heat flux scenario	Reference
1	40	100 x 100 x 100	Lab-made clay plasters* ClaySU04** ClaySF04	reed mat	1	(Liblik, 2015; Liblik et al., 2016)
2	33	100 x 100 x 100	ClaySU04 ClaySU01 ClayCT04 ClayCT02 ClayCT01	reed mat	2	(Liblik et al., 2017, 2023)
3	56	50 x 100 x 100 100 x 100 x 100	LimeSU04 LimeSAK LimeUNI LimeSF04	non/ reed mat	3	(Nurk, 2021; Liblik et al., 2022)
4	16	50 x 100 x 100 100 x 100 x 100	non	non	2; 4	(Liblik et al., 2022)

\*Details on the plaster mixes is found in the master thesis (Liblik, 2015).

\*\*ClaySU04 consisted of straw fibre instead of hemp fibre.

Table 5-7 provides a description and specifics of test specimens. Before applying plaster, the density of timber samples was measured at room temperature. Before testing, the density of plaster systems (including the plaster carrier) was calculated by weighing the whole test specimen (including the timber specimen) and subtracting its weight. The thicknesses of the prepared plaster ranged from 10 to 40 mm. To assess the repeatability of testing, selectively duplicated models were prepared. Before testing, TP1 and TP2 test specimens were conditioned for about one month in a climate chamber at  $20 \pm 2^\circ\text{C}$  and  $\text{RH } 65 \pm 5\%$ . Prior to testing, TP3 and TP4 specimens were conditioned in a climate chamber at  $23 \pm 2^\circ\text{C}$  and  $50 \pm 5\%$  RH for about one month; 48 hours of oven drying at  $120^\circ\text{C}$  indicated that the moisture content of timber specimens was  $\sim 9\%$ . The variance in conditioning was related to the particular testing facility and laboratories.

Various heating regimens were applied to specimens during testing. Figure 5-9 presents the heat flux scenarios applicable to each TP. TP1 used the same heat flux scenario as previous research by (Tiso et al., 2015). In TP2, the heat flux of  $50 \text{ kW/m}^2$  was raised to  $75 \text{ kW/m}^2$  in a single step after 20 minutes. The time needed to reach a steady heat flux level of  $75 \text{ kW/m}^2$  was not measured, thus the increase from  $50 \text{ kW/m}^2$  to  $75 \text{ kW/m}^2$  is illustrated as an approximation in Figure 5-9. Multiple heat flux scenarios were assessed in TP4.

Table 5-7. Test specimens and test set-ups used in test programs (TP).

TP	Density range of timber specimens [ $\text{kg/m}^3$ ]	Density range of plaster system [ $\text{kg/m}^3$ ]	Duration of cone test [min]	Heat flux scenario no. Figure 5-9
1	453 - 632	1225 - 2088	60	1
2	428 - 630	1540 - 2223	40	2
3	345 - 509	$\sim 1700$	30 - 60	3
4	367 - 457	-	20; 40	2; 4; 5

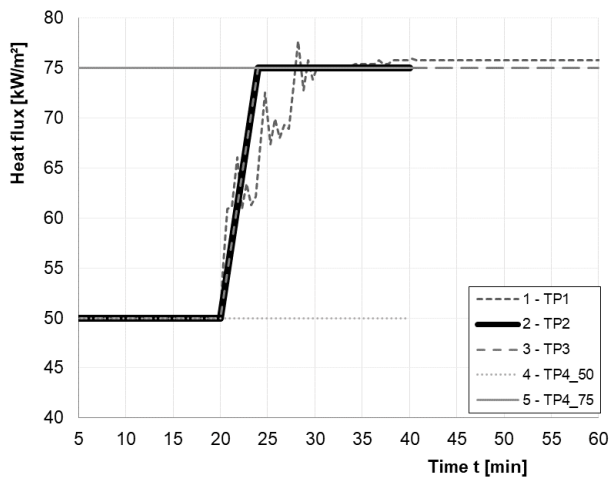


Figure 5-9. Heat flux scenarios used in cone heater tests.

### 5.3.2 Test set-up and procedure

The cone heater of a cone calorimeter (ISO 5660-1) was used to carry out the tests in horizontal position. Test preparation and set-up of specimens followed closely the instructions given in ISO 5660-1 to ensure the universality and repeatability of tests. All the test specimens were prepared alike and according to the same principles. The specimens were prepared so that the charring takes place perpendicular to the grain. The fire protection effect was assessed by means of temperature rise at the interface of plaster and timber surface and by the charring performance of timber specimens.

The preparation and test procedure of test specimens is given below:

1. Figure 5-10 illustrates the preparation of test specimen. Each test specimen was instrumented with thermocouples (TC) of chromel-alumel (0.25 mm, type K) at the interface of the plaster and timber specimen for temperature recordings. The TC were fixed on the top and in the centre of the timber surface (parallel to the isotherm) by using staples to ensure the exact measurement point (Figure 5-10b). The position of the TC marks also the centreline of the cross-section of the timber specimen where the charring of the timber element was later analysed.
2. In case of reed mat, it was fixed on the timber surface using staples to ensure their positioning. For plastering, temporary wooden frame was fixed to timber (Figure 5-10c). The frame was removed before testing. Plasterwork was carried out according to the manufacturers' instructions. A maximum thickness of 10 mm plaster layer was applied at once; subsequent layer was added after one week to ensure proper curing of previous layer (Figure 5-10d, e).
3. Before testing, the specimens were wrapped in an aluminium foil on the sides to eliminate the airflow and minimize the mass transfer. The bottom of the timber specimen was insulated with a rigid stone wool that enabled a firm fixation of the test specimen inside the retainer frame (see Figure 5-11). The frame was to prevent the combustion from the edges and was deliberately used to guarantee high repeatability and routine testing (Babrauskas, 2004). The retainer frame and specimen holder were analogue to the ones specified in ISO 5660-1; solely the depth of the frame was 179 mm instead of  $54 \pm 1$  mm to accommodate the prepared specimen. Due to the use of the frame, the exposed surface area of the test specimen was  $94.0 \pm 0.5$  mm in square. Figure 5-11 illustrates the fixation of test specimen for cone heater testing.
4. The test set-up is presented in Figure 5-11. The distance between the exposed surface of the test specimen and the bottom edge of the cone heater was  $25 \text{ mm} \pm 1 \text{ mm}$  as stated in ISO 5660-1. Tests were conducted by combining two predetermined heat flux levels of  $50 \text{ kW/m}^2$  and  $75 \text{ kW/m}^2$ , as the aim was to replicate similar thermal exposure conditions as in furnace. Slightly different heat flux scenarios and test durations were used for each TP (Table 5-7).
5. All test specimens were cooled down with water after termination of the test. Thereafter, the plaster coat was removed. The timber specimens were cut into half along the centreline of the specimen at the position of the TC. The charcoal was mechanically removed, and residual cross-section was measured along the position line of the TC. The charring rate of timber was calculated based on the charring depth and time.



a) TC and reed stems fixed on timber.



b) Top view of the test specimen before the application of plaster.



c) Temporary wooden frame for plasterwork.



d) Application of the first plaster layer.



e) Thicker plaster systems were built up with 10 mm layer at a time.

*Figure 5-10. Preparation of a test specimen for a cone heater test.*

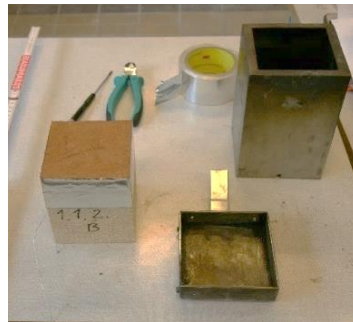
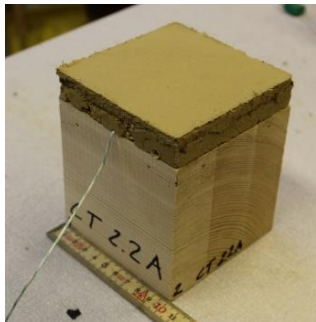


*Figure 5-11. The preparation and fixation of a test specimen in the cone heater tests.*

## 5.4 Furnace tests

### 5.4.1 Test materials and programs

The furnace tests were carried out in four test programs (referred later in text as TP1, TP2, TP3 and TP4), see Table 5-8. All furnace tests with respect to their test programs are described in Table 5-9. Figure 5-13 presents the principal set-ups of the test specimens consisting of the protection system and a timber element. In Figure 5-13-left, a plaster carrier is used; in Figure 5-13-right, a reed board as a plaster substrate is used.

The selection of timber elements was based on the size of the furnace and the handling of the whole test specimen, the latter being a challenge mainly due to the heavy weight of the plaster and solid timber element. TP1 and TP2 were performed at SP Wood Technology laboratory (now the RISE Fire Research) in Stockholm, Sweden (Liblik et al., 2020). TP3 and TP4 were carried out in cooperation with the iBMB, TU Braunschweig at the MPA fire laboratory in Germany (Liblik et al., 2022). An overview of the furnace tests and the layouts of test specimens are presented in Table 5-9, Figure 5-13 to Figure 5-15.

Table 5-8. Overview of furnace test programs.

Test program	No. of Tests	Test orientation	Fire exposed surface area	Size of the timber specimen	Plaster reference	Plaster carrier
			[mm x mm]	[mm x mm x mm]		
1	2	ver	1000 x 1000	120 x 1200 x 1200	ClaySF04	non / reed mat
2	8	ver	600 x 950	40 x 600 x 1200;	ClaySU04	reed mat/ reed board**
			470 x 470	40 x 1200 x 1200	ClaySU01	
		hor	950 x 950		ClayCT04	
					ClayCT02	
3	4*	ver	~450 x 450	38 x 500 x 500	ClaySU04	reed mat/ metal mesh
					ClaySF04	
					LimeSAK	
					LimeSUC04	
4	3	hor	980 x 1480	100 x 1400 x 1900	ClayCT04	reed mat
					LimeSU04	

\* A single furnace test comprised two test specimens tested in opposite sides of furnace walls.

\*\*Plaster applied directly on reed board; no plaster carrier was used.

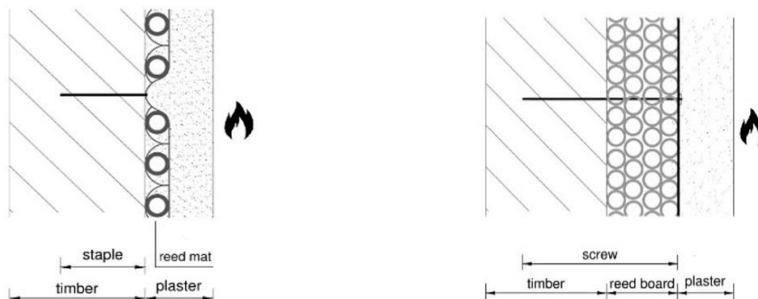


Figure 5-12. Schematic close-ups of the layered construction of test specimens tested in furnace: Left – Plaster system with a plaster carrier; Right – Plaster system and reed board on timber.

Table 5-9. Overview of furnace tests carried out in this research.

Test No.	Test orientation	Fire exposed surface area [mm x mm]	Plaster reference	Plaster thickness [mm]	Plaster reinforcement	Plaster carrier / Plaster substrate
<b>TP1 - Test program no 1</b>						
0	ver	1000 x 1000	SF04	10	-	-
01	ver	1000 x 1000	SF04	30	-	reed mat
<b>TP2 - Test program no 2</b>						
1	hor	600 x 950	SU04/SU01	17	jute	reed mat
2	hor	600 x 950	SU04/SU01	17	-	reed mat
3	hor	600 x 950	SU04/SU01	17	-	reed board
4	hor	600 x 950	SU04/SU01	16	jute	reed board
5*	ver	470 x 470 A	SU04/SU02	20	jute	reed mat
		470 x 470 B	SU02/SU01	20	jute	reed mat
		470 x 470 C	CT04/CT01	20	jute	reed mat
		470 x 470 D	CT02/CT01	20	jute	reed mat
6*	ver	470 x 470 A	SU04/SU02	23	jute	reed board
		470 x 470 B	SU02/SU01	23	jute	reed board
		470 x 470 C	CT04/CT01	23	jute	reed board
		470 x 470 D	CT02/CT01	23	jute	reed board
7	ver	950 x 950	SU04/SU01	44	jute	reed mat
8	ver	950 x 950	SU04/SU01	44	jute	reed board
<b>TP3 - Test program no 3</b>						
9a	ver	450 x 450	ClaySU04	30	-	reed mat
9b	ver	450 x 450	ClaySF04	30	-	reed mat
10a	ver	450 x 450	LimeSAK	30	-	wire mesh
10b	ver	450 x 450	LimeCSU04	30	-	wire mesh
11a	ver	450 x 450	LimeSU04	30	-	reed mat
11b	ver	450 x 450	LimeSU04	30	-	wire mesh
12a	ver	450 x 450	LimeSU04	20	-	reed mat
12b	ver	450 x 450	LimeCSU04	20	-	reed mat
<b>TP4 - Test program no 4</b>						
13	hor	980 x 1480	ClayCT04	20	flax	reed mat
14	hor	980 x 1480	LimeSU04	20	glass fibre mesh	reed mat
15	hor	880 x 1380	LimeSU04	30	glass fibre mesh	reed mat

\*The surface area of test specimen was divided by four smaller areas for various plaster types (Figure 5-13b).

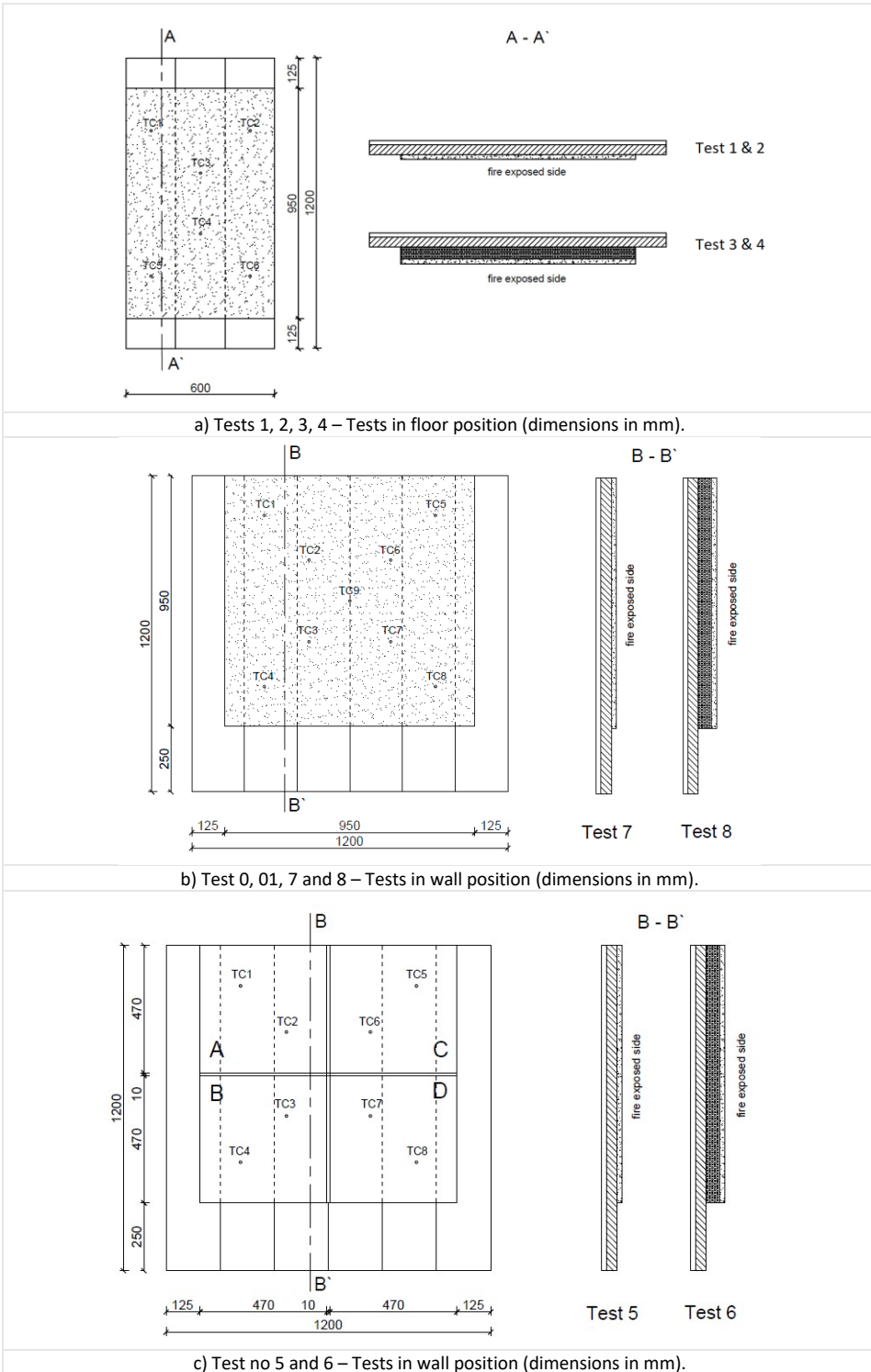
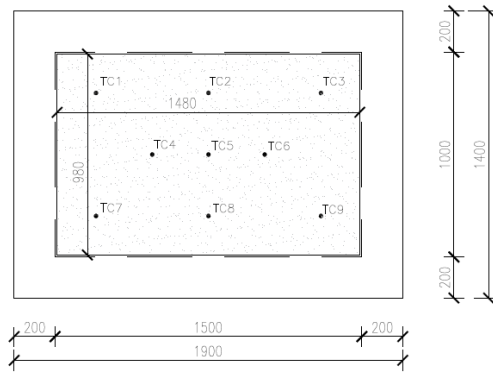


Figure 5-13. TP1 and TP2 – The layout of the fire-exposed side of the test specimens (with TC placements).



a) View of the furnace

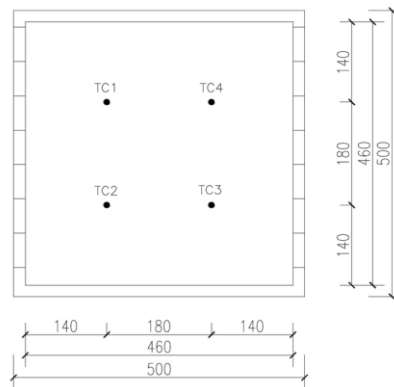


b) Test no 13, 14, 15 (dimensions in mm)

Figure 5-14. TP3 – Furnace and the layout of the fire-exposed side of the test specimens tested in floor position (with TC placements).



a) View of the furnace opening



b) Test no 9, 10, 11,12 (dimensions in mm)

Figure 5-15. TP4 – Furnace and the layout of the fire-exposed side of the test specimens tested in wall position (with TC placements).

TP1 comprised of two tests. A 120 mm thick 3-layer CLT panel (spruce) was selected. The dimensions of each board were 40 mm in thickness and 150 mm in width. A board thickness of 40 mm was chosen to ensure the solid timber effect in testing. The average density of timber elements was  $451 \text{ kg/m}^3$ , determined by the manufacturer, before the application of plaster.

TP2 is considered as the main set of tests due to the number and size of test specimens investigated. The timber specimens consisted of 40-mm thick (spruce) wooden planks (200 mm x 1200 mm) forming a solid background for the plaster system (gaps between the planks were  $\leq 2 \text{ mm}$ ). The average density of the timber specimens was  $428 \text{ kg/m}^3$ , measured in the preparation phase of the specimen, before the application of plaster. The wooden planks were secured with a 12 mm thick particleboard and a supporting construction on the unexposed side to guarantee the integrity and stiffness of the specimen throughout testing. In addition to tests in vertical position, floor tests (Test 1-4) were carried out to assess the plaster system in the most critical position.

TP3 was carried out in a smaller furnace that enabled to test more variations of test specimens. In addition, it served as a verification test method for the clay plaster systems tested in the larger furnace in TP1 and TP2. Test specimens were cut from glulam timber (pine) panels of 38 mm x 500 mm x 3000 mm. Each timber specimen was cut in size of 500 mm x 500 mm (tolerance of 2 mm). The average density of the timber elements before the application of plaster was 490 kg/m<sup>3</sup>.

TP4 aimed to investigate the worst-case scenario for plaster systems, i.e., the horizontal orientation (floor position). A 3-layer CLT panel was used with a total thickness of 100 mm (lamellas of 40–20–40, in cm) with dimensions of 1400 mm x 1900 mm. The density of timber panels was approximately 459 kg/m<sup>3</sup>. Before testing, an average moisture content of the timber panels was between 13.1–15.2%, measured by an electrical resistance moisture meter. Measurements were performed just before the fire testing; taken from the edges of the test specimen (without any plaster on top).

#### 5.4.2 Test preparation and procedure

All tests were prepared according to the size of furnace and the set-up of the test specimen, respectively (Table 5-8, Figure 5-13). Tests were carried out under the standard fire exposure conditions (EN 1363-1) following the standard temperature-time fire curve ISO 834. An overview of test programs and materials is given in Chapter 5.4.1, whereas all the test specimens were prepared alike and according to the same principles by professionals. Test specimens were built-up similarly as the ones tested in small-scale using the cone heater (see Chapter 5.3). The fire protection effect was assessed by means of temperature rise at the interface of plaster and timber and by the charring performance of timber specimens.

The preparation and test procedure of test specimens is given below:

1. The fire-exposed surface area of a timber specimen was instrumented with thermocouples (TC) of double glass fibre insulated bare wire type K specified in EN 1363-1 (wires with a diameter of 0.25 mm). The TC were placed at the centerline of the respective boards, thus avoiding the gap effect for charring. In case of a 50 mm thick reed board, additional thermocouples were fixed on the reed board before plastering. All thermocouples were fixed with staples to ensure the exact measurement points, Figure 5-16. In TP 1 and 2, the thermocouples were with crimped junctions (Figure 5-16a), produced by Pentronic AB, Sweden. In TP 3 and 4, NiCr-Ni copper disc thermocouples of type- K were used (Figure 5-16b).



Figure 5-16. Close-up on the fixation of thermocouples (TC) on the exposed side of the timber elements before the application of plaster systems: a) TP1 and TP2; b) TP3 and TP4.

2. A temporary wooden frame was fixed on top of the fire-exposed side of the timber elements that framed the specified area for the application of plaster, see Figure 5-17. The area for plaster was dependent on its layout and position in furnace, see Table 5-8. The frame ensured the exact thickness and quality of the plasterwork for each test specimens. In TP 3, the frame was additionally covered with a tape to prevent the cracking of plaster from the sides while removing the frame after plaster has hardened. The frame was removed before the preparation of the fire test in test laboratory.



a)



b)

*Figure 5-17. Temporary wooden frames fixed on timber element for the application of plaster: a) Framework fixed on timber element in TP2 (Test 6); b) Framework fixed on wooden panel in TP3.*

3. The plaster carrier was applied and fixed on timber elements according to the manufacturers' instructions. In case of a reed mat, staples of 25 mm in length and 10 mm in width were used (Figure 5-18a; Figure 5-18b). Staples were fixed along each wire of a reed mat, with a distance of about 10 cm (exception was made in TP4, where the distance of staples was around 10–20 cm, which is widely done in practice as the adherence to timber was considered to be sufficient for plastering). In case of a metal mesh, thin wooden stripes with a distance of ~10 cm were additionally used that provided the space for plaster to adhere around the mesh (Figure 5-18d). Staples were fixed along the wooden stripes with 10 cm apart. The reed board was fixed with screws (80 mm in length) using fastening clips on the wires (Figure 5-18c). The distance between screws on the wire support was not more than 150 mm.



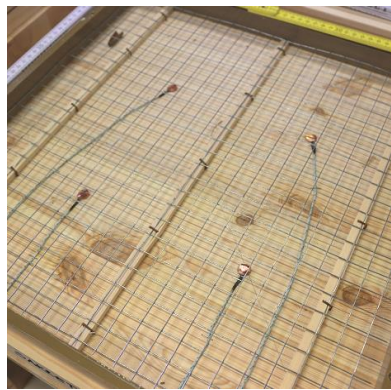
a) Fixation of reed mat with staples to timber



b) Reed mat fixed on timber panel in TP3



c) Fixation of reed board in TP2



d) Wire mesh on timber panel in TP3

*Figure 5-18. Application of plaster carriers (a,b,d) and a plaster substrate (c) to the timber element before plastering.*

4. Plasterwork was carried out by professional craftsman according to the manufacturer's instructions as referred in the European design and application methods given in EN 13914-2:2016. The plaster layers were built up with a 10 mm thick layer at a time (Figure 5-19). A 10 mm thick plaster layer was applied at once and left for hardening approximately one week before subsequent layer was added. Tests were mainly carried out solely with undercoat plasters, except in TP 2. In TP2, the undercoat plaster coats were finished up with a total thickness of 2–3 mm of topcoat plasters as this is commonly done in practice. In case of some plaster systems, a reinforcement mesh (e.g., jute) was used and it was applied into the last layer of the undercoat plaster layer (Figure 5-19).



*Figure 5-19. Plasterwork carried out in all test programs: Left – Application of a first plaster layer on a reed board; Right – Jute mesh applied on a plaster layer.*

5. All test specimens (except the ones prepared for TP4) were prepared at the workshops of the plaster manufacturers in Estonia. Specimens were left for hardening about one month, thereafter, shipped to the test laboratory. Test specimens were conditioned at ambient test hall conditions at  $20 \pm 2^\circ\text{C}$  and  $\text{RH } 50 \pm 5\%$  for a minimum time of two weeks prior testing. TP1 was exceptional due to the time constrains, thus the test specimens were conditioned in test hall for three days before testing. In TP4, the test specimens were prepared at the fire test laboratory. The total hardening time (as well as the carbonization time for lime-based plasters), calculated from the application time of the first plaster layer, was 2.5–3.5 months for lime plasters (TP3, TP4) and one month (TP4) for test specimens with clay plaster.
6. Before testing, the wooden frame (see point 2 above) was removed and the sides of a plaster system were sealed with an aluminum tape to prevent any airflow and mass transfer to the sides (Figure 5-20a). Additionally, a thin ceramic insulation or a rigid stone wool was fixed onto the aluminum tape to prevent a possible thermal exposure from the sides.
7. Before the fire testing of TP3, an additional supporting wooden frame was fixed on the unexposed side of the prepared test specimen to handle the specimen before and after the test, foremost to fix it firmly to the furnace (Figure 5-20b) and remove it afterwards for cooling down in water (Figure 5-21b).



*Figure 5-20. Preparation of test specimens for furnace testing: Left – Sides of plaster fixed with aluminum tape; Right – Test specimen fixed in furnace in TP3.*

8. Test specimens were carefully fixed to the furnace. In TP1, the surface area of plaster was prepared in accordance with the size of the opening of the furnace wall. In TP2 and TP4 (Test 13 and 14), the plaster system was prepared not to be in contact with the edges of the furnace sides, allowing it to fall-off during the test. In TP3 and TP4 (Test 15), the surface area of plaster systems was little larger than the fire-exposed furnace opening.
9. A visual observation of the fire-exposed surface of test specimens was made through the small window openings, when possible.
10. Test duration was determined by the fall-off time of the plaster system or a total test time of 60, 90 or 120 minutes.
11. After the fall-off of plaster system, the fire was stopped, and the specimens were removed from the furnace and directly cooled down with water (Figure 5-21).



*Figure 5-21. Cooling down the test specimens after its removal from furnace:  
Left – Furnace test in TP2; Right – Test specimen in TP3.*

12. The charring performance of timber specimens were analysed after the plaster system was removed. The charring depth was measured after the mechanical removal of charcoal until the virgin wood.

## 6 Results and analysis

### 6.1 Material tests and data for simulations

The material tests were performed, foremost to determine input parameters for the thermal simulations (Chapter 7). The required material properties are temperature-dependent thermal conductivity, specific heat, and density.

Indications about the material changes and relative mass loss of selected plasters was assessed by the TGA (Chapter 5.2.1). However, the determination of mass loss using TGA is not explicit in terms of the realistic mass loss of a plaster in a real application. This testing was limited to the sample size (crushed particles), test method, heating regime etc. In particular, no free water evaporation related to the moisture content in plaster is detectable, however in case of fire, the moisture content of materials is an important factor. Yet the results from TGA present clear insights on the chemical reactions and mass changes at different temperature levels to understand the different behaviours of dry-mix plasters regarding their specific composition.

The results discussed in Chapter 5.2.1 present a clear distinction between the mass loss performance of clay and lime-based dry-mix plasters, also a comparison to the gypsum plasterboard was shown (Figure 5-4). Based on the test results predictions on the change of mass (and accordingly the change of density) could be made. Table 5-4 presents the mass loss of plaster mixes up until 500°C, wherein the mass loss is minimal, as for clay and lime plasters it was not more than 2% and 4%, respectively. At 900°C, the mass loss for clay plasters was approximately in the range of 4–11%; for lime plasters the difference was 9–12%, except for LimeSU04 it was 26% (Liblik et al., 2019, 2020).

As discussed in earlier chapters (Chapter 3.2 and Chapter 4), the equilibrium moisture content of sand-based plasters is low, ranging around 1% at room conditions. For the fire testing, plasters were mainly applied with a plaster carrier directly to timber (Chapter 5.4.1). For these material combinations representing a whole test specimen, the exact initial density and moisture content of the plasters was not explicitly determined; mainly the conditioning of test specimens was assured (described in Chapter 5.4.2). In case of lime plasters, the carbonisation level, and its influence on the change of mass was not examined. Thus, a direct correlation between TGA test results and the actual change in the plaster's density (used as input data for thermal simulations) was not achievable.

In case of clay plaster, the product standard DIN 18947 classifies plasters according to their densities (plasters with a density between 1610–1800 kg/m<sup>3</sup> belong to a density class 1.8). This density class of 1.8 also applied to the selected clay plasters in this research, which was used as the foundation for discussing and deriving the effective thermal properties of interest (Chapter 7), primarily with a mean density value of 1700 kg/m<sup>3</sup>. Manufacturers have mainly determined a similar density range for the traditional type of lime-based plasters; thus, this density range was considered as the basis for all thermal investigations in Chapter 7. The determination of the initial density of plasters and the change in the temperature-dependent density of the plaster systems was somewhat complex due to the impact of the plaster carriers to the density of the whole plaster system and the influence from the manual application technique of the plaster.

While compared to the other relevant material thermal properties (i.e., thermal conductivity and specific heat), the change of density of a material has demonstrated the slightest influence on the thermal response (Mäger et al., 2017). Considering the preceding

explanation and the fact that the mass loss of all plasters remained relatively constant up to approximately 800°C in TG analysis (Chapter 5.2.1), a simplification was made. For the thermal simulations (Chapter 7), a constant density value was considered to be used, which would be indirectly considered by the other thermal properties in the simulations. The greatest total mass loss for most of the plasters was approximately 12%, which could be deemed insignificant when compared to the range of clay plaster densities in a respective material density class (i.e., approximately  $\pm 100 \text{ kg/m}^3$ ). This approach of using a constant density value eliminated the somewhat complex prediction of the change of density for the variety of tested plaster systems that comprised different plaster carriers and types of binders in plasters (e.g., the impact of the carbonization in lime plaster to its change in density). Thus, the plaster systems were considered with a constant density value at all temperature levels in the thermal simulations in Chapter 7.

The TPS testing provided information on the change of thermal conductivity and specific heat. The experiments demonstrated that plasters crack between 400–500°C, which corresponds to the results in the literature about the mineralogical changes and the release of crystallization water in clay at this temperature range. At this temperature range, lime-based plasters also undergo material-specific transformations, the decomposition of  $\text{Ca(OH)}_2$  (Chapter 4). Consequently, the mass loss indicated by TG analysis seems to provide explanation on the alterations (e.g., cracking) of plasters observed in the TPS tests.

Based on the TPS test results, the thermal conductivity of plasters decreased with rising temperature. This agrees to previous studies carried out with clay and soil by (Han et al., 2017) and (Sun, Zhang, & Qian, 2016; Sun, Zhang, Zhang, et al., 2016), discussed in Chapter 4. This phenomenon is explained by the absorbed water dissipation causing the pores to fill with air instead of water that lowers the thermal conductivity of the medium. Furthermore, the loss of moisture starts the splitting of clay, wherein the splits are also filled with air, additionally, the porosity increases due to the carbonisation and sublimation of organics until around 500°C. At higher temperatures the original minerals of clay start to transform, but this has a slight effect on the thermal conductivity of clay (Han et al., 2017). Thus, it may be concluded that the thermal conductivity determined around 500°C in this research (Figure 5-7) would not change significantly with increasing temperature. In case of ClaySF04, the thermal conductivity was rather constant until the last measurement at 494°C (Figure 5-7, right). On the other hand, the measurement at 396°C of ClaySF04 (average value of 0.905 W/mK) was similar to the one measured for ClaySU04 at 394°C (average value of 0.983 W/mK); despite the different values measured at lower temperatures. This seems to indicate to the differences of the plaster mixes and probably to the somewhat different initial moisture contents in the mixes, related to the composition of the plasters (e.g., various type of fibres and their influence on the thermal properties). Previous research by (Han et al., 2017) and (Zehfuß et al., 2020) have demonstrated that the thermal conductivity for mineral based materials decrease between 20 and 400°C. Taking into account the aforementioned, the TPS results of ClaySU04 should present more realistic behaviour of clay plaster (compared to the results of ClaySF04) and were chosen to be used as input parameters for the calibration of effective thermal properties (Chapter 7).

The specific heat is dependable on various factors (aggregate type, moisture etc.), thus the values of specific heat should correlate to the changes in material mix at respective temperatures, e.g., influence from water evaporation around 100–150°C. The TPS test results did not show any significant change (peak) in the specific heat for selected

plasters. This could also be explained by a low moisture content in the plaster mixes. For reference, the lower limit of temperature-dependent specific heat of concrete (with a moisture content of 1.5%, according to EN 1992-1-2) presents similar trend of rather constant value for specific heat (i.e., around 1000°C, (Zehfuß et al., 2020) over the whole temperature range, which was also obtained from the TPS test results in this research for plaster ClaySU04 and LimeSU04 (Table 6-1, Table 6-3). In case of ClaySF04, an increase in specific heat at around 400°C was determined that is in line with the decrease of sudden thermal conductivity, and which corresponds to the temperature range of the loss of chemically bond water from clay.

The specific heat capacity per unit volume ( $C_v$ ) can be derived from the obtained TPS measurements by dividing the thermal conductivity ( $\lambda$ ) by the thermal diffusivity ( $\alpha$ ) from the following equation:

$$\alpha = \frac{\lambda}{C_v} \quad (12)$$

When the density of material is known, the specific heat can be further calculated from the equation (12). The selected clay plasters belong to the density category of 1.8 (according to DIN 18947). This category implies to plasters with a bulk density of 1610–1800 kg/m<sup>3</sup>. Accordingly, the specific heat per mass was calculated using this density range; a mean constant value of 1700 kg/m<sup>3</sup>, and 1800 kg/m<sup>3</sup> were taken as the basis for calculations. The TPS testing comprised the weight measurements of the test specimen, wherein the mass loss of the plaster, was determined minimal (~1%) up until 500°C (Table 5-5). Thus, the change of density was rather constant at each temperature step. Table 6-1 and Table 6-2 present the average values for material properties determined for ClaySU04 and ClaySF04. Table 6-3 presents the results for lime plaster LimeSU04. The density of all plasters was considered constant at all temperatures points, for simplification reasons explained above.

Previous studies by (Küppers, 2020) have proposed thermal properties for clay plaster (purely mineral) and boards as well as for light-weight lime-based plasters exposed to high temperatures in furnaces and in façade fires. In this study, the density of the materials was considered constant. The properties proposed for light-weight lime plaster (Küppers, 2020) differ considerable to the ones determined for the heavy weight lime plaster tested in this current thesis. One of the main reasons is the materials' thermal conductivity that is significantly lower in case of light-weight lime plasters.

A joint publication has been written with Küppers (Liblik et al., 2019) were the first set of effective thermal properties for clay plaster were determined. In that research paper, the TPS results for mineral clay plaster (without any fibres) were presented that also showed a decrease of thermal conductivity (e.g., 1.192 W/mK measured at room temperature and 0.694 W/mK at 400°C); however, these values are somewhat lower than the ones obtained in this thesis for ClaySU04. The specific heat for mineral clay plaster was measured around 800–1250 J/kgK between 20–400°C, which agrees rather well to the values obtained in this thesis for ClaySU04 (Table 6-1).

Table 6-1. Average values of measured properties and derived specific heat for ClaySU04.

Temperature	Thermal conductivity	Thermal diffusivity	Volumetric heat capacity	Specific heat	Specific heat
T	$\lambda$	$\alpha$	$C_v$	$C_{p,1700}$	$C_{p,1800}$
[°C]	[W/ mK]	[mm <sup>2</sup> /s]	[MJ/m <sup>3</sup> K]	[J/ kgK]	[J/ kgK]
21	1.598	1.103	1.449	852.61	805.25
89	1.327	0.771	1.721	1012.21	955.98
113	1.312	0.790	1.661	976.78	922.52
201	1.184	0.647	1.830	1076.41	1016.61
296	1.103	0.568	1.942	1142.50	1079.02
394	0.983	0.515	1.908	1122.58	1060.21

Table 6-2. Average values of measured properties and derived specific heat for ClaySF04.

Temperature	Thermal conductivity	Thermal diffusivity	Volumetric heat capacity	Specific heat	Specific heat
T	$\lambda$	$\alpha$	$C_v$	$C_{p,1700}$	$C_{p,1800}$
[°C]	[W/ mK]	[mm <sup>2</sup> /s]	[MJ/m <sup>3</sup> K]	[J/ kgK]	[J/ kgK]
21	0.934	1.399	0.667	392.63	370.81
90	0.881	1.065	0.827	486.68	459.64
108	0.877	1.039	0.844	496.27	468.70
201	0.875	0.932	0.939	552.32	521.63
297	0.898	0.888	1.011	594.98	561.93
396	0.905	0.773	1.171	688.83	650.56
494	0.564	0.186	3.032	1783.79	1684.69

Table 6-3. Average values of measured properties and derived specific heat for LimeSU04.

Temperature	Thermal conductivity	Thermal diffusivity	Volumetric heat capacity	Specific heat	Specific heat
T	$\lambda$	$\alpha$	$C_v$	$C_{p,1700}$	$C_{p,1800}$
[°C]	[W/ mK]	[mm <sup>2</sup> /s]	[MJ/m <sup>3</sup> K]	[J/ kgK]	[J/ kgK]
21	0.947	0.662	1.432	842.26	795.47
101	0.887	0.499	1.777	1045.33	987.26
141	0.858	0.456	1.881	1106.28	1044.82
212	0.818	0.413	1.981	1165.52	1100.77
262.9	0.766	0.357	2.181	1283.23	1211.94
315	0.661	0.320	2.085	1226.28	1158.16
423	0.618	0.280	2.218	1304.76	1232.27

## 6.2 Cone heater tests

The fire protection effect of plaster systems against the charring of timber elements was primarily evaluated by means of temperature measurements and residual cross-section of timber, accompanied by visual documentation of plasters' performance made during testing. The following is a summary of the test results and analyses related to the TPs and fire scenarios (Liblik et al., 2019, 2020, 2022, 2023).

In TP1 and TP2, visual inspections showed that the surface of clay plasters did not change noticeably over the test period. However, when the plaster thickness was 10–30 mm, the wood specimen began to char and show some flames (coming from the edges of the specimen). Plasters were discolored consequently (Figure 6-1). However, after cooling there was not any apparent mechanical difference between the flamed plaster and the rest of the uncolored plaster. The blackened plaster edges did not detach or fall off. The plaster remained solid. When 40 mm plaster was tested, hardly any flames were observed. The plasters revealed no cracks throughout the whole test, except for 10 mm plaster systems, few cracks were observed (Figure 6-1c). No ignition of plasters occurred.

All clay plasters hardly cracked after cooling; it was simply removed in one piece from timber specimen (Figure 6-1d). Some exceptions were observed for a particular plaster mixture (Liblik, 2015), which exhibited some layer separation after cooling down with water, see Figure 6-2a. The reed stems were carbonized, but metal staples were still attached to the wooden elements, securing the plaster to the wood (Figure 6-2b). Figure 6-3 illustrates the cross-sections of plasters (placed upside down) after testing and cooling down with water.



a) Top view of the test specimen



b) Side view of the test specimen

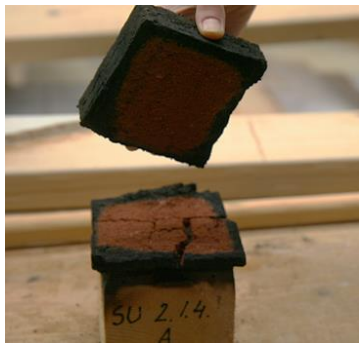


c) View of the plasters' surface after its removal from furnace and before extinguishment



d) Plaster system removed from timber and placed upside down

Figure 6-1. Test specimens (10 mm clay plaster system) after cone heater testing.



a) Detachment of plaster layers



b) Plaster intact with timber after fire test

Figure 6-2. Documentation of test specimen after cone heater testing.



Figure 6-3. Cross-section of clay plasters placed upside down, after cone heater testing.

Temperature measurements taken behind the plaster systems allowed for the assessment of the protective effect. The time when 300°C was reached on wood was considered as the start of charring ( $t_{ch}$ ). Figure 6-4 shows the mean temperature readings and determined start times of charring obtained from TP1. The  $t_{ch}$  values are shown in relation to the thickness of the plaster, which had the most effect on the charring of timber elements. A good agreement to reach the start times of charring was achieved for the whole range of plaster thicknesses.

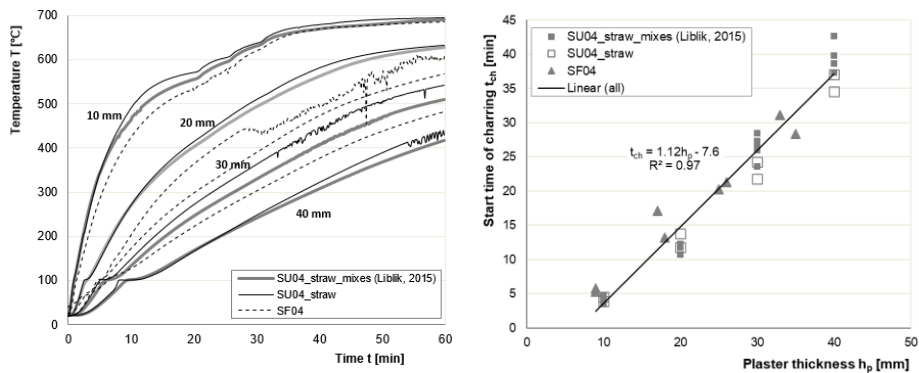


Figure 6-4. Mean temperature measurements and start time of charring obtained from cone heater tests in TP1.

The charring performance of timber was assessed by the cross-sections of timber specimen cut in half. The charcoal was mechanically removed to measure the residual cross-section (i.e., virgin wood) for the determination of the charring depth ( $d_{char}$ ). The point of analysis was along the centerline (position of the TC) of the specimen as shown in Figure 5-10. The relationship between the plasters' thickness and charring depth of timber is shown in Figure 6-5a. Despite the test specimens being prepared to char perpendicular to the grain, this aspect was further investigated. Figure 6-5 shows

wood specimens where the charring occurred perpendicular to the yearly rings of the sample (labeled 'Charring perpendicular\*'). However, in most experiments, the charring occurred parallel to the annual rings. A few wood specimens ('Charring perpendicular\*') corresponded closely (with minimal deviation) to the average trend in charring depths.

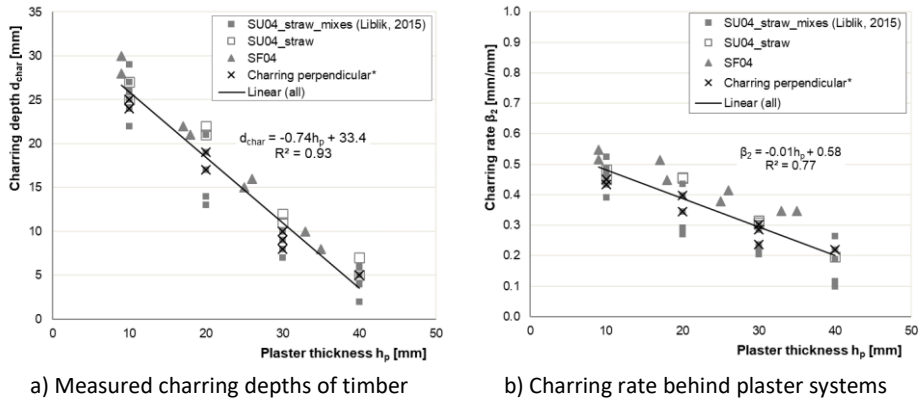


Figure 6-5. The charring performance of timber in relation to the plasters' thickness in TP1.

Compared to the test results of  $t_{ch}$  values presented in Figure 6-4, the charring of timber exhibited a greater degree of variability in test results. Figure 6-5a presents the measured char depths, probably various aspects compile to the deviation of results (e.g., variations in the material properties such as density, specifics of wood, micro cracks of plaster and the positioning of the reed stems in a reed mat). The total charring times of timber samples also varied in relation to the plasters' thickness. The differences in charring times and the somewhat uncertainty related to the time criterion of 300°C can be attributed to the deviation of test results.

The specimens demonstrated some edge burning along the sides, however a clear plateau of a charring depth in the middle of the test specimen demonstrated an evident one-dimensional charring (Figure 6-6). In TP1, the total test time was 60 minutes, thus in case of thinner plaster coats the charring time was rather significant, which resulted in greater char depth in the corner areas of the timber specimen. Indirectly, this phenomenon could add some influence on the charring rate of timber as the flames (coming from the edges of the specimen) during the testing may contribute to a higher fire exposure level compared to the tests without any flaming (in case of thicker plasters).

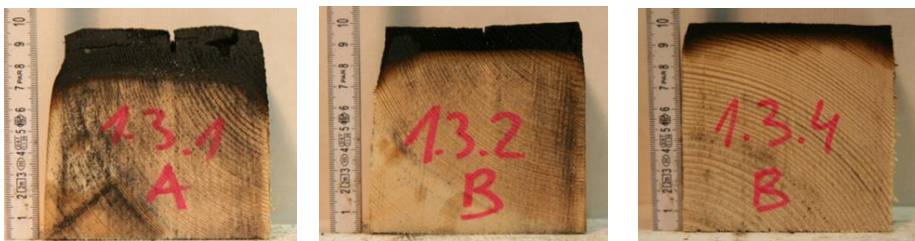


Figure 6-6. The cut cross-section of timber specimens protected by 10-, 20- and 40-mm plaster in TP1.

The  $t_{ch}$  values derived from TP2 are shown in Figure 6-7. All plasters demonstrated comparable performance in terms of thickness; however, a difference is shown between plasters with and without fibres (in case of 20 mm and 30 mm plasters), since only plasters

containing fibres were evaluated in TP1. One layer plaster has a wide range of  $t_{ch}$  values, which is mostly due to the impact of the reed mat since it makes up a larger portion of the whole plaster system than thicker plasters.

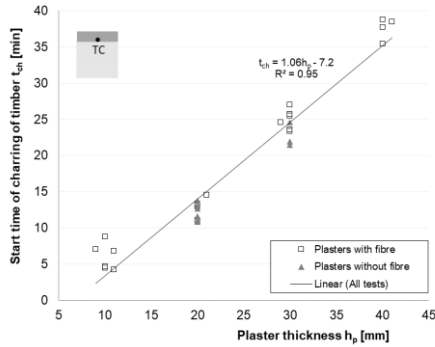


Figure 6-7. The start times of charring obtained from cone heater tests in TP2.

Figure 6-8 illustrates the charring performance of specimens. The measured charring depths and rates are presented in Figure 6-8a and Figure 6-8b, respectively. In comparison to the charring test results from TP1, the charring depths are smaller owing to the shorter test duration, but the mean charring rates for 10 to 20 mm plasters were very comparable. In the case of 30 mm plaster, TP2 provides a somewhat greater charring rate.

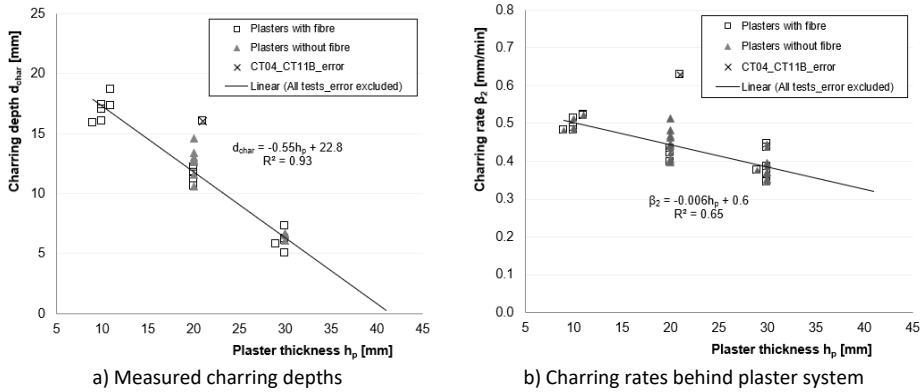


Figure 6-8. The charring performance of timber in relation to the plasters' thickness in TP2.

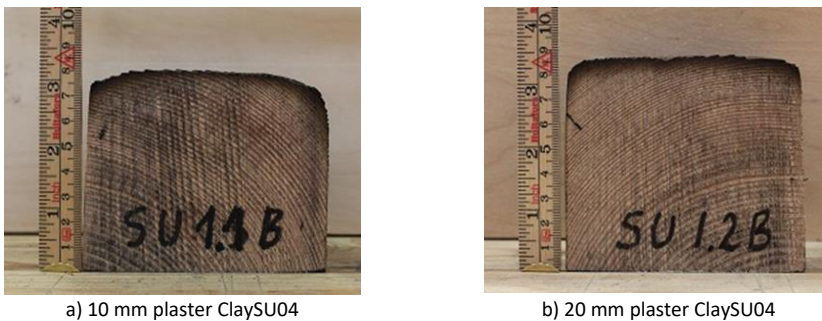


Figure 6-9. The residual cross-sections of timber specimens documented after testing in TP2.

In the following, a comparison of  $t_{ch}$  and  $\beta_2$  determined in TP1 and TP2 is presented in Figure 6-10. The difference between the programs was the heat flux scenario and test duration of 60 and 40 minutes, respectively. Figure 6-10a demonstrates that the time to achieve 300°C in both TPs agrees rather well. This was expected as the heat flux scenarios were very similar. Figure 6-7b presents the comparison of charring rates. Although the charring rates for 10 mm plaster in both TPs are comparable, there is a considerable difference for thicker plasters, and this difference increases with plaster thickness. This difference is directly linked to the total test duration. Table 6-4 presents test results.

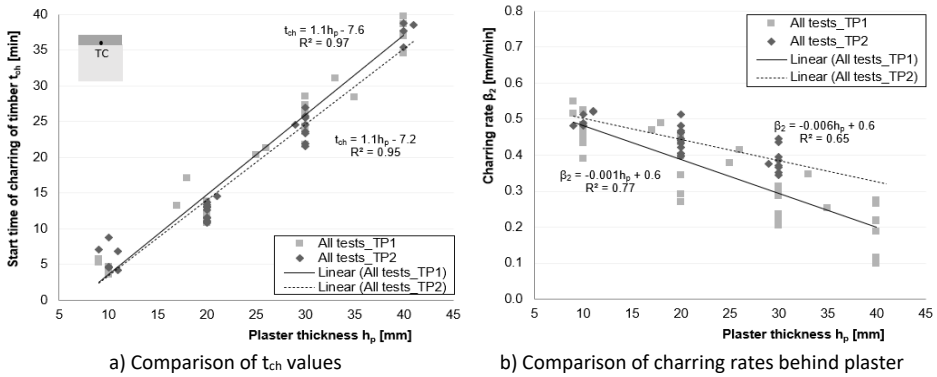


Figure 6-10. Comparison of test results obtained from TP1 and TP2.

Table 6-4. Mean values of start time of charring and charring rate behind plaster obtained from cone heater tests.

TP	Plaster thickness	Density of plaster system*	STD of	Start time of charring	STD of	Charring time	Charring rate behind plaster	STD of
	$h_p$ [mm]	$\rho$ [kg/m <sup>3</sup> ]	$\rho$ [kg/m <sup>3</sup> ]	$t_{ch}$ [min]	$t_{ch}$ [min]	$t_{char}$ [min]	$\beta_2$ [mm/min]	$\beta_2$ [mm/min]
1	10	1527.6	266.0	4.5	0.7	55.6	0.47	0.04
2	10	1456.5	122.8	6.0	1.7	29.1	0.50	0.00
1	20	1707.7	196.3	12.7	1.7	47.3	0.40	0.07
2	20	1589.8	47.2	12.3	1.2	27.7	0.46	0.06
1	30	1695.8	39.7	25.6	2.1	34.4	0.27	0.04
2	30	1482.7	58.1	24.2	1.7	15.8	0.39	0.03
1	40	1746.3	64.8	38.3	2.2	21.7	0.20	0.06
2	40	1413.2	26.5	37.6	1.3	2.4	-	-

\*Density of plaster system includes the reed mat. The only exception is 10 mm plaster in TP1, which did not use reed mat.

The lime-based plasters were tested in TP3. The preparation process and test duration in relation to the plasters' thickness is given in Table 6-5. Tests were carried out with four different types of plasters (Table 5-6) applied on 50 mm thick timber elements, see examples on Figure 6-11. Additional experiments were done to assess the effect of the reed mat and the 100 mm depth of the timber element. After testing, the specimens were directly cooled down with water.



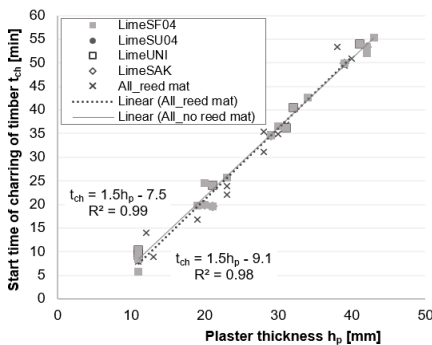
Figure 6-11. Test specimens prepared for the cone heater tests in TP3: Left – 10 mm thick lime plaster with a reed mat on timber specimen; Right – 30 mm thick lime plaster without reed mat.

Table 6-5. Preparation, hardening time of lime-based plasters and test duration in TP3.

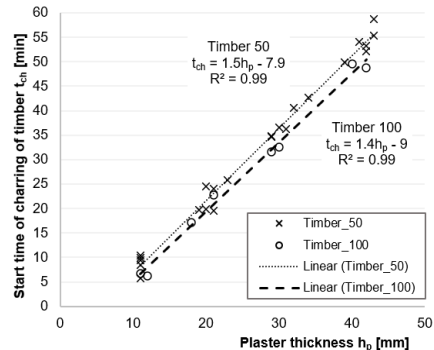
Plaster system thickness $h_p$ [mm]	Total time of plastering [week]	Hardening time at ambient room conditions [week]	Time of conditioning in climate chamber [week]	Total time of hardening before testing [week]	Test duration [min]
10	1	1	1	3	20..30
20	2	1	1	4	40..45
30	3	1	1	5	50..55
40	4	1	1	6	60

Figure 6-12 presents the obtained values for  $t_{ch}$  in relation to the different plasters and initial depths of timber elements. Figure 6-12a illustrates that the time needed to reach the start of charring is similar regardless of the usage of reed mat. Figure 6-12b displays the  $t_{ch}$  values obtained from experiments with 50 mm and 100 mm wood specimens, indicating that the 100 mm specimen starts charring slightly earlier. This behaviour may be partially attributable to the specimen's different moisture/vapour movement, yet the difference is considered minimal. Figure 6-13 presents the documentation of a test specimen after cooling down with water.

Figure 6-14 presents the measured charring depths and calculated charring rates of wood (50 mm) behind the plaster systems. In case of reed mat, there is a larger scatter of charring depths compared to the tests with no reed mat, see Figure 6-14a. Figure 6-14b which shows the charring rates, confirms the same result.



a) Comparison of  $t_{ch}$  values obtained with and without the reed mat on 50 mm timber element



b) Comparison of  $t_{ch}$  values in relation to the depth of the timber element used

Figure 6-12. The start times of charring obtained from cone heater tests in TP3.



Figure 6-13. A test specimen after cone heater testing and cooled down with water: Left – Top view of the timber specimen from which the plaster system was removed and put aside; Right – A close up of the plaster system (incl. the reed mat), placed upside down.

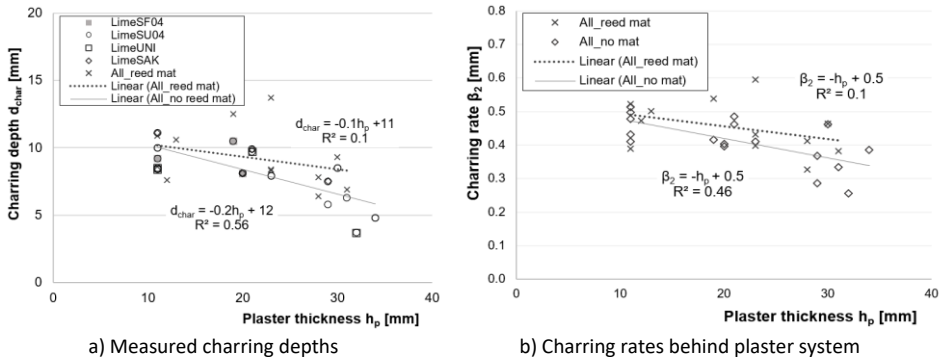


Figure 6-14. The charring depths and rates behind plaster systems obtained from cone heater tests (50 mm timber elements) in TP3.

Figure 6-15 shows the comparison of charring performance of 50 mm and 100 mm thick timber elements, when no reed mat was used. There is a larger scatter of results in case of 50 mm timber. This might be explained by the fact that the heat penetration through the 50 mm wood is more rapid and its heat loss from the sides is more scattered, resulting in a somewhat greater variation in the charring performance of wood. Figure 6-16 presents the documentation of residual cross-sections of timber specimens (cut in half from the middle of the timber specimen) from double testing (variant a and b). In case of various plaster thicknesses (e.g., 10 and 30 mm), the char line over the whole surface area of the fire-exposed side of the timber specimen was even.

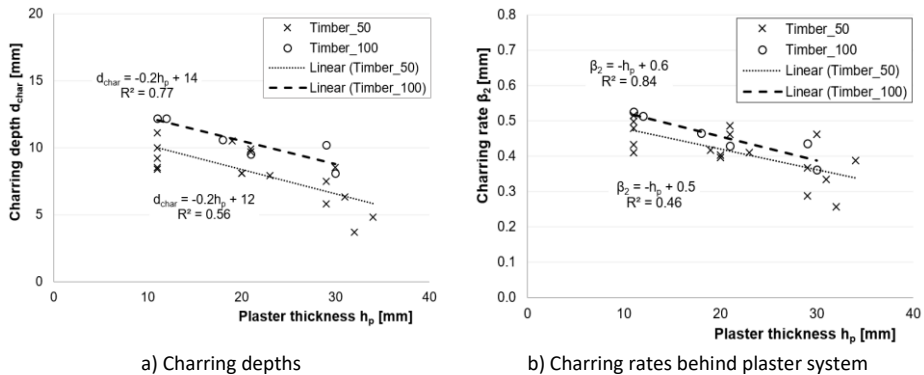


Figure 6-15. Comparison of the charring depths and rates behind plaster systems in relation to the depth of the timber elements (50 mm and 100 mm) in TP3.



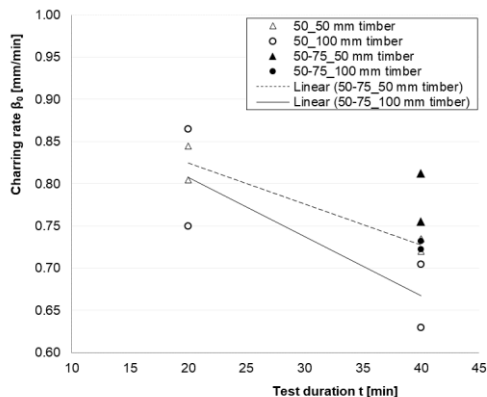
Figure 6-16. Residual cross-sections of timber specimens (50 mm) from double-testing after cone heater tests when protected by plaster: Left – 10 mm lime plaster; Right – 30 mm lime plaster.

Table 6-6 presents the overview of tests carried out in TP4. All different test set-up combinations included double testing, the mean values in Table 6-6 are provided. The results are presented in Figure 6-17; the charring rates obtained in case of the combined heat flux scenario (50–75 kW/m<sup>2</sup>, see Figure 5-9, no 2) are shown with trendlines linking the charring rates obtained from 20 and 40 minutes of testing. In case of 100 mm timber element, the mean charring rate of 0.67 mm/min (measured after 40 minutes) agree rather well with the basic design charring rate value given in EN 1995-1-2 that is 0.65 mm/min for softwood. This also confirms the conclusions made in previous studies by (Tsantaridis et al., 1998) explained in Chapter 4.

For the determination of protection factors for plaster systems, the basic charring rate of timber ( $\beta_0$ ) can be taken from the test results given in Table 6-6. The heat flux scenario no 2 is the same as used in TP2 and TP3, wherein after 20 minutes of constant 50 kW/m<sup>2</sup>, it was immediately raised to 75 kW/m<sup>2</sup>. For TP2, a basic charring rate of 0.73 mm/min should be taken (100 mm thick timber, 40 minutes of fire test). For TP3, a charring rate of 0.78 mm/min should be used due to the 50 mm thick timber element. The  $k_2$  factors derived from cone tests are calculated and given in Chapter 6.4, so that results can be compared with those determined in a furnace.

Table 6-6. Overview of tested timber specimens and charring rates obtained in TP4.

Test set-up	Height of the timber specimens [mm]	Mean density of timber specimens $\rho$ [kg/m <sup>3</sup> ]	Test time [min]	Heat flux scenario [kW/m <sup>2</sup> ]	Mean charring rate $\beta_0$ [mm/min]
1	100	435	20	50	0.81
2	100	420	20	75	0.87
3	100	430	40	50	0.67
4	100	443	40	50-75	0.73
5	50	414	20	50	0.83
6	50	373	20	75	0.95
7	50	383	40	50	0.73
8	50	367	40	50-75	0.78



a) Charring rates in relation to the test durations



b) Specimen after testing

Figure 6-17. The charring rates presented with respect to the test duration, heat flux scenario and depth of the timber specimens in TP4.

## 6.3 Furnace tests

### 6.3.1 Test results

The fire protection effect of plaster systems against the charring of timber elements was primarily evaluated by means of temperature measurements, accompanied by visual documentation of plasters' performance made through a small furnace window opening during the fire testing. Tests were carried out in small and intermediate scale furnaces. Each furnace test demonstrated some deviation of temperature measurements behind the same plaster system over the whole surface area of timber elements. According to the common practice and guidelines presented in technical documents (e.g., Annex G of EN 1995-1-2:2022, EN 1363-1), the mean temperature measurements are considered for presenting the main test results and analysis. Test data in detail are available in test reports (Liblik, 2016; Liblik, 2019a, 2019b) and main results are found in (Liblik et al, 2019, 2020, 2022, 2023).

In the following, overview of test results is presented in three parts regarding the plaster systems tested:

- i) Clay plaster and reed mat;
- ii) Clay plaster and reed board;
- iii) Lime plaster systems.

#### 6.3.1.1 Clay plaster and reed mat

Table 6-7 presents the test results regarding the visual documentation and performance of clay plaster systems with reed mat (except Test 0). Herein, the plaster reference is given solely with the symbol combination (without C marking), as all the plasters refer to clay plaster. There is also a reference to relevant figures demonstrating the surface of the plasters in fire.

Table 6-7. Furnace test results for clay plaster and reed mat – performance of plaster system.

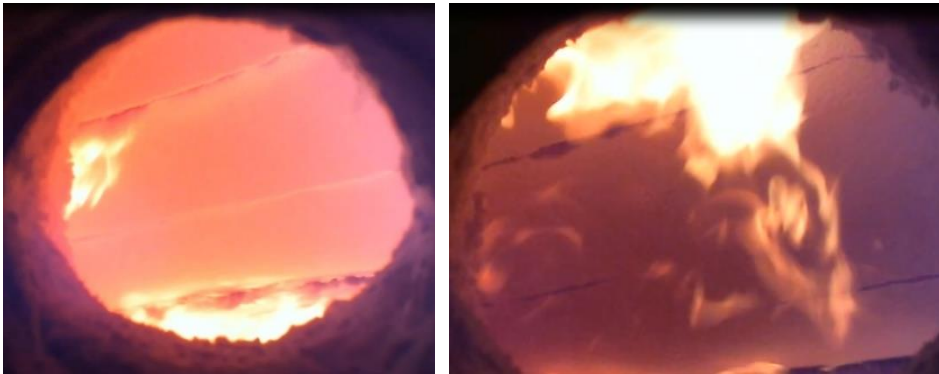
Test No	Test orientation	Plaster Ref.	Plaster thickness	First visible crack in plaster	Temp. behind plaster after first crack	Fall-off time of plaster	Total test time	Visual documentation
			$h_p$ [mm]	[min]	[°C]	$t_f$ [min]	[min]	Ref. to Figure
0	ver	SF04	10	13	479	-	90	Figure 6-21
01	ver	SF04	30	17	89	-	120	Figure 6-22
1	hor	SU0401	17	18	391	76	76	Figure 6-18a
2	hor	SU0401	17	22	414	63	63	Figure 6-18b
5A	ver	SU0401	20	29	506	-	90	Figure 6-19
5B	ver	SU0201	20	25	438	-	90	Figure 6-19
5C	ver	CT0401	20	no	-	-	90	Figure 6-19
5D	ver	CT0201	20	25	488	-	90	Figure 6-19
7	ver	SU0401	44	28	139	64*	76	Figure 6-20
9a	ver	SU04	30	39	444	-	60	Figure 6-23a
9b	ver	SF04	30	56	568	-	60	Figure 6-23b
13	hor	CT04	20	17	325	19	19 (23**)	Figure 6-24

\*Partial detachment of first plaster coats, when mean temperature on timber was 434°C.

\*\*The specimen was removed from furnace at 23 minutes, not directly after the fall-off.

In most cases, the start time of cracking of plaster (visually detected) was observed when the temperature behind the plaster coat (on timber) was around  $400 \pm 100^\circ\text{C}$ . Only for thicker plaster coats (Test 01, Test 7), the temperature was around  $100^\circ\text{C}$  on timber, when visual cracks started to develop, probably due to the greater temperature gradient within the plaster system. The cracking of plaster did not mean the plaster was thereafter fallen off. In many cases, it remained intact to timber until the termination of the test. In TP2, Tests 1 and 2 demonstrated that after some time of testing, the developed cracks started to visually disappear with the increasing test time (Figure 6-18). This may be explained by the mineralogical transformations and thermal expansion of clay at high temperatures. In Test 1 (with jute mesh), the plaster demonstrated only one dominant crack in the centre of the test specimen. In Test 2 (without jute), the plaster showed several smaller cracks on the plaster's surface. In both cases, the fall-off time of plaster happened after 60 minutes and no significant influence from the use of a jute mesh could be drawn.

The fall-off of the plaster system was only determined in floor position. A wall test (Test 7, Figure 6-20) showed some form of detachment of the first plaster layers (at around 64 minutes), yet no fall-off (of the plaster system as a whole) from the timber element was detected.



a) Test 1 – at 75 min of testing

b) Test 2 – at 32 min of testing

Figure 6-18. Visual documentation of the plaster systems ClaySU0401 tested in horizontal orientation in TP2 – view from the furnace window to the plasters' surface.

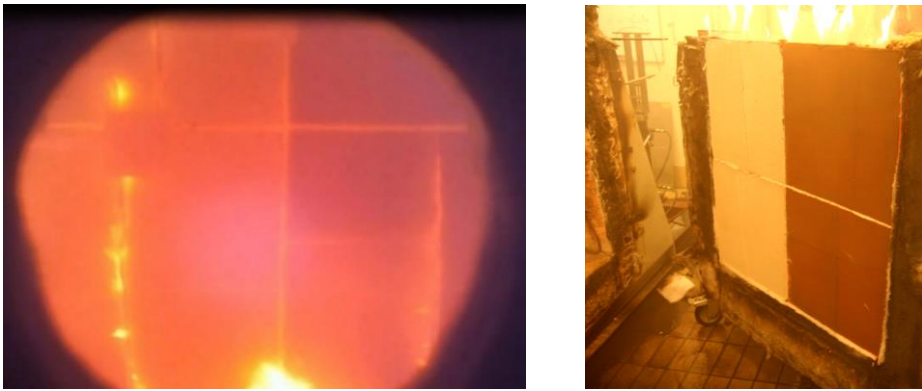


Figure 6-19. Documentation of clay plaster systems of Test 5 during the fire test at 53 min (Left) and after its removal from the furnace wall (Right).

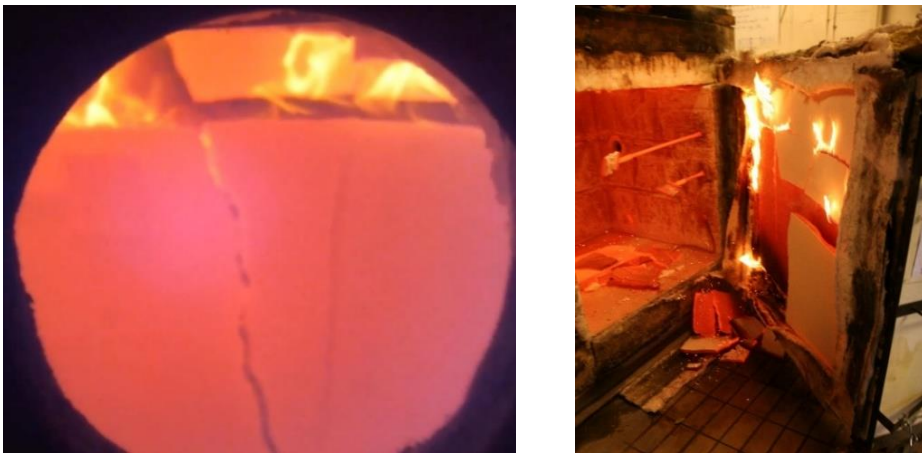
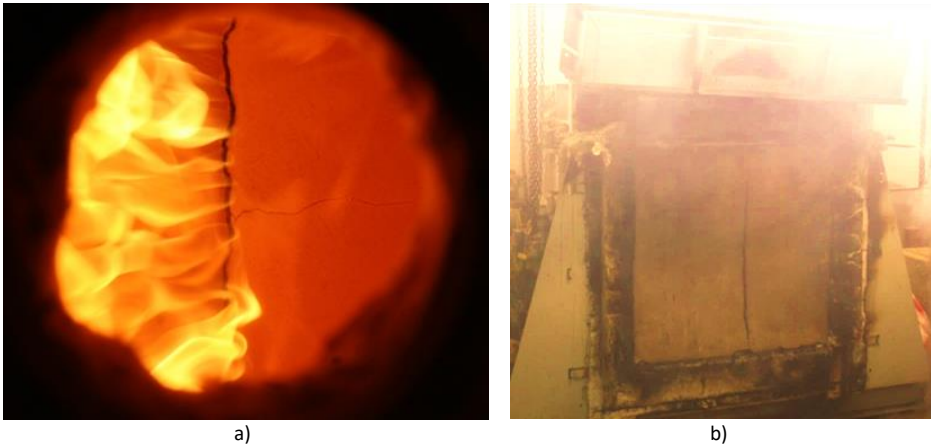
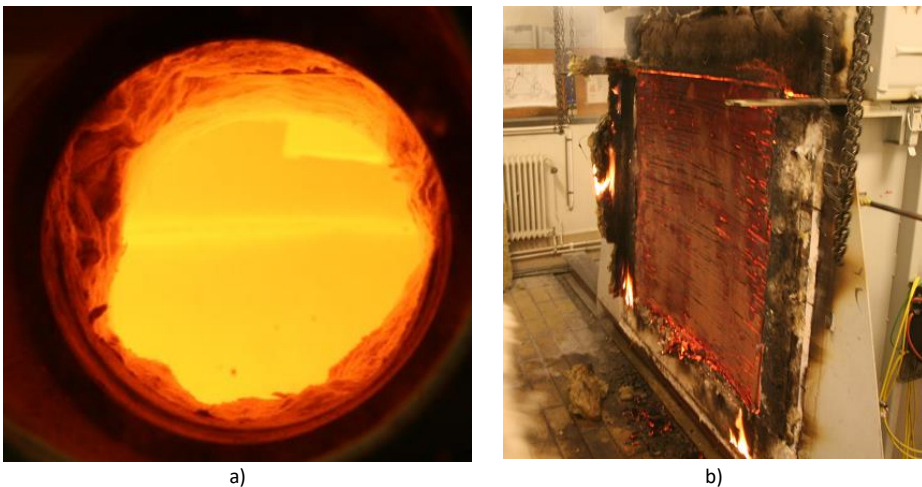


Figure 6-20. Documentation of Test 7 (44mm thick clay plaster system) during testing, approx. a minute before termination of the test (Left) and after its removal from furnace (Right).

The TP1 comprised the first set of tests (Test 0 and Test 01), where no fall-off of plaster was detected, despite visual cracks that developed on the plasters' surface (Figure 6-21a and Figure 6-22a). These test specimens were prepared in accordance with the size of the furnace wall opening, thus no space for material expansion was considered. In both tests, the plaster was attached to the furnace walls after the removal of the timber specimen from the furnace, see Figure 6-21b and Figure 6-22b. This probably prevented the plaster to fall-off during the test. Yet, the test results showed that clay plaster can withstand high temperatures without failing, while providing aspects that need further investigation.



*Figure 6-21. Documentation of Test 0 in TP1 during and after the termination of the fire test: a) View of the plaster systems' surface through the furnace window at 65 minutes of fire testing. b) Plaster attached to the furnace walls after the removal of the test specimen from furnace.*



*Figure 6-22. Documentation of Test 01 during and after the termination of fire test: a) View of the surface of plaster at 86 minutes of fire testing through the furnace window. b) Plaster attached to the furnace walls after the removal of the test specimen from furnace.*

Figure 6-23 shows the test specimens after their removal from the small furnace (TP3). Test 9b was analogue to the one tested in model scale furnace (Test 01, Figure 6-22). In a smaller furnace test, a single dominant crack also appeared (Figure 6-23a), although the crack was later visually seen (17 minutes in Test 01; 56 minutes in Test 9b). Both

plaster systems (ClaySU04 and ClaySF04) showed a one dominant crack forming in the middle of the test specimen. Figure 6-24 presents the observations made in TP4 for Test 13. A sudden fall-off occurred right after the small cracks were observed on the plasters' surface (Figure 6-24a). A piece of the plaster system and reed mat after fire test is shown in Figure 6-24b.

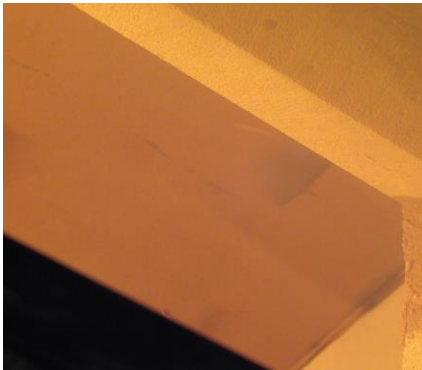


a) Test 9a – Plaster system ClaySU04



b) Test 9b – Plaster system ClaySF04.

Figure 6-23. Documentation of test specimens in TP3 after their removal from furnace.



a)



b)

Figure 6-24. Documentation of the test specimen of Test 13 in TP4 during and after the fire test:  
a) View of the ceiling through furnace window, 3 minutes before the fall-off of the plaster system.

b) A piece of the plaster system after fire test.

Figure 6-25 presents the comparison of temperature measurements between different thicknesses of clay plaster systems obtained from the furnace tests. Each temperature curve presents the mean recorded measurements in a test. There is a clear trend that the temperature rise is delayed with increasing plaster thickness. While most of the temperature curves demonstrate a continuous temperature increase throughout the testing, the floor tests revealed fluctuations in the temperature recordings (after reaching 500°C on timber), likely attributable to the test position and, as a result, gravitationally loosened plaster system allowing additional air circulation between the plaster and timber. As the thickness of the plaster increases, a plateau at 100°C is generated due to the evaporation of excess water from the plaster mix. Test O1 (TP1, 30 mm ClaySF04) had a slightly longer plateau at 100°C than Test 9b in TP3 for the same plaster system. Yet, after reaching 200°C on timber, the temperature curves of both tests are very comparable.

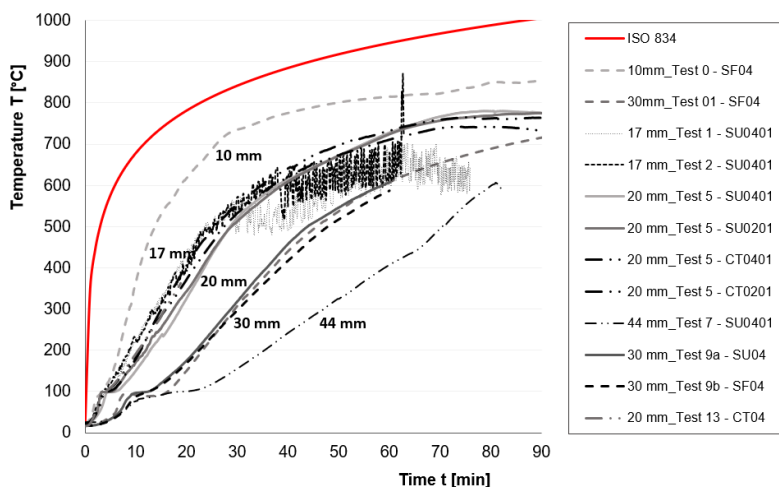


Figure 6-25. Mean temperature rise measured at the interface of clay plaster system and timber element in furnace tests.

### 6.3.1.2 Clay plaster and reed board

Table 6-8 provides an overview of the test results for the performance of the clay plaster systems on reed board, as well as references to photos taken during the fire testing (Figure 6-26 to Figure 6-28). Similarly, to the tests with reed mat, the first visible cracks appeared when 400°C was reached behind the plaster system (except in Test 8). In Test 6, the divided surface areas for plaster systems (Figure 5-13) likely prevented some crack development due to the small surface size; nevertheless, Test 6D showed a sudden fall-off of plaster system from the reed board when the mean temperature on reed board was 475°C.

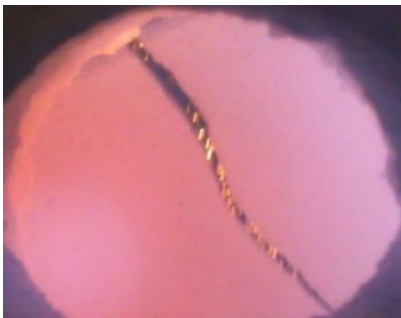
Table 6-8. Furnace test results for clay plaster system and reed board (50 mm) – observations.

Test No	Test orientation	Plaster Ref.	Plaster thickness $h_p$ [mm]	First visible crack in plaster [min]	Temp. behind plaster after first crack [°C]	Fall-off time of plaster $t_f$ [min]	Total test time [min]	Visual documentation of plaster Ref. to Figure
3	hor	SU0401	17	17	435	17	45	Figure 6-26a
4	hor	SU0401	16	18	503	18	45	Figure 6-26b
6A	ver	SU0401	23	no	n/a	no	120	Figure 6-27
6B	ver	SU0201	23	no	n/a	no	120	Figure 6-27
6C	ver	CT0401	23	no	n/a	no	120	Figure 6-27
6D	ver	CT0201	23	no	475	29*	120	Figure 6-27
8	ver	SU0401	44	10	21.6	(43);84**	100	Figure 6-28

\*Fall-off of plaster system (it fell down in one piece but remained solid while still covering most of the reed board from direct fire exposure).

\*\* (Partial detachment of first plaster coats ~15 mm); detachment of ~15mm plaster coat over the whole surface.

Tests 3 and 4 (Table 6-8, Figure 6-26) showed that the cracking of plaster system was directly related to its detachment from the reed board. As there was no mechanical mechanism to keep the plaster attached, its fall-off was expected. After the plaster system fell off, the fire test proceeded because the reed board maintained its structure and delayed the temperature rise on timber, despite being directly exposed to flames. These tests demonstrated good repeatability (solely Test 4 had a jute mesh embedded in the plaster system). The results indicated that the jute mesh had no significant influence on the fire performance of plaster system. In Test 6D, no cracks on plaster system were detected, but after 29 minutes at a temperature of about 475°C behind plaster system, it fell off from the reed board (Figure 6-27). This fall-off was comparable to those observed in the floor position, where it happened suddenly and at around the same temperature range. In Test 8, a clear detachment of plaster coats was observed, yet about half of the thickness of the plaster system stayed intact to timber specimen until the end of the test, see visual documentation in Figure 6-28.

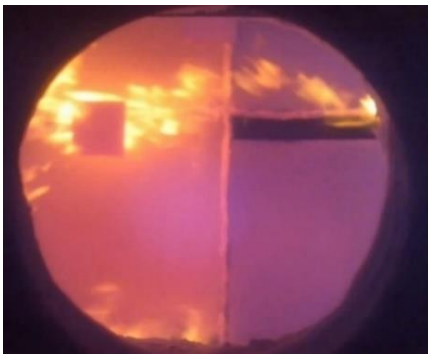


a) Test 3 – Fall-off of plaster system after 17 minutes of testing.



b) Test 4 – Reed board exposed to fire after the fall-off of plaster system.

*Figure 6-26. Furnace Test 3 and Test 4 – Visual documentation of test specimens in furnace.*



a) Fall-off of plaster CT0201 after 29 minutes.



b) Test specimen after removal from the furnace.

*Figure 6-27. Furnace Test 6 – Visual documentation of plaster through the furnace window during the fire test and after its removal from the furnace wall.*

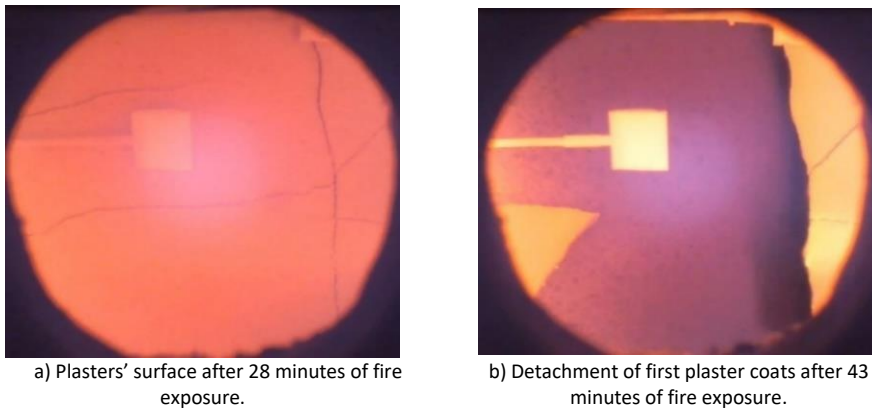


Figure 6-28. Furnace Test 8 – Visual documentation of plaster through the furnace window during the fire test.

Figure 6-29 presents the mean temperature rise recorded behind the clay plaster systems and reed board: dotted line refers to temperatures measured behind plaster system (on reed board); the continuous lines indicate the temperatures measured on the timber element (behind the reed board). The arrows show the difference of both recorded temperatures in each test. Tests 3 and 4 demonstrate that once the plaster system has fallen off (after 17 or 18 minutes), the temperature of the timber surface was still maintained at around 100°C for some time due to the protection effect provided by the reed board. In case of wall tests, the plaster systems stayed mainly in place and therefore, an increased protection time for timber was observed. In Test 6, 23 mm thick plaster system and 50 mm thick reed board, the temperature measured on the timber element was still below 300°C (i.e., start time of charring of timber) after 60 minutes of fire testing, see the black continuous line denoted as Test 6 – Timber\_23. The increase in temperature measured on reed board and on timber element is significantly delayed in case of 44 mm thick plaster system, the timber started to char at about 90 minutes after testing (Test 8 – Timber\_44).

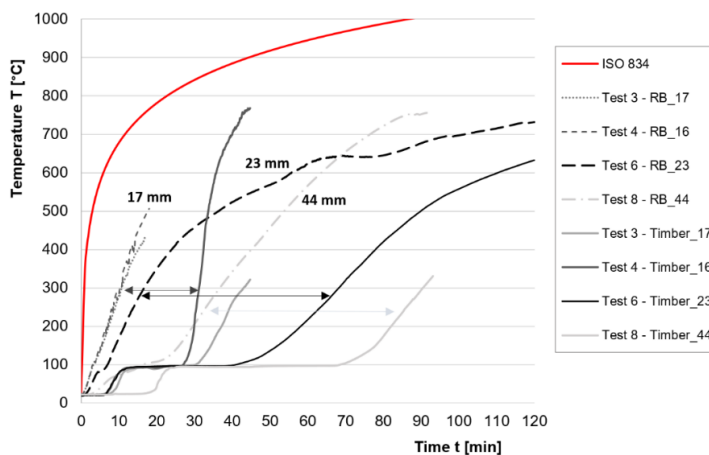


Figure 6-29. Mean temperature curves recorded on the fire-exposed side of the reed board (RB) and on the timber element (Timber) for each furnace test (Test 3, 4, 6, 8), protected by various clay plaster system thicknesses.

### 6.3.1.3 Lime plaster systems

Table 6-9 provides a summary of the test results for the lime plaster systems evaluated in the furnace tests in TP3 and TP4. Figure 6-30 and Figure 6-33 present documentation of the performance of the plaster systems. In TP3, the test results showed that the plaster thickness is the most influential factor determining the temperature rise behind the various types of lime plaster systems. When the lime plaster system (LimeSU04) was tested on a reed mat, crack development on the plasters' surface was observed (Test 11a, Test 12a). However, no cracks were detected when the cement component was added to the lime plaster (LimeSUC04, Test 12b).

Tests with wire mesh as a plaster carrier demonstrated almost no plaster cracking, except for Test 10a, in which a visible crack developed at the very end of the test. In Test 11, a direct comparison of the effect of the plaster carrier is observed: in case of a reed mat (Test 11a), cracks started to form 20 minutes after testing, but no cracks were detected for 60 minutes when a wire mesh was used (Test 11b).

Figure 6-31 presents the mean temperature measurements behind the plaster systems obtained during the furnace tests of TP3. The plaster thickness predominantly affects the increase of temperature on timber; a substantially slower temperature increase on timber is achieved by 30 mm thick lime plasters. The temperature increase behind 30 mm thick LimeSU04 on wire mesh and reed mat showed some slight difference (Test 11). It may be due to the air gaps formed by the reed stems; the rate of temperature rise is thereof slightly reduced compared to the use of a wire mesh which does not incorporate any air gaps. Herein, it may be further argued if the carbonisation of the lime plaster itself is influenced by the different plaster carriers used. However, the level of carbonisation was not examined within the scope of this work. The protection effect provided by different types of lime-based plasters (30 mm in thickness) tested on wire mesh did not show any significant difference in their performance. After 200°C measured on timber, only the LimeSU04 showed somewhat slower temperature rise that is most probably related to its higher calcite concentration in the plaster mix (Appendix 1).

Table 6-9. Furnace test results for lime plaster systems – observations.

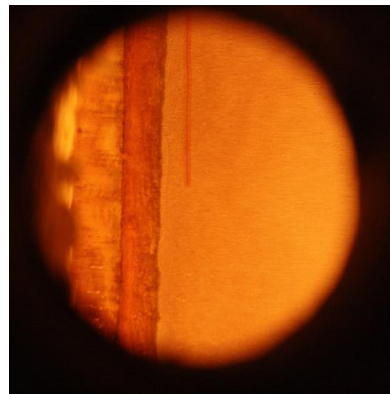
Test No	Plaster Ref.	Plaster carrier	Plaster thickness [mm]	First visible crack in plaster [min]	Mean temperature behind plaster after first cracks [°C]	Total test time [min]	Visual documentation Ref. to Figure
10a	LimeSAK01	Wire mesh	30	56	542	60	Figure 6-30a
10b	LimeCSU04	Wire mesh	30	no	-	60	Figure 6-30b
11a	LimeSU04	Reed mat	30	20	111	60	Figure 6-30c
11b	LimeSU04	Wire mesh	30	no	-	60	Figure 6-30d
12a	LimeSU04	Reed mat	20	17	231	60	Figure 6-30e
12b	LimeCSU04	Reed mat	20	no	-	60	Figure 6-30f
15	LimeSU04	Reed mat	30	30*	390	42**	Figure 6-33

\*Cracking was related to the performance of the reinforcement mesh.

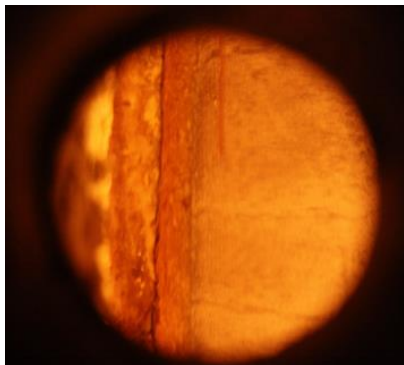
\*\*Fall-off of plaster system, partially linked to the failure of the reinforcement mesh.



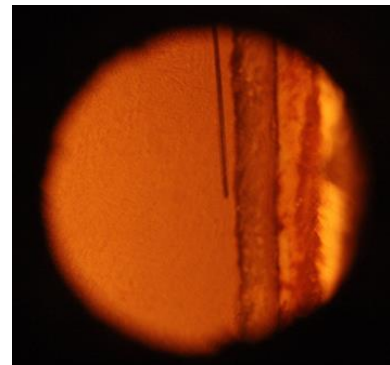
a) Test 10a – LimeSAK - Plaster surface after the removal of the test specimen from furnace.



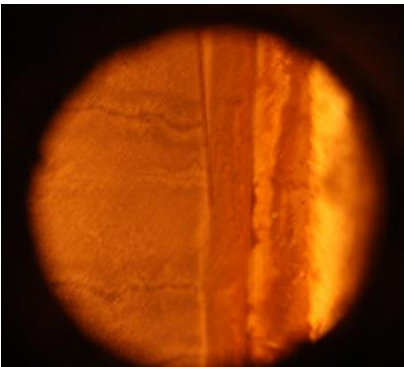
b) Test 10b – LimeCSU04 - View of the plaster's surface through the furnace window opening.



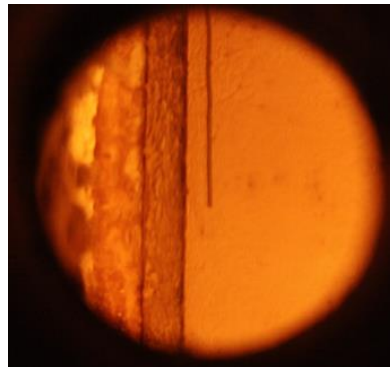
c) Test 11a – LimeSU04 - Visual cracks developed along the reed stems in a reed mat.



d) Test 11b – LimeSU04 – No visual cracks throughout testing when wire mesh was used.



e) Test 12a – LimeSU04 on reed mat - Cracks developed after 17 minutes of testing.



f) Test 12b – LimeCSU04 on reed mat - No visible cracks developed during the test.

*Figure 6-30. Visual observation of the performance of various lime plaster systems in TP3.*

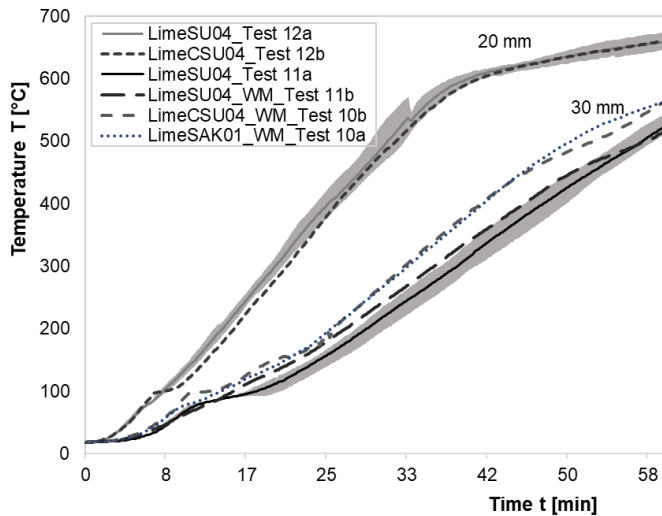


Figure 6-31. Mean temperature curves measured at the interface of plaster and timber in TP3.

Figure 6-32 presents the temperature rise behind the plaster system measured in Test 15. The temperature measurements vary rather significantly over the entire exposed side of the timber element. The temperature curves marked in solid lines in Figure 6-32 indicate the locations of TC positioned in the centre of the test specimen (see Figure 5-13). The temperature increase of TC4, TC5, and TC6 change noticeably after about 15 minutes of fire testing. This may indicate the probable separation of plaster system from timber and is likely to be connected to the performance of the glass fibre mesh in the plaster system. Outside of the element's core region, the rate of temperature increase is notably slower, which may also indicate a greater degree of carbonisation of the lime plaster towards the element's perimeter. The test indicated that the glass fibre reinforcement mesh influences the performance of the lime plaster system. After approximately 30 minutes, the first crack in the plaster system was developed, which was likely related to the beginning of the failure of the glass fibre mesh. The manufacturer has declared that the blackening decomposition temperature is  $> 350^{\circ}\text{C}$  and the classification temperature is  $500^{\circ}\text{C}$  for this certain mesh. Consequently, the plaster system retained its structural integrity until the failure time of this mesh (Figure 6-33). As indicated in Section 5.4.2, the sides of the plaster system were covered with a rock wool fibre of 10 cm in width fixed onto the exposed perimeter sides of the specimen, Figure 6-33a). This was done due to the sudden failure of the lime plaster system observed in Test 14 after just about 3 minutes of fire testing. Therefore, in Test 15, the stone wool fixed on sides appeared to have a directly influence on the longer test time, thus no early fall-off of the plaster system occurred.

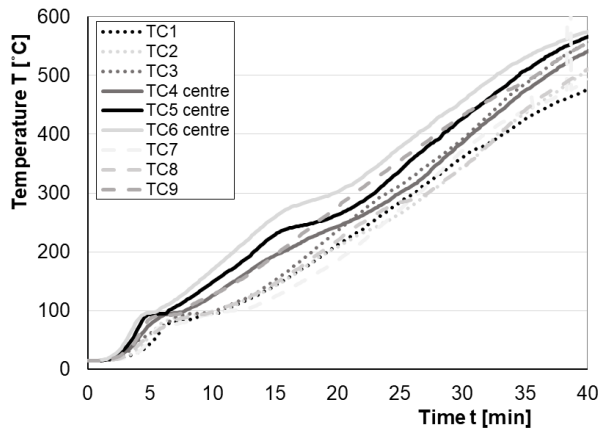


Figure 6-32. Temperature measurements at the interface of lime plaster system and timber element in Test 15 (TP4).



a) Test specimen is lifted to the furnace.

b) View from the furnace window opening – Plaster before its fall-off.

Figure 6-33. Test 15 carried out in TP4 – before and during the fire test.

### 6.3.2 Analysis of the charring performance of timber

The analysis of test data obtained from furnace tests is divided into three parts related to the tested fire protection systems and their comparison:

- i) Clay plaster and reed-based materials;
- ii) Lime plaster systems;
- iii) Comparison between lime and clay-based plasters.

#### 6.3.2.1 Clay plaster and reed-based materials

The furnace test results for clay plaster system are given with respect to its application on timber element. Table 6-10 presents the results when clay plaster was applied with a reed mat directly on timber. Table 6-11 presents the results when plaster system was applied on a reed board that was secured with screws to the timber element. In each test, there was some deviation in temperature recordings (e.g., to reach 270°C and 300°C) across the unexposed side of the plaster systems, thus a standard deviation (SD) is also included in the tables. For thinner plaster systems, the SD was lower. The highest SD was determined for the 44 mm thick plasters (Tests 7 and 8), which may be mainly attributed

to cracking and detachment of plaster layers observed throughout the test. Additionally, the positioning of the reed stems in the reed mat over the timber surface may also have had some impact on the heat transfer mode through the plaster system.

*Table 6-10. Furnace test results for clay plaster system with reed mat – mean values determined from temperature recordings and fall-off times.*

Test No	Test orientation	Plaster Ref.	Plaster system' thickness	Time reaching 270°C behind plaster	SD of time reaching 270°C	Time reaching 300°C behind plaster	Fall-off time of plaster
			$h_p$ [mm]	$t_{270}$ [min]	[min]	$t_{300}$ [min]	$t_f$ [min]
0*	ver	SF04	10	8.2	0.9	8.8	No
01	ver	SF04	30	27.6	0.6	29.5	No
1	hor	SU0401	17	12.5	0.8	13.7	75
2	hor	SU0401	17	12.2	0.4	13.6	62
5A	ver	SU0401	20	17.4	0.3	18.8	No
5B	ver	SU0201	20	16.3	2.0	18.1	No
5C	ver	CT0401	20	14.2	1.8	15.8	No
5D	ver	CT0201	20	13.9	1.6	15.3	No
7	ver	SU0401	44	42.9	2.4	46.6	64**
9a	ver	SU04	30	26.6	1.3	28.7	No
9b	ver	SF04	30	27.9	1.9	30.2	No
13	hor	CT04	20	14.3	1.7	15.8	19

\*No reed mat used.

\*\*Partial detachment of the first layers of the plaster system.

Figure 6-34 shows the times to reach 300°C (i.e., start time of charring) behind the clay plaster system in case of reed mat and reed board. In the wall tests carried out in TP2 and TP3, a high correlation between the plaster thickness and the time to reach 300°C behind plaster system was determined. In TP3, an analogue plaster system (ClaySF04) was tested so that a comparison with Test 01 (TP1) could be made. Comparing the mean test results obtained from Test 01 and Test 9b, the times that it took to reach 300°C behind the plaster systems was 29.2 and 30.2 minutes, respectively. This indicates that test results in terms of temperature measurements were very similar despite the different-sized furnaces and slightly different conditioning of the specimens before testing. In Figure 6-34, test results obtained in case of the reed board (Table 6-11) are also shown, which are indicated by the legend extension ‘\_RB’. In the case of clay plaster tested on a reed board, 300°C was reached earlier than compared to the use of a reed mat as a plaster carrier directly on timber. This was to be expected given that reed board is an insulation material with low thermal conductivity. In Test 8, the SD of test results is the highest (about 4.0 minutes). This could be further related to the somewhat shifted placements of TCs that were forced deeper into the reed board when the 44 mm thick plaster system was prepared layer by layer.

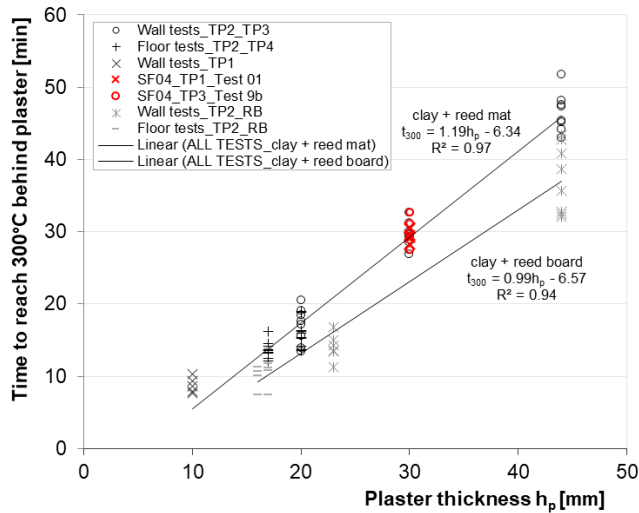


Figure 6-34. Relationship between the thickness of clay plaster systems and the time to reach 300°C behind plaster system in case of reed mat and on a reed board (\_RB).

Table 6-11. Furnace test results for clay plaster systems and reed board – mean values from temperature recordings and determined fall-off times.

Test No	Test orientation	Plaster Ref.	Plaster thickness	Time reaching 270°C on reed board (RB)	SD of reaching 270°C on reed board (RB)	Time of reaching 300°C on reed board (RB)	Time of reaching 300°C on timber	Fall-off time of plaster
			$h_p$ [mm]	$t_{270}$ [min]	[min]	$t_{300}$ [min]	$t_{300}$ [min]	$t_f$ [min]
3	hor	SU0401	17	10.0	1.7	11.0	42.8	17
4	hor	SU0401	16	8.9	1.3	10.2	35.6	18
6A	ver	SU0401	23	13.4	0.3	15.0	68.0	no
6B	ver	SU0201	23	11.7	1.4	12.8	64.7	no
6C	ver	CT0401	23	12.3	0.0	13.5	66.7	no
6D	ver	CT0201	23	13.8	1.6	15.1	74.9	29*
8	ver	SU0401	44	34.5	4.0	37.7	86.0	(43)**; 84**

\*Fall-off of plaster (it fell down in one piece but remained solid while still covering most of the reed board area from direct fire exposure). Charring rate was not determined for this case.

\*\* (Partial detachment of first plaster coats ~15 mm); detachment of ~15mm plaster coat over the whole surface.

The results on the charring of timber behind clay plaster systems with reed mat are presented in Figure 6-35 and given in Table 6-12. Figure 6-35 presents the derived charring rates behind the plaster system (incl. reed mat). In all tests, the total charring time of timber surpassed ~30 minutes, allowing for a reasonable foundation for comparing test results. The charring rate of timber behind the plaster system was determined by

the residual cross-section, by measuring the charring depth and considering the respective charring time. In a comparison of the mean test results for the charring rate of timber, Test 0 and Test 01 exhibited a somewhat slower charring rate than other tests. This may be influenced by the longest charring time compared to the other tests. In addition, as in these tests, the plaster adhered to the sides of the furnace, the plaster itself bent towards the furnace. This behaviour generated some additional air gap between the plaster system and timber, which might have had some effect on the charring rate.

There is a larger scatter of charring rates in case of floor tests (Test 1 and 2) and in one wall test (Test 7). As the temperature measurements from Tests 1 and 2 fluctuated significantly after reaching 500°C beneath the plaster, the difference in charring rates could be directly linked to this. In the case of 44 mm thicker plaster system (Test 7), cracking and layer detachment were observed that had an influence on the charring of timber. Moreover, the tests in TP2, conducted in the model-scale furnace, revealed somewhat uneven fire exposure to the exposed side of the test specimen, as various tests exhibited comparable phenomena that near some of the furnace's corner areas the 300°C was measured earlier than in other areas on the timber surface.

*Table 6-12. Furnace test results for clay plaster and reed mat – mean values of charring of timber behind plaster system.*

Test No	Plaster Ref.	Plaster thickness	Charring time	Charring depth	Charring rate	Protection factor	SD of $k_2$ factor
		$h_p$ [mm]	$t_{char}$ [min]	$d_{char}$ [mm]	$\beta_2$ [mm/min]	$k_2$	
0*	SF04	10	81.2	43.0	0.53	0.81	0.05
1	SF04	30	90.4	33.8	0.37	0.58	0.05
1	SU0401	17	61.4	33.7	0.55	0.84	0.10
2	SU0401	17	48.4	26.0	0.54	0.83	0.05
5A	SU0401	20	71.2	40.0	0.56	0.86	0.00
5B	SU0201	20	72.0	40.0	0.56	0.86	0.03
5C	CT0401	20	74.3	40.0	0.54	0.83	0.02
5D	CT0201	20	74.8	40.0	0.54	0.82	0.02
7	SU0401	44	32.4	11.6	0.36	0.55	0.09
9a	SU04	30	31.3	13.8	0.44	0.68	0.02
9b	SF04	30	29.8	13.0	0.44	0.67	0.04

\*No reed mat used.

Tests with plaster thicknesses of 20 mm and 30 mm (T2, TP3, Figure 6-35) revealed that the charring of the timber element varied less, which is consistent with the fewer cracking observed on the surface of the plasters. Overall, all test results showed a good correlation in view of the plaster systems' thickness and respective charring rates. Figure 6-37 shows the documentation of a timber specimen directly after the fire tests (Figure 6-37a) and the residual cross-section of the timber lamella (Figure 6-37b).

The protection factor  $k_2$  was calculated using the basic design charring rate given in EN 1995-1-2 that is 0.65 mm/min for softwoods. Table 6-12 shows the calculated values for each plaster system tested, and the results are presented in Figure 6-36. With respect to the thickness of the plaster systems, a mean trendline (solid line) and a worst-case trendline (dashed line) are presented for the protection factor. The results from TP1 are

separately shown. In addition,  $k_2$  values obtained from the midsection of the test specimen (positions of TC) are shown in Figure 6-36 as “All tests\_C\_TP2\_TP3” marked with red crosses. An apparent variation of  $k_2$  values is evident in case of the floor tests (Tests 1 and 2), which can be further explained by the formation of cracks that increase heat transfer to the timber element (Figure 6-18). In addition, the self-weight of plaster may have gravitated to some degree, creating more space for air circulation at the interface between plaster and timber. For the 44 mm thick plaster system, the deviation of values is related to the development of cracks and, ultimately, the detachment of the outer plaster layers from the plaster system (Figure 6-20). The higher  $k_2$  values (in most cases) indicate the locations of the plaster system where cracks were observed.

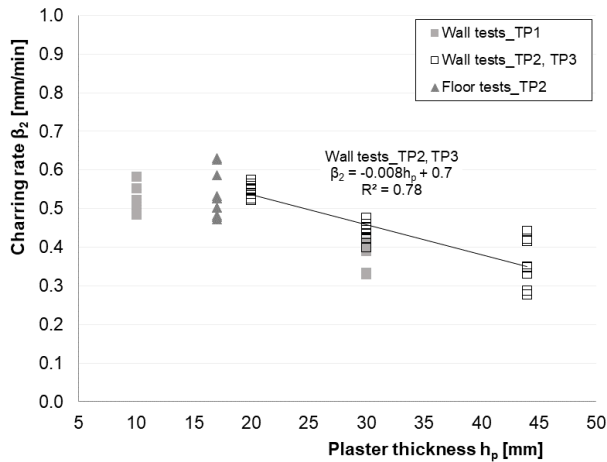


Figure 6-35. The charring rates of timber protected by clay plaster systems in relation to the thickness of plaster, determined in furnace tests.

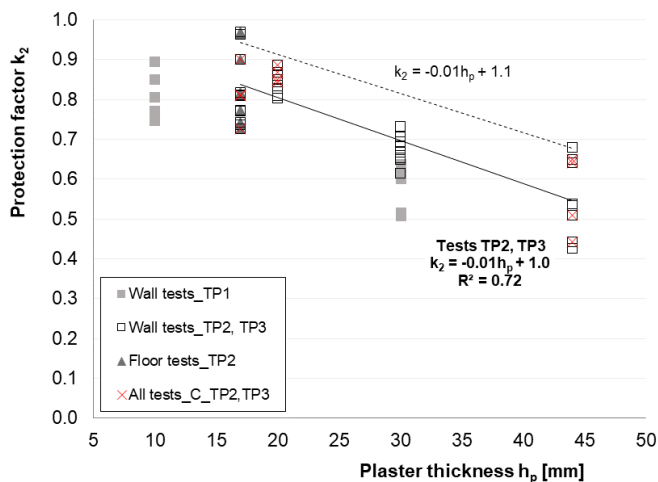


Figure 6-36. The protection factors for clay plaster systems (with reed mat) in relation to the thickness of plaster; obtained from the furnace tests.

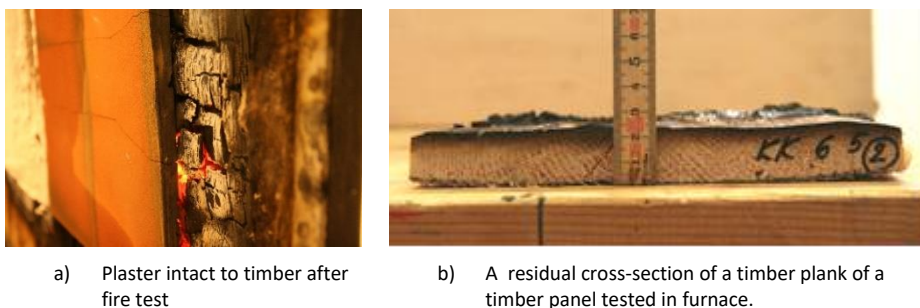


Figure 6-37. Documentation of the timber specimen after furnace tests (TP2).

In TP2, clay plaster systems were additionally tested on reed board. In case of the tests performed in horizontal position, the plaster fell off from the reed board after some time of testing (when the temperature at the interface of plaster and reed board was about 400–500°C); yet, the reed board remained in place after the fall-off of plaster and protected the timber element from charring up to some time. The visual documentation of the board after fire test is presented in Figure 6-38. As the protective effect of the 50 mm thick reed board for timber was evident, its protection ability was calculated based on the temperature recordings (measured by the inserted TC) on both sides of the reed board. The charring rates of reed board (i.e., recession speed), which represent the propagation of the 300°C isotherm through the board, was calculated from the test results and are given in Table 6-13. The charring rate was calculated by dividing the boards' thickness to the calculated charring time of the board, see Table 6-13. The charring time was calculated by the temperature measurements of reaching 300°C on both sides of the reed board (behind plaster and on timber).

Table 6-13. Furnace test results for clay plaster and reed board (50 mm) – mean values of charring of timber behind plaster system.

Test No	Test orientation	Plaster Ref.	Plaster thickness [mm]	Charring time of reed board	Start time of charring of timber	Recession speed of reed board
				$t_{\text{char, RB}}$ [min]	$t_{\text{ch}}$ [min]	$v_{\text{rec}}$ [mm/min]
3	hor	SU0401	17	33.7	42.8	1.48*
4	hor	SU0401	16	25.2	35.6	1.98*
6A	ver	SU0401	23	54.3	69.3	0.92
6B	ver	SU0201	23	51.9	64.7	0.96
6C	ver	CT0401	23	52.0	65.5	0.96
6D**	ver	CT0201	23	59.8	74.9	0.85
8	ver	SU0401	44	53.3	76.7	1.07

\*Minimal influence from the protection effect from the plaster system due to its fall off.

\*\* The plaster system fell down after 29 minutes but stayed in front of the reed board until the end of test.

In case of floor tests (Test 3 and Test 4), the recession speed of the reed board was determined in the range of ~1.5–2.0 mm/min. Herein, the calculation of recession speed only considered the TC measurements taken from the centre of the test specimen (see the positioning of TC3, TC4 in Figure 5-13a), thus the extensive flaming and effects from

the sides of the specimen were neglected. This recession speed of  $\sim 1.5\text{--}2.0$  mm/min represented little influence from the plaster system due to its early fall-off. In the wall tests, the average recession speed was calculated about  $\sim 1$  mm/min, but which was influenced by the protection effect from the plaster systems that did not fall-off and stayed in place during the whole test. This different recession speeds determined in floor and wall tests is foremost attributable to the influence from the fire protection contribution provided by the plaster systems in case of wall tests. In Test 8, a recession speed of 1.07 mm/min was determined that is roughly similar to the one determined in case of 23 mm plaster. This could be explained by the detachment of the first layers in Test 8, which increased heat transfer through the remaining plaster system and resulted in an increased recession speed of the reed board. Test results showed that if the plaster system stays intact to the reed board, the recession speed of the reed board is slower. The results of clay plaster systems have also been published in conference papers (Liblik et al., 2017; Liblik et al., 2018; Liblik et al., 2018) in view of their potential use in historical buildings.

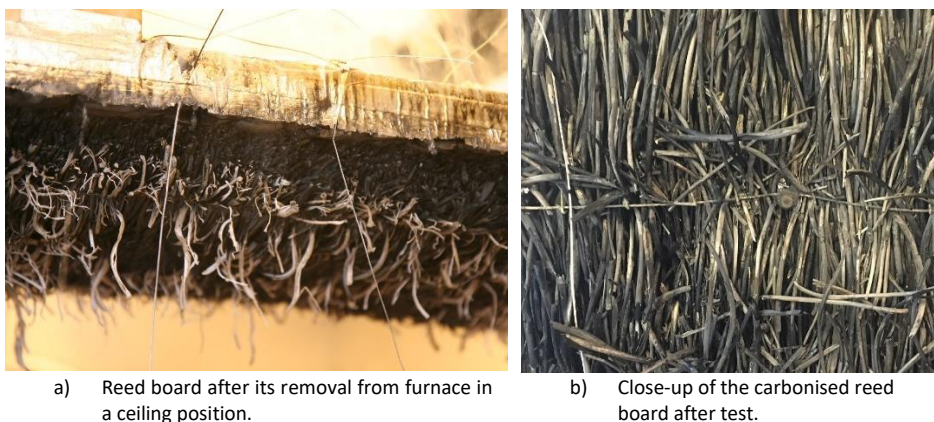


*Figure 6-38. Documentation of reed boards after cooled down with water.*

### **6.3.2.2 Failure time of clay plaster systems**

The fall-off times of plaster systems were observed in several tests. All tests in floor position showed that clay plaster system eventually falls off. When a reed board was applied to timber instead of a reed mat, the plaster system fell off significantly faster (compare Test 1 and 2 to Test 3 and 4, in Table 6-14, values of 'Fall-off in furnace test'). Once the reed board started to carbonize, there was no mechanical key holding the plaster in place, which resulted in the earliest fall-off times. Plaster system fell off because adhesion was lost. The temperatures recorded behind the plaster system at the time of fall-off were between  $400\text{--}500^{\circ}\text{C}$ , which corresponds to the mineralogical changes in the clay plaster itself as well as the carbonisation process of reed board is already undergoing. The reason that the plaster system did not immediately fall off after the start time of charring of  $300^{\circ}\text{C}$  was recorded on reed board may be also influenced by the plaster system's adhesion to the metal wires of the reed board.

The furnace tests showed that the clay plaster functions as a uniform fire protection system with a reed mat by creating a strong bond with the fine metal wires of the reed mat. As a result, when the reed mat is stapled to timber, the fastening system of a reed mat prevents the plaster from falling off. In Tests 1 and 2, when the fall-off times

occurred after 60 minutes of testing, the plaster should have fallen off earlier than the observed time (Table 6-14). The timber element was completely charred to the length of the staples by the time the fall-off times were determined. This finding was further supported by the additional test conducted in TP4, where the fall-off time correlated with the charring of timber behind the plaster system (Test 13). However, due to the use of staples, it was expected that the plaster would stay attached to the timber panel for a longer time than observed in Test 13. In Figure 6-40b, a visual documentation of a lamella of a timber specimen after a fire test is shown, where it is evident that the wood around the metal staple has been charred compared to the rest of the virgin wood (due to the faster heat transfer in metals). This weakens the bond between the timber and staple, resulting in an earlier fall-off, particularly in floor position. In a vertical position, this does not seem to be such a significant issue since there is no pull-out force from the plaster (gravity). The tests also proved that the plaster stays attached to a timber element for an extended time in case of walls, despite that the total length of the staples were in charred wood.

In Figure 6-39, the fall-off times determined in a furnace are presented. Additionally, calculations based on the 25 mm long staples used to fasten the reed mat to the timber are included to the fall-off times determined in furnace, see Table 6-14 and Figure 6-39. Two calculations (Cal 1 and Cal 2) are presented, wherein Cal 1 implies that the fall-off time occurs when the timber is fully charred over the entire length of the staple (25 mm). The second calculation (Cal 2) was based on the design equation specified in EN 1995-1-2:2004 for estimating the fall-off time of gypsum plasterboards, given that 10 mm of the fastener must remain in the uncharred wood.

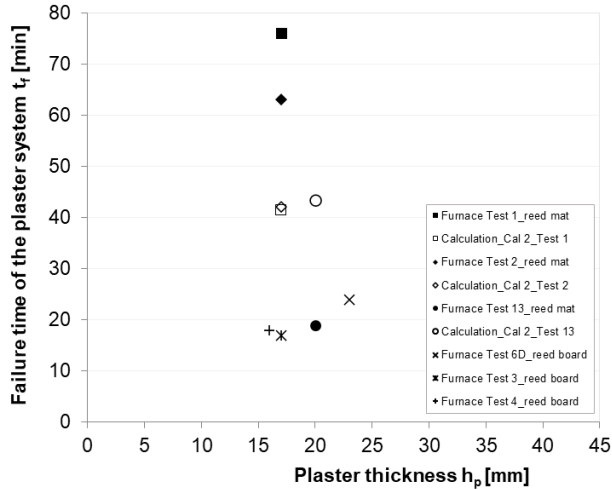


Figure 6-39. The fall-off times of clay plaster systems obtained from furnace tests, accompanied by estimations based on calculations.

Table 6-14. The test results of fall-off times and calculated fall-off times for clay plaster systems.

Test No	TP	Plaster thickness $h_p$ [mm]	Plaster carrier	Fall-off time determined in furnace test $t_{f,test}$ [min]	Time till complete charring of anchorage length $t_{f,cal 1}$ [min]	Calculated fall-off time Cal 2 $t_{f,cal 2}$ [min]
1	TP2	17	reed mat	76	60	41
2	TP2	17	reed mat	63	61	42
3	TP2	17	reed board	17	n/a	n/a
4	TP2	16	reed board	18	n/a	n/a
6D	TP2	23	reed board	24	n/a	n/a
7	TP2	44	reed mat	64*	116	88
8	TP2	44	reed board	43*	n/a	n/a
13	TP4	20	reed mat	19	62	43

\*Partial detachment and fall-off of first plaster layers.

There was no fall-off of plaster system detected when the clay plaster and reed mat were tested in vertical position. In the case of a thicker plaster system (44 mm, Test 7), a detachment of plaster layers was observed. In Figure 6-39, results from Tests 7 and 8 (noted with an asterisk) correspond to the times of detachment of the first layers, not the whole plaster system (as in the other tests). Figure 6-40a shows the inner layers of the plaster system that remained affixed to the timber after a fire test and its cooling down with water (Test 7). This phenomenon of a layer detachment may be linked to the large temperature gradient within the thick plaster system and the movement of moisture and vapour inside the plaster layers, which generates excessive thermal stresses in the plaster system and results in cracks and layer detachment. In case of 30 mm thick clay plaster systems (TP1 and TP3), no layer detachment was detected. In TP3, it may be argued that the furnace size was too small to determine this phenomenon; however, Test 01 (TP1) was performed in the same furnace as Test 7 in TP2 that also did not show any layer detachment, solely the cracking of plaster itself. Thus, the detachment of plaster layers appears to be attributable to a relatively thick plaster systems, e.g., more than 40 mm.



a) Clay plaster after the detachment of the outer plaster layers on timber.



b) Close-up of a timber plank of a timber panel with a pulled-out staple.

Figure 6-40. Documentation of test specimens after fire test.

### 6.3.2.3 Lime plaster systems

Lime-based plasters were tested in TP3 and TP4. The test results are shown in Table 6-15 for the relevant temperature points of interest, 270°C and 300°C. Despite the different compositions of plaster mixes (Table 5-2), all plaster systems (tested in TP3) of the same thickness had a similar protection effect, e.g., Test 12a and Test 12b; Test 10a, Test 10b and Test 11b).

The test results from both TPs are shown in Figure 6-41 as a function of plaster systems' thickness, since the thickness of the plaster was the most significant factor influencing the temperature rise behind plaster systems. However, the type of plaster carrier also seemed to have some impact on the heat transfer mode. Consequently, the results are mainly discussed with regards to the TP and the type of plaster carrier.

Table 6-15. Furnace test results for lime plaster systems – mean values of temperature measurements.

Test No	Plaster Ref.	Plaster carrier	Plaster thickness $h_p$ [mm]	Time reaching 270°C behind plaster $t_{270}$ [min]	Time reaching 300°C behind plaster $t_{300}$ [min]	SD of time reaching 300°C behind plaster [min]
10a	LimeSAK01	wire mesh	30	30.9	33.2	1.3
10b	LimeSUC04	wire mesh	30	30.6	32.9	1.1
11a	LimeSU04	reed mat	30	37.1	39.9	3.1
11b	LimeSU04	wire mesh	30	33.3	36.1	1.5
12a	LimeSU04	reed mat	20	19.7	21.4	3.3
12b	LimeSUC04	reed mat	20	19.1	20.7	1.8
14	LimeSU04	reed mat	20	-	-	-
15	LimeSU04	reed mat	30	22.0	24.5	2.5

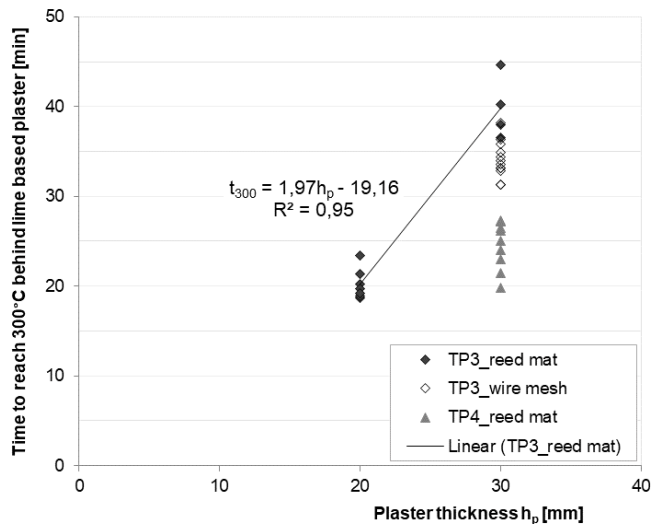


Figure 6-41. Relationship between the lime plaster systems' thickness and time to reach 300°C behind lime-based plasters tested in TP3 and TP4.

In TP3, a reed mat and a wire mesh were used to assess the effect of the plaster carrier on the performance of one of the plaster systems (LimeSU04). The results of Tests 11a and 11b (30 mm thick plaster, LimeSU04) showed that the average start times of charring in case of reed mat and wire mesh are 39.9 and 36.1 minutes, respectively. The reed mat appears to act as an air pocket in the plaster system, delaying the heat transfer and extending the time it takes for the timber to char by a few minutes. The reed mat showed a greater standard deviation of  $t_{ch}$  values than wire mesh, 3.1 minutes as compared to 1.5 minutes. This is likely due to the air gaps present in reed mats, which disperse heat transfer. However, it may have also influenced the carbonisation level of the plaster that is unknown.

The comparison of average  $t_{ch}$  values obtained for 30 mm thick plasters on a wire mesh in Tests 10a, 10b, and 11b indicates that timber starts to char somewhat earlier in case of the plasters that had the cement component included in the plaster mixture. However, most probably it is the influence from the amount of calcite in the plaster and the total carbonisation level, which slows down the heat transfer in the plaster. The average  $t_{ch}$  values for plaster systems LimeSAK and LimeSUC04 (which both included cement) were 33.2 and 32.9 minutes, respectively. The average  $t_{ch}$  value for plaster LimeSU04 (without cement) was 36.1 minutes. Based on the comparable  $t_{ch}$  values, it became clear that the differences in the plasters' densities have no significant effect on the start time of charring; rather, the composition of the plaster appears to have a greater impact.

The average  $t_{ch}$  values for 20 mm thick plasters and a reed mat (Tests 12a and 12b) were 19.5 and 20.7 minutes, respectively, indicating that there is no real difference in the time to reach the charring of timber. Thus, the addition of cement component to the pure lime plaster has no significant influence on the heat transfer mode through the plaster. The standard deviation of  $t_{ch}$  seems to correlate to the type of plaster carrier used, as the standard deviations were around 3 minutes compared to the test results with wire mesh that were less than 2 minutes.

In TP4, a similar plaster system (30 mm thick LimeSU04 with reed mat) as tested in Test 11a showed a significantly different average start time of charring, 24.5 minutes (Test 15) compared to 39.9 minutes determined in TP3. While comparing the results, the following differences of tests can be made: i) the position of the specimens in the furnace; ii) the size of the specimen; and iii) the carbonisation time and level of the plaster system. The same test hall conditions were used for specimen preparation and conditioning. Despite the different sizes of the specimens and furnaces, comparable testing series have previously been conducted with clay plaster systems, with agreeable test results (TP2, TP3, TP4). This indicates that the cause of this notable difference observed in case of this lime plaster is a material-specific characteristic, most likely connected to its carbonisation and hardening processes. In addition, a potential influence from the specific timber specimen and the size and thickness of the test specimens could have had some impact on the hardening process of the plaster layers. This should be further evaluated to better understand these phenomena (e.g., moisture movement and evaporation; also, the exposed surface area for carbonisation). According to previous research (Pachta et al., 2018), the compressive strength (which is directly related to the carbonisation time and depth) is said to be one of the most relevant metrics for the behaviour of mortars at high temperatures. These mechanical properties of plasters were not assessed in this study; plasters were applied by professionals, and

preparation of plaster systems followed the preparation guidelines as implemented in practise.

Figure 6-42 presents the calculated protection factors with respect to the thickness of plaster systems. The results for 20 mm thick plasters show a large scatter of  $k_2$  values, despite of demonstrating a similar average time to reach the start time of charring (19.5 and 20.7 minutes, respectively). In case of 20 mm plasters, the LimeSU04 seems to have slightly higher fire resistance as the protection factors are somewhat lower than for LimeCSU04. Lower protection factor results in a slower charring rate of timber behind the plaster system.

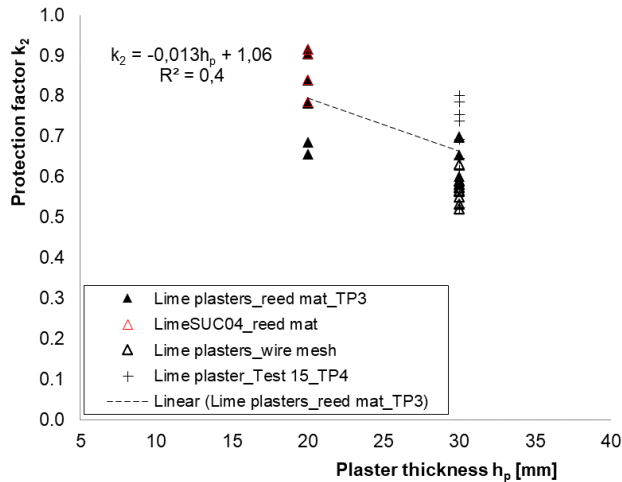


Figure 6-42. The protection factors for lime plaster systems obtained from the furnace test results.

Table 6-16. Test results on the charring of timber protected by lime plaster systems in furnace.

Test No	Plaster Ref.	Plaster carrier	Plaster thickness $h_p$ [mm]	Charring time $t_{char}$ [min]	Charring rate $\beta_2$ [mm/min]	Protection factor	SD of $k_2$
						$k_2$	
10a	LimeSAK01	wire mesh	30	26.8	0.37	0.57	0.01
10b	LimeSUC04	wire mesh	30	27.5	0.39	0.60	0.03
11a	LimeSU04	reed mat	30	20.2	0.43	0.66	0.04
11b	LimeSU04	wire mesh	30	23.9	0.36	0.55	0.02
12a	LimeSU04	reed mat	20	38.6	0.47	0.73	0.06
12b	LimeSUC04	reed mat	20	39.3	0.56	0.86	0.05
15	LimeSU04	reed mat	30	17.5	0.44	0.68	0.09

On the basis of the charring profiles of cut timber specimens (see Figure 6-43) and measurements, it was observed that, in addition to the plaster thickness, the charring is somewhat influenced by other factors: i) the edge-glued joints; ii) the grain orientations of timber specimens and iii) presence of the knots (Figure 6-43, below). Test results include this indirectly. Nevertheless, the charring of wood panels may still be considered relatively uniform across their cross-section.



Figure 6-43. The cross-section of timber panels protected by 30 mm thick plasters:  
Above – LimeSU04 and reed mat; Below – LimeSU04 and wire mesh.

The 30 mm thick plasters tested on wire mesh (Test 10a, 10b, and 11b) showed relatively similar charring rates of timber (0.37, 0.39, 0.36 in mm/min, respectively). Despite the differences in their composition and density, as well as the cracking of LimeSU04, there is a strong correlation of  $k_2$  values when wire mesh is used as plaster carrier. Wire mesh appears to have a smaller effect on the heat transfer mode in comparison to reed mat, which explains why there is less variation in the charring performance of timber when using wire mesh. The average calculated  $k_2$  values for 20 mm thick plasters, LimeSU04 and LimeSUC04, were 0.73 and 0.86, respectively. Herein, the difference appears to be related to the specifics of the plaster mix (and cracking of plaster) as both plasters were tested on reed mat.

In TP3, the largest scatter of  $k_2$  values apply to the test results for 30 mm thick plaster LimeSU04 (SD 0.04) compared to the same plaster tested on wire mesh (SD 0.02). In case of Test 15, the SD was 0.09. Same plaster system was tested in Test 11a and Test 15, and despite the different times to reach the start time of charring, the charring rates obtained in Test 11a and Test 12 are comparable: 0.43 mm/min and 0.44 mm/min. The comparison seems adequate due a similar charring time of timber, 20.2 and 17.1 minutes, respectively. Interestingly, in TP3, the comparison of charring rates behind 20 mm and 30 mm thick same plaster LimeSU04 showed very similar charring rates 0.43 mm/min and 0.47 mm/min. However, in this case the charring times differed significantly 20.2 minutes in case of 30 mm plaster and 38.6 minutes for 20 mm plaster. This might indicate that in order to compare the charring rates behind plaster systems, the charring times should be as similar as possible or at least 30 minutes long (Chapter 4). However, the impact of the reed mat should also be considered here, as it may alter the hardening process of the plasters, including the differences in their thicknesses, e.g., resulting in different carbonisation levels and thereof different protection effect.

While Test 15 indicated a significant difference in the time to reach the start of charring in comparison to a similar plaster system evaluated in TP3, the protection factor appeared to be in good agreement with those found in Test 11a. In both instances, the charring period was around 20 minutes, and the mean protection factors were 0.68 (Test 15) and 0.66 (Test 11a). This may imply that, after the timber starts to char, the carbonisation level of lime plaster has little effect on the charring rate behind the plaster; rather, the carbonisation level and application process and hardening of lime plaster seem to have the greatest impact on the start time of charring. Test 15 showed

that lime plaster system fell-off after 42 minutes. At about 15 minutes of fire testing, the central part of the plaster system appeared to have slightly separated from the timber element (Figure 6-32). Because the plaster system was reinforced with glass fibre mesh, it seemed to be stayed intact until the mesh lost its mechanical strength (related to its critical temperature point). This phenomenon demonstrates that the reinforcement mesh could contribute to the fire performance of plaster systems, preventing their cracking and earlier failure time.

### 6.3.2.4 Comparison between clay and lime-based plasters

This comparison is made between tests in which reed mat was used as a plaster carrier. Figure 6-44 presents a comparison of furnace test results on the start times of charring between clay and lime plaster systems. Test 14 and Test 15 of TP4 were not included in this analysis due to the performance of the lime plaster (LimeSU04) described in Chapter 6.3.1, making them not directly comparable.

Based on a comparison, the start time of charring is more delayed in case of lime plaster systems and this time appears to increase with increasing thickness. This phenomenon could be mainly attributed to the different binders (composition) used in the plaster. The TGA test results indicated that lime plasters had a significant mass loss at high temperatures compared to clay plasters, which likely delays the heat transfer because of the decomposition of calcium carbonate. Also, the impact of the reed mat to the heat transfer mode could be considered lesser than in case of 20 mm plaster, thus the effect from the thermal properties of lime plaster is more emphasised. This could additionally explain the more significant difference in time to reach 300°C behind lime and clay plasters.

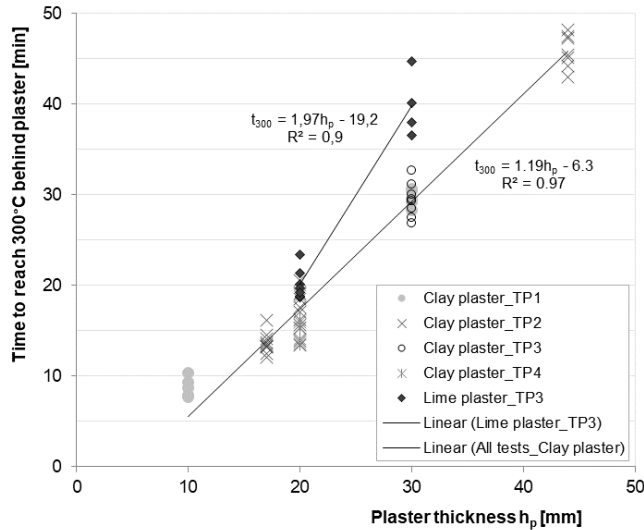


Figure 6-44. Comparison of furnace test results to reach the start time of charring behind clay and lime plaster systems.

The protection factors in relation to plaster thickness are shown in Figure 6-45. The  $k_2$  values for 20 mm and 30 mm lime and clay plasters are within the same range. There is a variation of  $k_2$  values for each plaster system thickness, that is impacted by the specifics of the reed mat, the plaster's compactness on the reed mat, and the cracking. In case of

clay plaster systems, the detachment of plaster layers during the test also had an influence. Regarding the charring performance of timber, the mean protection factor values obtained for both plaster systems are in good agreement. This shows that the charring rates of timber behind these clay and lime-based plaster systems are similar until their failure time. In both cases, the highest protection factors regarding a certain plaster thickness were mainly determined when the plaster systems were tested in ceiling position (see the protection factors for plaster thicknesses 17 mm, 20 mm, and 30 mm in Figure 6-45).

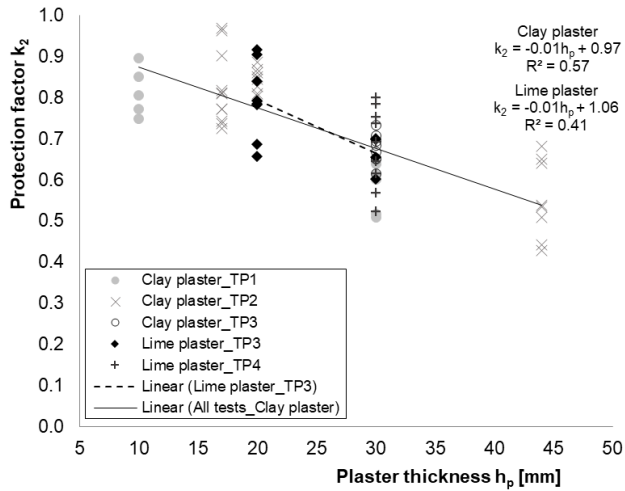


Figure 6-45. Comparison of protection factors between clay and lime-based plaster systems obtained from the furnace tests.

## 6.4 Comparison of test results between cone and furnace tests

The relevant design values of  $t_{ch}$  and  $k_2$  derived from various tests are compared and presented. The comparison of test results is undertaken separately for clay plaster and lime plaster systems due to their specific test programs presented in Chapter 5.3 and Chapter 6.2. The comparison of test results is also published in (Liblik et al., 2022, 2023).

### 6.4.1 Clay plaster systems

Figure 6-46 compares the recorded values for the start time of charring of timber ( $t_{ch}$ ) from both test methods in case of a clay plaster (incl. a reed mat). Solely in case of 10 mm plaster, no reed mat was used. Results from cone tests (TP1 and TP2) are reported separately owing to a difference in the heating scenario used (Figure 5-9). The comparison of these tests was presented in Figure 6-10a. The results of both cone test programs (TP1 and TP2) indicate a somewhat earlier onset of charring for all types of plaster systems compared to the ones obtained in furnace. This is acceptable given the range of  $t_{ch}$  values recorded in the furnace and the fact that the cone test results should provide a conservative estimate. In cone testing, there was no evidence of plaster cracking; hence, the average values are a valid basis for comparison, as they also demonstrate a good correlation with the earliest start times of charring obtained in furnace tests (i.e., the worst-case scenario).

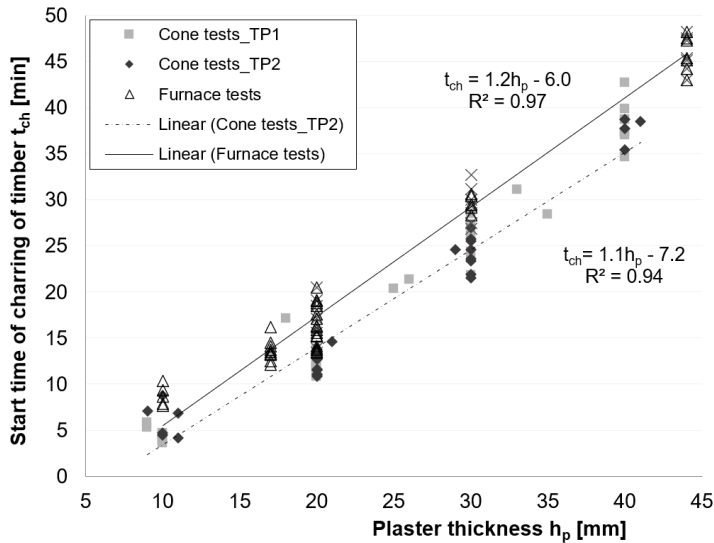


Figure 6-46. Comparison of start times of charring of timber protected by clay plaster system and reed mat as a plaster carrier.

Figure 6-47 compares the charring rates obtained from the cone tests and furnace. The results indicate that the charring of timber specimens determined in the cone heater tests do not agree to the charring of timber in furnace when protected by plaster systems. Despite of the acceptable agreement to reach the start time of charring of timber in cone and furnace tests behind plaster systems, the charring rate behind plaster is underestimated in cone tests. When comparing the cone test results, it is apparent that the charring rates determined in TP1 for plasters thicker than 20 mm are much lower than the ones obtained in TP2. This is principally because of the total test duration of 60 minutes in TP1, whereas in TP2 it was 40 minutes. In case of 10 mm plaster thickness, there is rather good agreement between all test results. In view of cone tests, this might be explained by the relatively thin plaster layer, which resulted in lesser heat loss from the sides (compared to thicker plasters) and a respectively faster charring rate of timber in general (as some of the 10 mm thick plasters also showed some cracks). In case of unprotected timber specimens, the basic charring rate in cone testing was found to be 0.73 mm/min (see Chapter 6.2), which is greater than the rate typically used in furnace tests that is 0.65 mm/min. Unlike to the determination of  $t_{ch}$  values, the charring rates are influenced by the material specific properties of the timber specimen itself, which leads in some variations in the test results as well. Contrary to furnace testing, heat losses from the whole specimen during cone testing may result in lower charring rates than expected. Furthermore, after some time of testing, the heat flux levels do not correlate to the ones in furnace, thus underestimating the heat exposure.

The cone tests of TP2 showed the closest fit to the furnace test results, Figure 6-47. There is a slight overlap between the greatest and lowest charring rates determined (i.e., the lowest charring rate in furnace agrees to the highest one determined in cone tests TP2). In case of 30 mm plaster, a rather close fit to the furnace tests could be related to the fact that the charring time in cone tests was shorter compared to the charring time of timber in case of thinner plaster and to the charring time in furnace.

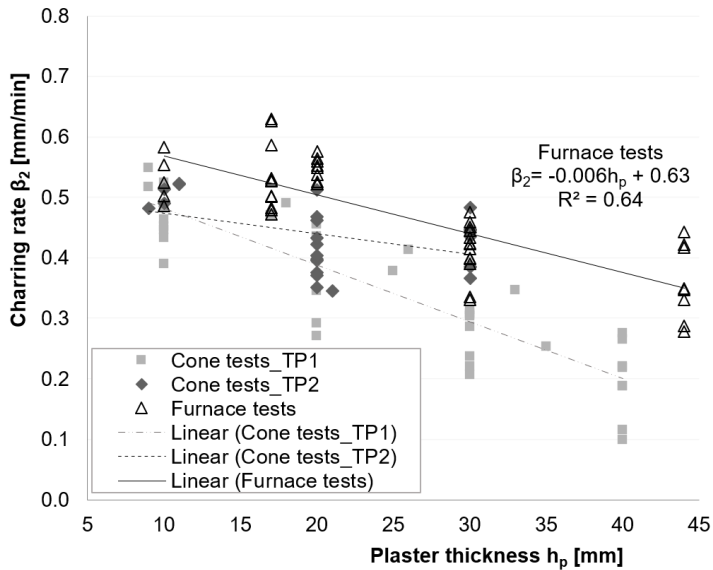


Figure 6-47. Comparison of charring rates of timber protected by clay plaster systems.

The charring performance of timber behind the protection system is expressed by the protection factor  $k_2$ . The  $k_2$  factor is derived from the test results, based on the determined charring rate behind the plaster system and using the basic design charring rate  $\beta_0$ . In case of cone testing, the basic charring rate was determined (Chapter 6.2) and used in this analysis. In the following, only the cone tests of TP2 are included since they indicated a greater correlation with the furnace results.

The comparison of the  $k_2$  values derived from the cone and furnace tests is shown in Figure 6-48. The  $k_2$  values for the furnace tests were calculated using a basic charring rate ( $\beta_0$ ) value of 0.65 mm/min. For cone heater tests (TP2) two different basic charring rates were used 0.65 mm/min and 0.73 mm/min for calculating the  $k_2$  values. In Figure 6-48, the results are presented, denoted as 'Cone tests\_TP2\_0.65' and 'Cone tests\_TP2\_0.73', respectively. The  $\beta_0$  value of 0.73 mm/min was used as it was determined for unprotected timber specimens using the same test setup and heat flux scenario of 50 to 75 kW/m<sup>2</sup> as was used in cone tests with plaster systems in TP2, see Table 6-6. Figure 6-48 illustrates how the  $k_2$  values derived from cone tests significantly overestimate the fire protection performance of plasters since lower values of  $k_2$  indicate slower charring. Although the basic charring rate of 0.65 mm/min is deemed suitable in a furnace (given in EN 1995-1-2), the use of a basic charring rate determined in cone (0.73 mm/min) is inadequate when compared to the test results obtained from furnace. The cone heater test results clearly indicate lower charring rates of timber behind plaster that is partly related to the heat flux scenario that is not capable of following the ISO834 curve after about 20 minutes (Chapter 4) accompanied with heat losses from the specimen during the cone testing. Yet, it must be said that this underestimation appears to occur only when timber is protected, as in case of unprotected timber specimens, the obtained charring rates were rather similar to the ones measured in furnace and also determined by previous studies (Chapter 4), see cone heater test results from this thesis presented in Chapter 6.2.

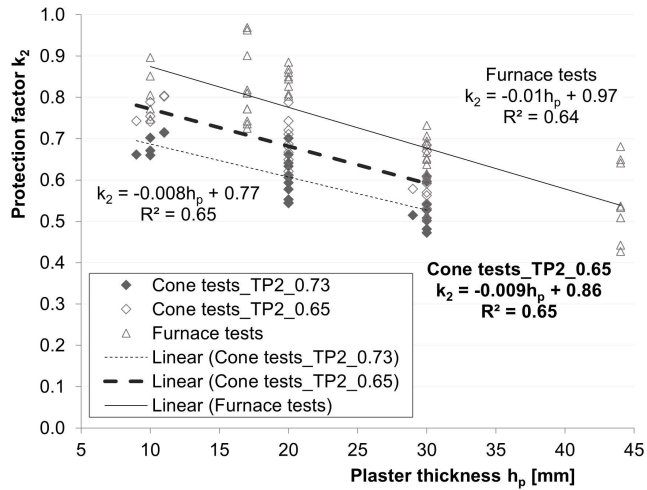


Figure 6-48. Comparison of protection factors of clay plaster systems.

Regarding the range of plaster thicknesses, however, the general trend in the charring performance of timber indicates a similar decrease in the  $k_2$  factor for both cone and furnace tests. Compared to the  $k_2$  values obtained in furnace, the values from cone testing in case of 'Cone tests\_TP2\_0.73' and Cone tests\_TP2\_0.65' were about 20% and 10% lower, respectively. In addition, the values presented as 'Cone tests\_TP2\_0.65' roughly indicate the lowest  $k_2$  values determined in furnace tests. It can be concluded that there is no need to consider the basic charring rate determined in cone (0.73 mm/min) when calculating the  $k_2$  values from cone test results. Instead, it is simpler to use the same basic design charring rate of 0.65 mm/min as in case of furnace tests. The estimation of  $k_2$  values from cone heater testing is inadequate if the test results are compared directly to the ones in furnace, hence an additional modification factor should be used. When  $\beta_0$  of 0.65 mm/min is used in the analysis of cone test results (TP2), the obtained  $k_2$  value should be multiplied by 1.15 for an estimation. This would provide a good agreement with the mean values obtained in furnace. The design values of  $t_{ch}$  and  $k_2$  derived from cone and furnace tests are listed in Table 6-17.

Table 6-17. The mean design values derived from cone and furnace tests for clay plaster systems.

Plaster thickness	Cone	Furnace	Cone	Cone	Furnace
	Test result	Test result	Test result	Modification**	Test result
	Start time of charring	Start time of charring	Protection factor	Protection factor	Protection factor
$h_p$ [mm]	$t_{ch}$ [min]	$t_{ch}$ [min]	$k_2$	$k_2$	$k_2$
10	3.8	6.0	0.77	0.89	0.87
17	11.5*	14.4	0.71*	0.81*	0.80
20	14.8	18.0	0.68	0.78	0.77
30	25.8	30.0	0.59	0.68	0.67
40	36.8	42.0*	0.50	0.58	0.57*
44	41.2*	46.8	0.46*	0.53*	0.53

\*Determined by the equation presented in Figure 6-48.

\*\* The  $k_2$  values derived from cone tests are multiplied by 1.15.

### 6.4.2 Lime plaster systems

A comparison was made between the results of cone tests of TP3 and the furnace tests of TP3. Herein, the cone tests were performed using two different depths of timber specimens: 50 mm and 100 mm (test results with 100 mm timber are separately marked as `_Timber 100` in the legend). Test results are shown in Figure 6-49 for the start time of charring. The mean values of the two test methods are closely correlated. There is a greater correlation between the furnace test results and the cone tests with 50 mm timber specimens. However, it may be argued that the results of cone tests with 100 mm wood specimens would be preferable since they correspond more closely to the earliest start times of charring obtained in furnace, thus a safe estimation could be guaranteed. This also be corroborated by the clay plaster experiments presented above, where the depth of the timber specimen was 100 mm.

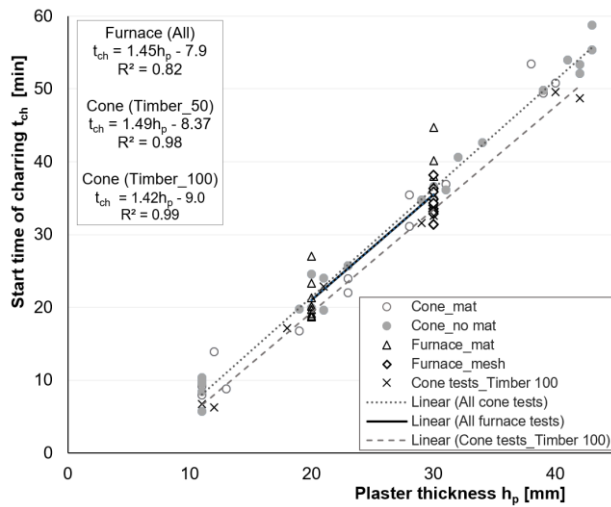


Figure 6-49. Comparison of start times of charring of timber protected by lime-based plaster system obtained from cone and furnace tests of TP3.

Figure 6-50 presents the comparison of  $k_2$  factors. Similarly, to the results obtained with clay plasters (Figure 6-48), the cone test results demonstrate unsafe  $k_2$  factors. The cone heater tests presented ~28–36% and ~19–26% lower  $k_2$  values for 50 mm and 100 mm thick timber specimens, respectively. For the calculation of  $k_2$  factors, the mean basic charring rates determined in cone tests TP4 were used (for 50 mm thick timber sample: 0.78 mm/min; for 100 mm timber sample: 0.73 mm/min). In case of 100 mm timber specimens, the derived  $k_2$  factors are somewhat higher than the ones obtained in case of 50 mm thick specimens. This phenomenon could be related to the difference in the boundary conditions due to the difference in the whole thickness of the test specimen and therefore the related heat transfer mode and heat losses.

Similarly, to the test analysis of clay plaster systems, herein the cone test results are also reported in the case when the basic charring rate is assumed to be 0.65 mm/min. In Figure 6-50, the mean trendline value is denoted as 'Cone\_Timber100\_0.65', for tests with 100 mm timber specimens. There is no sufficient agreement between the 'Cone\_Timber100\_0.65' and the furnace tests results. In case the basic charring rate of 0.65 mm/min is used, the obtained  $k_2$  values still position on the nonconservative side (~7–18% lower values) compared to furnace test results. In case of 30 mm plaster,

the agreement is significantly improved compared to the 20 mm plaster, as the rough mean difference in  $k_2$  values for 20 mm and 30 mm plaster is about 0.1 and 0.05, respectively.

The  $k_2$  values of 30 mm thick plaster and wire mesh ('Furnace tests\_mesh') are in a rather good agreement with the cone test results of 'Cone\_Timber100\_0.65'. However, if a better estimation of  $k_2$  is to be achieved for the plaster systems with a reed mat, a modification factor should be used. A modification factor of 1.15 may be applied to the  $k_2$  values derived from cone tests when the 0.65 mm/min as the basic charring rate is used. Table 6-8 presents the comparison of test results obtained from cone and furnace tests.

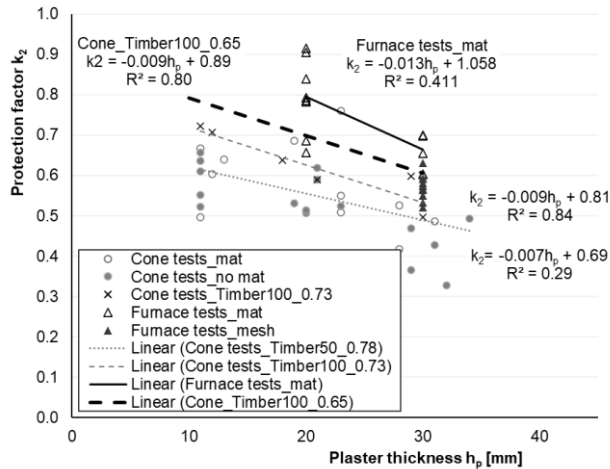


Figure 6-50. Comparison of protection factors of lime-based plaster systems obtained from cone and furnace tests of TP3.

Table 6-18. The mean design values derived from cone and furnace tests for lime plaster systems.

Plaster thickness	Cone	Furnace	Cone	Cone	Furnace
	Test result	Test result	Test result	Modification**	Test result
Start time of charring	Start time of charring	Start time of charring	Protection factor	Protection factor	Protection factor
$t_{ch}$ [min]	$t_{ch}$ [min]	$t_{ch}$ [min]	$k_2$	$k_2$	$k_2$
10	5.2	5.3*	0.80	0.92	0.93*
20	19.4	21.8	0.71	0.82	0.80
30	33.6	38.9	0.62	0.71	0.67

\*Determined by the respective equation presented in Figure 6-50.

\*\* The  $k_2$  values derived from cone testing are multiplied by 1.15.

### 6.4.3 Discussion

In case of all performed cone heater tests, the estimation of design values appears to be achievable. Whilst there was a good agreement to reach 300°C behind plasters determined in cone tests and furnace, an underestimation of the charring rate of timber (lower  $k_2$  values) behind plaster systems was evident in cone tests. This was influenced by several factors. By the time timber starts to char in cone tests (particularly in case of

thicker plasters), the heat flux level is already underestimating the fire exposure level in furnace (ISO 834). The heat exposure condition applied to the test specimens in cone tests is unable to deliver sufficient heat flux levels to replicate the aggressive furnace environment, especially in case of longer fire tests (COST Action FP1303, 2017). This difference of fire exposure conditions also influences the material changes and the water vapour movement within the specimen influencing the results. Thus, the increase in heat flux levels from 50 kW/m<sup>2</sup> to 75 kW/m<sup>2</sup> appeared justified as a comparable trend (inclination angle) of  $t_{ch}$  values among all plaster thicknesses was achieved as well as a similar trend in the reduction of  $k_2$  values with increasing thickness. The shorter test duration of 40 minutes seems to represent the best fit to the furnace results (Figure 6-48). Lower heat flux levels could have resulted in a longer time required to reach 300°C for thicker plaster coats, resulting in a considerable underestimation in their charring rates (as described in Chapter 4).

Furthermore, when test results are compared, the underlying differences related to the test methods should be understood as different boundary conditions to the test specimens apply. In cone heater tests, the specimens are predominantly exposed to radiation from the cone heater and cooled by convection as the tests are carried out at ambient air conditions. In furnace tests, the specimens are exposed to radiation and convection in a controlled furnace according to EN 1363-1. In this work, the tests differed from scale, oxygen content, thermal loads, and test specimens' insulation peculiarities (i.e., related to heat loss from the specimen during cone testing). The heat loss from the test specimen in cone tests seems to be significant due to the height and test set-up of the whole specimen. The apparent heat loss phenomena (not examined in this work) is related to the set boundary conditions (e.g., influence from the retainer frame, which acts as a heat sink). In addition, the total height of the test specimens varies with increasing plaster thickness, which also has some effect on the heat transmission mode. This is not the case regarding furnace testing. All these factors contribute to an underestimating of the charring performance of protected timber specimens in cone tests. When an adequate estimation is to be made, a modification factor for the  $k_2$  value must be applied.

It is important to acknowledge the limitations of cone testing. For example, no cracking of plaster was observed, however in furnace tests the cracking of plaster had some influence on the local charring performance of timber. This phenomenon should be considered when the cone test results are modified and used for estimation. The failure time of the plaster system is not feasible to study in cone tests. However, some indication from the heat transfer mode and its interpretation to the possible failure times could be made, this is further discussed in the next Chapter 6.5.

The cone test results with clay and lime-based plasters demonstrated a sufficient estimation to be comparable to the ones determined in furnace. Whilst the tests with lime-based plasters were performed with different timber specimen thicknesses, it was concluded that the use of thicker timber specimen yields better fit to the furnace test results. Furthermore, the thinner timber specimens seem to be more sensitive to the influencing factors such as the characteristics of wood, its positioning in the retainer frame throughout the test and the boundary conditions. The guidance on the use of cone heater testing for estimation of design values  $t_{ch}$  and  $k_2$  is given in Chapter 9.

## 6.5 Discussion on experimental work

Material test results offered sufficient insight into the composition and performance of selected plasters to be used as a first input for thermal simulations (Chapter 6.1). However, this current study about the plaster's performance could be considered somewhat limited as in a wider context the temperature-dependent material specific properties can be divided as: i) thermal properties (thermal conductivity, specific heat, density); ii) mechanical properties (tensile strength, compressive strength, modulus of elasticity); iii) deformation properties (i.e., thermal expansion) and iv) transport properties (e.g., porosity and pore pressure). At elevated temperatures, the chemical and physical changes of materials depend greatly on their specific compositions. The micro and macro structure of a material experiences significant changes because of high temperature gradients, loss of moisture, dehydration, and crystal transformations.

One of the most influential material properties is thermal conductivity. It is very sensitive to the microstructure of the material. It is strongly influenced by such factors as mineral composition, degree of crystallinity, impurities in the crystal structure, average grain size, grain orientation, and porosity. Consequently, the thermal conductivity of materials with the same general name might vary. This difference was also demonstrated in this thesis (Chapter 6.1). However, the furnace tests (TP3) showed that in case of standard fire exposure conditions, the plasters still perform very similarly with respect to the charring performance of timber behind the plasters (e.g., ClaySU04 and ClaySF04). In TP2, the furnace test of Test 5 (Table 6-10) indicated a three-minute difference between plaster systems of ClaySU and ClayCT for the start of time of charring of timber. Regardless of the origin and composition of the selected plaster mixes (Estonian vs German, Appendix A), the difference in their mineralogical components appears to have no significant effect on the heat transfer mode through the clay plaster. In contrast, in case of lime-based plasters, the amount of calcite in the plaster mix as well as the addition of cement component had somewhat influence on the heat transfer mode and to the development of cracks (furnace tests of TP3). According to the tests in this experimental program, the thickness of the plaster system is the most influential component in determining its protective effect.

Besides the specifics of material properties, the characteristics of fire exposure (such as fire load, maximum temperature, and fire duration) also have an impact on the properties and overall performance of building materials. Because of this, attention should be paid when interpreting the material test results to determine how effectively the plasters perform under standard fire exposure conditions. However, certain indications were obtained from the material testing, since the formation of cracks in clay plasters at certain temperatures was found to correspond to its behaviour in furnace, e.g., at about 400°C behind clay plaster, the first visible cracks started to develop in furnace, which agrees with the mass loss of the dry-mix plasters determined in TGA and cracking of the specimen halves in TPS tests. The lime plasters (furnace tests TP3) revealed somewhat better fire protection capabilities in terms of the start time of charring (higher  $t_{ch}$  values) compared to the clay plaster, which could be seen to correlate with their greater mass loss reported in TGA (i.e., more energy is needed for the material changes that consequently slow down the heat transfer). However, the degree of carbonisation of the lime plaster appears to be a critical factor (furnace tests, TP4, Test 15), and no definitive conclusions can be made since more investigation is required. This is further discussed below.

In case of thicker clay plasters, significant cracking and detachment of layers was observed after some time of testing (Chapter 6.3.1). This behaviour's underlying phenomena could be related to the one described by (van der Heijden et al., 2011). As the temperature rises, the water inside the pores starts to boil and the chemically bond water is released by dehydration. The released water vapour needs to be transported out. When fire test starts, the dehydration front is close to the surface, so the vapour can easily escape from the material. As the temperature increases, the front moves into the material increasing the resistance of the vapour flow towards the surface. The resistance is determined by the vapour permeability. As a result, a large temperature gradient can generate stresses on the fire-exposed side of the surface. When temperature increases, the strength of the material weakens (also due to the dehydration as the pore geometry changes leading to the change in permeability and strength loss). These processes can result in sudden explosion or a significant cracking of the material. The processes leading to cracking are generally believed to be similar to those which generate spalling in concrete. This has been recognised in case of concrete structures and gypsum (van der Heijden et al., 2011) and now also in the furnace tests presented in this thesis (Chapter 6.3.1).

In some test specimens, reinforcement meshes were used in the plaster systems. Observations indicated that the jute mesh had no influence on the performance of the plaster; no detachment of the plaster layer occurred at the location where it was placed. In case of lime plasters, a strong bond between the plaster and the glass-fibre reinforcement mesh was observed. It appeared to prevent the cracking of plaster (in case of floor test in TP4) up to a certain time until the failure of the mesh itself. Similar performance of the reinforcement fabric's impact on concrete structures has been investigated to assess reductions in spalling (Jansson, 2013). It has been demonstrated that wrapping concrete member in a steel fabric reduces spalling by providing lateral confinement pressure to the concrete member which is greater than the internal vapour pressure causing spalling. The effect of carbon and glass fibre fabrics have shown reduced effect due to the bond strength of these materials reducing at high temperatures and the corresponding reduction of the ability of the fabric to provide confinement. It does not appear that the technique induces cracking deeper within the structure. It was found that a metal fabric had a beneficial effect on spalling resistance, with less effect using carbon fibre and glass fibre fabrics. Future research may apply this knowledge to the use of reinforcement meshes in plaster systems to increase their mechanical strength and thereby avoid cracking and contributing to the integrity of the plaster systems for a prolonged time. In this thesis. tests were carried out solely with the jute mesh as a reinforcement for clay plaster systems. The performed tests showed that the detachment of first plaster layers only occurred in case of 44 mm thick clay plaster systems, confirming the descriptions above about the thermo-hydral process associated with the transfer of mass in the porous network (air, vapor, liquid water), which results in the build-up of high pore pressures and pore pressure gradients (Kalifa et al., 2000).

It is also important to address the effect of the plaster carrier as it may influence the performance of plaster itself. The same type and thickness of lime plaster (30 mm) tested in furnace (TP3) developed cracks on reed mat but not when a steel wire mesh was used. It seems that, particularly in the case of thinner plaster systems, the reed mat may enhance rather than prevent the formation of cracks. Furthermore, the plaster carrier in a form of a thin layer in a plaster system such as a reed mat used in this study, has a slight impact on the heat transfer mode through the plaster to the timber element. In the TP3

furnace experiments with different lime-based plasters, the same plaster tested on metal mesh started to char about 3 minutes (in average) earlier than the same plaster tested on a reed mat. The somewhat better protection effect may be attributed to the reed stems of a reed mat as the heat transfer is influenced by its air voids. Therefore, a reed mat is likely to somewhat delay the heat transfer regardless of the type of plaster used. It was detected that the fastest temperature increase behind plaster, determined in case of a reed mat, was comparable to the mean temperatures recorded in tests with a wire mesh, so there was an overlap. The cracking of clay plaster was observed when plaster was applied on a thin reed mat on timber (furnace tests TP2). However, when a reed board was used, no crack development was observed but only a sudden fall-off occurred in the floor position (Test 3, Test 4, in TP2). Interestingly, the determined fall-off times corresponded to the time of the development of cracks in a similar thickness of plaster system tested in other floor tests when a reed mat was used (Test 1, Test 2, in TP2).

This study revealed two distinct types of failure modes for the clay plaster systems, the first of which was associated with the fastening system (including the type of plaster carrier, i.e., reed mat) and its fixation to the timber element, and the second with the loss of adhesion between the plaster and its substrate (i.e., reed board). When the moisture is driven out of the plaster and the underlying substrate (e.g., reed board) begins to char, adhesion is lost as there is no other means to keep plaster in place at high temperatures. The same loss of adhesion may also occur when plaster is applied on wooden laths (often found in old structures) or other building boards when no mechanical fastening to the substrate is done. This phenomenon can further be argued by the adhesion between plaster and timber at ambient temperatures that starts to weaken with increasing temperature in case of fire: the water is driven out from the plaster and timber starts charring at around 300°C. This indicates that (at the latest) by the time timber starts to char, there is no adhesion left to keep plaster attached to timber. Therefore, the presence or lack of a mechanical fastening system (i.e., plaster carrier fixed into the substrate) becomes an important indicator to estimate the probability and the fall-off time of the plaster system. The relevance of a sufficient key between the existing wooden floors and plaster system has also been pointed out in a technical guideline by (BRE, 1988). Based on the conducted furnace tests in this thesis and considering the statements given in some technical guidelines referred to in Chapter 1 and 4, there seems to be no guarantee to state that the plaster will stay intact to timber without any mechanical fixation.

In the case of reed mat fixed to the timber element with staples, the floor tests (Test 1 and Test 2, TP2) demonstrated that plaster was attached to timber for a long time, which must be due to the material characteristics of clay expanding and strengthening at high temperatures (e.g., sticking to the sides of the furnace), preventing it from falling off. Additionally, a strong bond between the plaster and the reed mat's wires was observed, indicating that they functioned as a single system. In Test 1 and Test 2, according to the plaster's fastening system and the length of the staples in the uncharred wood, gravity should have forced the plaster to fall off, therefore the test results were unexpected. In addition, the furnace tests of TP1 demonstrated that the clay plaster could adhere to the furnace walls, preventing it from falling off even though clear cracks developed during the fire tests (Test 0 and Test 01, TP1). In TP4, however, a floor test in a larger scale was conducted (Test 13), and the clay plaster system fell off at a time that correlated rather well with the start time of charring of wood (the somewhat unexpected earlier fall-off is described before). One possible explanation to the early fall-off could be

that heat is transferred faster by the metal fasteners, and the wood is heated up around the fasteners and the bond between the staple and wood is getting weaker, thus the early fall-off may be a consequence of this phenomena. In this regard, it might be suggested that, in the case of ceilings, where the fixation of fasteners is more crucial than in the case of walls, the failure time of the plaster system is exclusively related to a certain temperature criterion reached behind the plaster, e.g., 270°C that corresponds to the protection time. Previous studies by (König et al., 1997) have reported that critical fall-off temperatures for ceiling linings (gypsum plasterboards) is 600°C and for walls 800°C. According to (Schleifer, 2009), the failure times for gypsum boards type F in relation to the temperature increase behind the board was considered 400°C in ceilings and 600°C in walls. However, a research work by (Just, 2010) has demonstrated that the dependence between the temperatures and fall-off times of the gypsum plasterboards was not found. The fall-off times and failure modes of the plaster systems, especially in ceilings, should be further studied in future due to numerous influencing factors such as the types of plaster carriers and its fastening methods, plaster thicknesses, test scale etc.

In contrast to the performance of clay plaster, furnace test results of lime plasters tested in floor position (TP4) provided basis for some further discussion on the sudden failure of the lime plaster detected in Test 14. This observed fall-off could be listed as a third possible failure mode for certain plaster systems, which may occur due to the material thermal degradation. This phenomenon appears to be highly complex, as a similar behaviour of 'explosive spalling' has been recognised in concrete members. Work by (Fletcher et al., 2007) explains that this process is often assumed to occur only at high temperatures, yet it has also been observed in the early stages of a fire. The mechanism leading to spalling is generally thought to involve high thermal stresses resulting from rapid heating and/or large build-ups of pressure within the porous concrete, which the structure of the concrete is not able to dissipate, due to moisture evaporation (Fletcher et al., 2007). These actions lead to the development of cracks and expulsion of chunks of material from the surface layers. Furthermore, it is stated that the temperature gradients are dependent not only on gas-phase temperatures but also heating rates, so that it is not possible to define a threshold temperature. However, these critical values for spalling may also be affected by the type of concrete, including the strength of the material and the presence of fibres. In view of the test results observed in Test 14, the low mechanical strength of the lime plaster could be one of the reasons of causing the early failure. The mechanical strength of lime plaster is related to its level of carbonisation (Chapter 3.2.2 and Chapter 4). In case of fire, the certain preparation and hardening process accompanied by the respective carbonisation level of the lime plaster seems to be one of the important factors influencing the heat transfer mode through the lime plaster system. It may be argued that the application and preparation process of the lime plaster was not carried out as intended in TP4, e.g., there was not enough water inside the material pores for the carbonation to proceed as it should which hindered the hardening process and resulted in plaster with low mechanical properties (i.e., uncarbonized lime). This may be further attributable to the fact that the thick CLT element absorbed the free water from the lime plaster mix that was intended for the carbonisation process. In addition, the moistening of the plaster layer's surface during its hardening prior to the addition of the next layer may have been not sufficient. Thus, this current work proves the need for future studies related to this phenomenon, as also pointed out in previous research that the level of carbonization influences the physical and mechanical properties of lime-based plasters (Chapter 4).

Several key conclusions may be drawn by comparing the results of small-scale experiments to those obtained from the furnace tests. The cone heater tests were not able to detect any fall-off time; nevertheless, the observed fixation of staples after the cone testing may still offer an indicator to some limited estimation of the fall-off time of plaster from timber (Figure 6-2b). However, the charring rate behind plaster was much slower according to the cone test results; thus, the findings about the anchorage length of the fasteners must be carefully analysed if any estimation is to be made. In addition, the effect of self-weight and the development of tensile stress in plaster seems not to be addressable nor obtainable in cone tests due to the horizontal specimen orientation and very small specimen size. Similar limitations of testing with cone heater apply to assessment of the thermal degradation and the integrity of plaster systems (i.e., cracking, detachment of layers). Whilst the cone heater testing did not show any crack development in plaster, the tests in furnaces demonstrated clear crack development in the plaster systems; tests in a smaller furnace with clay plasters (TP3) showed only minimal crack development during 60 minutes of fire exposure compared to the tests in TP2. It may be argued that a relatively limited surface area of plaster (such as the separated sections tested in Test 5 and Test 6 (TP2) is not explicit to analyse the stress development inside plaster system, as would be the case at a larger scale. Despite this, the heat transfer through the specimen was in good agreement with the data obtained from various scales of furnace testing.

Tests in small and intermediate scales demonstrated some deviation of test results for the same plaster thickness, which is a result of a combination of various factors: the influence of a reed mat; variations in the initial density of test materials (compactness of the plaster and the final plaster systems' density), specific of timber specimens etc. Furthermore, it was recognised that the heat exposure was not uniform in the whole furnace (e.g., some tests showed higher temperature recordings in the corner areas of the specimen), which has also been noticed in other research works (Niemann, 2010). The scatter in the obtained charring rates also indicate to some additional factors that influence the analysis of results such as the different charring times that may indicate slightly different charring rate values, properties of timber specimen itself as well as the specifics of plasterwork (i.e., influence from the handicraft technique itself that may result in some differences in the compactness of plaster coats on the reed stems over the whole specimen). Yet, these aspects are inevitably variables in practice that could not be fully avoided. Consequently, the test results are used as mean values for further analysis. This recommendation is also given in standardised test methods described in EN 1995-1-2 and EN 13381-7.

The performed cone tests provided an evident distinction of the protection ability of plasters to rank their fire resistance. Similar conclusions have been made by (Wachtling et al., 2013), where different plaster compositions were tested to assess their fire protection ability. This mentioned research is not directly comparable to this current study due to the significant variations in the test set-up, procedure, and applied heat flux levels. To generalize, this fact proves to be an example of the overall situation in small-scale testing that despite of numerous studies, the differences between test set-ups and procedures complicate an accurate comparison of different tests. Consequently, within this work a test method is introduced that aims to replicate the requirements stated in ISO 5660 as close as possible (e.g., regarding the preparation of the test specimen and the procedure of testing) to provide a universally reliable and simple test method that guarantees high repeatability of test results. Recommendations to determine the design

equations for plaster systems as fire protection materials from cone test results are given in (Liblik et al., 2023) and presented in Chapter 9.

While testing the plaster system on a reed board in a furnace, it was found that the quantity of fuel load (gas) required to follow the ISO 834 curve increased significantly compared to other tests with only a reed mat on timber. It is known that surfaces with greater thermal inertia absorb more heat energy from a fire-induced environment, hence lowering gas temperatures, whereas materials with lower thermal inertia absorb less heat energy. This data obtained from the conducted furnace tests might be investigated further in the future, for example for performance-based design and advanced calculation methods.

## 7 Thermal simulations

### 7.1 Aim

According to prEN 1995-1-2:2022, the verification of the separating function of timber assemblies is performed by the separating function method (SFM). This method is explained in Chapter 2.2.2. For SFM, material specific design equations are required. To implement new materials into the SFM, the procedure specifies that thermal simulations should be performed to determine the effective material properties for developing the design equations in accordance with prEN 1995-1-2:2022.

The general steps for the development of relevant design parameters include:

- 1) Thermal simulations with initial material properties (e.g., obtained from TGA tests, TPS tests, literature) and comparison with the fire test data;
- 2) Determination of effective thermal properties (material properties calibrated on the basis of fire tests);
- 3) Thermal simulations and comparison with fire test data;
- 4) Systematic thermal simulations for developing the design equations.

The design equations for the plaster systems investigated in this research were mainly determined based on the calibration procedure developed by (Mäger, 2016). The furnace test results (Chapter 6.3) were used for the calibration of the thermal properties. First results have been published in papers (Liblik et al. 2019, 2020). In the following chapter, a comprehensive overview of simulations and a proposal for a new set of effective thermal properties for clay and lime plaster systems are presented in order to determine the design equations.

### 7.2 Simulation program and model

The software used for the thermal simulations was SAFIR, versions SAFIRv2014a1 and SAFIR2019a3. It is a commercial software developed in the University of Liège that is used to model the behaviour of building structures subjected to fire. It uses the finite element method (FEM) (Franssen et al., 2017). On the surface of a material heat is exchanged with the environment via convection and radiation. These phenomena are considered by specifying the appropriate coefficients (EN 1995-1-2).

The main concept for calculation in SAFIR is that heat is distributed in the structure by conduction as building elements are made of solid materials. This means that for some materials (e.g., wood, plaster systems) the calculation is an approximation. Temperature calculations within solid materials are based on the Fourier equation (13), a simplified expression of one-dimensional conduction is presented in the following equation:

$$k \frac{\partial^2 T}{\partial^2 x} = c\rho \frac{\partial T}{\partial t} \Rightarrow \frac{\partial T}{\partial t} = \frac{k}{c\rho} \cdot \frac{\partial^2 T}{\partial^2 x} \quad (13)$$

where:

- $T$  is the temperature [K];
- $x$  is the coordinate in the direction of heat transfer [m];
- $k$  is the thermal conductivity [W/(mK)];
- $\rho$  is the density [kg/m<sup>3</sup>];
- $c$  is the specific heat [J/(kgK)];
- $t$  is time [s].

As shown by equation (13) thermal conductivity is divided by the product of specific heat and density. This indicates that, theoretically, only one of these values could be calibrated to fit the test data for determining the effective thermal properties of a material if the values of the others are known.

It must be noted that SAFIR does not take into account the mass transfer of water (and its re-condensation), steam and gases nor heat transfer within the material via radiation between the fibres and air or by air convection, thus these effects must be accounted for by using effective conductivity values rather than real ones (Franssen et al., 2017). This also applies to the formation of cracks, e.g., in the char layer or protection material, causing increasing heat flux which is taken into account by using higher conductivity values. Also, effects which such as anisotropy of conductivity in cracked materials and contact resistance between two adjacent materials that have (somewhat) separated cannot be accounted for with this tool.

### Concept of thermal simulations

The concept map of the simulations is presented in Figure 7-1. To account for the changes in test specimens and plaster types used in different TPs, the first simulations were divided into two main sets, Model 1 and Model 2. The simulation models are further described in Table 7-1.

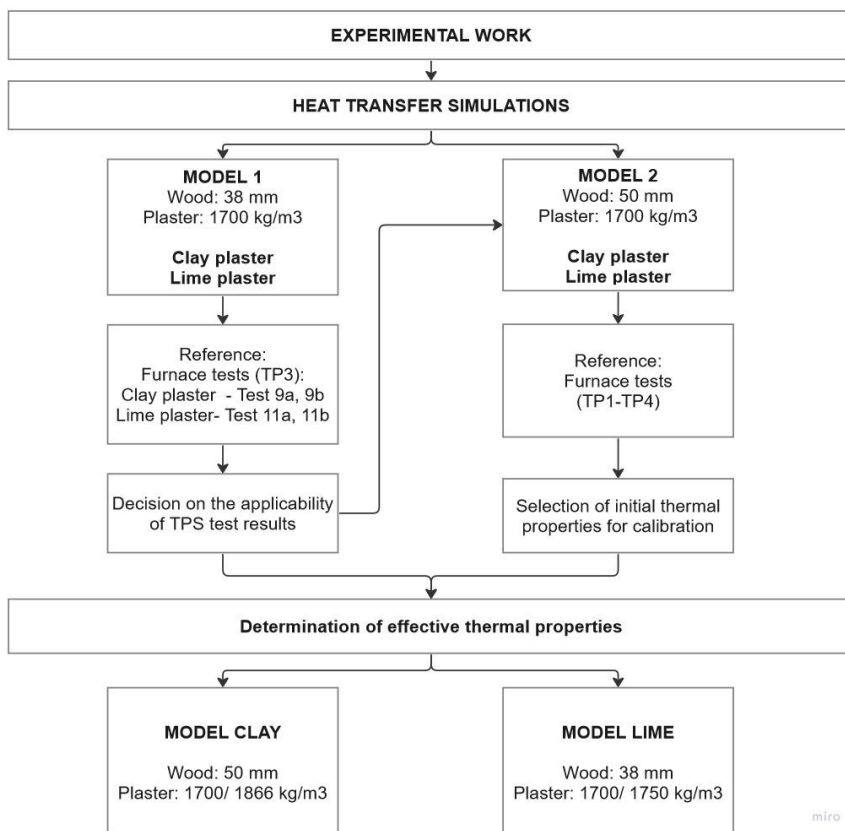


Figure 7-1. The concept map about the heat transfer simulations.

## Simulation model

A two-dimensional specimen with 1D heat transfer path was used. Thermal properties of plasters obtained from TPS tests (Chapter 6.1) were used as first input, see Table 7-1. In Model 1, only the TPS and furnace test results (TP3) for 30 mm plasters were used. In Model 2, for reference, an additional set of properties of clay plaster denoted as 'Clay\_mineral' was used (Küppers et al 2018). It was a mineral clay plaster (no fibres) with a density class of 2.0, building material class A1 (DIN 18947, 2018). The thermal properties of this plaster were the closest ones to the clay plasters tested in this thesis due to its composition and origin.

In this current thesis, the TPS testing demonstrated limited capacity to determine thermal properties at higher temperatures (Chapter 6.1). To run the simulations, it was assumed that the input values for the thermal properties at higher temperatures would be the same as the last measured value (at ~400°C). As the density is regarded to have a minor impact on heat transfer mode compared to other two properties (Mäger, 2017), it was considered as constant at all temperatures. This approach was deemed sufficient to compensate for its influence by the other thermal properties.

In the majority of fire tests, the plaster was tested with a reed mat that altogether formed the plaster system. Thus, in simulations, a simplification was made and the reed mat as a separate material was neglected due to its characteristics and the fact of being part of the plaster system. Its influence was considered indirectly (by temperature measurements obtained in furnace tests).

Table 7-1. Description of the FE-models for simulations using TPS test results as input.

Properties		MODEL 1	MODEL 2
Plaster system	Type	1.ClaySU04 2.ClaySF04 3.LimeSU04	1.ClaySU04 2.Clay_mineral
	Thickness (mm)	30	10–44
	Thermal properties	1.Table 6-1 2.Table 6-2 3.Table 6-3	1.Table 6-1 2.TPS (Küppers et al., 2018)
	Density (kg/m <sup>3</sup> )	1700	1700
	Timber	Thickness (mm)	38
	Thermal properties	EN1995-1-2:2004	EN1995-1-2:2004
Boundary conditions (sides)		Adiabatic	
Ambient temperature		20°C	
Fire exposure		ISO 834; $\alpha = 25 \text{ W/m}^2\text{K}$ (EN 1995-1-2:2004)	
Unexposed side		20°C; $\alpha = 4 \text{ W/m}^2\text{K}$ (EN 1995-1-2:2004)	
Emissivity coefficient		0.8 (EN 1995-1-2:2004)	
Simulation model		2D	
Element type		Quadric, 1 mm x 1 mm	
Measurement point		Plaster system-wood interface	
Ref. temperature-time curve		Mean calculated temperature-time curve from test	
TP of furnace tests		TP3	TP1 - TP4

In Model 1, a base layer of 38 mm thick wood element was used as it corresponds to the thickness of the timber panel tested in furnace (TP3). In Model 2, a 50-mm-thick wood corresponded to the furnace tests conducted in TP2 and was considered adequate

for the analysis of tests in TP1 and TP4. The timber element was described in accordance with prEN 1995-1-2:2022, where it is stated that a solid timber used in thermal simulations shall have a density of 450 kg/m<sup>3</sup> and temperature dependent material properties given in the respective standard in Table 8.1. The simulation results were plotted against the mean TC recordings at the interface of the plaster system and timber element. The main temperature points of interest were 150°C, 300°C and 550°C behind the plaster system on timber.

### 7.3 Heat transfer simulations

The simulations were run based on Table 7-1 in accordance with the concept map shown in Figure 7-1. The simulations were performed with the plaster systems (with a reed mat) applied on timber elements. In case of lime-based plaster systems, the tests carried out in TP4 are herein excluded mainly due to test results and conclusions made on the furnace tests. This subject was discussed in Chapter 6.5.

#### MODEL 1

Initial simulations with clay plasters were carried out with plasters denoted as ClaySU04 and ClaySF04. A direct comparison was made between the use of material test results obtained from TPS tests and the performance of both plasters in furnace tests in TP3. Figure 7-2 shows the properties of clay plasters obtained from TPS tests, based on the assumption of a linear relationship between the different measurement points. The density was considered constant value of 1700 kg/m<sup>3</sup> as it represents the mean value for the density class of the tested clay plasters.

Figure 7-3 presents the comparison of temperature measurements at the interface of plaster system and timber; the temperature rise on the unexposed side of the timber element is also shown. For both plasters (ClaySU04 and ClaySF04), the simulation results (SIM\_ClaySU04 and SIM\_ClaySF04) show faster temperature rise behind the plasters compared to the ones in furnace. After 400°C, SIM\_ClaySF04 starts to correlate rather well with the temperatures measured in furnace. In the instance of SIM\_ClaySU04, the discrepancy seems to stem from the lack of a plateau at 100°C, since the simulation's curve line generally resembles the one obtained in furnace. In furnace testing, the evaporation of free water from the specimen creates a distinct plateau at around 100°C, which hinders the temperature rise to a certain extent. This phenomenon is not represented by simulations. One distinction is the reed mat used in furnace tests, which may somewhat alter the heat transfer mode within the plaster system. Another distinction is the impact of the backing layer on the performance of the layer that precedes it. The TPS tests are material-specific according to the test specimen and have certain limitations (discussed in Chapter 6.1). The temperature measurements on the unexposed side of the test specimen agreed well with simulations. Based on the first comparison, the properties of ClaySF04 present weaker agreement to the furnace test result in the first 20 minutes, however this is an important temperature-time frame. The TPS test results obtained in this work and used for initial simulations seem to not give an adequate basis for the calibration of properties, particularly in the most critical temperature range up to 400°C.

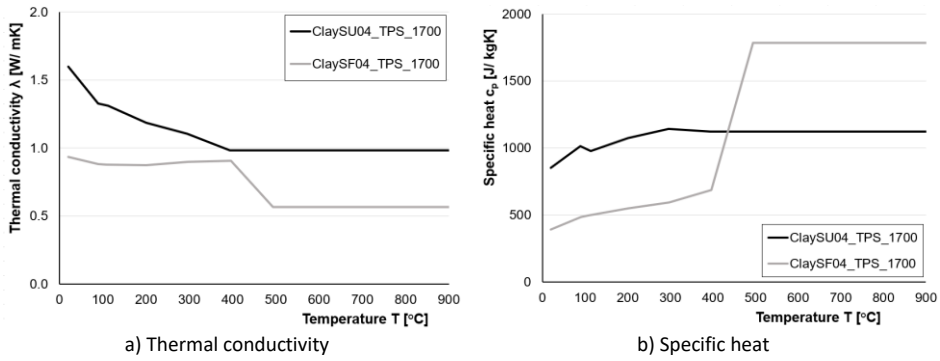


Figure 7-2. Comparison of mean values of thermal properties obtained from TPS tests and used for simulations in Model 1 – Clay plasters.

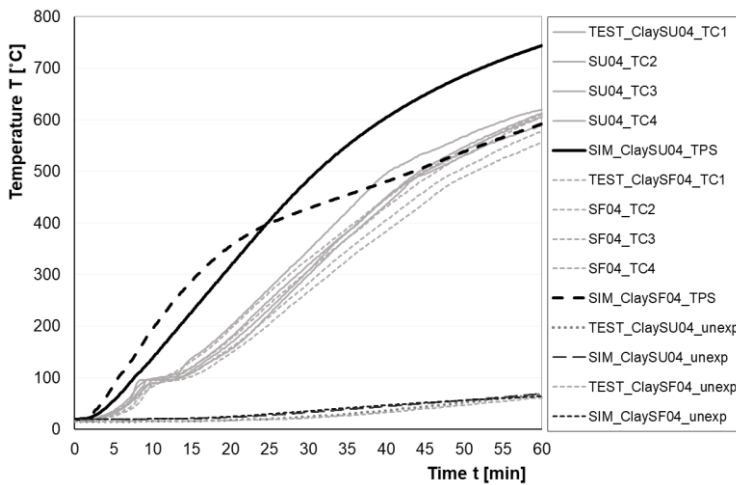


Figure 7-3. Comparison of temperature measurements recorded in furnace (Test 9a, Test 9b, TP3) and simulations based on TPS test results – clay plaster systems.

In case of lime plaster systems, first simulations were carried out with 30 mm thick plaster systems (with reed mat and wire mesh) tested in TP3 (Test 11a and Test 11b). The thermal properties were taken from the TPS tests, presented in Figure 7-4. The density was taken  $1700 \text{ kg/m}^3$  and considered constant at all temperatures. Test 11b only varied from Test 11a by having a wire mesh (WM) (instead of a reed mat (RM)), denoted as 'TEST LimeSU04\_WM' in Figure 7-5. Figure 7-5 presents the comparison of mean temperatures at the interface of plaster system and timber. A similar result (as in case of clay plaster) is also observed as the temperature rise behind lime plaster based on simulations (SIM\_LimeSU04) is much faster than the one determined in furnace tests. Similarly, to the performance of clay plasters in furnace, the temperature increase behind lime plaster is slower and a longer plateau at  $100^\circ\text{C}$  is formed that represents the water evaporation. Thus, it is further confirmed that this phenomenon is not captured by the material tests conducted in this research (Chapter 5.2); the temperature rise determined by simulations is significantly faster.

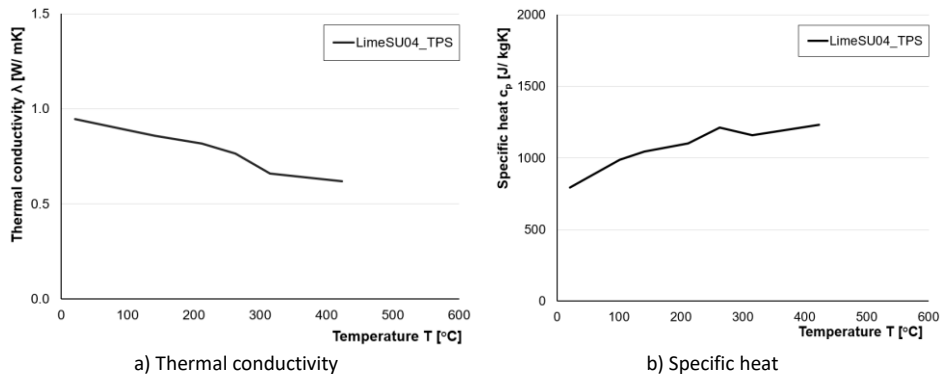


Figure 7-4. Mean temperature-dependent thermal properties obtained from TPS tests for lime plaster – LimeSU04.

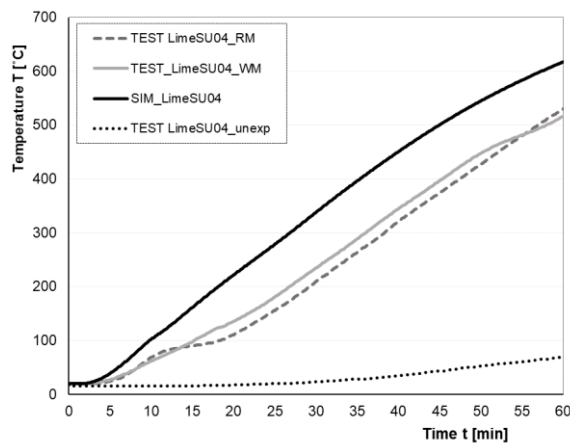


Figure 7-5. Comparison of temperature measurements between furnace tests (Test 11a, Test 11b) and simulations based on the TPS test results – 30 mm thick lime plaster systems.

Figure 7-6 presents a more detailed evaluation of the performance of 30 mm thick lime plasters. The difference in temperature rises behind the plaster systems between using a reed mat and a wire mesh appears to become apparent before 100°C is reached on timber. In the case of a wire mesh, the temperature increase behind plaster system is rather linear; however, in the case of a reed mat, a temperature plateau around 100°C is observed. The simulation results denoted as SIM\_LimeSU04 show a somewhat similar curve trend to that of Test 11b (with WM) compared to Test 11a; however, the temperature increase is more rapid from the start. Herein, the influence of timber specimen (e.g., the moisture movement and evaporation of free water from timber) cannot be ignored if comparison to the use of TPS test results is made. In addition, the level of carbonization of the lime plasters may have an effect on the material properties, hence influencing the simulation results, although this was not investigated in this work.

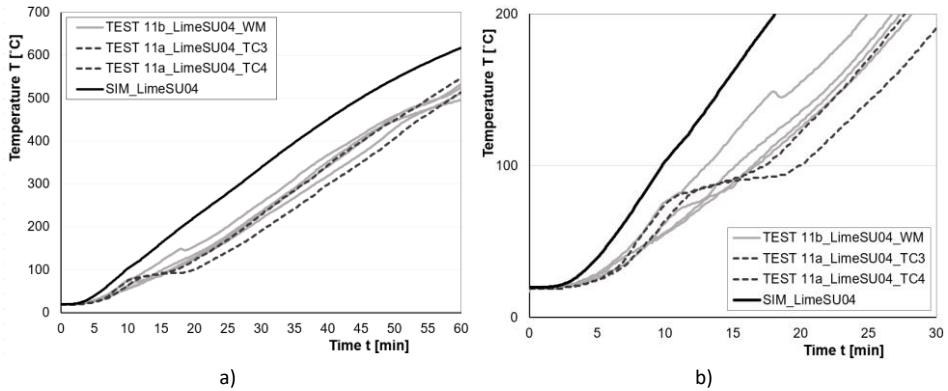


Figure 7-6. Comparison of temperature curves between furnace tests (Test 11a, Test 11b) and simulations based on the TPS test results – 30 mm thick lime plaster systems: a) Temperature curves up to 60 minutes; b) Close-up of the curves around 100°C.

A comparison of simulation results between the 30 mm thick clay and lime plaster systems (with a reed mat) is presented in Figure 7-8. Figure 7-7 illustrates the comparison of the thermal properties of tested lime (LimeSU04) and clay plasters (ClaySU04). The furnace results of clay plasters (ClaySU04, ClaySF04) are presented as a mean temperature curve from both tests in TP3. While the simulation and furnace test results diverge over time in case of clay plaster (SIM\_ClaySU04), the simulation results of 'SIM LimeSU04' seem to be in good agreement with the furnace test results of clay plasters 'TESTS Clay plasters'. This compliance can be directly related to the lower thermal conductivity values and slightly higher specific heat in TPS results obtained for LimeSU04 (compared to the ones of ClaySU04, Figure 7-7) that slow down the heat transfer mode. This data could be utilised to calibrate the effective thermal properties of the clay plaster system, given both plasters are within the same density range and include similar components. There was no good fit between the simulation and furnace results for LimeSU04, the reason may be also influenced by the carbonisation level of lime plaster. The results of Model 1 present the need for extended simulations in Model 2 as well as highlight the need for the calibration of material properties obtained from TPS tests to fit the furnace test results.

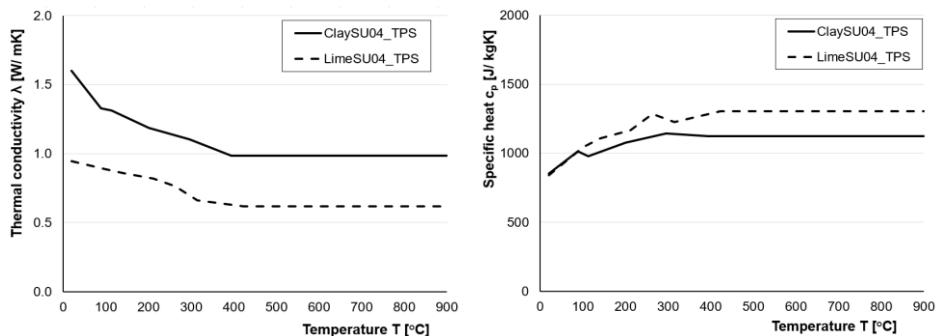


Figure 7-7. Comparison of the thermal properties of clay and lime plaster used as input for Model 1: Left – Thermal conductivity; Right – Specific heat.

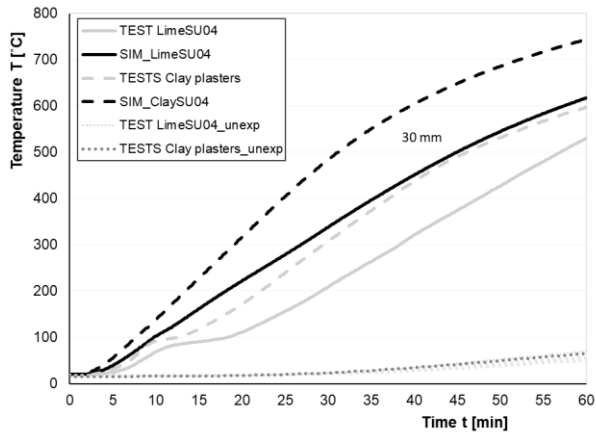


Figure 7-8. Comparison of mean temperature values between 30 mm thick clay and lime plaster systems (with a reed mat) obtained from furnace tests (TP3) and simulations.

## MODEL 2

The simulation model is specified in Table 7-1. Simulations were performed for the whole range of clay and lime plaster systems tested in furnace. Because the TPS results of ClaySF04 showed a more pronounced temperature increase than furnace tests within the first 20 minutes, these properties were not used in Model 2. Instead, properties previously determined by (Küppers et al., 2018) were utilised for extensive investigation, wherein the provided specific heat values were slightly modified by considering a constant density value of  $1700 \text{ kg/m}^3$  used in these current simulations of Model 2.

Figure 7-9 illustrates a comparison of temperature rise at the interface of clay plaster system and timber with respect to the different plaster thicknesses. The simulation results of 'SIM\_ClaySU04' considerably overestimated the increase in temperature behind plasters thicker than 20 mm, resulting in conservative results. Whereas the results of 'SIM\_Clay mineral' demonstrate rather good fit to the furnace tests within the whole range of plaster thicknesses. When comparing the thermal properties of 'ClaySU04' with 'Clay mineral', see Figure 7-10, the difference in their specific heat values at higher temperatures seems to be the most prominent difference. This is a clear limitation of the TPS testing conducted within this thesis, in which measurements of material properties were restricted to  $394^\circ\text{C}$ . However, it is known that clay plaster undergoes significant mineralogical changes at higher temperatures, which leads to the conclusion that the results reported by (Küppers et al., 2018) should be more reliable to be used for further investigations (as shown by the simulations).

However, the correlation between the 'SIM\_Clay mineral' and furnace results still do not correlate well at certain temperature range, Figure 7-9. In case of 10- and 20-mm plaster, the simulation results fall gradually on the non-conservative side after  $400^\circ\text{C}$ . For 30- and 44-mm plasters, the agreement between  $100^\circ\text{C}$  and  $300^\circ\text{C}$  is somewhat weak (though on the safe side), improves around  $300^\circ\text{C}$ , and then weakens again thereafter. The graph illustrates that the material properties require improvement to provide good agreement with the furnace test results.

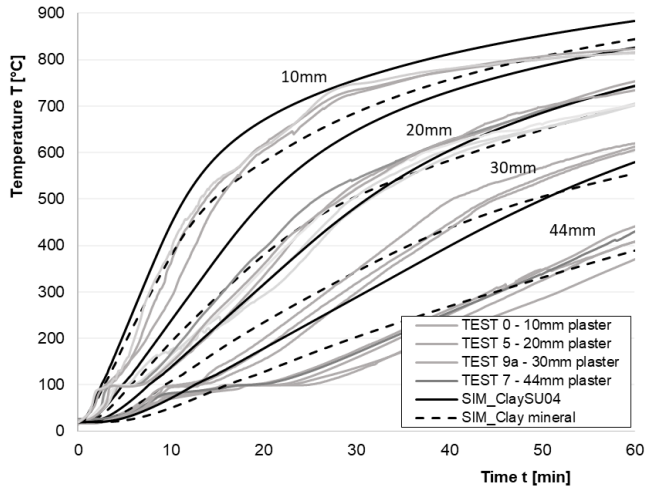


Figure 7-9. Comparison of temperature measurements obtained in furnace behind the clay plaster system (wall tests) and simulation results of Model 2.

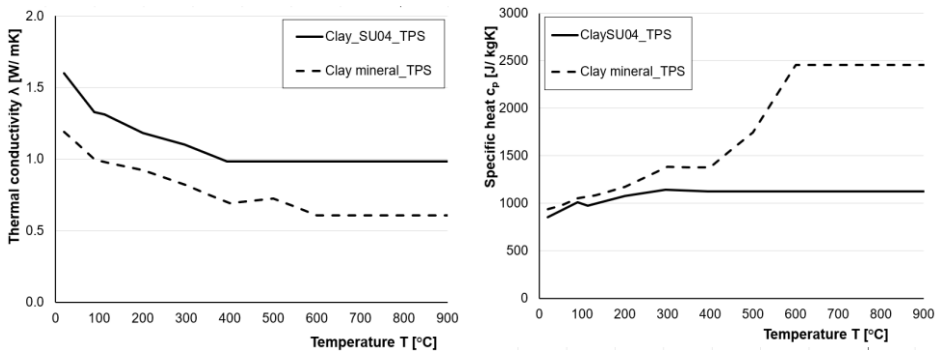


Figure 7-10. Comparison of the thermal properties obtained from TPS tests for 'ClaySU04' and 'Clay mineral' used as input for Model 2: Left – Thermal conductivity; Right – Specific heat.

The times required to reach certain temperatures (150°C, 300°C, and 550°C) behind the plaster system on timber seen in Figure 7-9 are listed in Table 7-2. Figure 7-11 illustrates the correlation between the start times of charring obtained in the furnace and in simulations. The results of 'SIM\_Clay mineral' yield the best fit to the ones obtained in furnace. However, as the temperature exceeds 500°C, the simulation results for thicker plasters start to show a slower rise in temperature behind the plaster than the furnace results, thus becoming unsafe. In Table 7-2, the results of 'SIM\_Clay mineral' to reach 550°C are gradually shifting toward the unsafe side with increasing thickness, although the results for 10 and 17 mm are comparable to the furnace test results.

Table 7-2. Comparison of times to reach 150°C, 300°C and 550°C behind clay plaster systems determined in furnace tests and simulations of Model 2 based on TPS results.

Test specimen			Time to reach certain temperature behind clay plaster system								
Test No	Plaster Ref.	Plaster system' thickness $h_p$ [mm]	150°C			300°C			550°C		
			TEST	SIM_ ClaySU04	SIM_ Clay mineral	TEST	SIM_ ClaySU04	SIM_ Clay mineral	TEST	SIM_ ClaySU04	SIM_ Clay mineral
			$t_{150}$ [min]	$t_{150,s1}$ [min]	$t_{150,s2}$ [min]	$t_{300}$ [min]	$t_{300,s1}$ [min]	$t_{300,s2}$ [min]	$t_{550}$ [min]	$t_{550,s1}$ [min]	$t_{550,s2}$ [min]
0	SF04	10	5.5	3.7	4.1	8.8	6.8	7.8	16.1	13.2	17.7
1	SF04	30	20.0	10.7	13.3	29.5	19.1	25.8	51.4	35.0	58.9
1	SU0401	17	7.1	5.8	6.8	13.9	10.5	13.0	28.7	19.7	29.5
2	SU0401	17	6.9	5.8	6.8	14.4	10.5	13.0	28.8	19.7	29.5
5A	SU0401	20	10.0	6.8	8.1	18.8	12.3	15.5	32.5	22.8	35.4
5B	SU0201	20	8.7	6.8	8.1	17.4	12.3	15.5	33.6	22.8	35.4
5C	CT0401	20	8.3	6.8	8.1	16.1	12.3	15.5	31.8	22.8	35.4
5D	CT0201	20	7.8	6.8	8.1	15.0	12.3	15.5	29.7	22.8	35.4
7	SU0401	44	28.7	17.4	22.8	46.6	31.0	44.9	74.9	56.1	101.3
9a	SU04	30	17.9	10.7	13.3	28.7	19.1	25.8	54.2	35.0	58.9
9b	SF04	30	18.4	10.7	13.3	30.2	19.1	25.8	54.4	35.0	58.9
13	CT04	20	7.7	6.8	8.1	15.8	12.3	15.5	n.a.	22.8	35.4

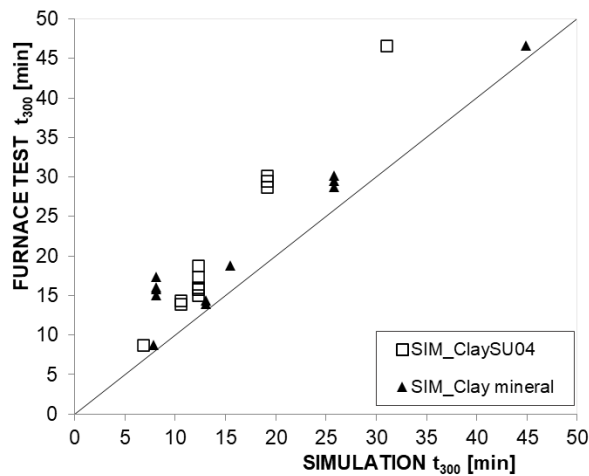


Figure 7-11. Relationship between the mean results of furnace tests and the first simulations on the time to reach 300°C on timber ( $t_{300}$ ) for clay plaster systems.

In case of lime plasters, a comparison of test results for the same plaster system 'LimeSU04' with a reed mat ('TESTS\_LimeSU04\_RM') and simulation results is shown in Figure 7-12. The presented test result denoted as 'TESTS\_LimeSU04\_RM' refers to a mean temperature curve for 20 mm and 30 mm thick plasters determined in Test 11a and Test 12a (Table 5-9), respectively.

In addition, the mean temperature curve of the same plaster (30 mm thick) tested on the wire mesh (Test 11b, Table 5-9) is presented as 'TEST\_LimeSU04\_WM'. In case of 30 mm plaster, the use of different types of plaster carriers does not appear to have a significant influence on the heat transfer mode; yet the use of reed mat has a slight influence until around 500°C. Therefore, the difference between the simulation and furnace test results for 30 mm thick plaster is most likely attributable to the limitations of the thermal properties used as input, including the absence of a plateau around 100°C, which slows down the heat transfer in furnace tests compared to the simulations results. Table 7-3 presents the results in view of temperature criteria obtained from furnace tests and simulations.

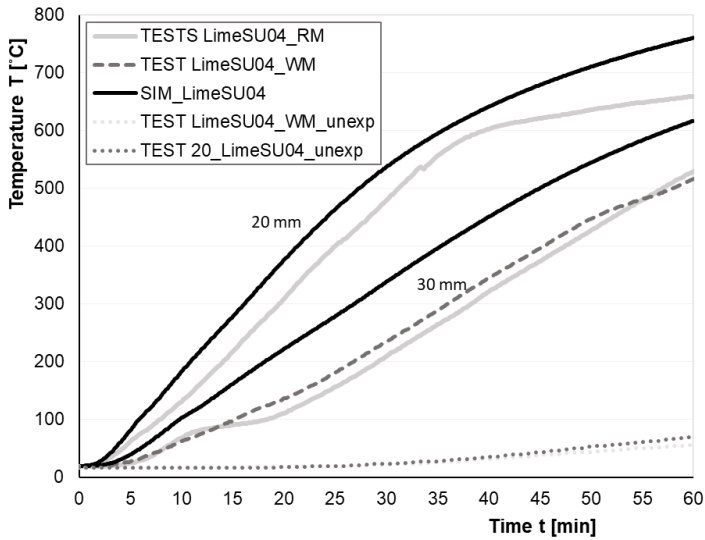


Figure 7-12. Comparison of temperature measurements obtained in furnace behind the lime plaster systems (with reed mat) and derived from the simulations of Model 2.

Table 7-3. Comparison of times to reach 150°C, 300°C and 500°C behind lime plaster systems (LimeSU04) determined in furnace tests and simulations of Model 2 based on TPS results.

Test specimen				Time to reach certain temperature behind lime plaster system					
Test No	Plaster Ref.	Plaster system' thickness $h_p$ [mm]	Plaster carrier	150°C		300°C		500°C	
				TEST	SIM_LimeSU04	TEST	SIM_LimeSU04	TEST	SIM_LimeSU04
				$t_{150}$ [min]	$t_{150,s}$ [min]	$t_{300}$ [min]	$t_{300,s}$ [min]	$t_{550}$ [min]	$t_{550,s}$ [min]
11a	LimeSU04_RM	30	reed mat	24.5	14.1	39.9	26.8	57.2	44.9
11b	LimeSU04_WM	30	wire mesh	21.7	14.1	36.1	26.8	58.2	44.9
12a	LimeSU04_RM	20	reed mat	11.2	8.4	21.4	16.1	31.2	27.3

## 7.4 Determination of effective thermal properties

The determination of effective thermal properties followed mainly the calibration method developed by (Mäger, 2016). This calibration procedure uses a MATLAB code, which changes the values of the thermal properties (thermal conductivity and specific heat) in the input file of the simulation software SAFIR and compares the results with fire test data (temperature-time curve) in the same point. The code for finding the input curve is based on simple principles. The software changes one value by a set percentage and then calculates the difference between the simulated and test result curves. It was found by (Mäger, 2016) that executing three consecutive loops with different increments yielded good results. This process is repeated until an acceptable correlation with test results is obtained and the temperature graphs are shifted iteratively closer. This calibration method is described in detail in a Master thesis by (Mäger, 2016), presented in a paper (Mäger et al., 2018) and it has been previously used to determine the effective material properties for some insulation materials (Tiso et al., 2016).

The determination of effective properties was carried out for two simulation models (clay and lime plaster systems): 1) MODEL CLAY and 2) MODEL LIME, respectively, see Table 7-4. Both models comprise two materials: a plaster and timber element. The influence of the plaster carrier was considered indirectly by the thermal properties of the whole plaster system.

*Table 7-4. Simulation model for the determination of effective thermal properties for clay and lime-based plasters.*

Properties		MODEL CLAY	MODEL LIME
Plaster system	Type	1. ClaySU04 2. ClaySF04 3. Clay_mineral	LimeSU04
	Thickness (mm)	10–44	20; 30
	Thermal properties	1. Table 6-1 2. Table 6-2 3. TPS results (Küppers et al., 2018)	Table 6-3
	Density (kg/m <sup>3</sup> )	1700; 1800	1750; 1800
Timber	Thickness (mm)	50	50
	Thermal properties	EN1995-1-2:2004	EN1995-1-2:2004
Boundary conditions (sides)		Adiabatic	
Ambient temperature		20°C	
Fire exposure		ISO 834; $\alpha = 25 \text{ W/m}^2\text{K}$ (EN 1995-1-2:2004)	
Unexposed side		20°C; $\alpha = 4 \text{ W/m}^2\text{K}$ (EN 1995-1-2:2004)	
Emissivity coefficient		0.8 (EN 1995-1-2:2004)	
Simulation model		2D	
Element type		Quadric, 1 mm x 1 mm	
Measurement point		Plaster system-wood interface	
Ref. temperature-time curve		Mean calculated temperature-time curve from each furnace test from the TP	
TP of furnace tests		TP1 – TP4	TP3

For this current thesis, Katrin Nele Mäger performed the calibration procedure using the MATLAB tool. The author of this thesis provided the input data for calibrations, assessed the calibration results, and performed the analysis for extensive modification of the calibrated material properties, which resulted in the determination of the proposed effective thermal properties.

### MODEL CLAY

First, a calibration procedure for both 30 mm thick clay plasters (ClaySU04 and ClaySF04) tested in TP3 is presented. The thermal properties are presented in Figure 7-13, where the comparison of properties obtained from the TPS tests (Chapter 6.1) and calibrated thermal properties (denoted with a symbol \_CAL30) is shown. A linear trend was assumed between the determined temperature points. Herein, a constant density value of 1800 kg/m<sup>3</sup> was considered.

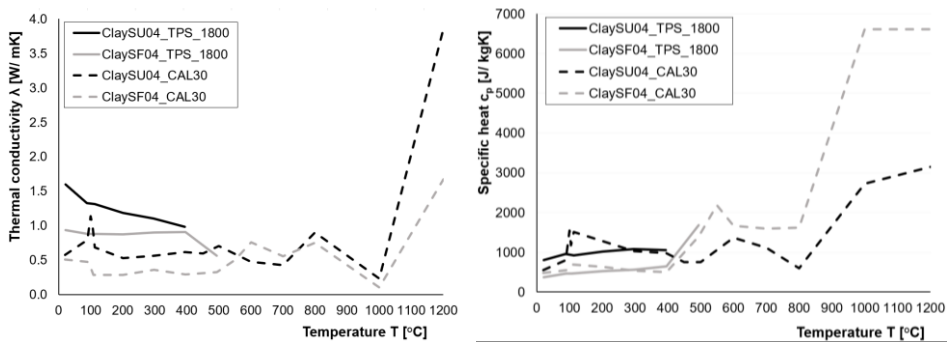


Figure 7-13. Comparison of thermal properties obtained from TPS tests and effective thermal properties determined by first calibrations.

Figure 7-14 presents the overview of the comparison of temperature curves between tests and simulations for ClaySU and ClaySF04. Although the agreement between the reference curve (30 mm thick plaster system) and simulations was excellent, the fit with temperature curves of varying thicknesses did not provide a similarly good match. In the case of thinner plasters of ClaySU (Figure 7-14a), the simulations underestimate the rise in temperature up to 300°C. In case of ClaySF04, there is a rather good agreement with tests of 10 mm and 30 mm thick plaster and simulations (SIM\_ClaySF04\_CAL30) (Figure 7-14b). For further comparison, the furnace test of a 44 mm thick plaster system (Test 7 – 44mm plaster ClaySU0401) was simulated using the effective properties of 'ClaySF04\_CAL30', however in this case, the simulation result demonstrated slower temperature increase compared to the mean measurements in furnace. Thus, there is space for improvement in order to determine a sufficient match between the tests and simulations for the whole range of plaster thicknesses.

Furthermore, the calibrated thermal properties appear not to truly capture the (theoretically realistic) material thermal performance; hence, there could be some improvement made. The thermal properties could be determined with a better correlation to their actual behaviour when exposed to high temperatures, e.g., the thermal conductivity should decrease when water is evaporated from the plaster (Chapter 4). As the calibrated values indicated a strong link with the provided input data (see the graphs in Figure 7-13), the key for developing more material specific properties is to supply more appropriate input data, which present the material changes at various temperatures (that may also include the modification of TPS test results) for the calibrations.

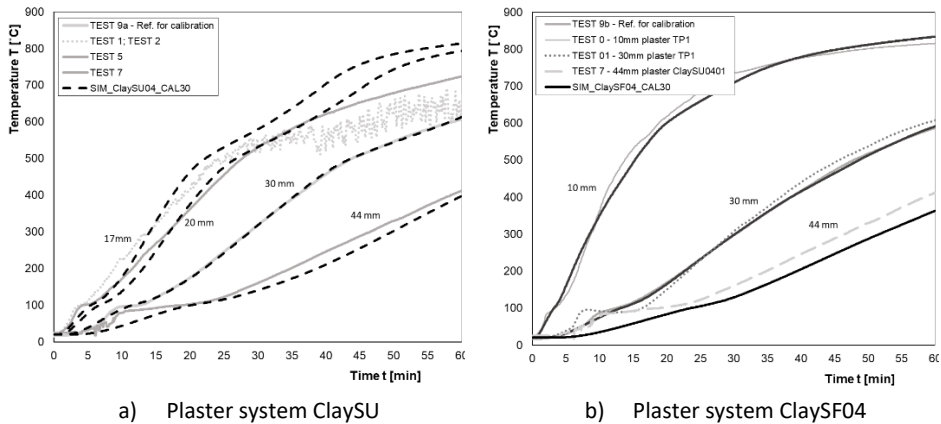


Figure 7-14. Comparison of temperature curves for different plaster thicknesses on timber determined by simulations using the effective thermal properties calibrated based on furnace tests in TP3 (Test 9a, Test 9b).

A more comprehensive study on the determination of effective properties for clay plaster systems was carried out in collaboration with Judith Küppers from TU Braunschweig, Germany. A joint publication (Küppers et al., 2018) has been published. In this paper, two distinct FEM software packages and mathematical computing software were introduced and compared regarding the determination of effective thermal properties: i) SAFIR software and MATLAB tool (Mäger et al., 2016), ii) FEM software ABAQUS and WOLFRAM MATHEMATICA (Küppers et al., 2018). Both methods used a distinct calibration sequence for the thermal conductivity and specific heat, which made them different in terms of how the calibration cycle runs were carried out. This comparison was expected to provide a better understanding of the properties' development and their compatibility with a wider range of plaster thicknesses.

The selected material properties for the initial calibrations are presented in Table 7-5, also presented in the respective paper. As the use of thermal properties of 'Clay mineral' demonstrated the closest fit to the furnace test results for the whole range of plaster thicknesses shown in Figure 7-9, this certain set of material properties were used for input. A mean temperature curve (at the interface of plaster and timber) obtained from Test 5A of TP2 (Table 5-8) was selected as the reference curve as it represents a common plaster thickness, and as the same plaster system was tested with various thicknesses. The TGA analysis of clay plasters showed that the total mass loss after around 900°C was rather little. Although the precise moisture content of the plasters was not explicitly determined but was expected to be around 1%, the density was taken constant (1866.65 kg/m<sup>3</sup>) at each temperature step. This value corresponded to the average density of the plaster tested by (Küppers et al., 2018).

Table 7-5 presents the input properties for the calibrations ('Clay\_mineral') considering a constant density value of 1866.65 kg/m<sup>3</sup>; and the calibrated thermal properties obtained using the two different methods carried out with SAFIR and ABAQUS software, designated 'Clay\_SAF1866' and 'Clay\_ABA1866', respectively. Figure 7-15 compares the combination of thermal properties by showing the change in the thermal diffusivities with temperature in both cases. There is a significant difference in thermal diffusivity values up to 150°C, which is also apparent in the temperature curves (Figure 7-16), where the 'SIM\_SAF1866' demonstrates a somewhat faster temperature increase up to this

temperature point. Afterwards, the diffusivity is slightly greater for Clay\_ABA1866 that seem to relate to its faster temperature increase at higher temperatures (Figure 7-16).

Table 7-5. Effective thermal properties based on the TPS test results (Clay mineral, constant density of 1866.65 kg/m<sup>3</sup>) and furnace test results from Test 5A.

Temperature	Thermal properties from TPS tests Clay_mineral (Küppers et al., 2018)		Calibrated thermal properties 'Clay_SAF1866' (Mäger, 2016)		Calibrated thermal properties 'Clay_ABA1866' (Küppers et al., 2018)	
	Thermal conductivity	Specific heat	Thermal conductivity	Specific heat	Thermal conductivity	Specific heat
T [°C]	$\lambda$ [W/ mK]	$c_p$ [J/ kgK]	$\lambda$ [W/ mK]	$c_p$ [J/ kgK]	$\lambda$ [W/ mK]	$c_p$ [J/ kgK]
20	1.192	821.43	2.36	361.43	2.36	887.15
50	1.109	868.97	2.20	535.29	2.22	938.48
90	0.998	932.34	1.32	664.57	1.98	1006.93
130	0.968	955.41	1.11	889.52	0.64	1054.77
150	0.955	999.53	0.50	1034.39	0.62	1410.53
200	0.923	1109.82	0.65	1059.57	1.02	1491.6
250	0.869	1198.13	0.66	1214.62	0.96	1351.49
300	0.816	1286.44	0.53	1589.42	0.87	1383.38
350	0.755	1270.46	0.60	1630.05	0.72	1424.34
400	0.694	1254.49	0.55	1609.56	0.68	1354.85
450	0.709	1452.17	0.61	1495.15	0.8	1386.42
500	0.724	1649.85	0.88	1811.93	0.86	1267.09
550	0.666	2014.06	1.25	1015.09	0.96	1015.08
600	0.608	2378.26	0.77	2012.96	0.76	2283.13

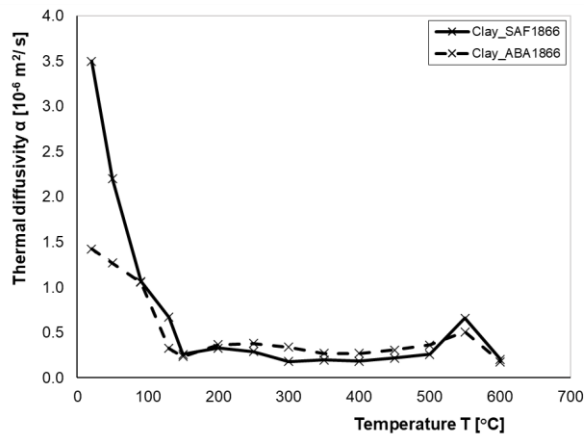


Figure 7-15. Comparison of effective thermal diffusivity values between simulation results of Clay\_SAF1866 and Clay\_ABA1866.

Figure 7-16 presents the overview of comparison of simulation results and mean temperature curves from furnace tests for 10–44 mm thick clay plaster systems. The times to reach certain temperature criteria are given in Table 7-6. The results of SIM\_ABA1866 demonstrated a somewhat faster temperature increase than those of SIM\_SAF1866, resulting in values that are consistently on the conservative side when compared to test results. In case of 44 mm thick plaster, the results of SIM\_SAF1866 fall on the nonconservative side after reaching 200°C on timber compared to test result. In both cases, the correlation between simulation and test results is weakest for 30 mm thick plaster at temperatures below 300°C. As the furnace test results for each test indicated some variation of temperature measurements throughout the exposed surface area during the test, a few-minute difference from the mean value for the simulation result was deemed acceptable so long as the simulations provide a conservative (safe) result. The comparison between the two methods of using SAFIR (SIM\_SAF) and ABAQUS (SIM\_ABA) to reach 300°C behind the plaster system in relation to the test results is presented in Figure 7-17.

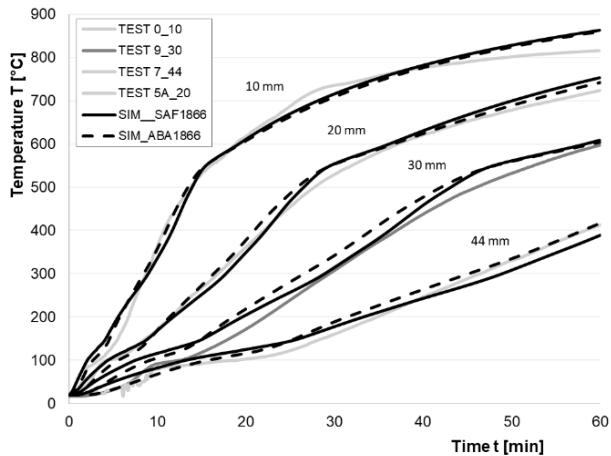


Figure 7-16. Comparison of temperature curves obtained in furnace and simulations with calibrated thermal properties based on “Clay mineral” input (Küppers et al., 2018).

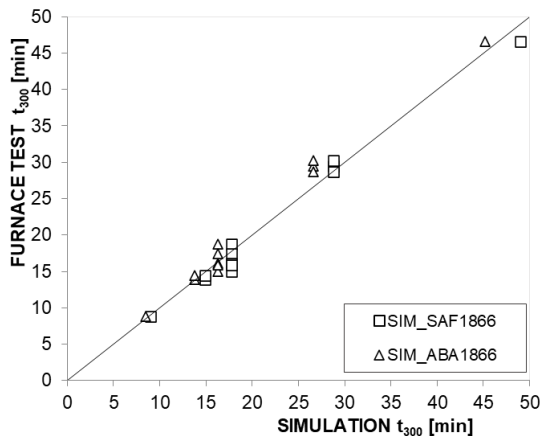


Figure 7-17. Comparison of the agreement between the times to reach the 300°C behind plaster system in furnace and simulations based on calibrated thermal properties (Table 7-5).

Table 7-6. Comparison of times to reach 150°C, 300°C and 550°C behind clay plaster determined in furnace tests and simulations based on calibrated thermal properties (Table 7-5).

Test specimen		Time to reach certain temperature behind clay plaster system								
Test No	Plaster system thickness $h_p$	150°C			300°C			550°C		
		TEST $t_{150}$	SIM_ SAF1866 $t_{150}$	SIM_ ABA1866 $t_{150}$	TEST $t_{30}$	SIM_ SAF1866 $t_{300,s1}$	SIM_ ABA1866 $t_{300,s2}$	TEST $t_{550}$	SIM_ SAF1866 $t_{550,s1}$	SIM_ ABA1866 $t_{550,s2}$
	[mm]	[min]			[min]			[min]		
0	10	5.5	4.2	4.6	8.8	9.0	8.5	16.1	15.5	15.4
1	30	20.0	15.2	15.1	29.5	28.8	26.6	51.4	47.9	48.2
1	17	7.1	7.3	7.7	13.9	14.9	13.8	28.7	24.8	24.9
2	17	6.9	7.3	7.7	14.4	14.9	13.8	28.8	24.8	24.9
5A	20	10.0	8.9	9.2	18.8	17.8	16.3	32.5	29.6	29.6
5B	20	8.7	8.9	9.2	17.4	17.8	16.3	33.6	29.6	29.6
5C	20	8.3	8.9	9.2	16.1	17.8	16.3	31.8	29.6	29.6
5D	20	7.8	8.9	9.2	15.0	17.8	16.3	29.7	29.6	29.6
7	44	28.7	26.0	25.5	46.6	49.0	45.2	74.9	80.8	81.3
9a	30	17.9	15.2	15.1	28.7	28.8	26.6	54.2	47.9	48.2
9b	30	18.4	15.2	15.1	30.2	28.8	26.6	54.4	47.9	48.2
13	20	7.7	8.9	9.2	15.8	17.8	16.3	n.a.	29.6	29.6

In Table 7-6, the obtained values from the simulations start to lose their agreement (at higher temperatures) with the furnace test results in case of thicker plasters (30 mm and 44 mm). In the example of SIM\_SAF1866, the time required to reach 300°C for 44 mm of plaster is underestimated by approximately 3 minutes; at 550°C, the difference between the simulation and the test had increased to 6 minutes. It was observed that the calibrated thermal properties for both cases demonstrated a significant decrease in thermal conductivity at around 100°C, which was preceded by a sudden rise in the conductivity (see the calibrated thermal conductivities of \_SAF and \_ABA around 100–200°C in Figure 7-18a). Consequently, a modification was made to the calibrated properties to combat this phenomenon in effective thermal properties. The modified thermal properties are shown in red on Figure 7-18 and presented in Table 8-1. Herein, the most significant change was made for the values of specific heat at around 150°C, which corresponds to the evaporation of free water, see Figure 7-18b. Thus, the thermal conductivity decreased more steadily at this temperature range compared to the one determined by the calibration.

Figure 7-19 compares the simulation results to the mean temperature data obtained from furnace tests from evaluating various thicknesses of plaster systems. Herein, a comparison was made between the simulations based on the calibrated thermal properties (in the legend marked as \_SAF and \_ABA, Table 7-6) and the simulation results based on the modified thermal properties wherein two different constant densities were selected 1700 kg/m<sup>3</sup> and 1866.65 kg/m<sup>3</sup>, results are marked as ‘SIM\_MOD1700’ and ‘SIM\_MOD1866’, respectively. A constant density value of 1700 kg/m<sup>3</sup> was selected as it

represents the mean value of tested clay plasters (density class 1.8), which should be used as the effective thermal property for density to determine the design equations. Table 8-1 lists the modified properties for clay plaster system that were proposed and used for the determination of the design equations in Chapter 8.

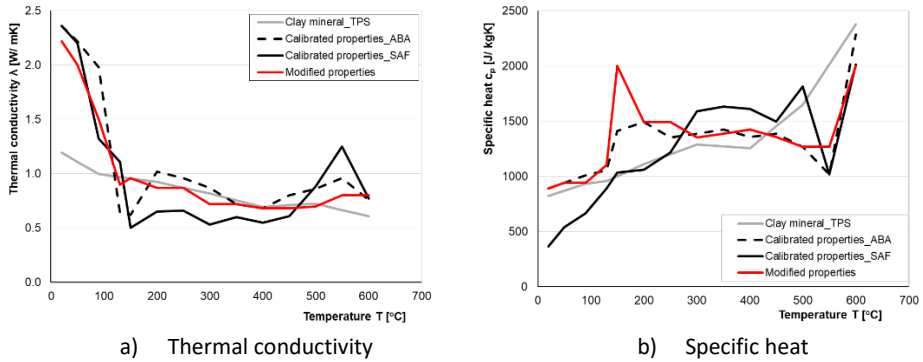


Figure 7-18. Comparison of the thermal properties determined by TPS tests (Küppers et al., 2018), calibrations and modifications for clay plaster systems.

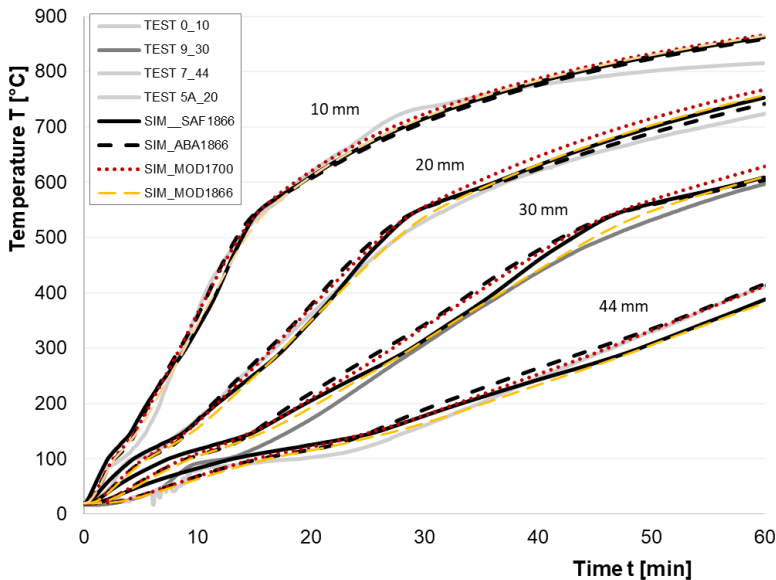


Figure 7-19. Comparison of temperature curves obtained from furnace tests and simulations with calibrated and modified thermal properties for clay plaster systems.

## MODEL LIME

The aim was to determine effective properties applicable to all tested lime-based plaster systems, independent of the type of plasters and the plaster carriers. Only the furnace tests of TP3 were used for calibration. As all types of lime-based plasters demonstrated a comparable level of protection with respect to their thickness, LimeSU04 was used as the basis for the simulations as it was also used in the TPS tests (Chapter 5.2.3). A constant density value of  $1750 \text{ kg/m}^3$  was chosen for calibrations.

The determination of effective properties was performed using the MATLAB tool and SAFIR software described above. The mean temperature curve of Test 11a (30 mm thick lime plaster ‘LimeSU04’ with a reed mat) was used as a reference for calibration. The input data is given in Table 6-3, Table 7-7 presents the calibrated thermal properties denoted as ‘LimeSU04\_Cal’. Despite the excellent correlation between the simulation with calibrated properties (SIM\_LimeSU04\_Cal, Figure 7-22) and the furnace test result (Test 11a) for 30 mm plaster; the calibrated properties didn't provide a good agreement with furnace test result of a 20-mm thick lime plaster (Test 12a), see Figure 7-22, ‘SIM\_LimeSU04\_Cal’. In this case, the temperature increase was considerably slower, resulting in a delay of more than 5 minutes after temperatures higher than 150°C behind plaster. Thus, the modification of calibrated properties was deemed necessary.

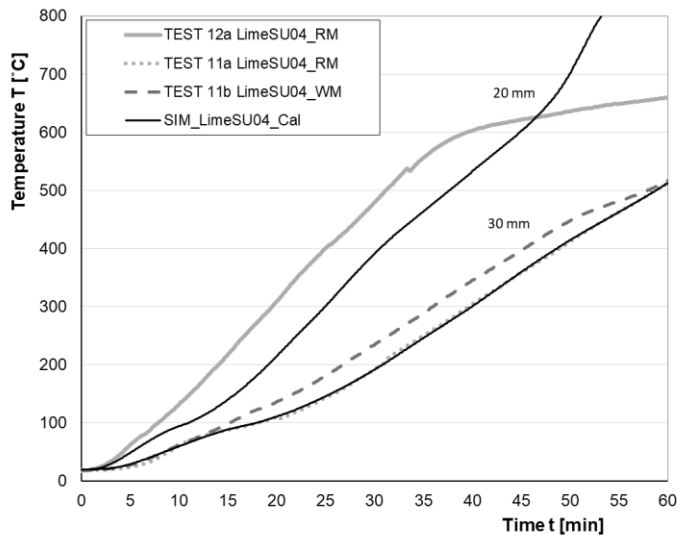


Figure 7-20. Comparison of furnace test results of lime plaster system LimeSU04 and first simulations based on calibrated thermal properties.

The first step in modifying the calibrated material properties (LimeSU04\_Cal) included decreasing the values of the thermal properties. This was done by using the same thermal diffusivity values as determined for ‘LimeSU04\_Cal’, with the exception that the values of thermal conductivity and specific heat was reduced by half. Following this, additional modifications were made to optimise the fit to obtain a realistic trend of change in material properties in response to temperatures. The improvement of properties was based on the try to follow theoretical approach in the change of material performance at high temperatures, such as an increase in specific heat round 100°C owing to the evaporation of free water, etc. The modified properties are presented in Table 7-7.

Figure 7-21 compares the thermal properties determined from TPS tests with the initial calibration results (Table 7-7), which vary significantly. The performance of the modified properties is somewhat comparable to that of LimeSU04 determined by TPS testing, except for the thermal conductivity being notably higher at lower temperatures and the specific heat being somewhat higher. Compared to the effective thermal properties of concrete, the sudden decrease of lime plasters’ thermal conductivity until around 100–200°C is caused by the evaporation of free water while the gaps in the plaster are filled with air having lower conductivity values. The higher values for specific

heat in range of 140–160°C are directly related to the higher heat capacity of water compared to air and solids. The properties should ideally also show some increase in specific heat around 600–800° due to the decomposition of the limestone. This process is associated with a reduction in the plasters’ density due to the mass loss associated with carbon dioxide generation. However, in this thesis, the developed properties for lime-based plasters do not represent all the material specific transformations the plaster undergoes. The peak of specific heat around 100°C is not significant since lime plasters have a low moisture content. The specific heat is approximately stable over the whole temperature range, similarly, to concrete after 200°C. It might be argued that the higher specific heat values of lime plaster compared to those of concrete (EN 1995-1-2) are attributable to its composition, which includes calcium hydroxide and calcium carbonate, which requires more energy to decompose.

*Table 7-7. Determined effective thermal properties based on the TPS test results (LimeSU04) and furnace test results from Test 11a (TP3).*

Temperature T [°C]	Thermal properties from TPS test 'LimeSU04'		Calibrated thermal properties 'LimeSU04_Cal'		Modified calibrated properties 'LimeSU04_Mod'	
	Thermal cond. $\lambda$ [W/ mK]	Specific heat $c_p$ [J/ kgK]	Thermal cond. $\lambda$ [W/ mK]	Specific heat $c_p$ [J/ kgK]	Thermal cond. $\lambda$ [W/ mK]	Specific heat $c_p$ [J/ kgK]
	20	0.95	818.2	3.71	3117.5	2.20
90	-	-	3.17	3430.0	2.00	1558.8
101	0.89	1015.5	1.52	4064.3	1.50	1558.8
141	0.86	1074.7	1.49	4214.9	1.00	3000.0
212	0.82	1132.2	1.19	3310.4	0.80	1800.0
263	0.77	1246.6	1.26	3364.4	0.80	1682.2
315	0.66	1191.2	1.09	3150.8	0.80	1575.4
423	0.62	1267.5	1.27	3352.4	0.70	1676.2
500	0.62	1267.5	1.12	3777.7	0.60	1676.2
600	0.62	1267.5	1.32	3931.2	0.60	1000.0
700	0.62	1267.5	1.12	1954.9	0.60	1000.0
800	0.62	1267.5	1.99	503.1	0.60	1000.0
1000	0.62	1267.5	2.42	1258.3	0.60	1000.0
1200	0.62	1267.5	2.42	15217.6	0.60	1000.0

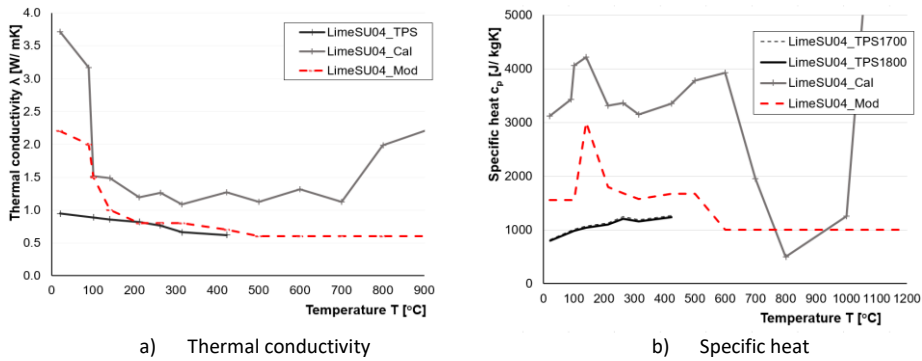


Figure 7-21. Comparison of thermal properties determined for lime plaster (LimeSU04).

Figure 7-22 illustrates the comparison of mean temperature curves obtained in furnace tests (TP3) plotted against the simulation results of SIM\_LimeSU04\_Mod. The simulations overestimate the temperature increase in case of 30 mm plaster system with a reed mat, however the results show a good agreement to the same plaster system with a wire mesh. Therefore, the simulation result is considered satisfied for both cases. In case of 20 mm plaster, there is a satisfactory agreement between test and simulation as the difference is very minimal. The simulation result yields good agreement also for the 20 mm thick lime plaster that composed some cement component (LimeSUC04) until 600°C. At temperatures higher than 600°C, there is gradual increase in temperatures according to the simulation compared to the test result. However, the critical temperature points of 150°C and 300°C provide a sufficient fit to the test results and is deemed sufficient for the development of design equations in Chapter 8.

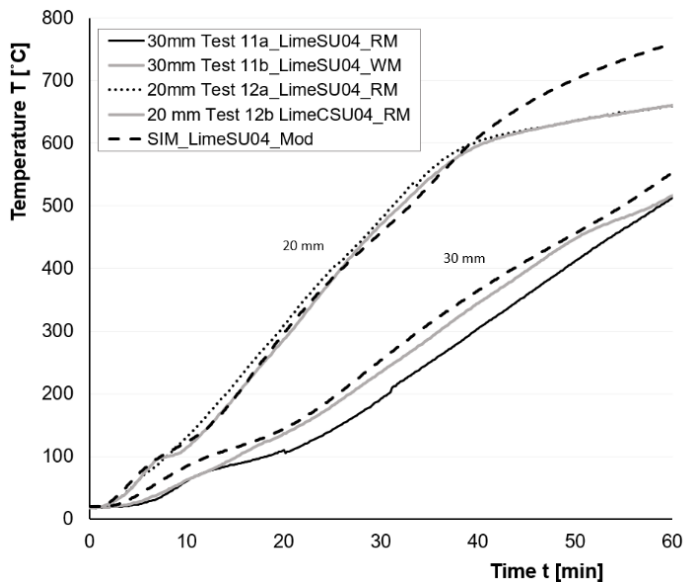


Figure 7-22. Comparison of temperature curves obtained from the furnace tests (TP3) for LimeSU04 plaster systems and simulations with (modified) effective thermal properties.

Table 7-8. Comparison of times to reach 150°C, 300°C and 500°C behind plaster determined in furnace tests and simulations based on modified thermal properties.

Test specimen		Time to reach certain temperature behind clay plaster system							
Test No	Plaster Ref.	Plaster system' thickness	Plaster carrier	150°C		300°C		500°C	
				TEST	SIM_LimeSU04_Mod	TEST	SIM_LimeSU04_Mod	TEST	SIM_LimeSU04_Mod
		$h_p$ [mm]		$t_{150}$ [min]	$t_{150,s1}$ [min]	$t_{300}$ [min]	$t_{300,s1}$ [min]	$t_{500}$ [min]	$t_{500,s1}$ [min]
10a	LimeSAK*	30	WM	20.6	17.6	33.2	29.1	50.2	47.7
10b	LimeCSU04	30	WM	19.4	20.8	32.9	33.9	52.5	54.9
11a	LimeSU04	30	RM	24.5	20.8	38.5	33.9	57.2	54.9
11b	LimeSU04	30	RM	21.7	20.8	36.0	33.9	58.2	54.9
12a	LimeSU04	20	RM	11.2	12.4	19.5	20.2	31.2	32.9
12b	LimeCSU04	20	RM	11.9	12.4	19.9	20.2	30.9	32.9

\*A constant density value of 1400 kg/m<sup>3</sup> was used as declared by the product specification.

With the use of a reed mat, it appears that a longer plateau forms at around 100°C, causing a slower increase in temperature behind the plaster throughout 60 minutes. When using wire mesh, the temperature rises faster, especially when the plaster comprises cement component (LimeSAK01 and LimeCSU04). It may be concluded that the type of plaster carrier appears to have an influence on the fire protection effect of the plaster system. In case of plaster carriers like reed mat, the air gaps in the reed stems reduce the thermal conductivity of the whole protection system. As contrasted to a wire mesh, which is relatively thin and, due to the high thermal conductivity of metals, may potentially have some opposite effect.

Lime plaster is a porous material comprising various types of volumetric constituents of materials (all undergoing their specific processes of heat transfer, including the specifics related to the hydrated lime), thus the determination of its effective thermal properties was somewhat challenging. Consequently, simplifications were made that could be referred to roughly comparable to those for concrete, since it is somewhat a similar mixture of numerous constituents. As the thermal properties are strongly dependent on various factors such as moisture content, porosity and quantities of aggregates, the determination of 'realistic' thermal properties is a highly complex matter that should be a study on its own. Thus, the determined properties for lime plaster systems in this thesis are deemed sufficient as they provide a good fit to the furnace test results and cover all the different types of lime plasters (including the plaster carriers). In contrast to clay plasters, the calibration of thermal material properties for lime-based plasters appears to be more complex due to the carbonisation of the lime and its influence on the thermal properties of the plaster system.

## 8 Determination of the design equations

The design equations for clay and lime plaster systems were determined in view of the guidance given in a paper by (Mäger et al., 2017) and prEN 19951-2:2022 (Annex G). The design equations for lime-based plasters were developed in the range of 20 to 30 mm and for clay plaster systems in the range of 10 to 44 mm, as tested in furnace. All plasters were assigned the same density value of 1700 kg/m<sup>3</sup>, which best represents the mean values of the investigated plaster systems.

The effective thermal properties of clay and lime-based plasters used for the determination of the main design equations (determined in Chapter 7.4) are presented in Table 8-1. The density value of 1700 kg/m<sup>3</sup> was considered constant at all temperatures. As a component of the plaster system, the impact of the plaster carrier was considered indirectly.

*Table 8-1. Effective thermal properties for clay and lime plaster systems used for the determination of design equations.*

Clay plaster system			Lime plaster system		
Temp.	Thermal conductivity	Specific heat	Temp.	Thermal conductivity	Specific heat
T	$\lambda$	$c_p$	T	$\lambda$	$c_p$
[°C]	[W/ mK]	[J/ kgK]	[°C]	[W/ mK]	[J/ kgK]
20	2.22	887.2	20	2.20	1558.8
50	2.00	938.5	90	2.00	1558.8
90	1.50	938.5	101	1.50	1558.8
130	0.90	1100.0	141	1.00	3000.0
150	0.96	2000.0	212	0.80	1800.0
200	0.87	1491.6	263	0.80	1682.2
250	0.87	1491.6	315	0.80	1575.4
300	0.72	1351.5	423	0.70	1676.2
350	0.72	1383.4	500	0.60	1676.2
400	0.68	1424.3	600	0.60	1888.8
450	0.68	1354.9	700	0.60	1000.0
500	0.70	1267.1	800	0.60	1000.0
550	0.80	1267.1	900	0.60	1000.0
600	0.80	2000.0	1000	0.60	1000.0
1200	0.80	2000.0	1200	0.60	1000.0

### 8.1 Basic protection time

The basic protection time ( $t_{\text{prot},0,i}$ ) from simulations  $t_{\text{prot},0,\text{sim}}$  is taken as the time from the start of standard fire exposure until the temperature rise on the unexposed side of the investigated layer reaches 270°C. The configuration of simulations is illustrated in Figure 8-1, where the investigated material (plaster system) is considered as a layer 1 (L1) and a 19 mm thick wooden particleboard as a layer 2 (L2). In the new generation of Eurocode 5 Part 1-2 (prEN 1995-1-2:2022), the basic protection time is also considered as the start time of charring of timber ( $t_{\text{ch}}$ ).

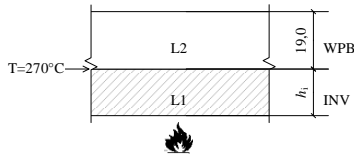


Figure 8-1. The simulation configuration to determine the basic protection times (prEN 1995-1-2:2022).

The results for clay and lime plaster systems are shown in Figure 8-2. The comparison of simulations and mean test results from furnace tests are given. Table 8-2 presents the times to reach 270°C behind plaster system in furnace tests and in simulations. Note that the simulation result for 30 mm thick lime plaster with a reed mat (\_RM) is rather conservative. However, as shown in Figure 8-2b, the effective thermal properties were developed to propose design equations independent of the type of plaster carrier used. As the furnace tests (TP3) with lime plaster showed cracking when applied on reed mat, the conservative estimation in case of 30 mm lime plasters is considered to be adequate (Figure 8-2b). In case of clay plasters, the presented design equation based on simulations is proposed based on tests with clay plaster and reed mat. There is a good agreement between the test results and simulations for the whole range of plaster thicknesses (Figure 8-2a).

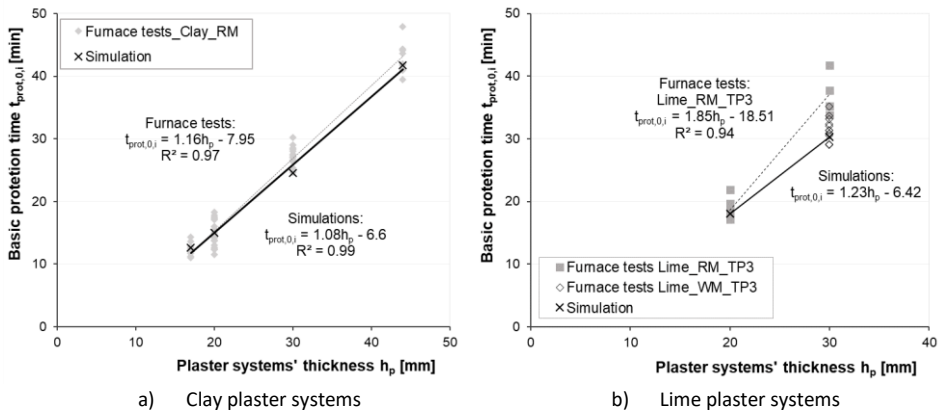


Figure 8-2. Comparison of the basic protection times determined by simulations and tests.

Table 8-2. Comparison of basic protection times and the mean test results of reaching 270°C behind plaster system with a reed mat.

Plaster system' thickness	Clay plaster system		Lime plaster system	
	TEST	SIMULATION	TEST	SIMULATION
$h_p$ [mm]	$t_{270}$ [min]	$t_{prot,0,i}$ [min]	$t_{270}$ [min]	$t_{prot,0,i}$ [min]
17	12.3	12.6	-	-
20	14.8	15.0	18.6	18.1
30	27.0	24.6	37.1/ 31.6*	30.0
44	43.0	41.8	-	-

\*Lime-based plasters with a wire mesh.

## 8.2 Basic insulation time

The basic insulation time ( $t_{ins,0,n}$ ) from simulations  $t_{ins,0,sim}$  is taken as the time from the start of standard fire exposure until the temperature rise on the unexposed side of the investigated layer reaches 160°C. Figure 8-3 presents the simulation configuration. The temperature on the unexposed side of the layer (L1) is taken as 20°C. Figure 8-4 shows the simulation results for both types of plaster systems. A comparison to furnace test findings (temperature increase behind plaster) is made, despite the fact that the plaster was not tested on the unexposed side as a last layer. In simulations, however, the air on the opposite side of the plaster should have a cooling effect compared to wood as a backing layer.



Figure 8-3. The simulation configuration to determine the insulation times (prEN 1995-1-2:2022).

For clay plaster systems, with reed mat (Figure 8-4a), the simulation results agree with the furnace results for the whole range of thickness. In case of lime plasters, the simulation aimed to provide good fit to all test results, independent from the plaster carrier used. Table 8-3 presents the comparison of mean values determined by simulations and tests.

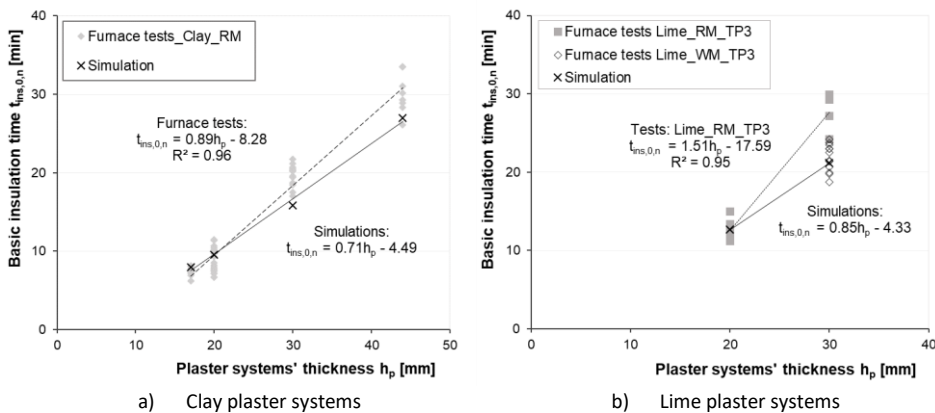


Figure 8-4. Comparison of test results and insulation times determined by simulations.

Table 8-3. Comparison of basic insulation times and the mean test results of reaching 160°C behind plaster system with a reed mat.

Plaster system' thickness	Clay plaster system		Lime plaster system	
	TEST	SIMULATION	TEST	SIMULATION
$h_p$ [mm]	$t_{160,timber}$ [min]	$t_{ins,0,sim}$ [min]	$t_{160,timber}$ [min]	$t_{ins,0,sim}$ [min]
17	7.4	8.0	-	-
20	8.7	9.6	12.6	12.7
30	18.7	15.8	27.7 / 21.8*	21.2
44	30.1	27.0	-	-

\*Lime-based plasters with a wire mesh.

### 8.3 Position coefficients

Position coefficients consider the influence of the layers that are backing and preceding the investigated layer. The  $k_{pos,exp}$  considers the effect of the preceding layer on the investigated layer, whilst the  $k_{pos,unexp}$  takes into account the effect of the backing layer.

In the furnace test program TP2 (Chapter 5.4.1), the clay plaster systems were tested in two distinct configurations, with a timber element and a reed board ( $\rho = 225 \text{ kg/m}^3$ ) serving as the backing layer (substrate). In Figure 6-34, it is presented that heat transfer through the plaster system was significantly faster when plaster was backed by a reed board, i.e.  $270^\circ\text{C}$  was reached earlier. Thus, a coefficient  $k_{pos,unexp}$  can be proposed. Figure 8-5 presents the comparison of times to reach  $270^\circ\text{C}$  behind the clay plaster backed by timber and reed board. For the whole range of plaster thicknesses, a fairly similar difference between the results is apparent. The position coefficient for plasters backed by reed board was developed based on the test data and may be assumed as  $k_{pos,unexp} = 0.75$ . Table 8-4 presents the comparison of mean test results in comparison to the calculation results when the coefficient of 0.75 is used in case of reed board as a backing layer.

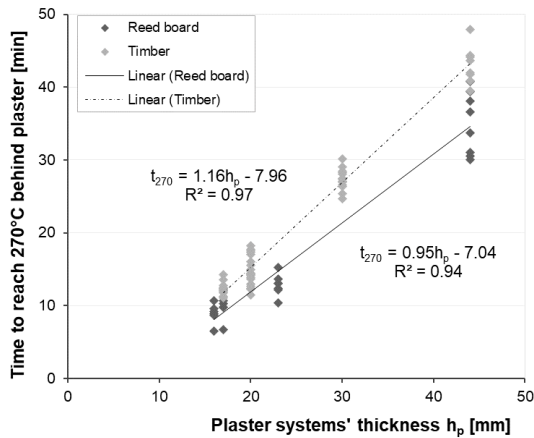


Figure 8-5. Comparison of test data to reach  $270^\circ\text{C}$  behind the plaster systems on timber element and reed board.

Table 8-4. Mean times to reach  $270^\circ\text{C}$  behind clay plaster system on timber and reed board in furnace tests and calculation results when position coefficient is used in case of reed board.

Plaster system' thickness	TEST		CALCULATION
	TIMBER	REED BOARD	REED BOARD
$h_p$ [mm]	$t_{270,timber}$ [min]	$t_{270,RB}$ [min]	$t_{270,timber} \cdot k_{posunexp}$ [min]
17	12.30	9.90	9.23
20	14.80	11.96*	11.10
23	18.72*	12.80	14.04
30	27.00	21.46*	20.25
44	43.00	35.00	32.25

\*This plaster thickness was not tested; thus, the values are calculated by the equations given in Figure 8-5.

Although lime-based plasters have been tested only on timber, it may be assumed that the same proposed value for  $k_{pos,unexp}$  could be used in case of lime plasters on a reed board. This approach may be considered adequate due to the similar material characteristics of a heavy weight plaster and test results obtained in TP3.

When plaster is backed by timber (as tested in this work) or other building panels (described in FSITB and prEN1995-1-2:2022), a generic value of  $k_{pos,unexp} = 1$  may be used.

This current work did not evaluate the  $k_{pos,unexp}$  for plaster systems as a backing layer. Herein a reference could be made to a previous work by (Rauch et al., 2021), wherein the contribution of floor screeds as a fire protection layer for timber floor elements was assessed. It was noted that the floor screeds backed by another layer of screed or concrete (EN1992-1-2) provide more conservative results than the simulations with panels or a timber member as there appears to be a cooling effect due to the high thermal conductivity of the screeds. This approach may be alike attributed to the plasters tested in this thesis due to their similarities in material compositions and thermal properties. Thus, in case clay or lime-based plaster system is considered as a backing layer, the position coefficient for other materials could be taken as  $k_{pos,unexp} = 1$ .

### 8.4 Protection factor

The charring rates of the timber element behind plaster system (Phase 2, Chapter 2.2.1) are determined by multiplying the basic design charring rate ( $\beta_0$ ) by a protection factor  $k_2$ . The analysis of the charring of timber specimens in this work was presented in Chapter 6. The design equations for clay and lime plaster systems are provided based on test results. An overview of test specimens and programs was given in Chapter 5.4.

Figure 8-6a shows the results of protection factors obtained from furnace tests for clay plaster systems. The protection factors shown with crosses are the values determined from the specimen's midsection (i.e., excluding the measurements of TC that positioned near the edges or corner areas of the specimen). The somewhat higher protection factors were determined mostly in the corner areas of the test specimen; in case of 44 mm thick clay plaster, two values indicate the locations where crack development was observed during testing (partial fall-off of the first plaster layers was observed at around 64 minutes).

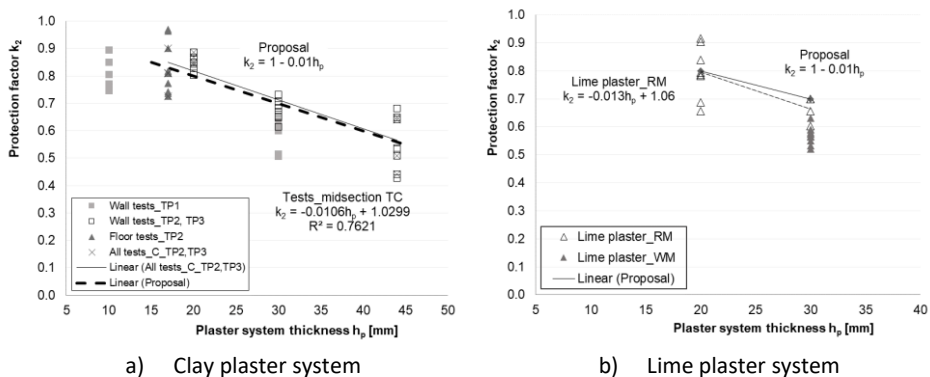


Figure 8-6. Furnace tests results on the relationship between the plaster thicknesses and the determined protection factors: a) Clay plaster system; b) Lime plaster system.

Figure 8-6b shows all furnace test results obtained from TP3 for lime-based plaster systems. The results are presented with regards to the type of plaster carrier used (reed mat as  $\_RM$  and wire mesh as  $\_WM$ ). In the case of  $WM$  as a plaster carrier, the protection factors have lower  $k_2$  values, but it was considered not necessary to differentiate between plaster carriers and the  $k_2$  factor. In Chapter 6, Figure 6-45 presented the comparison of the protection effect provided by clay and lime plasters. While the mean values for clay and lime plaster systems presented a comparable protection in terms of the mean charring rates of timber behind the plaster systems, the same design equation was proposed for both type of plaster systems. The design equation derived from the mean values is deemed adequate as it follows the common approach when determining design parameters for other materials. Considering the mean values could be further supported by the charring analysis of timber specimens, which showed a relatively uniform charring depth across the entire specimen; hence, there does not seem to be a significant risk associated with providing a safer proposal.

### 8.5 Failure time

The failure of the fire protection system is regarded as its fall off which is followed by the post-protection charring phase of the substrate (Phase 3, Chapter 2.2.1). The failure times of the plaster systems were observed mainly in tests carried out in horizontal position, except Test 6D in TP2 (clay plaster applied on reed board). The results were analysed in Chapter 6.3.2.

Tests with clay plaster systems indicated two distinct failure modes, depending on how the plaster was applied to the substrate. When a plaster carrier (reed mat mechanically fixed to timber) was used, the failure of the clay plaster system was attributed to the fastening system to timber. In the case of reed board as a plaster substrate, the failure of the clay plaster system was due to the loss of adhesion between the two materials at a certain temperature range. Figure 8-7 presents the test results observed in horizontal furnace tests in case a reed mat on timber (Figure 8-7a) and a reed board (Figure 8-7b). Based on the test results, design equations are proposed in Chapter 10.2.

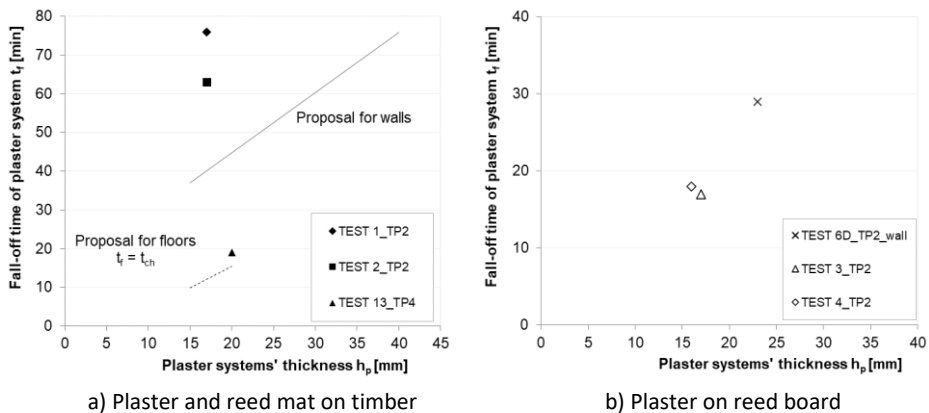


Figure 8-7. The failure times of clay plaster systems.

The performance of plaster and reed mat as a plaster system demonstrated that the fall-off is predominantly related to the start time of charring but is also influenced by the charring of timber and the length of fasteners. In Figure 8-7a, the presented trendlines

for  $t_f$  in case of wall and floor position are illustrated in relation to the plaster systems' thickness. Here, in case of walls, the proposal is given when staples of 25 mm in length are used (considering 10 mm left in uncharred wood), according to the design equation (20). This proposal is deemed sufficiently safe since furnace testing in wall position showed no fall-off times, although fire tests lasted 60 minutes or more. In floor position, gravity demonstrated a major influence on the fall-off of the plaster system; hence, no contribution from the fastening system to the protection effect can be proposed. Thus, the failure time in ceilings could be taken equivalent to the start time of charring of the substrate, see equation (14) for clay plaster system. In case of lime plaster, its performance in case of ceilings should be further tested and no design equation could be proposed.

In Figure 8-7b, the fall-off times of clay plaster system from the reed board were observed when the temperature at the interface of plaster and reed board was measured in all cases in range of 400–500°C. Based on the test data, recommendation about the loss of adhesion could be made regarding the temperature increase behind plaster system. It is adequate and safe to propose that the loss of adhesion corresponds with the start time of charring of the substrate. This may apply to wall and ceiling positions in case of clay plaster systems.

In the case of 44 mm thick clay plaster systems (Test 7 and Test 8, TP2), the plaster coats detached from the plaster system after some time of testing, but as the timber was not directly exposed to fire throughout the test, this was not regarded a failure time. The influence of this phenomenon on the charring performance of timber was taken into account when determining the protection factor  $k_2$ .

The lime-based plasters were mainly tested in a smallest furnace (in TP3), where no fall-off time was determined. In the case of walls, it may be presumed that lime-based plasters stay attached to timber similarly to clay plaster systems, as was observed in furnace tests in TP3. However, further testing is required to assess the failure modes of lime-based plasters due to its material specifics as the horizontal furnace tests in TP4 (Test 14) presented a sudden fall off. This appears to be attributed to the thermal degradation of the material, which is linked to the plaster's mechanical strength (linked to the carbonisation level of the lime plaster itself). The thermal degradation should be considered as a third type of failure mode for certain types of lime plasters.

## 8.6 Validation by full-scale tests

There are limited fire test data available for timber structures with traditional plaster systems. The application of plaster to timber may be encountered in furnace tests with straw bale structures where the plaster is applied directly on the straw bales. The overview of available full-scale test results thus mostly consists of different types of building elements where the plaster has been utilized as the finishing layer exposed directly to fire. This is particularly a case for clay plaster that is combined with various building boards used in contemporary building practice in contrast to traditional building methods, in which plaster was directly applied on solid timber.

The following overview and comparison of existing full-scale tests aims to provide the closest feasible validation for the test findings in this thesis, based on the available test reports and literature to the author, listed in Table 8-5. Table 8-6 presents the test data obtained from the test reports, e.g., development of cracks and fall-off times of plaster. In Table 8-6, the plaster substrates are denoted as SB – straw bales; SP – straw panel; CB – clay board; WP – wood panel; WFB – wood fibre insulation board; PLY – plywood;

SOF – softwood lumber boards with groove and tongue joints. It must be emphasised that since test results were in many cases presented in a general manner, it was challenging to pinpoint specific temperature points of interest, such as the times to reach 300°C behind plaster. Hence, there may be some inaccuracies or deviations in some of these presented results. Still, the collected information should offer the best possible approximation of the level of protection effect provided by plasters that can be presented at this moment. The Test Report 14 describes two large-scale furnace tests (Test 14A and Test 14B) in which the test specimen dimensions were 2500 mm x 3000 mm, which is somewhat smaller than the standard size. Yet, this test report presents the most direct comparison to the intermediate scale furnace tests carried out in this thesis.

*Table 8-5. Full-scale test reports.*

No.	Test Report	Report date	Test facility
1	32487/3833 -CM vom 14.08.2003	14.08.2008	MPA, TU Braunschweig, Germany
2	Chilt/RF13217/AR1	05.10.2013	Ireland, UK
3	FIRES-FR-021-18-AUNE	21.02.2018	Slovakia
4	Chilt/RF09001	21.01.2009	Bath, UK
5	Project No. 3098054B	09.07.2007	USA
6	FIRES-FR-052-21-AUNE	26.03.2021	Slovakia
7	PGA12221A	20.01.2023	Denmark
8	PGA12221B	20.01.2023	Denmark
9	3066/490/07 - CM vom 21.04.2008	21.04.2008	MPA, TU Braunschweig, Germany
10	3067/491/07 11.06.2008	11.06.2008	MPA, TU Braunschweig, Germany
11	3798/999/13 - NB vom 18.02.2014	18.02.2014	MPA, TU Braunschweig, Germany
12	Nr. PB 3.2/16-288-3	02.10.2017	MFPA Leipzig GmbH
13	O100402-1101398-2	09.12.2022	RISE, Sweden
14	RAK/2683/2022	22.02.2023	Tampere University, Finland

The test findings indicate that the clay plaster (described mainly as a basecoat) falls into a similar density range as tested in this thesis. Based on the reported observations, the cracking of plaster was not directly followed by a fall-off of plaster, but the development of cracks over the surface was observed in time. In some cases, the fall-off of parts of plaster has been determined. The test data and total test times indicate that the plaster contributes to the fire resistance of timber structures. When the fall-off time of plaster is noted as ‘no comment’ in Table 8-6, it denotes that this was not determined/observed. In Test 3 (Table 8-5), for example, the clay plaster (with glass fibre mesh as a reinforcement) was applied directly to the straw surface and the timber studs. At around 61 minutes, the only observation made was the formation of cracks.

Majority of the test reports have limited data with respect to the plasters’ performance, as they lack temperature measurements behind the plaster and limited observations have been made regarding the crack developments and failure times. However, two recent tests with 25 mm thick clay plaster (as a finishing material) have been performed (in horizontal position) to meet the K-class criteria. Both tests (Test 7 and 8, Table 8-6) demonstrated a strong adhesion between the clay plaster and its substrate throughout the test. In test report 7, the plaster was applied directly on the straw panels, in case of the timber frame, a wood fibre underlay strips ( $\rho = 250 \text{ kg/m}^3$ ) were used before the plaster was applied. The test succeeded the K<sub>10</sub> criteria as the minimum and maximum temperature rise on the substrate (straw) was 125°C and 174°C. The results indicate that the relatively thick clay plaster is able to stay intact to its substrate without any mechanical fixation (plaster carrier) for at least 10 minutes on

straw panel in ceilings. No detachment of plaster coats or any failure of the plaster was detected. Another test (Test report 8) was conducted with a 25 mm clay plaster on a wood fibre insulation board ( $\rho = 246 \text{ kg/m}^3$ ), where the mean temperature rise after 10 minutes behind plaster was  $238^\circ\text{C}$ . Until this temperature, no failure of plaster system was determined. Interestingly, after the test was terminated, a delamination of the 60 mm (20–20–20) thick wood fibre insulation board occurred, as the first fire-exposed layer of the board (20 mm) delaminated and fell down together with the plaster system. This may be of further evidence on the good adhesion strength between the plaster and the fibreboard, since the plaster did not detach from the board, but the board failed itself.

Table 8-6. Test data obtained from the full-scale fire test reports.

No	Test standard	Plaster type	Plaster substrate	Plaster thickness [mm]	Plaster density [kg/m <sup>3</sup> ]	First cracks in plaster* [min]	300°C behind plaster system [min]	Fall-off time of plaster system [min]	Total test time [min]	Classification
1	EN1365-1	clay	SB	30	1665-1820	37/74***	15-23	no comment	95	REI90
2	EN 1365-1	clay	SB	25	basecoat	70	n.a.	no fall-off detected	135	REI135
3	EN1365-1	clay	SB	25-30	basecoat/fine coat	61	37****	no comment	121	REI120
4	EN1364-1	lime	SB	30	basecoat	76/89**	n.a.	110	135	-
5	ATME E119	clay	SB	25	basecoat	13	n.a.	42**	60	REI60
6	EN1365-1	gypsum	SB	25	800	33	n.a.	no comment	107	REI90
7	EN 14135	clay	SP	25	1650	-	-	no fall-off detected	10	K <sub>1</sub> 10 K <sub>2</sub> 10
8	EN 14135	clay	WFB	25	1650	-	-	-	10	-
9	EN 1365-1	clay	SP	8	n.a.	7/11**	2-3	22**	53	REI45
10	EN 1365-1	clay	SP	30	1600	17/30**	15-22	30**/ 35	37	REI30
11	EN 1365-1	lime	WFB	10	800	-	-	no fall-off detected	92	90
12	EN 1364-1	clay	CB	5	1610 - 1800	11/11**		38 (45 with CB)	60	EI45/ F30
13	EN 1365-1	clay	CB	6	1641	11.5	40 (behind 24mm CB)	99 (with CB and WP)	114	114
14 A	EN 1364-1	clay	PLY	30	1734	-	25.5	no fall-off detected	49	-
14 A	EN 1364-1	clay	SOF	30	1734	-	24	no fall-off detected	49	-
14 B	EN 1364-1	clay	PLY	30	1741	33	27	no fall-off detected	71	-

\*Noted by the observations made during the test

\*\*Fall-off of parts of plaster

\*\*\*Cracks all over the surface

\*\*\*\*Measured inside the insulation

When comparing the test result on temperature measurements obtained in Test Report 8 (Table 8-5) to the temperature rise measured behind a 23 mm thick clay plaster on a reed board (Chapter 6.3) in this thesis, the results are very comparable. The time to reach  $\sim 238^{\circ}\text{C}$  on reed board was 13 minutes in average, compared to 10 minutes measured on the WFB in Test 8), resulting in a rough difference of 3 minutes. The wood fibre insulation board and reed board fall into a similar density range and the thermal conductivity of these two substrates appears to be comparable. Thus, it may be assumed that a rather similar protection time for clay plasters backed by reed board (Chapter 8.3) also applies to similar other boards, e.g., WFB. Furthermore, the observed failure mode of plaster system from reed board found in this research may also be applicable to wood fibre (insulation) boards. Table 8-7 presents the comparison of full-scale test results to the calculations based on the design equations for plaster systems presented in this Chapter and proposed in Chapter 10.2. When plaster system is applied on a wooden based substrate, the start time of charring is considered to equal the protection time of the respective plaster system, see design equations (14) and (16). In the case of straw as a substrate, the position coefficient of 0.75 for unexposed side was used in calculating the  $t_{ch}$  behind plaster system, Table 8-7. For lime plaster systems (Test 4, Table 8-7), an equation (16) was used.

Table 8-7. Validation of full-scale test results by proposed design equations.

Test Report No.	Plaster system' thickness	Plaster substrate	TEST			CALCULATION	
			300°C behind plaster	Last comment made on cracking of plaster	Fall-off time of plaster system	Start time of charring behind plaster	Fall-off time of plaster system
			$t_{300}$ [min]	[min]	$t_f$ [min]	$t_{ch}$ [min]	$t_f$ [min]
1	30	SB	15-23	71	no comment	19.8	19.8
2	25	SB	-	70	no fall-off	15.7 <sup>d</sup>	15.7
3	25-30	SB	-	61	no comment	15.7 <sup>d</sup>	15.7
4	30 (lime)	SB	-	89 <sup>c</sup>	110	22.2 <sup>d</sup>	22.2
5	25	SB	-	13	42 <sup>c</sup>	15.7 <sup>d</sup>	15.7
9	8	SP	2-3	11 <sup>c</sup>	22 <sup>c</sup>	1.7 <sup>d</sup>	n.a.
10	30	SP	15-22	30 <sup>c</sup>	35	19.8 <sup>d</sup>	19.8
12	5	CB22	38 <sup>a</sup>	38 <sup>c</sup>	38 <sup>c</sup> / 45 <sup>b</sup>	23.1 <sup>a</sup>	n.a.
13	6	CB22	40 <sup>a</sup>	34 (bending)	99 <sup>b</sup>	24.2 <sup>a</sup>	n.a.
14A	30	PLY15	25	no comment	29-33 <sup>c</sup>	26.4	33.5
14A	30	SOF	24	no comment	29-33 <sup>c</sup>	26.4	52.8
14B	30	PLY18	27	38	>71	26.4	37.8

<sup>a</sup>Behind clay paster and clay board (Test 12 – total thickness 27 mm; Test 13 – total thickness 28 mm) on wood.

<sup>b</sup>Failure time of the fire protection system: clay plaster and board (in Test 13 also including the WP).

<sup>c</sup>Fall-off of parts of plaster, but no failure time of plaster system was determined.

<sup>d</sup>Position coefficient  $k_{pos,unexp} = 0.75$  is applied.

The failure times of clay plaster systems, when plaster carrier is used, are calculated according to equation (20). The comparison of test results and calculations show a good agreement to reach the start time of charring. The calculated failure times of plaster system are very conservative in comparison to the test results. In case of wooden based substrate (Table 8-7), the vertical position seems to be favorable for plaster systems to

not fall off, despite the charring behind it. The tests with straw bale structures mainly report on the fall-off of parts of plaster that occur significantly later than the  $t_{ch}$ . Plaster and straw appear to have a very strong adhesion, which presents a sufficient mechanical key for keeping plaster in place for such a long time. In the case of timber (and comparable materials) as a substrate, this would likely not be the case, since the plaster has no means to adhere to the wood (when no plaster carrier is used), unlike straw, which has air spaces and a rough (fibrous) surface for the plaster to stick to.

Test report 14 presents the results obtained from two furnace tests (timber frame and a wood shaving infill with a density of 132–157 kg/m<sup>3</sup>), wherein different plaster substrates were tested (Test 14A comprised two separate situations: 15 mm plywood, 22 mm thick diagonal lumber boards (SOF); Test 14B: 18 mm plywood). In both tests, a galvanized steel plaster mesh was used as a plaster carrier to fasten the clay plaster system onto the wooden substrate. In both tests, the steel mesh was fastened with rivets 1,2 x 38 mm (distance 150 mm) through a first layer of 15 mm plaster to the substrate. In the second test (Test 14B), the plaster carrier was additionally fixed to timber studs with screws of 70 mm in length. In both tests, no failure of the plaster system was determined. Only in Test 14A, a fall off of small pieces of plaster was observed. In Table 8-7, there is a good agreement of  $t_{ch}$  values between the mean values obtained from test reports and the calculations according to the design equations presented in Chapter 10.2. In tests, the observations on times of the fall-off of parts of plaster somewhat comply with the calculated times for the failure times of plaster system according to equation (20).

Figure 8-8 presents a comparison of data obtained from the test reports (Table 8-5) and the calculated failure times for the clay plaster systems based on the equation (20). Figure 8-8a shows the results for clay plaster system when a plaster carrier is used. The respective figure shows two results presenting the end of both tests, no failure time of the plaster system was determined. The presented design equations (linear lines) are presented based on equation (20), wherein the penetration length of the fasteners into the wooden substrate (plywood or the lumber boards) depended on the substrates' thickness. Figure 8-8b presents the failure times of the clay plaster systems when no plaster carrier is used. In both cases, the proposed design equations for the failure times of clay plaster systems are conservative.

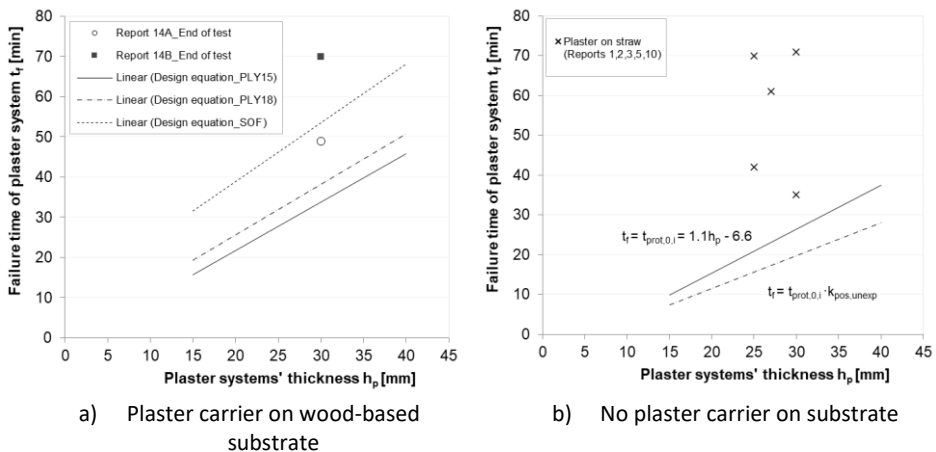


Figure 8-8. Comparison of failure times of clay plaster obtained from test reports and calculations.

In case of lime-based plasters, there is hardly any test data that is suitable for comparison due to the lack of available test reports as well as due to the large variety of different types of limes, additives, components of dry mixes and densities. A reference to a study carried out by (Niemann, 2010) using the cone heater and small-scale furnace could be made, wherein various types of lime-based plasters on strawbale panels were tested to meet an encapsulation criterion of 60 minutes. The cone heater tests showed that the temperature rise behind the heavy weight lime plaster was significantly faster compared to light-weight lime plasters. Yet, compared to a clay plaster (with straw fibers), the temperature rise was somewhat slower, thus presented slightly better fire resistance properties. This result also complies with the results obtained in this thesis, as the lime plaster appears to have somewhat greater protection effect regarding the start time of charring of timber compared to clay plasters.

In the scope of the European funded research project (Interreg) UP STRAW, an expert opinion has been published about the performance of straw bale structures protected by plasters in fire (IBB GmbH of Groß Schwülper, 2018). The opinion is based on numerous full-scale fire resistance tests conducted over the years, mainly at the iBMB, MPA fire laboratory in Germany (some of these test results are also reported in Table 8-6). According to this statement, if the composition, material properties, and thickness of clay and lime-cement plasters from different manufacturers are fundamentally the same, we can assume that the adhesion and their protective effect in fire would be comparable. This agrees with the results obtained from this thesis as no significant distinction between the different protection effects from various types of plasters (with the same binder) was detected. In addition, it was stated that there are no restrictions about the use of wood fibre boards as a plaster base as opposed to reed mats. The component testing showed that the adhesive bond between clay plaster and wood fibre panels or reed mats is comparable (IBB GmbH of Groß Schwülper, 2018). On this basis, it may be further concluded that the reed board performs similarly to the wood fibreboards as a substrate for plasters.

In case of the use of plaster carriers such as reed mat, tests with straw bales structures in the past frequently used the reed mat on timber studs (Niemann, 2010) to ensure the attachment of the plaster. Since any of the reported full-scale tests did not show early failure time of the plasters, it is reasonable to assume that the reed mat had a positive effect. Thus, it appears that a good mechanical bond with the metal wires of the plaster carrier and plaster is achieved at high temperatures, thus accordingly the failure time of the plaster may be linked to the fastening system to timber. The positive effect from the reed mat has been explained by (Niemann, 2010) as the plaster can secure itself to the mat from both sides, also adding that the reed mat provides enhanced flexibility and improved performance that may occur due to the shrinkage and movements in the building structure. A technical sheet published in earlier times (Metal lath technical bulletin no. 141, n.d.) has provided some fire resistance times for timber floors protected by various lime, gypsum, or cement-based plasters, while making a comment on the positive effect provided by the metal mesh as it keeps the calcined plaster in place even at extremely high temperature over 1000°C.

In case of historic structures, limited number of test reports are available. A report from UK (Papworth et al., 1995) presents investigations on the fire performance of historical lath and plaster constructions. Some test results and comments are made about the fire tests performed in 1940s with timber and wire lath (as a plaster carrier). Interestingly, it was noted that there were identical tests with lime plaster (with animal

hair), yet they showed significantly differently test results in view of the effective fire resistance times, whilst the only mentioned difference was the aging time of the plasters, 38 days, and 13 days. Thus, in view of all tests, slight evidence was noted that the longer curing times tended to give better performances, but the most interesting aspect of all results was the variation in performance achieved using nominally identical ceiling constructions. This remark also agrees to the observation made on the tests with lime plasters in this thesis, whilst the furnace tests in TP4 with lime plaster showed poor performance accompanied by large variations in temperature measurements behind the lime plaster compared to the ones tested in TP3. In this thesis, the preparation method and drying times between the layers for the plaster systems was carried out similarly as it would have been done in practise. However, the performance of lime plasters appears to be a more complex phenomenon in terms of how to evaluate the contribution of the traditional type of lime-based plasters as a fire protection material regarding their level of carbonisation related to the thickness, substrate etc. Thus, it was not possible to validate the performance of lime plasters in full scale; yet there appears to be a common ground between the findings reported in this thesis and those from the literature. This highlights the need for further studies.

## 9 Small scale method for estimation of fire protection effect

Based on the research presented in this thesis, the following guidance is provided. In Chapters 6.4, the comparison between results obtained from cone heater tests and furnace tests was given and discussed. The design parameters of fire protection materials for timber structures, which are commonly determined in a furnace under standard fire exposure conditions, may be estimated using the cone heater of a cone calorimeter (ISO 5660-1). The results have been previously published, and the test method has been presented in respective journal papers (Liblik et al., 2022, 2023).

The test method should be used in accordance with the following guidelines. For the estimation of **the basic protection time ( $t_{\text{prot},0,i}$ )** and **the start time of charring ( $t_{\text{ch}}$ )**, the results of the cone heater tests obtained from the temperature measurements by inserted thermocouples may be used directly.

For the estimation of **protection factor ( $k_2$ )**, the obtained cone heater test results shall be modified. Firstly, after cone testing, the charring rate behind the plaster system must be determined by the respective charring depth and charring time. The protection factor is calculated by dividing the determined charring rate (behind plaster) in cone tests by the basic design charring rate of 0.65 mm/min and then multiplying the result by a modification factor of 1.15. Note that no failure time can be estimated by this method.

For estimation purposes, the following bullet points must be followed:

- i) The estimation of design values is limited to 40 minutes.
- ii) The test specimen comprises plaster system and timber element, wherein the plaster thickness may vary between 10–40 mm and the timber element shall have dimensions of 100 mm x 100 mm x 100 mm.
- iii) The test specimen should be prepared in accordance with Chapter 5.3.2, which emphasises following the ISO 5660-1 test specimen preparation requirements as closely as possible to guarantee the repeatability and comparability of tests.
- iv) The application and hardening of plasters should be carried out with special care, following the manufacturers' instructions. The test specimens shall be conditioned at similar conditions as the furnace tests,  $20 \pm 2^\circ\text{C}$  and RH of  $50 \pm 5\%$ .
- v) The cone heater test set-up and procedure shall be followed as described in Chapter 5.3.2.
- vi) The test specimen should be exposed to predetermined heat flux scenario of  $50 \text{ kW/m}^2$  for the first 20 minutes, which is followed by an instant heat flux change to  $75 \text{ kW/m}^2$  for another 20 minutes. A total test duration is limited up to 40 minutes.
- vii) After 40 minutes, the test specimen must be immediately removed from cone heater and cooled down with water.
- viii) The charring of the timber specimen is exclusively examined along the specimen's centreline, where the thermocouples are positioned. The timber specimen is halved to determine the residual cross-section, which is assessed after the removal of charcoal. This procedure is described in Chapter 5.3.2.

## 10 Design principles and parameters

### 10.1 Limits of applicability

The design equations are limited to clay- and lime-based plaster systems that represent plaster compositions comparable to those tested in this work and used in the past, i.e., they should not include any additives that may significantly change the plaster's origin and performance, hence altering the material thermal properties.

#### PLASTER MATERIALS

Certain requirements must be adhered to in order to ensure the performance and quality of the plaster materials. In the case of clay plasters, the material should be tested and classified in accordance with the product standard DIN 18947 with a density class of 1.8 (1610–1800 kg/m<sup>3</sup>). It is highly recommended that the plaster applies to a strength class of SII and the linear shrinkage should correspond to DIN 18947.

The lime-based plasters should be tested and classified in accordance with EN 998-1. Lime plasters with higher strength classes are recommended to be used. The density should be in range of 1400–1800 kg/m<sup>3</sup> (as tested in this work). In case of lime plasters, a cement component (no more than 4% of the total volume of dry-mix lime plaster) may be added as sometimes used in plaster mixes for renovation purposes in practice.

#### PREPARATION AND APPLICATION OF PLASTER SYSTEMS

The application of plaster systems must be carried out strictly according to the manufacturers' instructions and follow the principles of design guidance given in EN 13914-2. Plasters of historic origin are most often applied in multiple layers to build up the whole plaster system. Consequently, it is essential to adhere to the maximum plaster thickness applied at once (to build up the plaster system) that is specified by the manufacturer. The preparation of the plaster mix with water is specified by the product manufacturer to guarantee its application and mechanical performance. In case of lime plasters, the hardening of plaster system due to the carbonization process requires special care. A reinforcement mesh may be used as instructed by the product guidelines.

Plaster systems may be applied to various substrates such as wooden structures or insulation boards (e.g., reed board). To ensure the adhesion and performance of a plaster system applied directly to wooden surfaces and other rigid panels (such as clay boards), a plaster carrier is recommended to be used.

#### PLASTER CARRIER

The fire protection effect of a plaster system is dependable on its application method to its substrate. When plaster carrier is used, the plaster system's fall-off time could be delayed. Plaster carrier is a mechanical support that is attached to the substrate onto which plaster is applied. In case of a thin plaster carrier such as a reed mat or a steel wire mesh, staples at least 25 mm in length should be used. Every longitudinal wire of the carrier must be fastened with staples at a spacing of 10–15 mm apart. It is highly advised to use screws (> 25 mm in length) for extra fixation.

When the plaster system is applied to a substrate without any plaster carrier (e.g., reed board), the failure time of the plaster occurs faster as there is no means of keeping the plaster adhered to the substrate after certain temperature criteria is reached behind the plaster (e.g., protection time).

## PLASTER SYSTEM THICKNESS

The thickness of a plaster system is measured from the substrate it is applied on (e.g., timber member). In case of the fire design parameters, the orientation of the structural element determines the plaster thicknesses which apply (wall or ceiling). The experiments conducted for this thesis primarily outline the limitations. Thus, it is recommended that lime-based plasters be applied only to walls. In case of ceilings, further furnace testing is required.

For walls, clay and lime plaster systems should have a minimum thickness of 15 mm and maximum thickness of 40 mm.

For ceilings, clay plaster system should have a minimum thickness of 15 mm and maximum thickness of 20 mm. In order to account for the contribution of a thicker plaster system, it is necessary to conduct a full-scale furnace test, as the influence of the added weight to the plaster on the failure time of the plaster system cannot be guaranteed based on existing tests.

## 10.2 Design equations for plaster systems

According to the principles specified in EN 1995-1-2, the design parameters for the plaster systems investigated in this thesis are provided. The design equations proposed for implementation are in line with the new version of Eurocode 5 (prEN 1995-1-2:2022) and are also applicable to the current EN 1995-1-2:2004.

The design equations are given with respect to the SFM and the effective cross-section method described in prEN 1995-1-2:2022. To ensure the application of the proposed design equations, Chapter 10.1 outlines the relevant principles and limitations.

### SEPARATING FUNCTION METHOD

For the SFM, the following design equations may be assumed.

#### Clay plaster systems

Design parameter	Design equation [min]
Basic protection time $t_{prot,0,i}$	$t_{prot,0,i} = 1.1h_p - 6.6$ (14)
Basic insulation time $t_{ins,0,n}$	$t_{ins,0,n} = 0.7h_n - 4.5$ (15)

#### Lime plaster systems

Design parameter	Design equation [min]
Basic protection time $t_{prot,0,i}$	$t_{prot,0,i} = 1.2h_p - 6.4$ (16)
Basic insulation time $t_{ins,0,n}$	$t_{ins,0,n} = 0.8h_n - 4.3$ (17)

$h_p$  is the plaster systems' thickness, measured from the underlying substrate, in mm.

$h_n$  is the thickness of the last layer n, in mm.

### Position coefficients

For clay and lime-based plaster systems, same values for position coefficients may apply. The position coefficient  $k_{pos,exp,i}$  for the fire-exposed side of the considered layer may be assumed as the same generic value given in FSITB and prEN1995-1-2:2022 for panels, as follows:

$$k_{pos,exp,i} = \begin{cases} 1 - 0.6 \frac{\sum t_{prot,i-1}}{t_{prot,0,i}} & \text{for } \sum t_{prot,i-1} \leq \frac{t_{prot,0,i}}{2} \\ 0.5 \sqrt{\frac{t_{prot,0,i}}{\sum t_{prot,i-1}}} & \text{for } \sum t_{prot,i-1} > \frac{t_{prot,0,i}}{2} \end{cases}$$

The position coefficient  $k_{pos,unexp,i}$  for the unexposed side for plaster systems backed by panels (density > 290 kg/m<sup>3</sup>) may be assumed as follows:

$$k_{pos,unexp,i} = 1$$

The position coefficient  $k_{pos,unexp,i}$  for the unexposed side for plaster systems backed by reed board (or other similar boards) may be assumed as follows:

$$k_{pos,unexp,i} = 0.75$$

### THE EUROPEAN CHARRING MODEL

In the following, the main design parameters are given for fire protection systems consisting of clay or lime plaster systems applied on a timber member or panels (density > 290 kg/m<sup>3</sup>). In addition, the design guidance is presented in case of reed board as a plaster substrate (without any plaster carrier).

#### Clay plaster systems

Design parameter	Design equation [min]	
Start time of charring	$t_{ch} = \sum t_{prot}$	(18)
Protection factor	$k_2 = 1 - 0.01 \cdot h_p$	(19)
Failure time of plaster in walls with plaster carrier	$t_f = t_{prot,plaster} + \frac{l_f - 10}{\beta_{n,Phase2}}$	(20)
Failure time of plaster in walls without plaster carrier	$t_f = t_{prot,plaster}$	(21)
Failure time of fire protection system consisting only of plaster in walls	$t_{f,pr} = t_f$	(22)
Failure time of fire protection system consisting of combinations of plaster with other panels in walls	$t_{f,pr} = \max \left\{ \sum t_{prot}, t_f \right\}$	(23)
Failure time of fire protection system in ceilings	$t_{f,pr} = t_{ch}$	(24)

## Lime plaster systems

Design parameter	Design equation [min]	
Start time of charring	$t_{ch} = \sum t_{prot}$	(25)
Protection factor	$k_2 = 1 - 0.01 \cdot h_p$	(26)
Failure time of plaster in walls with plaster carrier	$t_f = t_{prot,plaster} + \frac{l_f - 10}{\beta_{n,Phase2}}$	(27)
Failure time of plaster in walls without plaster carrier	$t_f = t_{prot,plaster}$	(28)
Failure time of fire protection system consisting only of plaster in walls	$t_{f,pr} = t_f$	(29)
Failure time of fire protection system consisting of combinations of plaster with other panels in walls	$t_{f,pr} = \max \left\{ \sum t_{prot}, t_f \right\}$	(30)
Failure time of fire protection system in ceilings	by testing	

$h_p$  is the plaster systems' thickness, measured from the substrate, in mm.

$l_f$  is the penetration length of the fastener, in mm.

$\beta_{n,Phase2}$  is the notional design charring rate in charring phase 2, in mm/min.

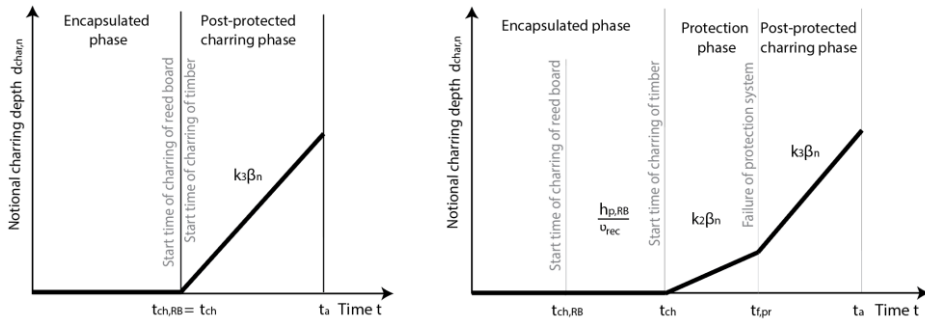
For the calculation of the load-bearing capacity of timber structures, the effective cross-section shall be calculated by reducing the initial cross-section by the effective charring depth from each side exposed to fire. It is assumed that the reduction of strength and stiffness properties of the material close to the char-line as well as the variation of the charring rate are allocated to the zero-strength layer depth  $d_0$ , while the strength and stiffness properties of the effective cross-section are assumed to be unreduced (prEN 1995-1-2:2022). The assessment of the zero-strength layer was outside the scope of this thesis. All tests were performed unloaded. However, for estimation, it may be proposed to comply to the design principles for  $d_0$  values described in prEN 1995-1-2:2022.

### Reed board as a plaster substrate on timber structures

In case of a reed board as a plaster substrate on a timber member, additional design guidelines are presented for walls. Figure 10-1 illustrates two different situations (a and b) that are dependent on the method of plaster systems' application to the reed board. The first scenario (Figure 10-1a) is presenting the most conservative approach when the start time of charring of the reed board is considered as the start time of charring of timber. Thereafter, the post-protection factor  $k_3$  must be applied.

Scenario 2 may be applicable if the plaster system could be prevented from falling off for an extended period of time. This is the case if the plaster system could be attached to the reed board by plaster carrier, such that the plaster system falls off after the reed board has started to char (e.g., later than the start time of charring of timber, Figure 10-1a). In this case, the start time of charring is dependable on the protection time of the whole fire protection system and its fastening system to the timber member. In the encapsulation phase, the contribution from the reed board is based on its thickness and its recession speed (e.g., carbonization rate).

In case of 50 mm thick reed board, a conservative approach would be to use the highest recession speed ( $v_{rec}$ ) of 2.0 mm/min as determined in this thesis; whilst considering that the start time of charring of timber determines the failure time of the protection system. In the protection phase, a protection factor  $k_2$  of the relevant plaster system may be applied.



1) Scenario 1:  $t_{ch, RB} = t_{ch}$

2) Scenario 2:  $t_{f, pr} > t_{ch}$

Figure 10-1. Charring models for plaster systems and reed board on timber structures.

In this current proposal of design parameters, only the first scenario is considered. Reed board without the plaster system is not regarded a fire protection material in this context. Thus, the failure time of the plaster system (from the reed board) determines the start time of charring of timber. This limitation is adequate because there are insufficient data about the joint coefficients and the performance of reed boards on a larger scale which may include additional risk factors that have an impact on the heat transfer mode. The proposed design equations are based on test results presented in Chapter 6.3.2.

The following design values may be applicable to reed boards (or other similar boards). The proposed design values are limited to walls.

The start time of charring of the reed board ( $t_{ch, RB}$ ) protected by the plaster system may be assumed as follows:

$$t_{ch, RB} = t_{prot, 0, plaster} \cdot k_{pos, unexp} \quad (31)$$

The failure time of the fire protection system consisting of the plaster system (without plaster carrier) and reed board may be assumed as follows:

$$t_{f, pr} = t_{ch, RB} \quad (32)$$

In case of scenario 2 (Figure 10-1b), the start time of charring of timber is dependable on the protection times of both materials and their fastening system into the timber member. The failure modes could be investigated in future to propose additional equations.

# 11 Conclusions and outlook

## 11.1 Conclusions

This thesis investigated the performance of **traditional type of clay and lime-based plasters**, primarily used in historic buildings, as a fire protection system for timber structures under fire-related conditions. A comprehensive experimental program accompanied by numerical investigations was conducted with the main objective of establishing the fire design principles and parameters for selected clay- and lime plaster systems that comply with Eurocode 5 Part 1-2.

This research topic was motivated by the lack of design parameters and guidelines for the use of a traditional plaster system as a means of fire protection for timber structures and to allow a fire risk assessment of such plasters found in existing buildings. A practical need has been recognized, stressing the lack and inadequacy of available literature and research study about **plaster as a fire protection material**. Understanding the fire resistance performance of plaster systems could result in more suitable design alternatives for old buildings, thereby preserving the craftsmanship as part of the cultural built heritage. Additionally, this research subject is applicable to current construction industry demands to increase the use of low-carbon, healthy building materials.

A test program consisting of material tests, cone heater tests, and furnace tests was conducted, all of which have not previously been carried out on such a broad scale for traditional type of plasters. The fire testing comprised of test programs divided as small-scale tests using the **cone heater of a cone calorimeter** (ISO 5660-1) and an **intermediate scale furnace tests** that provided the means to expose test specimens to ISO 834 in line with EN 1363-1. The use of different sizes of furnaces was related to specific conditions and availability of the test facilities; yet this provided content for more critical analysis. Utilizing common test methods and analysing test results by developing design parameters based on the European design codes enables the plasters' performance to be compared to other well-known protection materials.

The experimental program consisted of a selection of clay- and lime-based plaster systems and their plaster carriers, primarily based on their availability and utilization in Estonia. As plaster is a complex mix of constituents, **material-specific tests** (XRD, TGA) were performed to mainly specify the composition of the plasters for furnace test analysis and to offer future comparisons with other similar plasters. The TGA provided means to show fundamental differences existing between clay and lime-based dry-mix plasters regarding their mass loss change. The TPS testing was limited to 400–500°C due to the cracking of plaster samples. However, this temperature range agreed well to the first notable mass losses representing the material transformations detected by TGA. At around the same temperature range, the first visible cracks developed on the plaster surface in furnace tests, and in case of reed board as a substrate, the clay plaster fell-off. Hence, material changes identified at such a small scale may provide useful information on their performance at a larger scale, particularly about their integrity (e.g., cracking).

Despite the **material-specific differences between the dry-mix plasters** (XRD, TGA), the furnace tests with clay plaster systems showed that the charring performance of timber is very similar, regardless of the origin of the clay plaster mixes, thus their variations in mineralogical components appear to have no significant effect on the heat transfer mode. This observation may be attributable to various combinations of clay plasters in a similar density range that comprise different grain sizes and/or fibres, as also

no detachment between the different undercoat or topcoat layers was detected in tests. In contrast, in case of lime-based plasters, the addition of cement component to the lime plaster mix had an influence on the plaster's performance as it appears to prevent the crack formation. The composition of the lime plaster and the addition of components such as a new type of binder into the plaster mix alters its performance. The density range of the tested lime plasters was more varied than that of the chosen clay plasters, although it had no significant effect on the furnace test results. However, given the limited number of tests carried out, further experimental research with different types of lime-based plasters is required.

In practice, it is common to use a **reinforcement mesh in a plaster system**. Performed furnace tests (in TP2) with and without the use of a jute mesh (flax mesh in TP4) showed no detachment of the plaster layers at the location where it was placed. In case of a lime plaster, a strong bond between the plaster and the glass-fibre reinforcement mesh was observed, it appeared to prevent the cracking of plaster (in TP4) until the failure of the fibre mesh itself. Thus, certain reinforcement meshes with high temperature resistance, may contribute to the integrity of the plaster systems.

All performed fire tests showed that the **thickness of the plaster system** is the most influential factor in determining its protective effect against the charring of timber. With increasing thickness of the plaster system, the start time of charring of timber was gradually delayed, and the charring rate of timber protected by plaster reduced. This applies to the plasters of similar origin and density range. In this thesis, tests showed that although the measured charring rates of the timber elements behind the lime plasters were similar to those in case of clay plasters, lime plasters indicated somewhat greater protection effect in time to reach the start time of charring than clay plasters. The variation of test results regarding the charring of timber was greater when reed mat was used as opposed to wire mesh, indicating a slight influence on the heat transfer mode. In the performed tests, the plaster systems with a maximum thickness of 30 mm did not show any **detachment of plaster layers**, slowly the crack development was observed. However, the 44 mm thick clay plaster system demonstrated clear evidence of detachment of the first plaster layers (20–25 mm) after one hour testing, primarily related to the thermal stresses and material changes occurring in such a thick plaster.

The furnace tests enabled to determine the performance of plaster systems in different scales, orientations, and set-ups. The **horizontal furnace tests** with clay plaster and reed mat (TP2) showed a long time for the plaster system to fall-off (possibly influenced by the stickability of plaster to the furnace sides). In contrast, in case a reed board as a plaster substrate in TP2, the fall-off of plaster occurred suddenly after the reed board started to char. Thus, the use of a reed mat provided the means to hold the plaster in place due to the strong bond between the plaster and the metal wires of the mat and its **mechanical fastening system into the timber element** ensured by staples. However, further study on the fastening system is still required, as in TP4, a fall-off of a clay plaster with reed mat was observed prior to the failure estimation, though it occurred after 300°C recorded on timber. Tests with lime plasters in horizontal position (TP4) provide basis for some further discussion on its sudden failure detected in Test 14 that appears to be related to a highly complex phenomena of the drying and carbonisation process of traditional type of lime plasters. However, the furnace tests in a wall position in a smaller scale (TP3) did not show any detachment or degradation of lime-based plasters; no fall-off or other failure modes were detected when handling the specimens after its removal from furnace.

The horizontal tests in TP2 showed that when no plaster carrier is used (plaster applied directly to the reed board), the fall-off of plaster occurs when the reed board starts to char. At increasing temperature, moisture is driven out from the plaster, and adhesion between the two materials is weakened. A similar type of **loss of adhesion** may occur when plaster is applied on other type of substrates that start to degrade at around 200–300°C (e.g., wooden laths or wood-based boards). A comparable validation to the described test result can be made by a full-scale test (Test Report no. 8, Table 8-5), which demonstrated strong adhesion strength between a clay plaster and a wooden fibreboard up to 238°C measured at the interface (marking the end of the test).

**Furnace tests in vertical position** showed no fall-off of clay plaster system with a reed mat from timber elements, except the detachment of plaster coats in case of 44 mm thick plaster. The relatively long fire tests of more than 60 minutes indicated that the mechanical fastening of the plaster provided by the reed mat to the wood element increases its fixation to its substrate. This enabled to account for the plasters' protection effect in terms of slowing down the charring rate of timber for a certain time limit. Herein, it cannot be stated that the plaster (without any plaster carrier) in walls would definitely fall-off when the charring of the substrate starts, but this needs further testing. Due to the absence of negative impact from the self-weight of plaster and the pull-out of fasteners in wall position, the performed floor tests (TP2) could serve as a guarantee for wall tests to estimate the plasters' performance in full-scale. The available full-scale tests with plasters could be regarded sufficient to show their ability to stay intact to its substrate for a considerable time. The testing of lime-based plasters in a small furnace did not reveal any failure modes in vertical position.

The furnace tests demonstrated that the plaster systems resist significantly longer in place in walls compared to its position in ceilings. The study has identified three distinct types of **failure modes for the plaster systems**:

- i) failure of the mechanical fastening system;
- ii) loss of adhesion between the plaster and its substrate;
- iii) material thermal degradation.

In the first case, the fall-off of plaster system is dependent on the start time of charring and the charring rate of timber along the plaster carriers' fasteners, e.g., staples. Thus, the penetration length of the fasteners into the uncharred wood is a relevant design parameter to prevent an early fall-off of plaster system. In the event of a loss of adhesion, an increase in temperature at the interface between the plaster and its substrate becomes a key factor mainly due to the thermal degradation of the substrate, e.g., charring around 300°C. The third failure mode may occur due the mineralogical changes in the plaster that result in thermal degradation.

To provide means of predicting the charring performance of timber in furnace, **a test program with the cone heater** was conducted. Test results on the charring of timber behind plaster were plotted against the ones determined in furnace. The cone tests provided useful insight and estimation about the heat transfer mode through the plaster systems, as the start times of charring of timber ( $t_{ch}$ ) were obtained in a good agreement with the ones measured in the furnace. The cone heater testing was found limited in its capacity to provide sufficient heat flux levels and therefore the charring rate behind the plasters was not possible to be estimated from test results directly. For the determination of the protection factor ( $k_2$ ), a modification factor is proposed to approximate the values to the ones received in furnace. The cone heater tests were limited to distinguish the plasters' performance with respect to their crack development, detachment of plaster

layers and fall-off. However, it serves as a useful tool of testing various compositions, mixes, and combination of materials in a simple manner. The cone heater test method is proposed for a 40-minute fire duration and 40 mm maximum plaster thickness. The method enables to test different types of plasters under same test conditions to rank their fire performance. This method may be also used for development of fire resistance properties of plasters.

In this thesis, the **development of fire design parameters** was determined based on the obtained furnace test results. Firstly, numerical investigations on the thermal response through the plaster systems using input data from various TPS test results were carried out. The thermal properties from material tests were calibrated and modified to present the best fit to the furnace test results for the whole range of plaster thicknesses. Certain simplifications were made, e.g., the plaster carriers were considered as part of the plaster system. Thus, the thermal properties were defined independent from the type of plaster carrier. The proposed design parameters, provided in accordance with prEN 1995-1-2:2022, are mainly dependent on the thickness of the plaster systems. The design principles are accompanied by certain limitations in their application and declared material properties to guarantee their performance.

This research work demonstrated that the traditional plaster systems can perform as fire protection for timber structures. The results facilitate the planning of full-scale fire testing according to EN 13381-7 to study different failure modes. The performed work provides means to rate the fire resistance performance of existing plasters in view of the design principles presented in EN 1995-1-2. This study is believed to provide a framework for expanding the current work to various type of plasters, plaster carriers, and substrates, as well as a platform for product development in fire.

## 11.2 Outlook

This research study revealed numerous new insights regarding clay and lime plaster systems and their applications using different plaster carriers and substrates on structural timber elements in case of fire. However, the study is still limited to the certain plaster systems and the scale of testing. In the following, key topics are listed for future developments, based on the obtained test results and observations made.

- **Plaster materials**

Future research should investigate the material specific properties such as the level of carbonisation and effect of dry-mix components in relation their fire resistance performance to understand the thermal degradation as a failure mode for traditional type of lime plaster systems.

Lime-based plasters should be further tested, varying different types, additives, and densities.

To fully understand the failure modes of a relatively thick plaster systems (> 40 mm), full-scale tests should be conducted to assess the detachment of plaster layers.

Different types of plasters, e.g., gypsum plaster and lightweight plasters with low thermal conductivity, should be examined. A more universal design approach could be established considering the binder and composition of the plaster, its density and thickness.

In the case of clay plaster systems, a European product standard should be established in order to facilitate their recognition and implementation to building codes and guidelines at European level.

- **Plaster substrates and carriers**

The results from this thesis highlighted the relevance of the application method of plaster to its substrate and its relation to the potential failure modes. Thus, the performance of different types of plaster carriers used on wooden structures (e.g., a wooden lath often found in historic buildings; various type of wire meshes used in modern construction) and their influence on the plaster systems' contribution as a fire protection could be further studied.

Different type of fasteners (e.g., screws for fixing the plaster carrier) could be tested to analyse their contribution to the fall-off time of the plaster systems. In case of ceilings, more efficient fastening systems and types of plaster carriers should be studied or developed.

Little is known about the adhesion strength between the plaster and building boards at elevated temperatures and the corresponding failure times. Plaster and board combinations should be studied in the future to increase the flexibility of plaster applications in case of fire.

- **Effective thermal properties of plasters**

In case an explicit understanding about the thermal properties of the tested plasters is required, the material properties should be determined independently for the plaster and plaster carrier. In this thesis, the change in density of the plaster systems was considered indirectly. The effect of the change of density to the thermal properties could be further investigated.

In addition, the calibration tool and procedure for developing effective properties may be further customized based on material specific characteristics and different thicknesses.

- **Cone heater testing**

The proposed test method could be further validated with other materials.

The cone testing presents a universal comparison tool for fire technical properties of various plasters to create a comprehensive database.

In future, materials should be tested on various building boards to assess the protection time of the material combinations.

It is important to strictly adhere to the specimen preparation and testing procedures. The wooden specimens must have similar properties (e.g., the orientation of year rings, density) to minimize variables in charring rates while comparing the protection effect of plasters.

- **Furnace testing**

Full-scale tests should be carried out with traditional plaster systems that are directly applied on timber elements as the validation of obtained test results are currently based on tests with straw bale panels or other building boards. Testing according to EN 13381-7 is required for verification.

The results from this thesis could serve as a basis to estimate the K-classes. This data is rather limited, however appears to become more relevant in modern timber buildings with bio-based materials.

## List of figures

Figure 2-1. The European charring model according to prEN1995-1-2:2022. ....	23
Figure 2-2. Notional charring depth $d_{char,n}$ (prEN 1995-1-2:2022).....	24
Figure 2-3. Minimum penetration length of the fastener and minimum anchorage length into the uncharred part of the timber member (prEN 1995-1-2:2022). ....	26
Figure 2-4. Numbering and function of the layers in the assembly (prEN 1995-1-2:2022). .	27
Figure 3-1. Different type of timber constructions in Europe: Left – half-timbered buildings in Germany; Right – Wooden apartment buildings in Estonia. ....	31
Figure 3-2. Examples of plaster support fixed on horizontal-log construction for the mechanical fixation of plaster: Left – Wooden sticks and plaster layers; Right – Reed mat fixed to timber by using staples. ....	32
Figure 3-3. Different plant fibres used in clay plasters. ....	34
Figure 3-4. Application of reinforcement mesh into the clay plaster system:.....	34
Figure 3-5. Application of lime plaster system.....	37
Figure 5-1. Types of reinforcement meshes used in plaster systems. ....	47
Figure 5-2. Reed board as a plaster substrate on timber structures. ....	48
Figure 5-3. An example of a plaster system and a reed mat on timber element. ....	48
Figure 5-4. TGA test results of the relationship between mass loss and temperature...	50
Figure 5-5. Preparation of test samples for TPS method: Left – MICA sensor fixed on one of the sample halves; Right – Test specimen after hardening and before the removal of the metal cylinder. ....	52
Figure 5-6. Documentation of test specimens after TPS tests: Left – Close-up of ClaySU04 removed from the furnace; Right – Cracking of LimeSU04 in furnace. ....	52
Figure 5-7. TPS test results of thermal conductivity of plasters: Left – ClaySU04; Right – ClaySF04. ....	53
Figure 5-8. Results of thermal conductivity of plaster LimeSU04. ....	53
Figure 5-9. Heat flux scenarios used in cone heater tests. ....	55
Figure 5-10. Preparation of a test specimen for a cone heater test. ....	57
Figure 5-11. The preparation and fixation of a test specimen in the cone heater tests.	57
Figure 5-12. Schematic close-ups of the layered construction of test specimens tested in furnace: Left – Plaster system with a plaster carrier; Right – Plaster system and reed board on timber. ....	58
Figure 5-13. TP1 and TP2 – The layout of the fire-exposed side of the test specimens (with TC placements).....	60
Figure 5-14. TP3 – Furnace and the layout of the fire-exposed side of the test specimens tested in floor position (with TC placements).....	61
Figure 5-15. TP4 – Furnace and the layout of the fire-exposed side of the test specimens tested in wall position (with TC placements). ....	61
Figure 5-16. Close-up on the fixation of thermocouples on the exposed side of the timber elements before the application of plaster systems: a) TC in TP1 and TP2; b) TC in TP3 and TP4. ....	62
Figure 5-17. Temporary wooden frame fixed on timber element for the application of plaster: a) Framework fixed on timber element in TP2 (Test 6); b) Framework fixed on wooden panel in TP3.....	63
Figure 5-18. Application of plaster carriers (a,b,d) and a plaster substrate (c) .....	64
Figure 5-19. Plasterwork carried out in all test programmes: Left – Application of a first plaster layer on a reed board; Right – Jute mesh applied on a plaster layer.....	65

Figure 5-20. Preparation of test specimens for furnace testing: Left – Sides of plaster fixed with aluminum tape; Right – Test specimen fixed in furnace in TP3. ....	65
Figure 5-21. Cooling down the test specimens after its removal from furnace: .....	66
Figure 6-1. Test specimens (10 mm clay plaster system) after cone heater testing. ....	71
Figure 6-2. Documentation of test specimen after cone heater testing.....	72
Figure 6-3. Cross-section of clay plasters placed upside down, after cone heater testing.	72
Figure 6-4. Mean temperature measurements and start time of charring obtained from cone heater tests in TP1.....	72
Figure 6-5. The charring performance of timber in relation to the plasters' thickness in TP1. ....	73
Figure 6-6. The cut cross-section of timber specimens protected by 10-, 20- and 40-mm plaster in TP1. ....	73
Figure 6-7. The start times of charring obtained from cone heater tests in TP2. ....	74
Figure 6-8. The charring performance of timber in relation to the plasters' thickness in TP2. ....	74
Figure 6-9. The residual cross-sections of timber specimens documented after testing in TP2. ....	74
Figure 6-10. Comparison of test results obtained from TP1 and TP2. ....	75
Figure 6-11. Test specimen (lime plaster and reed mat on timber) in cone heater tests TP3. ....	76
Figure 6-12. The start times of charring obtained from cone heater tests in TP3. ....	76
Figure 6-13. A test specimen after cone heater testing and cooled down with water: Left – Top view of the timber specimen from which the plaster system was removed and put aside; Right – A close up of the plaster system (incl. the reed mat), placed upside down.	77
Figure 6-14. The charring depths and rates behind plaster systems obtained from cone heater tests (50 mm timber elements) in TP3. ....	77
Figure 6-15. Comparison of the charring depths and rates behind plaster systems in relation to the depth of the timber elements (50 mm and 100 mm) in TP3. ....	77
Figure 6-16. Residual cross-sections of timber specimens (50 mm) from double-testing.	78
Figure 6-17. The charring rates presented with respect to the test duration, heat flux and depth of timber specimens in TP4. ....	79
Figure 6-18. Visual documentation of the plaster systems ClaySU0401 tested in horizontal orientation in TP2; approximately a minute before the fall-off of plaster system. ....	81
Figure 6-19. Documentation of clay plaster systems of Test 5 during the fire test at 53 min (Left) and after its removal from the furnace wall (Right). ....	81
Figure 6-20. Documentation of Test 7 (44mm thick clay plaster system) during testing, approx. a minute before termination of the test (Left) and after its removal from furnace (Right).....	81
Figure 6-21. Documentation of Test 0 in TP1 during and after the termination of the fire test: .....	82
Figure 6-22. Documentation of Test 01 during and after the termination of fire test: ..	82
Figure 6-23. Documentation of test specimens in TP3 after their removal from furnace.	83
Figure 6-24. Documentation of the test specimen of Test 13 in TP4 during and after the fire test:.....	83
Figure 6-25. Mean temperature rise at the interface of clay plaster system (with reed mat) and timber element measured in furnace tests. ....	84
Figure 6-26. Furnace tests no 3 and 4 – Visual documentation of test specimens in furnace. ....	85

Figure 6-27. Furnace Test 6 – Visual documentation of plaster through the furnace window during the fire test and after its removal from the furnace wall. ....	85
Figure 6-28. Furnace Test 8 – Visual documentation of plaster through the furnace window during the fire test. ....	86
Figure 6-29. Mean temperature curves recorded on the fire-exposed side of the reed board (RB) and on the timber element (Timber) for each furnace test (Test 3, 4, 6, 8), protected by various clay plaster system thicknesses. ....	86
Figure 6-30. Visual observation of the performance of various lime plaster systems in TP 3. ....	88
Figure 6-31. Mean temperature curves measured at the interface of plaster and timber element in TP3. ....	89
Figure 6-32. Temperature measurements at the interface of lime plaster system and timber element in Test 15 (TP4). ....	90
Figure 6-33. Test 15 carried out in TP4: ....	90
Figure 6-34. Relationship between the thickness of clay plaster systems and the time to reach 300°C behind plaster system in case of reed mat and on a reed board (_RB). ....	92
Figure 6-35. The charring rates of timber protected by clay plaster systems in relation to the thickness of plaster, determined in furnace tests. ....	94
Figure 6-36. The protection factors for clay plaster systems (with reed mat) in relation to the thickness of plaster; obtained from the furnace tests. ....	94
Figure 6-37. Documentation of the timber specimen after furnace tests (TP2). ....	95
Figure 6-38. Documentation of reed boards after cooled down with water. ....	96
Figure 6-39. The fall-off times of clay plaster systems obtained from furnace tests and theoretical calculations. ....	97
Figure 6-40. Documentation of test specimens after fire test. ....	98
Figure 6-41. Relationship between the lime plaster systems' thickness and time to reach 300°C behind lime-based plasters tested in TP3 and TP4. ....	99
Figure 6-42. The protection factors for lime plaster systems obtained from the furnace test results. ....	101
Figure 6-43. The cross-section of timber panels protected by 30 mm thick plasters:..	102
Figure 6-44. Comparison of furnace test results to reach the start time of charring ...	103
Figure 6-45. Comparison of protection factors between clay and lime-based plaster systems .....	104
Figure 6-46. Comparison of start times of charring of timber protected by clay plaster system and reed mat as a plaster carrier. ....	105
Figure 6-47. Comparison of charring rates of timber protected by clay plaster system and mat. ....	106
Figure 6-48. Comparison of protection factors of clay plaster system and reed mat...	107
Figure 6-49. Comparison of start times of charring of timber protected by lime-based plaster system obtained from cone and furnace tests of TP3. ....	108
Figure 6-50. Comparison of protection factors of lime-based plaster systems obtained from cone and furnace tests of TP3. ....	109
Figure 7-1. The concept map about the heat transfer simulations. ....	118
Figure 7-2. Comparison of mean values of thermal properties obtained from TPS tests and used for simulations in Model 1 – Clay plasters. ....	121
Figure 7-3. Comparison of temperature measurements recorded in furnace (Test 9a, Test 9b, TP3) and simulations based on TPS test results – clay plaster systems. ....	121
Figure 7-4. Mean thermal properties obtained from TPS tests – LimeSU04. ....	122

Figure 7-5. Comparison of temperature measurements between furnace tests (Test 11a, Test 11b) and simulations based on the TPS test results – 30 mm thick lime plaster systems. ....	122
Figure 7-6. Comparison of temperature curves between furnace tests (Test 11a, Test 11b) and simulations based on the TPS test results – 30 mm thick lime plaster systems: a) Temperature curves up to 60 minutes; b) Close-up of the curves around 100°C.....	123
Figure 7-7. Comparison of the thermal properties of clay and lime plaster used as input for.....	123
Figure 7-8. Comparison of mean temperature values between 30 mm thick clay and lime plaster systems (with a reed mat) obtained from furnace tests (TP3) and simulations. .	124
Figure 7-9. Comparison of temperature measurements obtained in furnace behind the clay plaster system (wall tests) and derived from Model 2 simulation results.....	125
Figure 7-10. Comparison of the thermal properties obtained from TPS tests for ‘ClaySU04’ and ‘Clay mineral’ used as input for Model 2: Left – Thermal conductivity; Right – Specific heat. ....	125
Figure 7-11. Relationship between the mean results of furnace tests and the first simulations on the time to reach 300°C on timber ( $t_{300}$ ) for clay plaster systems.....	126
Figure 7-12. Comparison of temperature measurements obtained in furnace behind the lime plaster systems (with reed mat) and derived from the simulations of Model 2. .	127
Figure 7-13. Comparison of thermal properties obtained from TPS tests and effective thermal properties determined by first calibrations. ....	129
Figure 7-14. Comparison of temperature curves for different plaster thicknesses on timber determined by simulations using the effective thermal properties calibrated based on furnace tests in TP3 (Test 9a, Test 9b).....	130
Figure 7-15. Comparison of effective thermal diffusivity values between simulation results of Clay_SAF1866 and Clay_ABA1866. ....	131
Figure 7-16. Comparison of temperature curves obtained in furnace and simulations with calibrated thermal properties based on “Clay mineral” input (Küppers et al., 2018). .	132
Figure 7-17. Comparison of the agreement between the times to reach the 300°C behind plaster system in furnace and simulations based on calibrated thermal properties (Table 7-5). ....	132
Figure 7-18. Comparison of the thermal properties determined by TPS tests (Küppers et al., 2018), calibrations and modifications for clay plaster systems. ....	134
Figure 7-19. Comparison of temperature curves obtained in furnace and simulations with calibrated and modified thermal properties for clay plaster systems. ....	134
Figure 7-20. Comparison of furnace test results of LimeSU04 and first simulations based on calibrated thermal properties. ....	135
Figure 7-21. Comparison of thermal properties determined for lime plaster (LimeSU04).	137
Figure 7-22. Comparison of temperature curves obtained from the furnace tests (TP3) for LimeSU04 plaster systems and simulations with (modified) effective thermal properties.	137
Figure 8-1. The simulation configuration to determine the basic protection times (prEN 1995-1-2:2022).....	140
Figure 8-2. Comparison of the basic protection times determined by simulations and tests.....	140
Figure 8-3. The simulation configuration to determine the insulation times (prEN 1995-1-2:2022). ....	141
Figure 8-4. Comparison of insulation times determined by simulations. and tests. ....	141

Figure 8-5. Comparison of test data to reach 270°C behind the plaster system on timber element and reed board. ....	142
Figure 8-6. Furnace tests results on the relationship between the plaster thicknesses and the determined protection factors: a) Clay plaster system; b) Lime plaster system. ....	143
Figure 8-7. The failure times of clay plaster systems. ....	144
Figure 8-8. Comparison of failure times obtained from test reports and calculations. ....	149
Figure 10-1. Charring models for plaster systems and reed board on timber structures. .	157

## List of tables

Table 5-1. Type of clay plasters selected for this research. ....	46
Table 5-2. Type of lime-based plasters selected for this research.....	46
Table 5-3. Plaster carriers used in this research. ....	47
Table 5-4. Test materials and results of TG analysis. ....	50
Table 5-5. Description of test samples in TPS tests.....	51
Table 5-6. Overview of test programs of cone heater tests.....	54
Table 5-7. Test specimens and test set-ups. ....	55
Table 5-8. Overview of test programmes of furnace tests. ....	58
Table 5-9. Overview of furnace tests carried out in this research. ....	59
Table 6-1. Average values of measured properties and derived specific heat for ClaySU04...	70
Table 6-2. Average values of measured properties and derived specific heat for ClaySF04. ..	70
Table 6-3. Average values of measured properties and derived specific heat for LimeSU04..	70
Table 6-4. Mean values of start time of charring and charring rate behind plaster obtained from cone heater tests.....	75
Table 6-5. Preparation, hardening time of lime-based plasters and test duration in TP3.	76
Table 6-6. Overview of tested timber specimens and charring rates obtained in TP4...	78
Table 6-7. Furnace test results for clay plaster and reed mat – plasters’ performance.	80
Table 6-8. Furnace test results for clay plaster system and reed board (50 mm) – observations.....	84
Table 6-9. Furnace test results for lime plaster systems – observations. ....	87
Table 6-10. Furnace test results for clay plaster system and reed mat – mean values determined from temperature recordings and fall-off times.....	91
Table 6-11. Furnace test results for clay plaster systems and reed board – mean values from temperature recordings and determined fall-off times.....	92
Table 6-12. Furnace test results for clay plaster and reed mat – mean values of charring of timber behind plaster system.....	93
Table 6-13. Furnace test results for clay plaster and reed board – mean values of charring of timber behind plaster system. ....	95
Table 6-14. The test results of fall-off times and calculated fall-off times for clay plaster systems. ....	98
Table 6-15. Furnace test results for lime plaster systems – mean values of temperature measurements. ....	99
Table 6-16. The charring values of timber protected by lime plasters in furnace. ....	101
Table 6-17. The mean design values derived from cone and furnace tests for clay plaster systems. ....	107
Table 6-18. The mean design values derived from cone and furnace tests for lime plaster systems. ....	109
Table 7-1. Description of the FE-models for simulations using TPS test results as input.	119
Table 7-2. Comparison of times to reach 150°C, 300°C and 550°C behind clay plaster systems determined in furnace tests and simulations of Model 2 based on TPS results.	126
Table 7-3. Comparison of times to reach 150°C, 300°C and 500°C behind lime plaster systems (LimeSU04) determined in furnace tests and simulations of Model 2 based on TPS results.....	127
Table 7-4. Simulation model for the determination of effective thermal properties for clay and lime-based plasters.....	128

Table 7-5. Effective thermal properties based on the TPS test results (Clay mineral) and furnace test results from Test 5A.....	131
Table 7-6. Comparison of times to reach 150°C, 300°C and 550°C behind clay plaster determined in furnace tests and simulations based on calibrated thermal properties...	133
Table 7-7. Determined effective thermal properties based on the TPS test results (LimeSU04) and furnace test results from Test 11a (TP3). ....	136
Table 7-8. Comparison of times to reach 150°C, 300°C and 500°C behind plaster determined in furnace tests and simulations based on modified thermal properties. ....	138
Table 8-1. Effective thermal properties used for the determination of design equations.	139
Table 8-2. Comparison of basic protection times and the mean test results of reaching 270°C behind plaster system with a reed mat. ....	140
Table 8-3. Comparison of basic insulation times and the mean test results of reaching 160°C behind plaster system with a reed mat. ....	141
Table 8-4. Mean times to reach 270°C behind clay plaster system on timber and reed board in furnace tests and calculation results when position coefficient is used in case of reed board.....	142
Table 8-5. Full-scale test reports.....	146
Table 8-6. Test data obtained from the full-scale fire test reports.....	147
Table 8-7. Validation of full-scale test results by proposed design equations.....	148

## References

- Abu-Hamdeh, N. H. (2014). *Specific Heat and Volumetric Heat Capacity of Some Saudian Soils as affected by Moisture and Density*.
- Adl-Zarrabi, B., & Boström, L. (2004). *Determination of Thermal Properties of Wood and Wood Based Products by Using Transient Plane Source*.
- Adl-Zarrabi, B., Boström, L., & Wickström, U. (2006). Using the TPS method for determining the thermal properties of concrete and wood at elevated temperature. *Fire and Materials*, 30(5), 359–369. doi: 10.1002/fam.915
- Alcaraz, J. S., Belda, I. M., Sanchis, E. J., & Gadea Borrell, J. M. (2019). Mechanical properties of plaster reinforced with yute fabrics. *Composites Part B: Engineering*, 178. doi: 10.1016/j.compositesb.2019.107390
- Alev, Ü. (2017). *Renovation and Energy Performance Improvement of Estonian Wooden Rural Houses*. 186.
- Alrtimi, A., Rouainia, M., & Haigh, S. (2016). Thermal conductivity of a sandy soil. *Applied Thermal Engineering*, 106, 551–560. doi: 10.1016/j.applthermaleng.2016.06.012
- Arumägi, E. (2015). *Renovation of Historic Wooden Apartment Buildings, Doctoral Thesis* [Tallinn University of Technology]. Retrieved from <https://digi.lib.ttu.ee/i/?2534>
- Arumägi, E., & Kalamees, T. (2014). Analysis of energy economic renovation for historic wooden apartment buildings in cold climates. *Applied Energy*, 115, 540–548. doi: 10.1016/j.apenergy.2013.10.041
- Asdrubali, F., Bianchi, F., Cotana, F., D'Alessandro, F., Pertosa, M., Pisello, A. L., & Schiavoni, S. (2016). Experimental thermo-acoustic characterization of innovative common reed bio-based panels for building envelope. *Building and Environment*, 102, 217–229. doi: 10.1016/j.buildenv.2016.03.022
- Ashour, T., Georg, H., & Wu, W. (2011). An experimental investigation on equilibrium moisture content of earth plaster with natural reinforcement fibres for straw bale buildings. *Applied Thermal Engineering*, 31(2–3), 293–303. doi: 10.1016/j.applthermaleng.2010.09.009
- Ashour, T., Wieland, H., Georg, H., Bockisch, F. J., & Wu, W. (2010). The influence of natural reinforcement fibres on insulation values of earth plaster for straw bale buildings. *Materials and Design*, 31(10), 4676–4685. doi: 10.1016/j.matdes.2010.05.026
- Babrauskas, V. (2004). Wood char depth: interpretation in fire investigations. *International Symposium on Fire Investigation*.
- Balen, K. Van. (2005). Carbonation reaction of lime, kinetics at ambient temperature. *Cement and Concrete Research*, 35(March 2004), 647–657. doi: 10.1016/j.cemconres.2004.06.020
- Barbero-Barrera, M. del M., Maldonado-Ramos, L., Van Balen, K., García-Santos, A., & Neila-González, F. J. (2014). Lime render layers: An overview of their properties. *Journal of Cultural Heritage*, 15(3), 326–330. doi: 10.1016/J.CULHER.2013.07.004
- Barbero-barrera, M. M., García-santos, A., & Neila-gonzález, F. J. (2014). Thermal conductivity of lime mortars and calcined diatoms. Parameters influencing their performance and comparison with the traditional lime and mortars containing crushed marble used as renders. *Energy & Buildings*, 76, 422–428. doi: 10.1016/j.enbuild.2014.02.065

- Bartlett, A. I., Hadden, R. M., & Bisby, L. A. (2019). A Review of Factors Affecting the Burning Behaviour of Wood for Application to Tall Timber Construction. *Fire Technology*, 55(1), 1–49. doi: 10.1007/s10694-018-0787-y
- Baumberger, A., Eggenberger, H., Löffler, C., Merk, C., & Müller, D. (2022). *Lehmbau und Brandschutz - Standortpapier*. Zürich.
- Berge, A., Adl-Zarrabi, B., & Hagentoft, C. E. (2013). Determination of specific heat capacity by transient plane source. *Frontiers of Architectural Research*, 2(4), 476–482. doi: 10.1016/j.foar.2013.09.004
- BRE. (1988). *BRE Drgest Concise reviews of building technology Increasing the fire of existing timber Digest 208 Building Research Establishment DEPARTMENT OF THE ENVIRONMENT*.
- Buchanan, A., & Abu, A. (2017). *Structural design for fire safety* (A. H. Buchanan & A. K. Abu, Eds.; Second Edition). United Kingdom: John Wiley & Sons, Ltd .
- Buchanan, A., & Östman, B. (2022). Fire Safe Use of Wood in Buildings. In *Fire Safe Use of Wood in Buildings*. doi: 10.1201/9781003190318
- Chorlton, B., & Gales, J. (2020). Fire performance of heritage and contemporary timber encapsulation materials. *Journal of Building Engineering*, 29(March). doi: 10.1016/j.job.2020.101181
- Claytec e.K. (n.d.). FACHWERK NEU ENTDECKEN - Restaureiren, Erneuern, Wärmedämmen mit Lehm - Baustoffen von Claytec. In *Technical guideline*.
- COST Action FP1303. (2017). *Performance of Bio-Based Materials* (D. Jones & C. Brischke, Eds.). Woodhead Publishing Series in Civil and Structural Engineering.
- COST Action FP1404. (2014). *COST Action FP1404 - MEMORANDUM OF UNDERSTANDING For the implementation of a European Concerted Research Action designated as COST Action FP1404 FIRE SAFE USE OF BIO-BASED BUILDING PRODUCTS*. Retrieved from <https://www.cost.eu/actions/FP1404/>
- Crewe, R. J., Staggs, J. S. J., & Phylaktou, H. N. (2010). The Temperature-dependent Cone Calorimeter: An Approximate Alternative to Furnace Testing. *Journal of Fire Sciences*, 29(2). doi: <https://doi.org/10.1177/0734904110382223>
- Dalmis, M., Colson, V., Le Cunff, T., Jadeau, O., & Lanos, C. (2019). Behaviour of bio-based material in multilayer wall during fire test. *3rd International Conference on Bio-Based Building Materials*, 405–411.
- Darling, E. K., Cros, C. J., Wargocki, P., Kolarik, J., Morrison, G. C., & Corsi, R. L. (2012). Impacts of a clay plaster on indoor air quality assessed using chemical and sensory measurements. *Building and Environment*, 57, 370–376. doi: 10.1016/j.buildenv.2012.06.004
- Darling, E., Morrison, G. C., & Corsi, R. L. (2016). Passive removal materials for indoor ozone control. In *Building and Environment* (Vol. 106, pp. 33–44). Elsevier Ltd. doi: 10.1016/j.buildenv.2016.06.018
- Despotou, E., Schlegel, T., Shtiza, A., & Verhelst, F. (2014). Literature study on the rate and mechanism of carbonation of lime in mortars. *9th International Masonry Conference*. doi: 10.1002/dama.201500674
- DIN 4102-4. (2016). *Fire behaviour of building materials and building components –Part 4: Synopsis and application of classified building materials, components and special components*, DIN Deutsches Institut für Normung e. V. (in german).
- DIN 18550-2. (2018). *Planung, Zubereitung und Ausführung von Außen- und Innenputzen - Teil 2: Ergänzende Festlegungen zu DIN EN 13914-2:2016-09 für Innenputze*, DIN Deutsches Institut für Normung e. V. (in german).

- DIN 18947. (2018). *Lehmputzmörtel - Anforderungen, Prüfung und Kennzeichnung (Earth plasters - Requirements, test and labelling), DIN Deutsches Institut für Normung e. V (in german)*. doi: <https://dx.doi.org/10.31030/2897115>
- Džidić, S. (2017). FIRE RESISTANCE OF THE STRAW BALE WALLS. *Zbornik Radova Građevinskog Fakulteta*, 33(30), 423–432. doi: 10.14415/konferencijagfs2017.044
- Ed. Kask, Ü. (2013). *GUIDEBOOK OF REED BUSINESS* (Ü. Kask, Ed.). Retrieved from <https://dspace.emu.ee/xmlui/handle/10492/4490>
- Eensalu, M., Jänes, L., Kuuskemaa, J., Lankots, E., Liivik, O., Lippus, M., Martin, A., Orro, O., Paju, R., Pantelejev, A., Sarv, K., Selg, L., Sepp, M., Talk, T., Tamm, E., Tammert, M., Tuuder, M., Välja, L., & Väljas, M. (2014). *Tallinna puitarhitektuur* (L. Välja, Ed.). Tallinn.
- Elert, K., Rodriguez-Navarro, C., Pardo, E. S., & Hansen, E. (2002). *Lime Mortars for the Conservation of Historic Buildings* (Vol. 47, Issue 1).
- Emiroğlu, M., Yalama, A., & Erdoğan, Y. (2015). Performance of ready-mixed clay plasters produced with different clay/sand ratios. *Applied Clay Science*, 115, 221–229. doi: 10.1016/j.clay.2015.08.005
- EN 459-1. (2015). *Building lime - Part 1: Definitions, specifications and conformity criteria, European Standard. European Committee for Standardization.*
- EN 998-1. (2016). *Specification for mortar for masonry - Part 1: Rendering and plastering mortar, European Committee for Standardization, CEN.*
- EN 1363-1:2016. (n.d.). *EN 1363-1 Fire resistance tests - Part 1: General Requirements, European Standard. European Committee for Standardization.* Brussels.
- EN 1364-1. (2015). *Fire resistance tests for non-loadbearing elements - Part 1: Walls, European Committee for Standardization, CEN.*
- EN 1364-2. (2018). *Fire resistance tests for non-loadbearing elements - Part 2: Ceilings, European Committee for Standardization, CEN.*
- EN 1365-1. (2012). *Fire resistance tests for loadbearing elements - Part 1: Walls, European Committee for Standardization, CEN.*
- EN 1995-1-2. (2004). *Eurocode 5: Design of timber structures- Part 1-2: General-Structural fire design, European Committee for Standardization, CEN.* Brussels.
- EN 13381-7. (2019). *Test methods for determining the contribution to the fire resistance of structural members - Part 7: Applied protection to timber members, European Standard. European Committee for Standardization.* Brussels.
- EN 13501-2. (2016). *Fire classification of construction products and building elements Classification using data from fire resistance tests, excluding ventilation services, European Committee for Standardization, CEN.*
- EN 13914-2. (2016). *Design, preparation and application of external rendering and internal plastering - Part 2: Internal plastering, European Standard. European Committee for Standardization.*
- European Commission. (2011). Regulation (EU) No 305/2011 of the European Parliament and of the Council of 9 March 2011 laying down harmonised conditions for the marketing of construction products and repealing Council Directive 89/106/EEC (OJ L 88, 4.4.2011, pp. 5–43). *Official Journal of the European Union.*
- Fahrni, R., & Frangi, A. (2021). Model scale standard fire experiments on solid timber panels Charring and mass loss investigation to determine the variability of the charring rate. *Report 2021-02.*

- Fletcher, I. A., Welch, S., Torero, J. L., Carvel, R. O., & Usmani, A. (2007). Behaviour of concrete structures in fire. *Thermal Science*, 11(2), 37–52. doi: 10.2298/TSCI0702037F
- Földvári, M. (2011). *Handbook of thermogravimetric system of minerals and its use in geological practice*. Geological Institute of Hungary.
- Franssen, J. M., & Gernay, T. (2017). Modeling structures in fire with SAFIR®: Theoretical background and capabilities. *Journal of Structural Fire Engineering*, 8(3), 300–323. doi: 10.1108/JSFE-07-2016-0010
- Friquin, K. L. (2010). *Charring rates of heavy timber structures for Fire Safety Design, A study of the charring rates under various fire exposures and the influencing factors, Doctoral theses at NTNU, 2010:128*. Norwegian University of Science and Technology.
- Fromme, I., & Herz, U. (2021). *Lehm- und kalkputze – Mörtel herstellen – Wände verputzen – Oberflächen gestalten Irmela Fromme*. Rastede: ökobuch Verlag GmbH.
- Gales, J. (2013). Structural Fire Testing in the 18th Century. *Fire Safety Science New*, 32–33.
- Garcia-Castillo, E., Paya-Zaforteza, I., & Hospitaler, A. (2021). Analysis of the fire resistance of timber jack arch flooring systems used in historical buildings. *Engineering Structures*, 243(September), 112679. doi: 10.1016/j.engstruct.2021.112679
- Garijo, L., Zhang, X., Ruiz, G., & Ortega, J. J. (2020). Age effect on the mechanical properties of natural hydraulic and aerial lime mortars. *Construction and Building Materials*, 236. doi: 10.1016/j.conbuildmat.2019.117573
- Georgiev, G., Theuerkorn, W., Krus, M., Kilian, R., & Grosskinsky, T. (2013). *The potential role of cattail-reinforced clay plaster in sustainable building* (Vol. 13, Issue 14). Retrieved from <http://www.mires-and-peat.net/>,
- Golden, E. (2012). Traditional materials optimized for the twenty-first century. *ACSA International Conference*.
- Graham, A. H. D. (2004). *Wattle and Daub: Craft, Conservation and Wiltshire Case Study*. doi: 10.13140/2.1.1875.2806
- Gulbe, L., Vitina, I., & Setina, J. (2017). The influence of cement on properties of lime mortars. *Procedia Engineering*, 172, 325–332. doi: 10.1016/j.proeng.2017.02.030
- Han, J., Sun, Q., Xing, H., Zhang, Y., & Sun, H. (2017). Experimental study on thermophysical properties of clay after high temperature. *Applied Thermal Engineering*, 111, 847–854. doi: 10.1016/j.applthermaleng.2016.09.168
- Hasemi, Y., Yasui, N., Akizuki, M., Kyoto, C., Yamamoto, J. K., & Yoshida, M. (2002). Fire Safety Performance of Japanese Traditional Wood/Soil Walls and Implications for the Restoration of Historic Buildings in Urban Districts. In *Fire Technology* (Vol. 38).
- Historic England. (2016). *Energy Efficiency and Historic Buildings - Insulating Timber-Framed Walls - Guidance, UK*.
- IBB GmbH of Groß Schwülper. (2018). *Expert opinion No. GA-2018/028 (UPSTRAW project EU) - Expert opinion on the fire behaviour of load-bearing, separating wall constructions in timber frame construction with a cavity insulation of construction straw in connection with various design variants in Germany*. Retrieved from [https://strawbuilding.eu/tag/fire\\_resistance\\_safety/](https://strawbuilding.eu/tag/fire_resistance_safety/)
- ICOMOS. (2017). *Principles for the conservation of wooden built heritage - Adopted by ICOMOS at the 19th General Assembly in Delhi, India, December 2017*.

- Ikonen, I., & Hagelberg, E. (2007). *Read up on reed! Reed Strategy -project, implementing Interreg IIIA -programme between Southern Finland and Estonia*. (I. Ikonen & E. Hagelberg, Eds.; Issue March 2006). Turku: Southwest Finland Regional Environment Centre. Retrieved from [www.ymparisto.fi/julkaisut](http://www.ymparisto.fi/julkaisut)
- Ingason, H., & Wickström, U. (2007). Measuring incident radiant heat flux using the plate thermometer. *Fire Safety Journal*, 42(2), 161–166. doi: 10.1016/j.firesaf.2006.08.008
- ISO 834-1. (1999). *Fire-resistance tests — Elements of building construction — Part 1: General requirements*, International Organization for Standardization, ISO.
- ISO 5660-1. (2015). *Reaction-to-fire tests- Heat release, smoke production and mass loss rate-Part 1: Heat release rate (cone calorimeter method) and smoke production rate (dynamic measurement)*, International Organization for Standardization, ISO.
- ISO 22007-2. (2008). *Plastics — Determination of thermal conductivity and thermal diffusivity — Part 2: Transient plane heat source (hot disc) method*, International Organization for Standardization, ISO.
- Jackman, p. (2009). Fire resistance of historic fabric. *The Building Conservation Directory*, 185–187. Retrieved from [www.chilternfire.co.uk](http://www.chilternfire.co.uk)
- Jansson, R. (2004). Measurement of Concrete Thermal Properties at High Temperature. *Conference: Proceedings from the Fib Task Group 4.3 Workshop "Fire Design of Concrete Structures: What Now? What Next?"*
- Jansson, R. (2013). *Fire Spalling of Concrete - Theoretical and Experimental Studies, Doctoral thesis in Concrete structures*. KTH Architecture and Built Environment.
- Just, A. (2010). *Structural Fire Design of Timber Frame Assemblies Insulated by Glass Wool and Covered by Gypsum Plasterboards, Doctoral Thesis*. Tallinn University of Technology.
- Kalifa, P., Menneteau, F. D., & Quenard, D. (2000). Spalling and pore pressure in HPC at high temperatures. *Cement and Concrete Research*, 30(12), 1915–1927. doi: 10.1016/S0008-8846(00)00384-7
- Klinge, A., Roswag-Klinge, E., Fontana, P., Hoppe, J., Richter, M., & Sjöström, C. (2016). Reducing the need for mechanical ventilation through the use of climate-responsive natural building materials Results from the EU research project H-House and building practice. *Conference: Lehm 2016 - 7th International Conference on Building with EarthAt: Weimar, Germany*.
- Köbbing, J. F., Thevs, N., & Zerbe, S. (2013). *The utilisation of reed (Phragmites australis): a review* (Vol. 13, Issue 14). Retrieved from <http://www.mires-and-peat.net/>,
- König, J., & Walleij, L. (1997). *Timber frame assemblies exposed to standard and parametric fires*. Sweden.
- Küppers, J. (2020). *Grundlagenuntersuchungen zum Brandverhalten von WDVS mit nachwachsenden Rohstoffen*. Technische Universität Carolo-Wilhelmina zu Braunschweig.
- Küppers, J., Gößwein, L., Liblik, J., & Mäger, K. N. (2018). Numerical investigations on heat transfer through claddings of bio-based building materials. *5th Symposium Structural Fire Engineering – TU Braunschweig 2018 115th Symposium Structural Fire Engineering –TU Braunschweig, Germany*, 1–19.
- Larsen, K. E., & Marstein, N. (2000). *Conservation of Historic Timber Structures An ecological approach*.

- Lawrence, M. (2006). *A study of carbonation in non-hydraulic lime mortars* [University of Bath]. Retrieved from <https://researchportal.bath.ac.uk/en/studentTheses/a-study-of-carbonation-in-non-hydraulic-lime-mortars>
- Liblik, J. (2015). *Protective effect of clay plaster for the fire design of timber constructions, Master thesis*. Tallinn University of Technology.
- Liblik, J. (2016). *Performance of Constructions with Clay Plaster and Timber at Elevated Temperatures - Comparison of different methods in small and model scale*. Stockholm.
- Liblik, J. (2017). *Scientific Report of STSM - COST FP1404 - Determination of the Fire Design Parameters for Clay Plaster as a Protection Material of Timber Constructions* (Issue 23). Stockholm.
- Liblik, J. (2019a). *Test SE-19-02 Horizontal furnace tests at iBMB TU Braunschweig, MPA Germany 2019*.
- Liblik, J. (2019b). *Test SE-19-03 Small-scale furnace tests with clay and lime plasters at iBMB TU Braunschweig, MPA Germany*.
- Liblik, J., Järnefelt, K., Just, A., Möller, H., Lynch, P., & Salminen, M. (2018). Renovation of a wooden building in a historic village - A case study from Finland. *WCTE 2018 - World Conference on Timber Engineering*.
- Liblik, J., & Just, A. (2016). Performance of Constructions with Clay Plaster and Timber at Elevated Temperatures. *Energy Procedia*, 96. doi: 10.1016/j.egypro.2016.09.133
- Liblik, J., & Just, A. (2017). Design parameters for timber members protected by clay plaster at elevated temperatures. *Proceedings of the International Network on Timber Engineering Research (INTER), Meeting 50, Kyoto, Japan: International Network on Timber Engineering Research Meeting*. Ed. Görlacher, R. Karlsruhe: Forschungszentrum Karlsruhe, 375–389.
- Liblik, J., & Just, A. (2023). Small-scale assessment method for the fire resistance of historic plaster system and timber structures. *Fire and Materials*, 47(1), 62–74. doi: 10.1002/fam.3069
- Liblik, J., Küppers, J., Just, A., Zehfuß, J., & Ziegert, C. (2018). Fire safety of historic timber buildings with traditional plasters in Europe. *WCTE 2018 - World Conference on Timber Engineering*.
- Liblik, J., Küppers, J., Maaten, B., & Just, A. (2020). Fire protection provided by clay and lime plasters. *Wood Material Science and Engineering*, 0(0), 1–9. doi: 10.1080/17480272.2020.1714726
- Liblik, J., Küppers, J., Maaten, B., & Pajusaar, S. (2019). *Material properties of clay and lime plaster for structural fire design*. November, 1–11. doi: 10.1002/fam.2798
- Liblik, J., & Maaten, B. (2019). *Test Report SE-19-01 - TGA analysis of dry-mix plaster mixes*. Tallinn.
- Liblik, J., Nurk, M., & Just, A. (2022). Charring performance of timber structures protected by traditional lime-based plasters. *Construction and Building Materials*, 347. doi: 10.1016/J.CONBUILDMAT.2022.128572
- Log, T., & Gustafsson, S. E. (1995). Transient plane source (TPS) technique for measuring thermal transport properties of building materials. *Fire and Materials*, 19(1), 43–49. doi: <https://doi.org/10.1002/fam.810190107>
- Mäger, K. N. (2016). *Implementation of new materials to the component additive method for fire design of timber structures, Doctoral Thesis*. Tallinn University of Technology.

- Mäger, K. N., Just, A., & Frangi, A. (2018, June). Improvements of Component Additive Method. *SIF 2018—The 10th International Conference on Structures in Fire, FireSERT, Ulster University, Belfast, UK*.
- Mäger, K. N., Just, A., Schmid, J., Werther, N., Klippel, M., Brandon, D., & Frangi, A. (2017). Procedure for implementing new materials to the component additive method. *Fire Safety Journal*. doi: 10.1016/j.firesaf.2017.09.006
- Melià, P., Ruggieri, G., Sabbadini, S., & Dotelli, G. (2014). Environmental impacts of natural and conventional building materials: A case study on earth plasters. *Journal of Cleaner Production*, 80, 179–186. doi: 10.1016/j.jclepro.2014.05.073
- Metal lath technical bulletin no. 141. (n.d.). *Technical bulletin no. 141 - Description - Specifications- Details - Metal lath and plaster: Fire protection*.
- Mikkola, E. (1991). Charring Of Wood Based Materials. *Fire Safety Science*, 3, 547–556. doi: 10.3801/iafss.fss.3-547
- Miljan, M., Miljan, M.-J., Miljan, J., Akermann, K., & Karja, K. (2013). Thermal transmittance of reed-insulated walls in a purpose-built test house. *J. in Internet Mires and Peat*, 13(07), 1–12. Retrieved from <http://www.mires-and-peat.net/>,
- Minke, G. (2006). *Building with Earth - Design and Technology of a Sustainable Architecture*. Basel: Birkhäuser – Publishers for Architecture.
- Navarro, A., Palumbo, M., Gonzalez, B., & Lacasta, A. M. (2015, June). Performance of clay-straw plasters containing natural additives. *First International Conference on Bio-Based Building Materials, Clermont-Ferrand, France*.
- Niemann, T. (2010). *Machbarkeitsstudie zur Verwendung von Strohballen als Dämmstoff für ein 4-bis 5-geschossiges Gebäude*. Technische Universität Braunschweig.
- Nogueira, R., Ferreira Pinto, A. P., & Gomes, A. (2018). Design and behavior of traditional lime-based plasters and renders. Review and critical appraisal of strengths and weaknesses. *Cement and Concrete Composites*, 89, 192–204. doi: 10.1016/J.CEMCONCOMP.2018.03.005
- Nurk, M. (2021). *Lubikrohviga kaitstud puitkonstruktsioonide söestumine (Charring of timber structures protected by lime plaster), Master thesis*. Tallinn.
- Oliveira, M. A., Azenha, M., Lourenço, P. B., Meneghini, A., Guimarães, E. T., Castro, F., & Soares, D. (2017a). Experimental analysis of the carbonation and humidity diffusion processes in aerial lime mortar. *Construction and Building Materials*, 148, 38–48. doi: 10.1016/j.conbuildmat.2017.04.120
- Oliveira, M. A., Azenha, M., Lourenço, P. B., Meneghini, A., Guimarães, E. T., Castro, F., & Soares, D. (2017b). Experimental analysis of the carbonation and humidity diffusion processes in aerial lime mortar. *Construction and Building Materials*, 148, 38–48. doi: 10.1016/j.conbuildmat.2017.04.120
- Östman, B. (2022). National fire regulations for the use of wood in buildings—worldwide review 2020. *Wood Material Science and Engineering*, 17(1), 2–5. doi: 10.1080/17480272.2021.1936630
- Östman, B., Mikkola, E., Stein, R., Frangi, A., König, J., Dhima, D., Hakkarainen, T., & Bregulla, J. (2010). *Fire safety in timber buildings Technical guideline for Europe*. Stockholm: SP Technical Research of Sweden, SP Trätek.
- Pacheco-Torgal, F. (2014). Eco-efficient construction and building materials research under the EU Framework Programme Horizon 2020. *Construction and Building Materials*, 51, 151–162. doi: 10.1016/J.CONBUILDMAT.2013.10.058

- Pacheco-Torgal, F., & Jalali, S. (2012). Earth construction: Lessons from the past for future eco-efficient construction. *Construction and Building Materials*, 29, 512–519. doi: 10.1016/j.conbuildmat.2011.10.054
- Pachta, V., & Stefanidou, M. (2021). *Evaluation of the Behaviour of Lime and Cement Based Mortars Exposed at Elevated Temperatures*. September. doi: 10.23967/sahc.2021.093
- Pachta, Vasiliki, Triantafyllaki, S., & Stefanidou, M. (2018). Performance of lime-based mortars at elevated temperatures. *Construction and Building Materials*, 189, 576–584. doi: 10.1016/j.conbuildmat.2018.09.027
- Papworth, J. P., & Towler, K. D. S. (1995). *Investigations into existing test evidence in the public domain on the fire performance of historical lath and plaster constructions - Report no. L9509*.
- prEN 1995-1-2. (2022). *Eurocode 5: Design of timber structures- Part 1-2: General-Structural fire design*, European Committee for Standardization, CEN.
- Randazzo, L., Montana, G., Hein, A., Castiglia, A., Rodonò, G., & Donato, D. I. (2016). Moisture absorption, thermal conductivity and noise mitigation of clay based plasters: The influence of mineralogical and textural characteristics. *Applied Clay Science*, 132–133, 498–507. doi: 10.1016/j.clay.2016.07.021
- Ranesi, A., Faria, P., & Veiga, M. D. R. (2021). Traditional and modern plasters for built heritage: Suitability and contribution for passive relative humidity regulation. *Heritage*, 4(3), 2337–2355. doi: 10.3390/heritage4030132
- Rauch, M., Werther, N., & Winter, S. (2021). Fire design methods for timber floor elements - The contribution of screed floor toppings to the fire resistance. *World Conference on Timber Engineering 2021, WCTE 2021, October*. doi: 10.13140/RG.2.2.16032.00004
- Richter, M., Horn, W., Juritsch, E., Klinge, A., Radeljic, L., & Jann, O. (2021). Natural building materials for interior fitting and refurbishment—what about indoor emissions? *Materials*, 14(1), 1–14. doi: 10.3390/ma14010234
- Röhlen, U., & Ziegert, C. (2011). *Earth Building Practice - Planning Design Building*.
- Ruus, A. (2020). *Test Report SE-20-01 - Assessment of equilibrium moisture content in clay plasters*. Tartu College.
- Ryan, J. V. (1962). Study of gypsum plasters exposed to fire. *Journal of Research of the National Bureau of Standards -C. Engineering and Instrumentation*, 66C(4).
- Schleifer, V. (2009). *Zum Verhalten von raumabschliessenden mehrschichtigen Holzbauteilen im Brandfall* [Eidgenössische Technische Hochschule Zürich, Switzerland]. doi: 10.3929/ethz-a-005771863
- Schroeder, H. (2018). The New DIN Standards in Earth Building—The Current Situation in Germany. *Journal of Civil Engineering and Architecture*, 12(2), 113–120. doi: 10.17265/1934-7359/2018.02.005
- Silcock, G. W. H., & Shields, T. J. (2001). *Relating Char Depth to Fire Severity Conditions*.
- Sjöstrom, J., Jansson, R., & Brandskyddslaget, M. (2012). Measuring thermal material properties for structural fire engineering. *15th International Conference on Experimental Mechanics*.
- Snow, J., Torney, C. (2014). *Lime Mortars in Traditional Buildings: Short Guide 6*. Retrieved from <https://www.researchgate.net/publication/264563855>
- Straube, J. F. (2000). *Moisture Properties of Plaster and Stucco for Strawbale Buildings - EBNet*. Ottawa.

- Sultan, M. A., Benichou, N., & Min, B. Y. (2003). Heat exposure in fire resistance furnaces: full-scale vs intermediate-scale. *Fire and Materials 2003 International Conference, August*, 43–53.
- Sun, Q., Zhang, W., & Qian, H. (2016). Effects of high temperature thermal treatment on the physical properties of clay. *Environmental Earth Sciences*, 75(7). doi: 10.1007/s12665-016-5402-2
- Sun, Q., Zhang, W., Zhang, Y., & Yang, L. (2016). Variations of Strength, Resistivity and Thermal Parameters of Clay after High Temperature Treatment. *Acta Geophysica*, 64(6), 2077–2091. doi: 10.1515/acgeo-2016-0090
- Test Report 16027. (2016). *Test Report - Project-No: 16027: Testing of Lime Plasters according to EN 998-1 "Rendering and plastering mortar"* (Issue July 2016). Berlin.
- Tian, X., Sohngen, B., & Kim, J. B. (2022). Climate impacts of wood / timber as a building material – investigated on three urban quarters in Germany (CIW ) Climate impacts of wood / timber as a building material – investigated on three urban quarters in Germany ( CIW ). *IOP Conf. Series: Earth and Environmental Science*. doi: 10.1088/1755-1315/1078/1/012029
- Tiso, M. (2018). *The Contribution of Cavity Insulations to the Load-Bearing Capacity of Timber Frame Assemblies Exposed to Fire, Doctoral thesis, Tallinn University of Technology*.
- Tiso, M., Just, A., & Mäger, K. N. (2016). Behavior of Wooden Based Insulations at High Temperatures. *Energy Procedia*, 96, 729–737. doi: 10.1016/j.egypro.2016.09.135
- Tiso, M., Schmid, J., & Fragiaco, M. (2015). Charring behaviour of cross laminated timber with respect to the fire protection, comparison of different methods. In *Proceedings 1st European Workshop Fire Safety of Green Buildings*. Retrieved from [http://www.costfp1404.com/en/Documents/N076-05\\_Book of abstracts meeting in BCN.pdf](http://www.costfp1404.com/en/Documents/N076-05_Book of abstracts meeting in BCN.pdf)
- Tooming, K. (n.d.). LUBI II - Traditsiooniline lubikrohv ja värv. In Muinsuskaitseamet. Tallinn. Retrieved from [https://www.muinsuskaitseamet.ee/sites/default/files/content-editors/kasiraamat/24.\\_lubi\\_ii.pdf](https://www.muinsuskaitseamet.ee/sites/default/files/content-editors/kasiraamat/24._lubi_ii.pdf)
- Tsantaridis, L. D., & Östman, B. A. L. (1998). Charring of Protected Wood Studs. *Fire and Materials*, 22(2), 55–60. doi: 10.1002/(sici)1099-1018(199803/04)22:2<55::aid-fam635>3.3.co;2-k
- Tsantaridis, L. D., Östman, B. A. L., & König, J. (1999). Fire protection of wood by different gypsum plasterboards. *Fire and Materials*, 23(1), 45–48. doi: 10.1002/(SICI)1099-1018(199901/02)23:1<45::AID-FAM662>3.0.CO;2-6
- Umar, U. A., Khamidi, M. F., & Tukur, H. (2012). Sustainable building material for green building construction, conservation and refurbishing. *Conference: Management in Construction Research Association (MiCRA) Postgraduate Conference 5-6*. Retrieved from <https://www.researchgate.net/publication/233996708>
- Ünal, M., & Latifov, F. (2017). HIGH TEMPERATURE EFFECT ON THE STRENGTH OF SAND-CEMENT PLASTER. In *Journal of Engineering Technology and Applied Sciences* (Vol. 2, Issue 3).
- van der Heijden, G. H. A., Pel, L., Huinink, H. P., & Kopinga, K. (2011). Moisture transport and dehydration in heated gypsum, an NMR study. *Chemical Engineering Science*, 66(18), 4241–4250. doi: 10.1016/j.ces.2011.06.024
- Volhard, F. (2016). *Light Earth Building - A Handbook for Building with Wood and Earth*. Birkhäuser.

- Wachtling, J., Hosser, D., & Zehfuß, J. (2013). Fire protection of multi-storey straw bale buildings. Zingoni (Ed.), *Research and Applications in Structural Engineering, Mechanics and Computation* (Issue Scharmer 2011, pp. 2011–2012). Taylor & Francis Group.
- Wall, K., Walker, P., Gross, C., White, C., & Mander, T. (2012). Development and testing of a prototype straw bale house. *Proceedings of Institution of Civil Engineers: Construction Materials*, 165(6), 377–384. doi: 10.1680/coma.11.00003
- Wegerer, P. (2011). Long-term Measurement and Hygrothermal Simulation of an Interior Insulation Consisting of Reed Panels and Clay Plaster. *9th Nordic Symposium on Building Physics*, 1(Bednar 2000), 331–338.
- White, R. H. (1971). Charring Rate of Wood Exposed to a Constant Heat Flux. *Methods*, 1988, 175–183.
- Xu, Q., Chen, L., Harries, K. A., Zhang, F., Liu, Q., & Feng, J. (2015). Combustion and charring properties of five common constructional wood species from cone calorimeter tests. *Construction and Building Materials*, 96, 416–427. doi: 10.1016/j.conbuildmat.2015.08.062
- Zehfuß, J., Robert, F., Spille, J., Rijaniaina, |, & Razafinjato, N. (2020). *Evaluation of Eurocode 2 approaches for thermal conductivity of concrete in case of fire*. doi: 10.1002/cend.202000001
- Zihms, C. S., Karstunen M, & Tarantino A. (2013). *Understanding the effects of high temperature processes on the engineering properties of soils Comprendre les effets des procédés a haute température sur les propriétés des sols*.

## Acknowledgements

First, and foremost I am extremely grateful to my Prof. Alar Just, for his continuous support, invaluable advice, and trust in me to carry out this work. I truly appreciate his assistance throughout my research and encouragement to establish partnerships with international organisations for fire testing. I am grateful for the opportunity to participate in COST Action PF1404, which supported my scientific missions to conduct fire experiments and provided a platform for sharing and receiving feedback on the results of my research. Herein, I also want to thank my closest colleagues, Katrin Nele Mäger and Mattia Tiso, for their presence and continuous support throughout the years.

I am highly grateful to RISE Research Institute of Sweden in Stockholm, wherein my special thanks go to Birgit Östman, Joakim Noren, Lazaros Tsantaridis. My deepest gratitude belongs to Magdalena Sterley and her family, whose support and knowledge in so many ways surpassed all my expectations while doing research overseas. Extended thanks go to Meeri Nurk, Birgit Maaten, Siim Pajusaar and Mari Sinisalu from Tallinn University of Technology. My gratitude extends to Martti-Jaan Miljan from Estonian University of Life Sciences for the co-operation and feedback to my thesis.

My special gratitude goes to Judith Küppers for her hospitality, knowledge, and support in my work; also, my thanks extend to Prof. Zehfuß for the opportunity to carry out the furnace tests at TU Braunschweig in Germany. Herein, my special thanks go to Christian Northe, David Kellermann and Patrick Wulfert for all their technical support and furnace testing.

My gratitude extends to the plaster manufacturer UKU (Saviukumaja OÜ) from Estonia for their indispensable contribution of sharing their knowledge and helping with the preparation and shipment of the test specimens for fire testing. Marko Kikas, Martin Hütt, Indrek Kerbo and Mikk Luht – thank you for your contribution to this research project. My thanks extend to Safran OÜ for the materials and preparation of test specimens. Alike gratitude extends to Claytec e.K. in Germany who showed their interest and contributed with their materials and know-how. The gratitude extends especially to Manfred Lemke and Prof. Christof Ziegert. My thanks also go to Paul Lynch and Kasper Järnefelt for the opportunity to contribute to the planning of a heritage building renovation project in Finland.

I would like to thank the organizations that have rewarded my studies with scholarships – Riigi Kinnisvara AS, Sihtasutus Professor Karl Õigeri Stipendiumifond, City Government of Tallinn, and Estonian Education and Youth Board (former Archimedes Foundation).

My sincere thanks also extend to Michael Rauch for reviewing my thesis and to official referees of my doctoral thesis, Prof. Andrea Frangi and Assoc Prof. John Gales.

My heartfelt thanks go to Lauri Hass, my family, and my closest friends, who have constantly supported and encouraged me throughout these years. This work is dedicated to all of you who have been together with me on this journey.

## Abstract

### Performance of timber structures protected by traditional plaster systems in fire

Traditional clay and lime-based plasters have been used in the past to protect timber structures from direct fire exposure. Yet, little is known about their fire protection effect, which hinders their use as a fire protection material today. Currently, there are some fire test data for certain plasters used in straw bale buildings, yet barely any fire tests utilizing modern fire testing equipment for traditional plasters applied on timber structures exist. At present, design guidelines lack flexible fire design options for traditional type of plaster systems and no design values are provided in the current Eurocode 5 Part 1-2. A greater understanding on the plasters in fire would contribute to their wider acceptance in construction projects to increase the use of low carbon building materials as well as it supports the fire risk assessment of existing plasters in buildings for improved fire design solutions.

This thesis investigated the fire resistance performance of traditional type of clay and lime-based plasters as a fire protection system for timber structures. Plasters are regarded a plaster system in this research owing to the variety of plasters based on their components, function (basecoat and topcoat), densities, layers (thicknesses) as well as the use of a reinforcement mesh and/or plaster carrier. A comprehensive experimental program accompanied by numerical investigations was conducted with the main objective of establishing the fire design principles and parameters for the plaster systems that comply with Eurocode 5 Part 1-2. Due to the drawbacks of furnace testing, this thesis also aimed to propose a small-scale test method as a tool for estimating the design values (EN 1995-1-2) for protection materials usually determined in furnace (EN 1363-1), i.e., the start time of charring and protection factor.

The experimental program consisted of a series of experiments including i) material tests to determine thermal properties of clay and lime plaster, ii) use of a cone heater of a cone calorimeter that enabled simple testing of various plaster systems, and iii) furnace tests to assess the performance of plaster systems under standard fire exposure conditions. All performed tests with different plaster systems (consisting of different dry-mixes, binders, grain sizes and densities) showed that the thickness of the plaster system is the most influential factor in determining its protective effect against the charring of timber. With the increasing thickness of the plaster, the start time of charring of timber was gradually delayed, and the charring rate of timber protected by plaster system reduced. Whilst the material tests presented differences in the composition, density and temperature dependent thermal properties of selected plasters, the charring rate of timber behind clay and lime-based plaster systems was very similar. Solely the start time of charring behind lime plaster was somewhat delayed compared to clay plaster in case of thicker plaster systems (30 mm). The plaster systems seem to benefit from the glass fibre reinforcement mesh as it prevents the cracking of plaster and thus contributes to the integrity of the whole plaster system until the failure of the mesh itself.

The furnace tests demonstrated that the plaster systems resist significantly longer in place in walls compared to its position in ceilings. The study has identified three distinct types of failure modes for the plaster systems: i) failure of the mechanical fastening system, ii) loss of adhesion between the plaster and its substrate, iii) material thermal degradation. In the first case, the attachment of plaster to timber is dependent on the

fixation of the plaster carrier (e.g., reed mat) into the wooden element by fasteners (e.g., staples). Thus, the failure time of plaster system in walls is dependent on the start time of charring and the charring rate of timber along the fasteners. In case of ceilings, the failure time of the plaster system should be taken equal to the start time of charring (given that no material degradation occurs before). In the event of a loss of adhesion, plaster has been applied to its substrate without any plaster carrier. The test results revealed that the start time of charring of the substrate marks the failure time of the plaster. The mechanical degradation was detected in case of lime plaster systems tested in horizontal position in furnace that was most probably related to its low mechanical strength (related to the carbonisation of lime plaster before testing). Results show that the failure modes of lime-based plasters require further testing.

In addition to the obtained results in furnace tests, this thesis proposed a small-scale test method to estimate the start time of charring and charring rate of timber behind plaster systems. The cone heater tests provided useful insight and estimation about the heat transfer mode through the plaster systems, as the start times of charring of timber were obtained in a good agreement with the ones measured in the furnace. The cone heater testing was found limited to directly determine the charring rate behind the plasters, thus a modification factor was proposed for the estimation of the protection factor  $k_2$ .

For the development of fire design parameters in view of prEN 1995-1-2:2022, numerical investigations on the thermal response through the various plaster systems were carried out. The thermal properties from material tests were calibrated to determine effective material properties presenting the best fit to the furnace test results for the wide range of plaster thicknesses. The proposed design parameters are primarily dependent on the thickness of the plaster system and are accompanied by specific application requirements and material properties to ensure their performance.

This research demonstrated that traditional plaster systems can serve as effective fire protection for timber structures. The proposed design equations for clay and lime plaster systems are provided in view of EN 1995-1-2, allowing their use in a format similar to that for other well-known fire protection materials. The results facilitate the planning of full-scale fire testing according to EN 13381-7:2019 to study different failure modes. The performed work provides means to rate the fire resistance performance plasters in existing buildings in view of EN 1995-1-2. This study provides a framework for expanding the current work to various plasters, plaster carriers, and their substrates, as well as presents a platform for product development in small-scale.

**Keywords:** fire protection, clay plaster, lime plaster, traditional plaster system, timber structures, historical timber buildings, fire resistance, fire design, Eurocode 5 Part 1-2

## Lühikokkuvõte

### Traditsioonilise krohvisüsteemiga kaetud puitkonstruktsioonide tulepüsivus

Ajalooliselt on savi ja -lubikrohve kasutatud puitkonstruktsioonide kaitsmiseks tulekahjuolukorras. Krohvide kasutamine puitkonstruktsioonide tulekaitsematerjalina on aga tänapäeval piiratud, sest puuduvad teadmised krohvilahenduste tulekaitsevõime kohta. Viimaste aastakümnete jooksul on katsetatud erinevaid krohve peamiselt põhuehituses tulekaitsematerjalina, kuid traditsiooniliste krohvilahendustega kaetud puitkonstruktsioone on väga vähe uuritud tänapäevaste katseseadmetega kõrgetel temperatuuridel. Hetkel puuduvad projekteerimisjuhised krohvide tulekaitsevõime arvutamiseks ja kehtiv Eurokoodeks 5 osa 1-2 ei sisalda ühtegi viidet krohvi kohta. Krohvide tulekaitsevõime suurem teadlikkus võimaldaks nende materjalide laialdasemat kasutust ehitusprojektides, pakkudes madalama süsinikusisaldusega ehitusmaterjali näol alternatiivi teistele siseviimistlusmaterjalidele; vanades (puit)hoonetes toetaks see sobivamate tulekaitse lahenduste leidmist ning aitaks hinnata juba olemasolevate krohvide käitumist tulekahjuolukorras, mis toetaks eksperthinnangute andmist.

Antud doktoritöö eesmärgiks oli uurida traditsioonilisi savi- ja lubikrohvilahendusi puitkonstruktsioonidele tulekahjuolukorras. Antud töös käsitleti krohve süsteemidena, sest krohvilahendused võivad koosneda erinevatest krohvidest ja krohvikihetidest (sh paksusest), mis erinevad oma koostisosade, funktsiooni (alus- ja viimistluskrohv), tiheduse kui ka armeerimisvõrgu kasutamise poolest. Lisaks kasutatakse krohvikandjat (nt pilliroomatti) krohvide paigaldamisel puitpindadele nakke tagamiseks. Antud töös käsitleti erinevaid savi- ja lubikrohvisüsteeme, erinevaid krohvikandjaid ja aluspindu (puit ja pillirooplaat), mida kasutatakse ka praktikas, vanade hoonete renoveerimisel. Töö põhieesmärk oli määrata projekteerimiseks vajalikud arvutusparameetrid valitud krohvisüsteemidele juhindudes Eurokoodeks 5 osa 1-2 esitatud arvutuspõhimõtetest. Tulenevalt täismõõtmeliste tulekatsete läbiviimise puudustest, oli käesoleva töö eesmärk välja töötada ka meetod väikesemõõtmeliste katsekehade katsetamiseks oluliste arvutusparameetrite (EN 1995-1-2) saamiseks, mis tavaliselt määratakse ahjukatsega (EN 1363-1).

Töö sisaldas eksperimentaalset osa koos analüütilise uuringuga. Eksperimentaalne osa koosnes erinevatest katseprogrammidest: i) materjaliuuringud savi- ja lubikrohvide termiliste omaduste määramiseks, ii) katsetamine koonuskuumutiga (*Cone Calorimeter*), mis võimaldas erinevate krohvisüsteemide lihtsat katsetamist ning iii) ahjukatsed standardtulekahju (ISO 834) olukorras. Töö analüütiline osa sisaldas termilisi simulatsioone, mis põhinesid katsete tulemustel ja erialasel kirjandusel, et välja töötada krohvisüsteemide arvutusvalemid vastavalt prEN 1995-1-2:2022, lisa G juhistele.

Katsetulemused näitasid, et vaatamata erinevatele katsetatud savi- ja lubikrohvisüsteemidele oli krohvi paksus peamine mõjur, millest sõltus puidu söestumine krohvisüsteemi taga. Krohvi paksuse suurenemisega muutus kaitstud puidu söestumise algusaeg hilisemaks ja vähenes puidu söestumiskiirus kuni krohvisüsteemi tõrketekkeajani. Kuigi materjalikatset näitasid, et nii savi- kui lubikrohvid erinevad oma koostise, tiheduse ja termiliste omaduste poolest, siis olenemata katsetatud krohvisüsteemidest oli kaitstud puidu söestumiskiirus väga sarnane. Ainuüksi söestumise algusaeg oli lubikrohvi puhul hilisem võrreldes savikrohviga. Ahjukatsete

puhul täheldati, et krohvisüsteemides kasutatav klaaskiust armeerimisvõrk aitab ära hoida krohvi pragunemist kuni võrgu enda lagunemiseni.

Ahjukaitses näitasid, et krohvisüsteemid püsivad seintel oluliselt kauem kui lagedel. Antud uurimistöös tuvastati kolm erinevat krohvisüsteemide tõrketekkega mõjutavat olukorda: i) krohvikandjast tingitud krohvi ära kukkumine, ii) krohvi ja selle aluspinna vahelise nakke kadumine, iii) materjali termiline lagunemine. Esimesel juhul sõltub krohvisüsteemi tõrketekkegaag krohvikandjast (nt klambritega kinnitatud pilliroomatt puidul). Katsetulemuste põhjal saab väita, et seinakonstruktsioonis sõltub krohvisüsteemi tõrketekkegaag söestumise algusajast ja puidu söestumiskiirusest piki kinnitusvahendit. Lagede puhul tuleb krohvisüsteemi tõrketekkegaag võrdsustada söestumise algusajaga (arvestades, et materjali lagunemist enne ei toimu). Nakke kadumise korral on tegemist olukorraga, kus krohvisüsteem on aluspinnale kantud krohvikandjata. Katsetulemustele põhinedes tähistab sellisel juhul krohvisüsteemi tõrketekkegaag söestumise algusaeg kui aluspinnaks on puit või pilliroomat. Materjali termiline lagunemine tuvastati ahjus horisontaalasendis katsetatud lubikrohvisüsteemi puhul, mis oli tõenäoliselt tingitud lubikrohvi väikesest mehaanilisest tugevusest (seotud lubikrohvi vähesest karboniseerumisest). Antud katsetulemus näitas, et lubjapõhiste krohvisüsteemide tõrketekkegaag mõjutavad olukorrad vajavad täiendavat katsetamist tulevikus.

Lisaks ahjukatsetest saadud tulemustele pakkus antud töö välja katsemeetodi (koonuskuumuti katsed) krohvisüsteemide tulepüsivuse arvutamiseks vajalike parameetrite määramiseks, millisteks on: i) puidu söestumise algusaeg ja ii) krohvisüsteemi kaitsetegur  $k_2$  kaitsefaasi jaoks. Koonuskuumuti katsete tulemused puidu söestumise algusaja määramiseks olid kooskõlas tulemustega, mis saadi ahjus standardtulekahju olukorras. Kaitseteguri  $k_2$  määramiseks on tehtud ettepanek kasutada modifikatsiooniteguri tulemuste interpreteerimiseks, et saada võrdväärne kaitseteguri  $k_2$  väärtus ahjukatses saadud tulemustele, sest koonuskuumuti katsed ülehindasid krohvisüsteemide kaitsevõimet.

Arvutusparameetrite väljatöötamiseks vastavalt standardile prEN 1995-1-2:2022, tehti termilisi simulatsioone erinevate krohvisüsteemidega. Doktoritöö tulemusena on esitatud arvutusvalemid, mis sõltuvad peamiselt nii savi- ja lubikrohvisüsteemi puhul krohvi paksusest. Krohvisüsteemi toimivuse tagamiseks on kirjeldatud krohvisüsteemidele esitatavad nõuded. Uurimistöös näitas, et traditsioonilised krohvisüsteemid võimaldavad kaitsta puitu tule eest kuni nende tõrketekkeajani. Esitatud valemid on antud standardi EN 1995-1-2 eeskujul, mis võimaldab uuritud krohvisüsteeme arvutada sarnaselt teistele tulekaitsematerjalidele. Antud doktoritöö annab olulist sisendit täismõõtmeliste ahjukatsete planeerimiseks (EN 13381-7:2019), et uurida erinevate krohvisüsteemide tõrketekkegaagid. Lisaks saab töö tulemusi kasutada hindamaks olemasolevate sarnaste krohvide tulepüsivust vastavalt EN 1995-1-2 arvutusjuhiste. Käesolev uurimistöös annab raamistiku edasiste uuringute tegemiseks katsetamiseks erinevaid krohvisüsteeme, krohvikandjaid ja krohvide aluspindasid kaitsmaks puitkonstruktsioone tulekahjuolukorras.

Märksõnad: tulepüsivus, tulekaitsematerjal, savikrohv, lubikrohv, traditsiooniline krohvisüsteem, puitkonstruktsioonid, ajaloolised puithooned, Eurokoodeks 5 osa 1-2

## Appendix 1

Seven different dry-mix plasters were selected for the XRD analysis. The XRD measurements were made from powder prepare. 100mg of sample was hand milled and wet prepared with spirit. Samples were analysed with Bruker D8 diffractometer using Lynxeye detector. Scans were made through 2theta range 5–75 degrees. Measurement results were modelled with Rietveld refinement method using Topas software. The findings are reported in a table below. The estimation of the mixture’s clay content was problematic and thus was not performed in this investigation. Tests were performed by Siim Pajusaar at Taltech University, School of Science, Department of Geology.

*Table A1-1. Proportions of crystal phases determined by XRD analysis.*

Dry plaster mix	Quartz	Calcite	Ca-dolomite	Dolomite	Albite low	Orthoclase	Portlandite	Alite	Clay
Clay_mineral	13.7	83.8			1.6	1.0			trace
ClayCT04	73.3	8.7		2.7	7.8	7.5			trace
LimeSAK01	62.0	20.9	1.9		9.3	5.9		trace	
ClaySF04	55.0	17.2		8.5	10.3	9.0			trace
LimeSU04	24.4	53.4		10.0	4.8	2.9	4.5		
ClaySU04	60.1	13.2		5.8	11.5	9.2			trace
LimeUNI01	44.3	25.1		3.9	7.8	4.3	11.3	3.3	

## Appendix 2

Visual documentation of selected furnace tests performed in TP2.

### TEST 1 – horizontal orientation

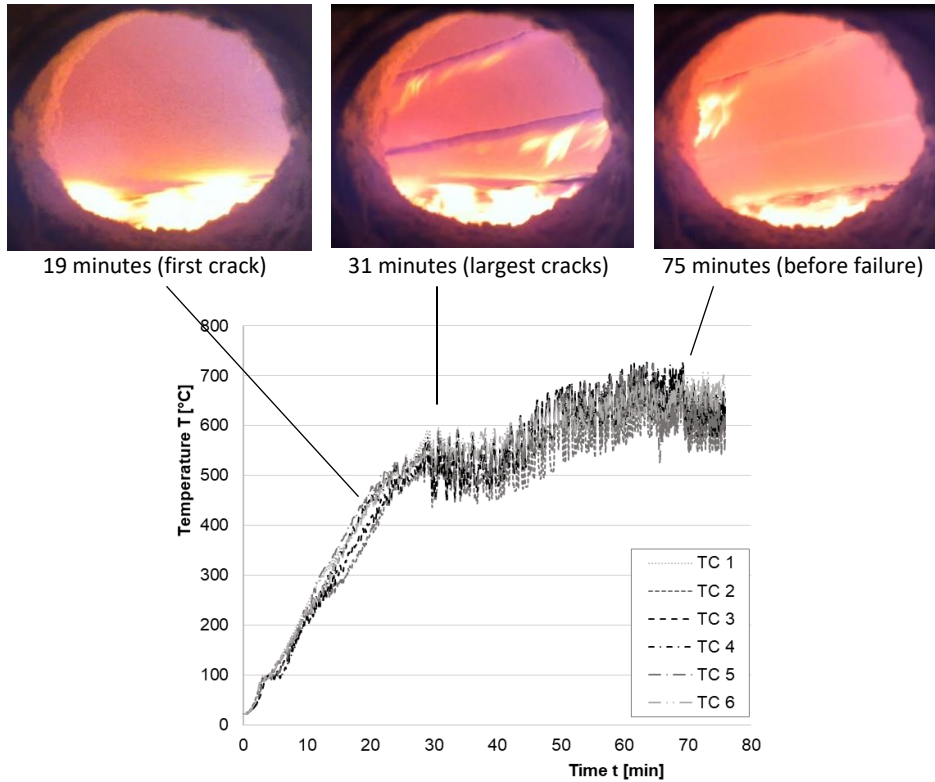


Figure A2-1. Temperature measurements at the interface of clay plaster (17 mm) and timber.

## TEST 7 – vertical orientation

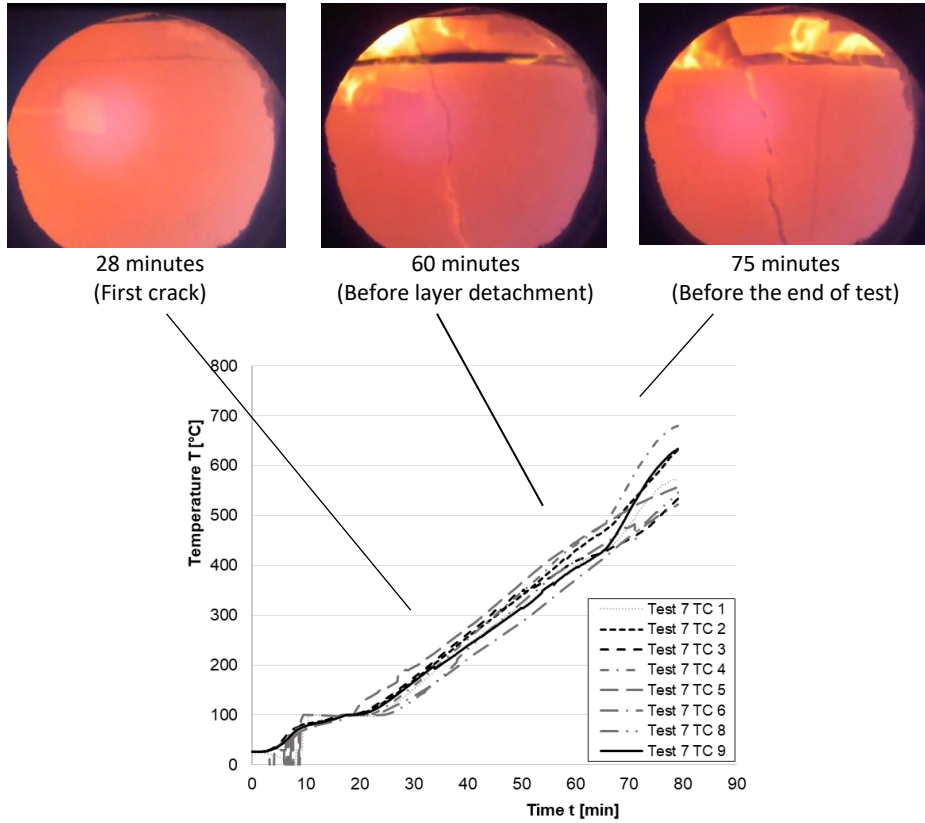


Figure A2-1. Temperature measurements at the interface of clay plaster (44 mm) and timber.

# Curriculum vitae

## Personal data

Name: Johanna Liblik  
Date of birth: 24.10.1988  
Place of birth: Tallinn  
Citizenship: Estonia

## Contact data

E-mail: johanna.liblik@taltech.ee

## Education

2016–2023 Tallinn University of Technology, Estonia – PhD  
2015–2016 Estonian Academy of Arts, In-Service Training for architectural, conservation and cultural heritage graduates  
2014–2014 Tartu College, Tallinn University of Technology, Estonia, In-Service Training for civil engineers in heritage protection and restoration  
2013–2014 VIA University College, architecture, Denmark – Exchange studies  
2008–2015 Tallinn University of Technology – MSC  
2006–2008 Tallinn Secondary School of Science, Estonia – High School

## Language competence

English Fluent  
Estonian Native

## Research experiences

2015 RISE Research Institutes of Sweden – fire testing  
2017 RISE Research Institutes of Sweden – fire testing  
2018–2019 TU Braunschweig, iBMB, MPA, Germany – fire testing

## Professional employment

2021– ... Tallinn University of Technology, School of Engineering, Expert  
2016–2021 Tallinn University of Technology, Junior Researcher

## Elulookirjeldus

### Isikuandmed

Nimi: Johanna Liblik  
Sünniaeg: 24.10.1988  
Sünnikoht: Tallinn, Eesti  
Kodakondsus: Eesti

### Kontaktandmed

E-post: johanna.liblik@taltech.ee

### Hariduskäik

2016–2023 Tallinna Tehnikaülikool, ehituse ja arhitektuuri instituut, doktorantuur  
2015–2016 Eesti Kunstiakadeemia, konserveerimise ja restaureerimise täienduskoolitus  
2014–2014 Tartu Kolledž, Tallinna Tehnikaülikool, muinsuskaitse ja restaureerimisalane täienduskoolitus ehitusinseneridele  
2013–2014 VIA University College, Taani – vahetusõpingud  
2008–2015 Tallinna Tehnikaülikool, tehnikateaduste magister  
2006–2008 Tallinna Reaalkool, keskharidus

### Keelteoskus

Inglise keel Kõrgtase  
Eesti keel Emakeel

### Teenistuskäik

2021– ... Tallinna Tehnikaülikool, inseneriteaduskond, ekspert  
2016–2021 Tallinna Tehnikaülikool, inseneriteaduskond, nooremteadur

ISSN 2585-6901 (PDF)  
ISBN 978-9949-83-992-6 (PDF)